NORTHWEST GEOLOGY

The Journal of The Tobacco Root Geological Society

Volume 40, July 2011

36th Annual Field Conference

The Superior Area, Montana

July 28—July 31, 2011

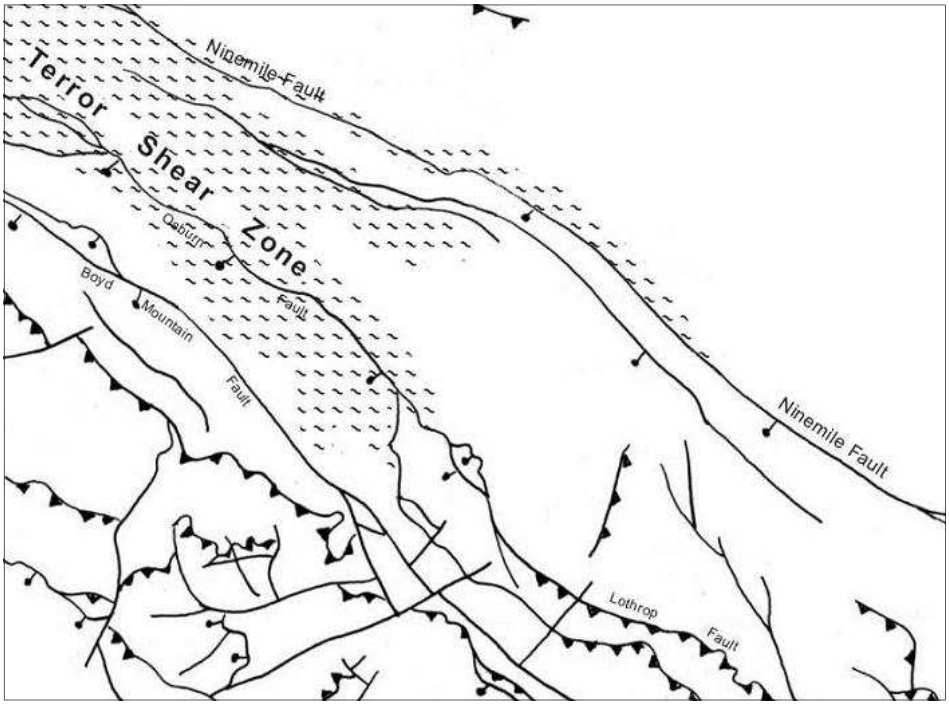

Published by The Tobacco Root Geological Society, Inc.
P.O. Box 2734
Missoula, Montana 59806
http://trgs.org

Edited by: Larry N. Smith and Richard I. Gibson

Cover: Boom operation in Gold Mountain mine placer along Trout Creek. See McCulloch (this volume).
Above: Structures of the Plains Quadrangle. See Lonn (this volume).

The Tobacco Root Geological Society, Inc.

P.O. Box 2734
Missoula, Montana 59806

Officers, 2011:

President: Mike Stickney, Montana Bureau of Mines and Geology, Butte, MT
Vice-President: Katie McDonald, Montana Bureau of Mines and Geology, Butte, MT
Treasurer: Ted Antonioli, Montana Mining Association, Missoula, MT
Secretary: Ann Marie Crites, Libby, MT
Webmaster: Dick Gibson, Consultant, Butte, MT

Board of Directors, 2011:

Bruce E. Cox, Hecla Mining Co., Idaho
Marie Marshall Garsjo, Natural Resources Conservation Service, Ft. Worth, TX
Richard I. Gibson, Gibson Consulting, Butte, MT
Larry Johnson, Consultant, Missoula, MT
Larry N. Smith, Dept. of Geological Engineering, Montana Tech, Butte, MT
Robert C. Thomas, Dept. of Environmental Sciences, U. of Montana-Western, Dillon, MT

Conference Organizer, Superior Field Conference:

Larry N. Smith

ISSN: 0096-7769

http://trgs.org

NORTHWEST GEOLOGY

The Journal of The Tobacco Root Geological Society

Volume 40, July 2011

The Superior Area

and other papers

Table of Contents

TRGS CHARTER MEMBERS

Stanley W. Anderson
Clyde Cody
William S. Cordua
Lanny H. Fisk
Richard I. Gibson
Thomas Hanley
Stephen W. Henderson
Thomas E. Hendrix
Mac R. Hooton
Inda Immega
Steven W. Koehler
Marian Millen Lankston
Robert W. Lankston
J. David Lazor
Joe J. Liteheiser, Jr.
Judson Mead*
Marvin R. Miller
Vicki M. Miller
Allen H. Nelson
Alfred H. Pekarek
Patricia Price*
Donald L. Rasmussen
Raymond M. Rene

TRGS HAMMER AWARD RECIPIENTS

Awarded for distinguished achievement in the study of the geology of the Northern Rocky Mountains

1993: Ed Ruppel
1994: Dick Berg
2003: Don Winston
2004: Dean Kleinkopf
2009: Betty Skipp
2010: Jim Sears
2011: John Childs

TRGS HONORARY MEMBERS

1980: Charles J. Vitaliano*
2008: Elizabeth Younggren
2010: Dick Berg
2010: Bruce Cox
2010: Dean Kleinkopf
2010: Dave Lageson

TRGS LIFETIME MEMBERS

Rob Foster
Joan (Mrs. Jack) Harrison*

* = deceased

Dedication

This volume of Northwest Geology is dedicated to two dedicated members: Isadore Million and John Whitmer. Both have faithfully attended TRGS meetings for many years, Isadore from Boulder/Longmont, Colorado, and John from Issaquah, Washington. Their camaraderie and cogent questions are a hallmark of the Society's meetings.

John Whitmer

Isadore Million

2011 Scholarship Recipients

- **Neal Auchter** (Michael Thompson Foster Scholarship) U. of Montana: *Analysis of incised channels in the Late Cretaceous Eagle Formation, south-central Montana*

- **Whitney G. Bausch** (TRGS Scholarship) U. of Montana: *Structural and thermochronological analysis of a lithologically-varied dike swarm, southwest MT*

- **Eduardo Francisco Guerrero** (TRGS Scholarship) Oregon State University: *Quantification of the landscape evolution over a mantle hot spot: deconvolving the uplift and geomorphic history of the Shoshone River drainage and the Yellowstone Crescent of High Terrain over the past 2 Ma*

- **Victor Guevara** (Harrison Scholarship) U. of Montana: *Constraints on the Structural and Thermal Evolution of the Clearwater Metamorphic Core Complex, ID*

- **William Thomas Jackson, Junior** (TRGS Scholarship) U. of Memphis: *Paleoseismites of the Elk Basin anticline: Indicators to early-formed joint development and fold growth during paleoseismic events*

- **Samantha Kaster** (Michael Thompson Foster Scholarship) U. of Montana: *Analysis of a marine transgression in the Cretaceous Eagle Formation in south-central Montana*

- **Lauren Kay** (TRGS Scholarship) Montana State University: *Tectonic deformation as a taphonomic process: using dinosaur bones as strain indicators*

- **Anita Moore-Nall** (Michael Thompson Foster Scholarship) Montana State University: *Physical and chemical characterization of brecciation and U-V mineralization in the Madison Limestone and adjacent units, Big Pryor Mountain mining district, Montana—Little Mountain mining district, Wyoming*

- **Laura Neser** (TRGS Scholarship) U. of North Carolina: *The timing of Laramide deformation in northwestern Wyoming*

- **Daniel L. Ross** (Michael Thompson Foster Scholarship) Montana State University: *Structural Geology of the North-Half of the Swift Reservoir Culmination, Northern Sawtooth Range, Montana*

Donate to scholarships at www.trgs.org/scholar.htm

2450 Ma METAMORPHISM RECORDED IN 3250 Ma GNEISSES, GALLATIN RANGE, MONTANA

Paul A. Mueller
Department of Geological Sciences, University of Florida, Gainesville, FL 32611

Joseph L. Wooden
Department of Earth Sciences, Stanford University, Stanford, CA

David W. Mogk
Department of Earth Science, Montana State University, Bozeman, MT 59717

Abstract

Zircons were separated from a sample of layered, migmatitic gneiss and from a sample of cross-cutting leucosome collected near the intersection of Greek Creek and the Gallatin River. Although there is some discordance in datasets from both samples, a coherent group of largely concordant data allows an estimate for the age of the primary gneiss protolith of 3261+/-13 Ma. Discordance is more prevalent in the zircons from the leucosome, but an age of 2434+/-30 Ma is representative of the metamorphic (Th/U <0.1) grains. One grain from the leucosomes also gave an age of ~1850 Ma and two low Th/U grains form the gneiss gave ages near 2400 Ma. These ages extend the spatial distribution of both the 3.2-3.4 Ga gneisses found throughout the Montana metasedimentary province and the most easterly record of the 2400 Ma event.

Introduction

Crystalline basement exposed in the cores of Laramide structures and in the soles of Sevier thrusts in SW Montana and eastern Idaho range in age from ~1.8 to ~3.5 Ga (e.g., fig. 1; Mueller et al., 1993; Mueller et al., 2005; Foster et al., 2006; Chamberlain and Mueller, 2007; Mueller et al., 2010). Gneisses exposed along the Gallatin River are similar in appearance and composition to the predominantly Mesoarchean TTG (tonalite-trondhjemite-granodiorite) gneisses previously described in the Madison Range and other parts of the Montana metasedimentary province (MMP; Mueller et al., 1993; Mueller et al., 2004a). In Gallatin Canyon, radiometric ages are limited to thermochronologic data (e.g., Giletti, 1966). These reports did not address the primary age of the protoliths to these gneisses, but did show that the gneisses near the intersection of Portal Creek and the Gallatin River were disturbed by elevated temperatures in the Proterozoic and that the resulting loss of Ar from biotites, and to a lesser extent amphiboles, occurred over a narrow interval with a steep thermal gradient at ~1600-1800 Ma. This zone of steep thermal gradients was later referred to as Giletti's line.

In contrast to the relatively homogeneous gneisses near Portal Creek described by Giletti, leucosomes (0.5 by 5 m) are well exposed near Greek Creek in Gallatin Canyon (Mogk, 1992). These leucosomes formed at near water-saturated conditions, at ca. 680-720^{o}C and 8-10 Kb. The leucosomes result from a melt reaction in which biotite tonalite (main lithology) melts to form K-spar rich melt, with horn-

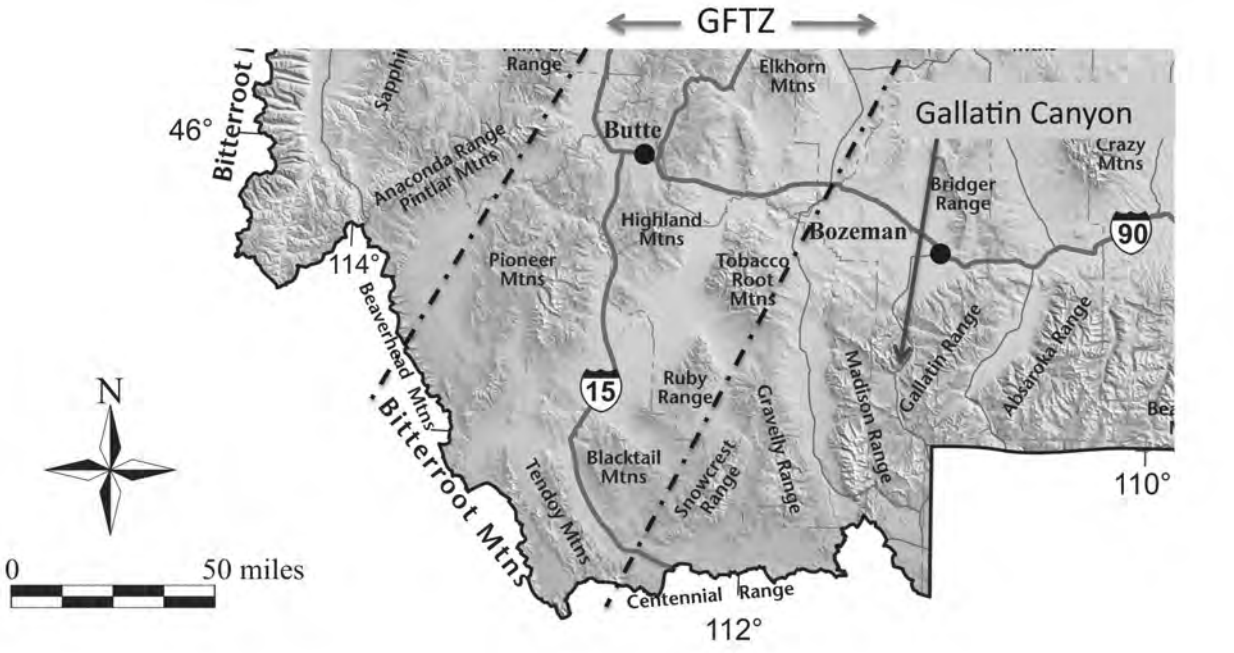

Figure 1. Generalized physiographic map showing major uplifts of SW Montana with sample location for Gallatin Canyon note by arrow (after Vuke et al., 2007). Dashed lines depict general limits of the Great Falls tectonic zone (GFTZ).

blende and magmatic epidote as restite phases. Mogk proposed a direct, genetic relationship between ductile shearing and migmatization such that the ductile shearing allowed infiltration of small amounts of water rich fluid into the system, inducing melting. The presence of melt, in turn, affected the rheology of the rock to localize ductile shearing. Locally generated melts occur both in shear zones and in domains of low strain, e.g., adjacent to boudins. These melts cannot escape the system because they are formed near the solidus and rapidly encounter the water-saturated solidus upon small degrees of either cooling or decompression. As a result, these localized melts produce veins that are sub-parallel to the gneissic layering over most of their length, but clearly crosscut the gneissic fabric in places. Samples collected for this study include biotite tonalite gneiss that is host to the K-spar-rich leucocosomes and a sample of one of the leucosomes, both from the Greek Creek location in Gallatin Canyon (fig. 1).

Methods and Results

Zircons were separated by standard hydraulic, magnetic, and density methods, mounted in epoxy, and ground to half thickness prior to analysis using the SHRIMP-RG ion microprobe (e.g., Compston and Williams, 1992). Where necessary, common Pb corrections are based on ^{204}Pb count rates and lead isotopic compositions based on the Stacey and Kramers (1975) model Pb. All ages discussed are given with errors at the 95% confidence interval and based on ^{207}Pb/^{206}Pb ratios. Seventeen analyses were made on 16 grains from one sample of layered gneiss (G01) with sub-parallel bands of melanosomes and leucosomes. Zircons ranged in age from 2365 to 3364 Ma (Table 1; fig. 2). Six of the 7 oldest grains that were <3% discor-

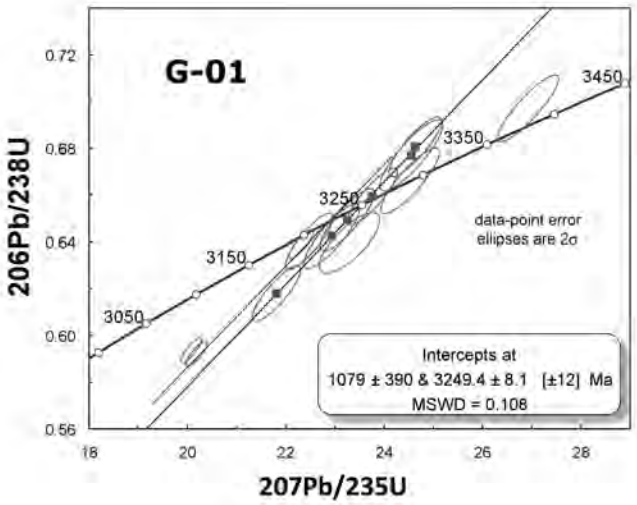

Figure 2. U-Pb concordia diagram shows scatter of data for G-01 (TTG gneiss). The concordia intercept age is within error of the calculated mean (2361 +/-13 Ma).

Spot Name	%comm 206	ppmU	ppmTh	232Th/ 238U	208corr206Pb /238UAge	1sigma error	204corr207Pb /206Pb Age	1sigma error	%Discordant
Gneiss									
G01-1	0.00	136	39	0.30	3185	21	3272	11	3%
G01-2	0.02	149	46	0.32	3342	21	3262	7	-3%
G01-3	0.03	724	601	0.86	2984	10	3155	4	5%
G01-4	0.10	654	471	0.75	2977	10	3167	4	5%
G01-5	0.43	1199	239	0.21	1726	5	2603	6	34%
G01-6	0.00	159	44	0.28	3184	20	3214	7	1%
G01-7	0.00	639	77	0.12	3184	10	3205	4	1%
G01-8	0.34	196	122	0.64	3402	24	3364	7	-1%
G01-9	0.00	126	67	0.55	3284	24	3289	8	0%
G01-10	-0.03	136	41	0.31	3221	22	3245	8	1%
G01-11	0.09	108	42	0.40	3338	25	3265	9	-2%
G01-12	0.02	121	37	0.31	3195	23	3240	8	1%
G01-13	0.00	846	67	0.08	2454	7	2446	5	0%
G01-14	0.02	171	82	0.49	3260	20	3255	7	0%
G01-15T	1.15	422	30	0.07	2661	12	3033	11	11%
G01-16	0.03	157	49	0.32	3093	20	3222	7	4%
G01-16T	2.36	1392	31	0.02	2178	9	2365	17	7%
Leucosome									
G02-1	0.50	3750	210	0.06	1803	3	2286	5	21%
G02-2	0.64	3839	54	0.01	1665	3	1852	8	10%
G02-3T	5.35	1217	130	0.11	273	4	1485	92	80%
G02-4	0.11	137	8	0.06	2416	21	2404	12	0%
G02-5	0.07	3900	204	0.05	2552	4	2430	2	-5%
G02-6	0.13	4021	194	0.05	2002	4	2410	4	17%
G02-7	0.06	93	6	0.07	2444	21	2490	14	2%
G02-8	0.36	4880	179	0.04	2042	3	2437	3	16%
G02-9	0.20	4692	186	0.04	1405	2	2350	4	40%

Notes: "T" designates analyses conducted on the tip or end of a grain.

Table 1.

dant form a coherent group with an age of 3261 +/-13 Ma, which we interpret as the age of crystallization of the gneiss protolith. The two youngest grains (2365 and 2447 Ma) have Th/U<0.1 and are best viewed as metamorphic. The oldest grain is interpreted as a xenocryst in the protolith's magma. Zircons from a band of partially crosscutting leucosome yielded a range of ages from 1485 to 2490 Ma. The youngest age is 80% discordant and the only grain with Th/U >0.1; it does not likely provide a meaningful chronologic constraint on either protoliths age or the time of metamorphism. Of the remaining 8 grains, 5 fall in the range 2286 to 2490 Ma, the sixth is 1852 Ma, and all have Th/U<0.1, suggesting a metamorphic origin. The most coherent group (5 grains) gives an age of 2434 +/- 30 Ma, which provides the best estimate of the time of metamorphism. If the low Th/U grains from sample G01 are combined with those from G02, the estimate of the time of metamorphism does not change significantly (2426+/-29 Ma). The single grain at 1852 Ma also has a low Th/U (<0.1) and likely grew during a later metamorphic event well documented in ranges to the west (e.g., Brady et al., 2004). The metamorphism at ~2430 Ma corresponds to an event that is recognized in other parts of SW Montana, but was extensively overprinted at ~1800 Ma during development of the Great

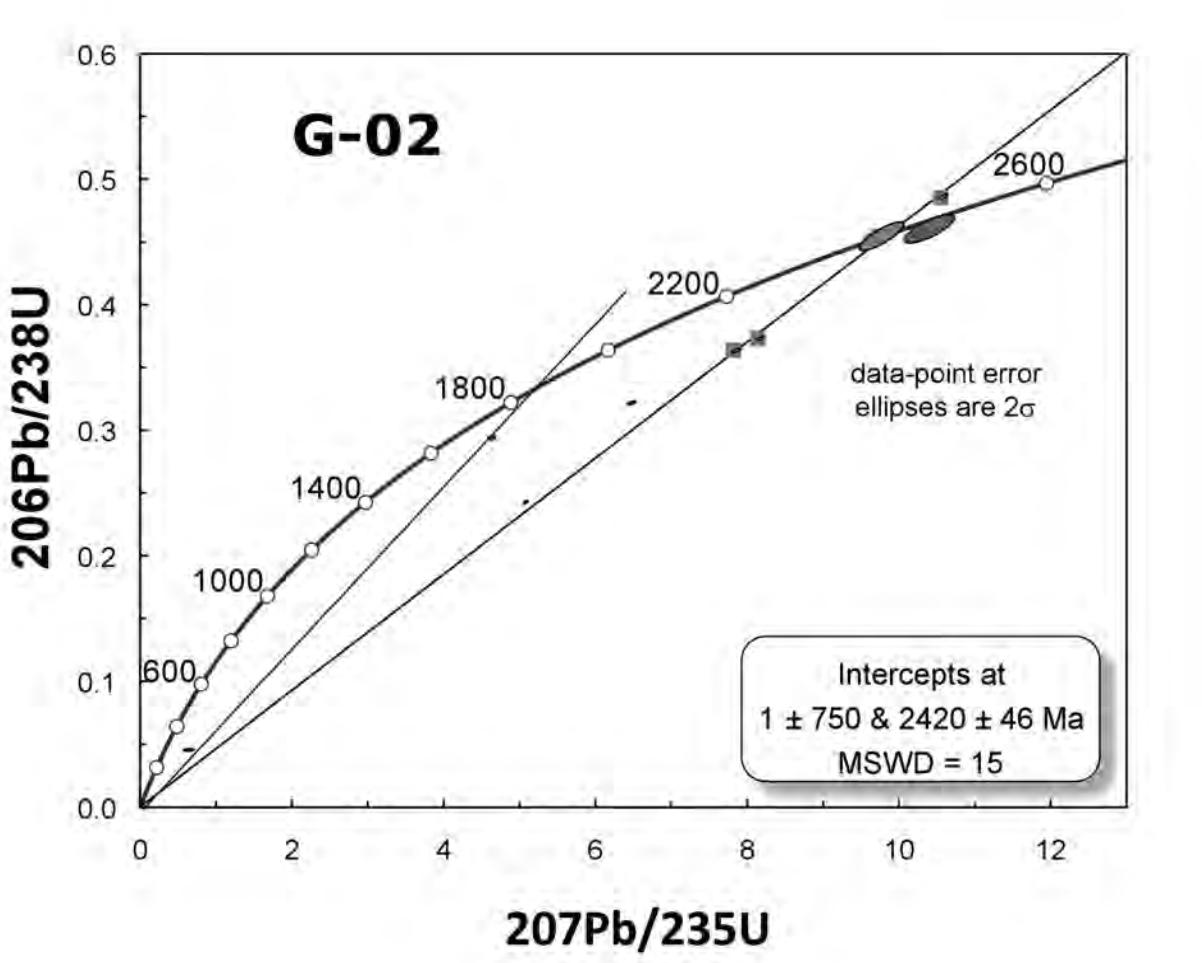

Figure 3. U-Pb concordia diagram for leucosome G-02 shows coherence of ~2400 Ma, low Th/U zircons and one ~1800 Ma grain. The concordia intercept age is within error of the calculated mean (2430 +/- 30 Ma).

Falls tectonic zone (1860 to 1770 Ma; Mueller et al., 2002, 2005).

Discussion

Our best estimate of the time of crystallization of the protolith of the gneiss of Gallatin Canyon falls within the range of the most populated age range (3200-3400 Ma) reported from Archean quartzites throughout the MMP as well as in the Beartooth Mountains (Mueller et al., 1998). In terms of direct measurements, protoliths with crystallization ages in this range are found throughout the Tobacco Root, Highland, Madison, and Ruby Ranges (e.g., Mueller et al., 1993; Mueller et al., 2004a; Krogh et al., 2011). Evidence for earliest Paleoproterozoic igneous and metamorphic activity in SW Montana is, however, much more limited in this region. Mueller et al. (1994) first noted the presence of ~2400 Ma overgrowths on zircons from the Dillon gneiss (Ruby Range). Roberts et al. (2002) reported Pb step leaching data experiments on garnet from the Tobacco Root Mountains that yielded an age of ~2470 Ma, which was attributed to monazite included within the garnet. This interpretation was confirmed by Cheney et al. (2004) who reported ion probe data for monazites separated from older gneisses in the Tobacco Root Mountains at ~2450 Ma. In addition, Krogh et al. (2011) report evidence of ~2450 Ma metamorphism in U-Pb systematics in zircons, also from the Tobacco Root Mountains. The only example of ~2450 Ma magmatic activity is exposed in the sole of a Sevier thrust in the Tendoy Mountains. This unit gave an U-Pb zircon age of ~2450 Ma with a strong overprint at ~1800 Ma (Foster et al., 2006).

In addition to these surficial occurrences, Mueller et al. (1996) reported a range of earliest Proterozoic xenocrystic zircons from the Tobacco Root batholith, suggesting that early Paleoproterozoic and Archean crust are intercalated at depth as far east as the Tobacco Root Mountains. The combined evidence for ~2450 Ma magmatic and metamorphic activity is limited in terms of specific chronologic determinations compared to the later ~1800 Ma metamorphism that has been recognized in data reported by many workers since the 1960s (e.g., Giletti, 1966; Roberts et al., 2002; Mueller et al., 2004a, Brady et al., 2004; Mueller et al., 2005). The ~2450 Ma tectonothermal event, however, is widespread in SW Montana's pre-Belt basement and must represent an episode of crustal thickening and metamorphism that predated the well established ~1800 Ma event. In addition, the new crust that formed at ~2450 Ma was likely in place along the western margin of the Wyoming craton prior to the crustal thickening at ~1800 Ma.

From a larger scale tectonic perspective, it is important to note that ~2450 Ma magmatism, and likely deposition, is recorded further south in the supracrustal rocks of the Farmington Canyon Complex, which is exposed along the Wasatch front immediately north of Salt Lake City (e.g., Bryant, 1988; Mueller et al., 2004b). These rocks were also subjected to Paleoproterozoic metamorphism, but significantly later than in the MMP/GFTZ, i.e., at ~1675 Ma (Mueller, in review). The occurrence of ~2450 Ma magmatism and metamorphism along the western margin of the Wyoming craton appears complementary to ~2450 Ma extension proposed for the eastern margin of the craton in the Black hills (e.g., Dahl et al., 2007). The later metamorphism of these rocks compared to those in SW Montana, however, suggests a fundamental boundary must exist along the western margin of the Wyoming craton that marks two distinct episodes of terrane accretion. Despite the differences in ages of these events along the western Wyoming margin, it is important to note that no corresponding magmatism has been

observed in the interior of the Wyoming craton corresponding to either of these events. This strongly suggests that any convergence associated with these events did not involve subduction of oceanic lithosphere beneath the Wyoming craton.

Acknowledgements

Financial support for this research was provided by NSF (EAR 0546751 and 0538133).

References

Brady, J.B., Kovaric, D.N., Cheney, J.T., Jacob, L.J., and King, J.T., 2004, $^{40}Ar/^{39}Ar$ Ages of Metamorphic Rocks from the Tobacco Root Mountains, Montana: *in* Brady, J.B., Burger, H. R., Cheney, J.T., and Harms, T.A., eds., Precambrian Geology of the Tobacco Root Mountains, Montana: Geological Society of America Special Paper 377, p. 131-150.

Bryant, B., 1988, Geology of the Farmington Canyon complex, Wasatch Mountains, Utah: U.S. Geol. Survey Professional Paper 1476, 54 p.

Chamberlain, K.R., and Mueller, P.A., 2007, Oldest rocks of the Wyoming Craton: *in* Earth's Oldest Rocks, Van Kranendonk, M.J., Smithies, R.H., and Bennett, V., eds., Developments in Precambrian Geology series, Kent Condie, series ed., Elsevier, Chapter 6.3, p. 775-791.

Cheney, John T., Webb, A., Coath, C., and McKeegan, K., 2004, In situ ion microprobe $^{207}Pb/^{206}Pb$ dating of monazite from Precambrian metamorphic rocks, Tobacco Root Mountains, Montana: *in* Brady, J.B., Burger, H.R., Cheney, J.T., and Harms, T.A., eds., Precambrian Geology of the Tobacco Root Mountains, Montana: Geological Society of America Special Paper 377, p. 151-180.

Compston, W., and Williams, I., 1992, Ion probe ages for the British Ordovician and Silurian stratotypes: *in* Webby, B., and Laurie, J., eds., Global Perspectives on Ordovician Geology: Rotterdam, Netherlands, Balkema, p. 59-67.

Dahl, P., Hamilton, M., Wooden, J., Foland, K., Frei, R., MacCombs, J., and Holm, D., 2006, 2480 ma mafic magmatism in the northern Black Hills, South Dakota: A new link connecting the Wyoming and Superior cratons: Canadian Journal of Earth Science, v. 43, p. 1579-1600.

Foster, D., Mueller, P., Vogl, J., Mogk, D., and Wooden, J., 2006, Proterozoic evolution of the western margin of the Wyoming Craton: Implications for the tectonic and magmatic evolution of the northern Rocky Mountains: Canadian Journal of Earth Science, v. 43, p. 1601-19.

Giletti, B., 1966, Isotopic ages from southwestern Montana: Journal Geophysical Research, v. 71, p. 4029-36.

Krogh, T., Kamo, S., Hanley, T., Hess, D., Dahl, P., and Johnson, R., 2011, Geochronology and geochemistry of Precambrian gneisses, metabasites, and pegmatite from the Tobacco Root Mountains, northwestern Wyoming craton, Montana: Canadian Journal of Earth Sciences, v. 46, p. 161-185.

Ludwig, K., 2002, SQUID 1.08 User's Manual: Berkeley Geochronology Center Special Publication, Berkeley, CA, 22 p.

Ludwig, K.R., 2003, User's Manual for Isoplot 3.00: A Geochronological Toolkit for Microsoft Excel: Berkeley Geochronology Center Special Publication, No. 4, 70 p.

Mogk, D., 1992, Ductile shearing and migmatization at mid-crustal levels in an Ar-

chean high-grade gneiss belt, Gallatin Range, Montana, USA: Journal of Metamorphic Geology, v. 10, p. 427-438.

Mueller, P., Wooden, J., Mogk, D., Henry, D., and Bowes, D., 2010, Rapid growth of an Archean continent by arc magmatism: Precambrian Research, v. 183, p. 70-88.

Mueller, P., Burger, H., Wooden, J., Brady, J., Cheney, J., Harms, T., Heatherington, A., and Mogk, D., 2005, Age and tectonic implications of Paleoproterozoic metamorphism in the northern Wyoming Province: Journal of Geology, v. 111, p. 169-179.

Mueller, P., Wooden, J., Heatherington, A., Burger, H., Mogk, D. and D'Arcy, K., 2004a, Age and evolution of the Precambrian crust of the Tobacco Root Mountains: *in* Brady, J.B., Burger, H. R., Cheney, J.T., and Harms, T.A., eds., Precambrian Geology of the Tobacco Root Mountains, Montana: Geological Society of America Special Paper 377, p. 181-202.

Mueller, P., Foster, D., Mogk, D., and Wooden, J., 2004b, New insights into the Proterozoic evolution of the western margin of Laurentia and their tectonic implications: Geological Society of America Abstracts, v. 36, no. 5, p. 404.

Mueller, P., Heatherington, A., Kelley, D., Wooden, J., and Mogk, D., 2002, Paleoproterozoic Crust within the Great Falls Tectonic Zone: Implications for the Assembly of Southern Laurentia: Geology, v. 30, p. 127-130.

Mueller, P., Wooden, J., and Mogk, D., submitted, Paleoproterozoic evolution of the Farmington zone: implications for terrane accretion in SW Laurentia: Lithosphere.

Mueller, P., Wooden, J., Nutman, A., and Mogk, D., 1998, Early Archean crust in the northern Wyoming Province: Evidence from U-Pb systematics in detrital zircons: Precambrian Research, v. 91, p. 295-307.

Mueller, P., Heatherington, A., D'Arcy, K., Wooden, J., and Nutman, A., 1996, Contrasts between Sm-Nd and U-Pb zircon systematics in the Tobacco Root batholith, Montana: Implications for the determination of crustal age provinces: Tectonophysics, v. 265, p. 169-79.

Mueller, P.A., Shuster, R., Wooden, J., Erslev, E., and Bowes, D., 1993, Age and composition of Archean crystalline rocks from the southern Madison Range: Implications for crustal evolution in the Wyoming craton. Geological Society of America Bulletin, v. 105, p. 437-446.

Mueller, P., Heatherington, A., Wooden, J., Shuster, R., Mogk, D., and Nutman, A., 1994, Paleoproterozoic evolution of the NW margin of the Wyoming craton: Evidence for 1.7 and 2.4 Ga terranes: Geological Society of America Abstracts, v. 26, no. 7, p. 340.

Roberts, H., Dahl, P., Kelley, S., and Frei, R., 2002, New ^{207}Pb-^{206}Pb and ^{40}Ar-^{39}Ar ages from SW Montana, USA: Constraints on the Proterozoic and Archean tectonic and depositional history of the Wyoming Province: Precambrian Research, v. 117, p. 119-143.

Stacey, J., and Kramers, J., 1975, Approximation of terrestrial lead isotope evolution by a two-stage model: Earth and Planetary Science Letters, v. 26, p. 381-399.

Vuke, S., Porter, K., Lonn, J., and Lopez, D., 2007, Geologic map of Montana—Information Booklet: Montana Bureau of Mines and Geology Geologic Map 62D, 73 p.

AN INTRODUCTION TO THE GOLD PLACERS AND LODE SOURCES OF THE QUARTZ-CEDAR MINING DISTRICT, MINERAL COUNTY, MONTANA

Robin McCulloch
Mining Engineer, Montana Bureau of Mines and Geology

Introduction

The eastern half of Mineral County has produced placer gold from many of the significant streams draining the area between the Clark Fork River and the Idaho border. After nearly 129 years, geologists and exploration company personnel are no closer to discovering the source for that gold. Lode exploration projects have not discovered significant auriferous sources. The small discoveries have no relationship to the known placer deposits.

The land is steep, rugged, and densely forested. Access and mineralized exposures are difficult to obtain. Other than similar environments in neighboring Idaho, it is located distant from other historic gold producing districts. Worst of all is that it has always been known as a good placer district. These points account for a historic avoidance of the area by exploration companies and researchers.

Location

The area is part of the historic Quartz-Cedar mining district that lies southwest of Superior, Montana. The district encompasses Fish, Quartz, Meadow, Trout, Cedar, Dry, and Little Joe creeks. The study area lies roughly ten miles south of Superior between and including the Trout and Quartz creek drainages.

History

Gold was discovered in Cedar Creek on October 9, 1869 by Louis Barrette (Horstman, 1996, unpublished report by the US Forest Service). By Christmas, he had filed claims 2.5 miles above his discovery. Newspaper articles report that by January 1, 1870, towns had sprung up along Cedar Creek. Companies had been formed to saw boards for sluice boxes, suppliers had built businesses, and companies had been formed to construct ditches and sluice the deposits. Exploration spread out rapidly to upper Cedar, Oregon, Rabbit, Illinois, Wolverine and Montreal gulches (Horstman, 1996, unpublished report by the US Forest Service).

By February, the miners had spread to Quartz, Lost, and Trout creeks. By April, the miners had located on Quartz, Meadow, and Little Bear creeks (a tributary to Meadow Creek). Between 1870 and 1877, most of the drainages were being heavily flumed (ground sluiced). Millions of yards of gravel were washed to the Clark Fork River. Deep ground was being drifted but many areas did not drain well because of the depth to bedrock, high volumes of water, and the flat gradient.

By 1878, the easy gold was gone and many of the camps had been abandoned. The remaining operations required sizeable investments for development. Some lode properties were developed in 1885 while the placer operations were starting to use hydraulic monitors to strip overburden.

By 1899, upper Cedar was the largest producer in the district with continued production through 1907 when a bucket-line dredge was constructed at the head end of the drainage. Hardrock operations enjoyed rich ore at the Amador, but newspaper articles of the times noted only development efforts on the other lode properties.

During the 1910 fire, many of the old camps and mines were destroyed. Most were not rebuilt. Fewer and fewer miners came to the Quartz-Cedar district but many of the original miners remained their entire lives. Production that started with a rush reached a sustainable level early in the century and produced consistently to World War II. Total production is estimated to exceed $13 million with approximately $10 million of that produced prior to 1900.

After World War II, gold prices were depressed while labor cost soared. Most jobs paid better than mining thus few people returned to the mines. Production has continued into the 1990s but at a much reduced rate.

Geology

The gold lode and placer deposits appear to be confined to steeply dipping, northwest- and northeast-trending faults in the middle and lower Wallace Formation (Middle Proterozoic) of the Ravalli Group. These rocks are part of the Belt Supergroup. The middle Wallace consists of dolomitic and calcareous siltite and quartzite, and black argillite. It also contains minor amounts of green siltite and argillite. Quartzite beds show evidence of scour, along with hummocky cross-stratification. Some of the quartzite is carbonate free. Tan weathering dolomitic siltite with black argillite caps is common. The presence of black argillite and abundant calcite distinguishes these rocks from the Shepard Formation.

Vertical fractures in quartzite are common, as are “birdsfoot” cracks on argillite surfaces. Orange-weathering, dolomite-rich sedimentary breccia is present within the middle member and is usually anomalous in gold. The breccias consist of angular fragments of quartzite and blocks of typical middle Wallace lithology suspended in a silty matrix and cemented by calcite, dolomite, iron carbonate, and quartz; these breccias are commonly dotted by crystals or pseudomorphs of scapolite (Harrison et al., 1986). The unit also contains rare salt casts. It is associated with large slump folds in zones as thick as 60 ft. The thickness of the middle Wallace is probably on the order of 2,500 to 4,500 ft (Lewis, 1998).

The lower member of the Wallace Formation consists of green siltite and light green argillite with the carbonate pods. It also contains dolomitic siltite and quartzite. The lower and middle parts are thinly bedded and are the least quartzitic. The thickness is indicated to be between 3,000 and 5,000 ft (Lewis, 1998).

The northwest trending high-angle faults are most likely associated with the Lewis and Clark Line which has had a history of intermittent movement from the Proterozoic into the Quaternary (Harrison et al., 1986). Although the faults can have easily recognizable features, most areas in the gold zones are not competent, form topographic lows, have few outcrops, heavy soil cover and are subsequently difficult to follow. Most mappers must use stratigraphy to identify the faults while steeply dipping bedding is commonly used as an indicator of the presence of a fault. Most faults in the mineralized zones appear to exhibit continuity for great length. In the central portion of the study area, the faults are relatively continuous for over 23 miles (Harrison et al., 1986).

Mafic sills and dikes (Late and Middle Proterozoic) are commonly associated near or in some of the fault zones. These are composed of dioritic to gabbroic rocks that show alteration of mafic minerals. These intrusives range in thickness from less than 3 ft to 1,500 ft. Thicker sills tend to have wide (600 ft) contact-metamorphosed zones around them. Sills commonly persist for many miles; some maintain approximately the same stratigraphic position, whereas others cut through the section. Intrusion occurred at least twice (at about 1,400 m.y. and 800 m.y. (Harrison, 1972, 1986)). In Deep Creek at the Gold Mountain mine, dozer cuts have exposed a mafic dike crosscutting the Middle Wallace. The dike was bisected by a 10-12 ft wide auriferous quartz zone with associated pyrite, magnetite, hematite, and aragonite.

Mineralized Structures

The mineralized structures have a corresponding relationship with regional fault systems. They are geochemically confined to gold and copper, however those two elements are unrelated and respond independently. Typical geochemical indicator elements such as arsenic, antimony, bismuth, and mercury are absent. In the placers, an occasional nugget of galena has been observed but lead has not been a good indicator of soils.

During the 1995-1997 field seasons, the author distinguished six identifiable structures. Four are parallel along the northwest trend and merge into a fifth structure on the west end. The sixth has a northeast trend and is located in the southern portion. The study area contains the first three zones from the east.

The northeastern zone is predominately copper, has no identified placers, and consequently was not studied in detail. This zone may include an oxide copper occurrence in Dry Creek, the Amador Mine in Cedar Creek, a sulfide copper property in Van Ness Creek, a tributary of Trout and a barren quartz outcrop in Quartz Creek.

The second zone from the northeast is not as easily traced. It has a good placer signature on the southern end, but is not as easily traced on the surface on the western end. No known significant placer signature exists west of the Trout Creek drainage. On this mineralized zone, the gold appears to be emplaced in small quartz veins in the gray argillite. The structure ranges in width from 200 to 500 ft in areas in the upper Meadow Creek/Sunrise Creek drainages to a 200 ft zone of widely spaced veinlets on the Trout Creek road between Tin Cup and Slaughterhouse creeks. The middle or third zone is the most continuous and appears to be the source for the majority of placer gold. It is 300-500 ft wide and has a close relationship in localized areas with a mafic dike. The northeast boundary is commonly the Wallace breccias that weather into blocky, red-brown to black, crusty boulders of dolomitic argillite. The southwest boundary of the zone is 500-1,000 ft of scapolite-filled argillite beds. In Rabbit Creek, those beds appear to be flooded with silica. But on the Rabbit Creek road cut, the scapolite forms a boxwork with quartz crystals and is filled with a red-orange soil. This material is anomalous in gold values but samples so far have not revealed any significant values.

Between the Wallace breccia and the scapolite zone is a mafic intrusive that ranges in width from approximately 100 ft in Lime Gulch (middle Deep Creek) to well over 1,000 ft in the middle Oregon Creek canyon. In none of the exposures seen was there any significant alteration related to the intrusive. The fault zone, however, seems to have the

emplacement of the mafic material. In the exposures in Lime Kiln Creek, the intrusive was faulted at a later period and massive quartz filled the space. Free gold was observed on pyrite gossan. Thickness of the quartz appears to range between 6 and 12 ft in exposures, but continuity is difficult to determine. Select samples of the quartz range between 0.1 and 1.0 opt Au. Crystalline magnetite, rare pyrite and limonite are associated with the zone.

The quartz is not confined to the intrusive nor is the fault zone. On the hillside above the confluence between Deep and Trout Creeks, there is a bedding plane emplacement of quartz that appears to be barren. The bottom of the vein is composed of 8-10 inches of siderite with specular hematite that is anomalous in gold. In Torino Creek, near the top of the divide between 4th of July and Sunrise creeks, the auriferous quartz occurs both as boudins in thinly bedded shales and as filling of en echelon joints. The depositional environment and preparation for porosity through faulting appears to be more critical than rock type. The gold in the third zone is typically coarse with many + ½ ounce nuggets. Historically, multi-ounce nuggets have been common. The mean size of the gold is 1/8 to 3/16 inch in diameter. Although many pieces are smooth and rounded, white quartz inclusions are quite common on the larger pieces and many have ragged edges. This zone also seems to have a distinct relationship with magnetite and hematite. Pieces of breccia 2-3 ft in diameter are often seen and concentrates are heavy in magnetite. Although outcrops of granite or granodiorite were not seen, placer deposits contain many 2-6 ft boulders of granodiorite exhibiting chloritic alteration that air-slack to sand within a few hours of exposure.

The fourth zone is as difficult to follow as the second zone. The mineralization appears to be confined to quartz pods and veins in an orange/tan argillite. Exposures are extremely rare. Placer deposits give hints to the location but the soils and geology are not conducive to outcrop.

The exposed subcrop in California Creek is highly fractured orange/tan argillite and quartz is not especially common in either the soils or the streams. Magnetite is not common in the placer deposits but hematite pseudomorphs of pyrite are exceedingly common in the Cedar Creek drainage starting at the upper end with Snowshoe Gulch.

Quartz veins up to 5 ft wide with good gold values are described in newspaper clippings of the 1860s-1880s period but little of that vein material is seen on mine dumps.

The gold is normally quite small with few nuggets. There are no mining operations on that zone thus detailed description of the gold related to the zone is impossible.

The fifth zone is also poorly exposed. It appears to be the source of the placer gold in the Deer and Ward Creek drainages. Although there is a history of placer activity, it is not recent and the workings do not exhibit any significant extent. Patented lode deposits at the head of Deer Creek indicate a gold bearing structure trending through Gold Peak and Rivers Peak. It may eventually intersect the Placer Creek fault in Idaho.

A potential exists that gold mineralization may also exist in a fault structure northeast of Gold Peak but only exploration will verify that.

The sixth zone follows a northeast trend from Shale Mountain in Idaho, along Cache Creek, bisecting Montana Creek and Fish Creek and continuing up Wig Creek. Placer activity was significant in the 1920s and 1930s but pro-

duction was limited. Field examination of the middle and lower Cache Creek indicates little production and minor exploration of placer bench gravels The zone is nearly vertical and hundreds of feet wide. The portion in Idaho is bounded by Tertiary granite with the main zone filled with Tertiary volcanic (rhyolite). In Montana, the structure cuts through middle Wallace and contains some zones of rhyolite. ASARCO staked claims in the Idaho side and indicated that the potential existed for a graben. The project never reached the drilling stage before the company's office was closed and all properties were dropped. (John Balla, oral commun. 3/26/98).

Following this introduction to the geology and mining history of the overall Quartz-Cedar Mining District, two field trips will cover the south-central segment of the district. The Quartz creek trip will focus on the geomorphologic aspects and the placers with some reference to the lode sources. The Trout Creek – Cedar creek trip will incorporate placer deposits as well as lode deposits along with the historical aspects of their development.

References

Harrison, J.E., 1972, Precambrian Belt basin of northwestern United States–Its geometry, sedimentation and copper occurrences: Geological Society of America Bulletin, v. 83, p. 1215-1240.

Harrison, J.E., Griggs, A.B., and Wells, J.D., 1986, Geologic and structure maps of the Wallace 1º x 2º quadrangle, Montana and Idaho: U.S. Geological Survey Miscellaneous Investigations Map I-1509-A, scale 1:250,000.

Lewis, R.S., 1998, Geologic map of the Butte 1º x 2º quadrangle, Montana: Montana Bureau of Mines and Geology Open-File Report MBMG 363, 16 p., scale 1:250,000.

IMPLICATIONS OF REFOLDED FOLDS IN THE MADISON LIMESTONE IN TROUT CREEK CANYON, BIG BELT MOUNTAINS, MONTANA

Matthew J. Rhoads

Trout Creek is a minor tributary to the Missouri River and is located approximately 26 miles northeast of the state capitol, Helena. Trout Creek Canyon is located approximately 4.5 miles east-northeast of York, Montana in the heart of the Big Belt Mountains. The canyon itself occurs almost entirely within repeated sequences of complexly thrust-faulted Lodgepole Limestone Formation and Mission Canyon Formation, which together comprise the Madison Group in this area of Montana. Folds related to the thrust faulting in the area have been complexly refolded, with subsequent fold axes that are nearly perpendicular to the fold axes associated with thrust faulting (fig. 1). Detailed regional mapping in the area, Reynolds (2003), has unveiled complex thrust relationships which established that successive thrusts sheets are younger to the west and have over-ridden older thrusts sheets with eastward displacement. Additionally, these thrusts have been subjected to a simultaneous north-south tectonic compression that created fold axes perpendicular to the direction of thrust faulting. Several of these complex refolds are preserved in vertical limestone walls of Trout Creek Canyon.

A potential source for the north-south oriented compression was brought forward by Sears, J.W., 2006, in which age-dating indicated that regional thrust faulting in northern Montana had a clock-wise, rotational nature with the pivot-point located somewhere near the Big Belt Mountains. It should also be noted that this location in the Big Belt Mountains corresponds to the intersection of the Lewis and Clark Line with the Montana Disturbed Belt. Competing compressive events have left the rootless refolded structures that are seen today.

References

Reynolds, M.W., 2003, Geologic map of the Hogback Mountain quadrangle, Lewis and Clark Counties, Montana: U.S. Geological Survey Geologic Investigations Map I-2773, Scale 1:24,000.

Sears, J.W., 2006, The Montana transform: Rotation along the northern boundary of the Wyoming foreland: Rocky Mountain Geology, v. 42, p. 65-76.

See photo, next page.

This is a view of the northwest wall of Trout Creek Canyon in the Big Belt Mountains. Shown in the view are faulted and folded beds of Mission Canyon Limestone and Lodgepole Limestone. Both are formations in the Madison Group. Trout Creek Canyon is oriented southwest-northeast and is located in the southeast quadrant of the Hogback Mountain 7 ½' Quadrangle (Sec. 20, T12N, R1E). View is to the north.

A STUDY OF THE STRUCTURE IN THE NORTHWESTERN MONTANA OVERTHRUST BELT USING SIDE-LOOKING AIRBORNE RADAR IMAGERY

D. H. Vice
Penn State Hazleton, 76 University Dr., Hazleton, PA 18202

Abstract

A remote sensing study of Northwestern Montana using side-looking airborne radar (SLAR) found five complex regional fault systems. The Pinkam-Dunsire system occurs on the west side of the Rocky Mountain trench while the Whitefish system occurs on the east side of the trench. There is some controversy in the literature over the subsurface structure of Rocky Mountain Trench. The Hog Heaven mining district is associated with the Pinkham-Dunsire system. A TIR survey of the Hog Heaven mining district did not find any geothermal activity.

Introduction

The Montana Overthrust Belt is part of a zone of eastward-directed thrusting that extends from Alaska to Mexico. The area was initially thought to consist of a narrow, structurally complex zone separating the Rocky Mountains from the plains (Erdmann, 1963). However, detailed mapping of much of Northwestern Montana indicates that the thrust and fold belt is much wider and includes most of the northwestern part of the state. The study area is bounded on the North by the Canadian border, on the West by the Idaho border, on the South by the Lewis and Clark Line, and on the East by the Montana plains. Much of this area has a heavy conifer forest cover.

Northwestern Montana is thought to have oil and natural gas potential because of the occurrence of oil and natural gas production in areas with a similar geology in Alberta (Erdmann, 1963) and in Western Wyoming and Eastern Utah.

Geologic mapping by Johns (1959 and 1970) and a remote sensing study of NW Montana using side-looking airborne radar (SLAR) imagery (Vice, 1984) suggests that five complex regional fault systems occur in the area. There is some debate about the subsurface structure underlying Northwestern Montana. Moulton (1984) shows a series of thin thrust sheets underlying Northwest Montana in two cross-sections he has drawn across northern Idaho to the Rocky Mountain Trench area of Northwestern Montana. Sears (2000) proposes that a massive thrust slab, the Lewis-Eldorado-Hoadley structure was emplaced during the Laramide orogeny adjacent to the disturbed belt and underlies most of the thrust structures to the west. He also suggests that eastward rotation has occurred with the north-

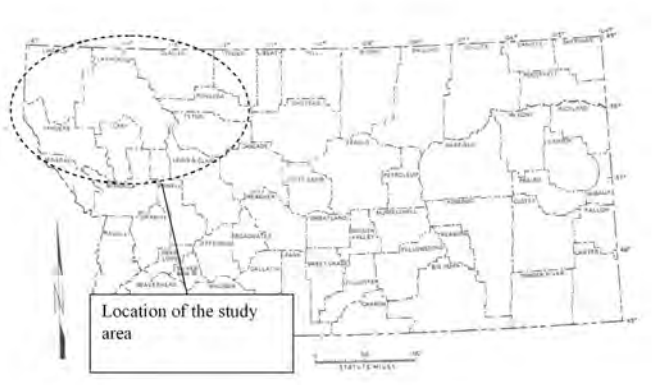

Figure 1. General location of SLAR imagery coverage.

ern part around Flathead Lake having rotated approximately 25°. Constenius (1996) suggests that thrusting ended in early to middle Eocene and extension caused by a change in the North America-Pacific plate convergence rate started in early Middle Eocene.

This paper is an update and expansion of part of a SLAR study of Northwestern Montana that was conducted for a client during the 1980s and on some work the author did for Burlington Northern. This paper concentrates on the Rocky Mountain Trench and some of the fault systems related to it.

Explanation of Side-Looking Airborne Radar

Side-looking airborne radar (SLAR) is an active remote sensing system because it provides its own source of energy, i.e., it sends out electromagnetic energy and then detects this energy as it has been reflected back by the terrain (Sabins, 1997). The advantage of an active system such as SLAR is that it can see through cloud cover or a heavy vegetative cover similar to the conifer forest of Northwest Montana to show topographic features that indicate the underlying structure.

The SLAR imagery of Northwestern Montana was obtained by the Seattle district of the U. S. Army Corps of Engineers in 1974. The survey was flown in a north-south direction and the SLAR strips were assembled into a mosaic. This imagery is printed out in shades of gray (Fig. 2) and can be interpreted visually similar to black-and-white air photos where tone (i.e., shades of gray) and landforms are used (Sabins, 1997). The SLAR imagery can be obtained from the Seattle district of the Army Corps of Engineers.

One problem with SLAR is that when a fault or structure parallels the topographic trend in an area of moderate to high relief, it may be masked by the radar shadow. An example of this masking is the Snowshoe fault on the east side of the Cabinet Mountains (Vice, 1984). However, the general north-northwest trend of the mountains in the study area indicates that most of the structures occur at oblique angles to the flight direction; therefore, most of the structures present in the study area should be readily seen in the SLAR imagery.

Fault structures are indicated by topographic features, e.g., the alignment of two or more stream drainages across the top of a ridge (or across a valley), straight stream segments, sharp changes in stream direction, saddles in ridgelines, or some combination of these and other landforms.

Description of Fault Systems

Five north- to north-northwest trending thrust faults systems are visible as a series of lineaments within the radar imagery. These thrust fault systems appear to consist of many separate faults that are related. The individual systems are: (1) the Leonia-Pine Creek system near Troy, (2) the Pipe Creek-Thompson Lakes system through Libby and the Thompson Lakes, (3) the Pinkham system on the west side of the Rocky Mountain trench, (3) the Whitefish system on the east side of the Rocky Mountain trench, and (5) the Tuchuck system on the east side of the Whitefish Range. A sixth system, the west-northwest striking Hope fault system occurs in the extreme southwestern part of the study area and is not described.

Sears (2000) suggests that Northwest Montana underwent compression when a massive slab, the Lewis-Eldorado-Hoadley structure was thrust eastward during the

Figure 2. Raw SLAR imagery (West Look). North-South flight lines.

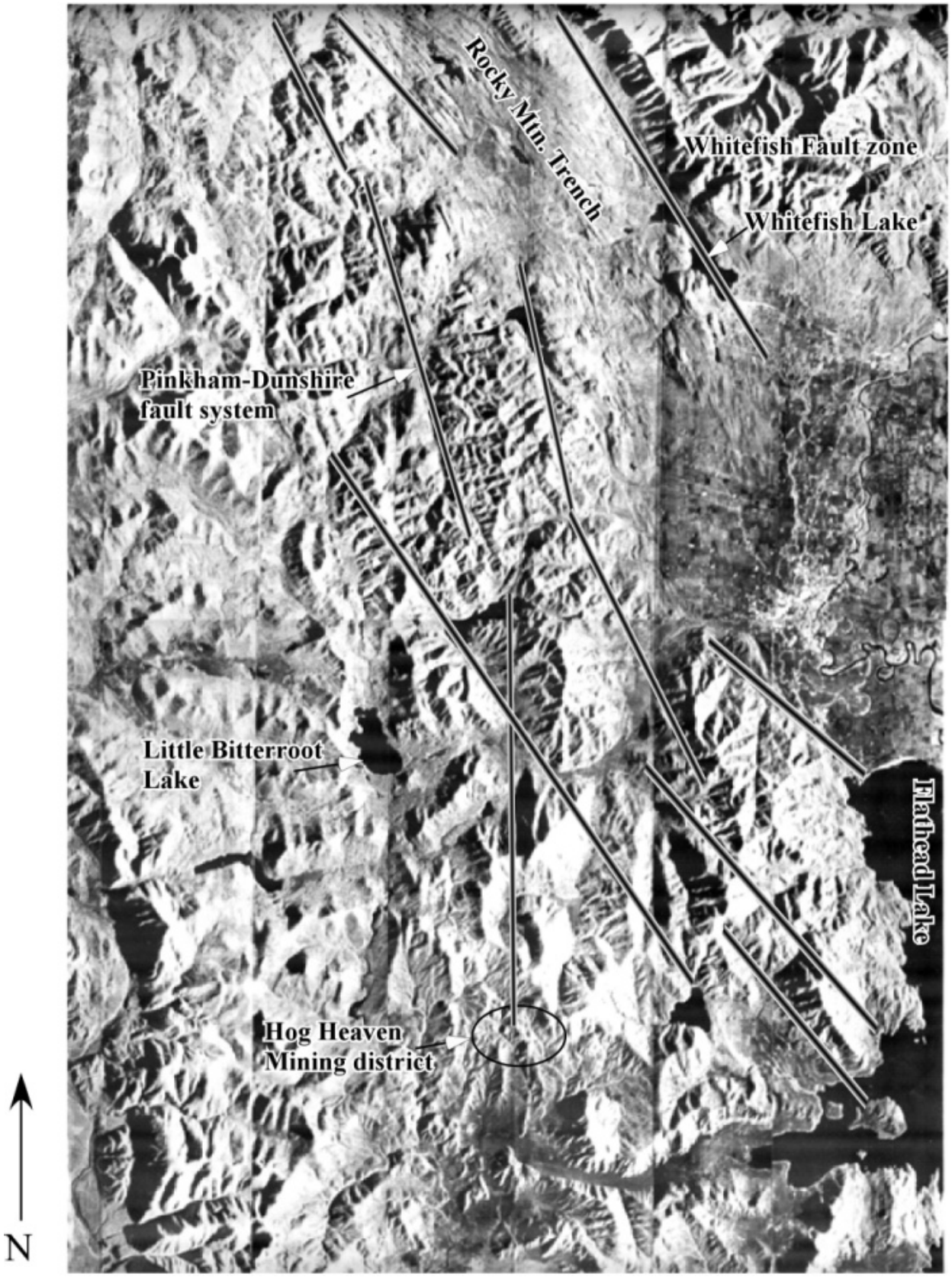

Figure 3. Interpretation of SLAR imagery.

Laramide orogeny. He also suggests that the region then underwent a period of normal faulting after the thrusting ceased. This fits with the occurrence of both thrust faults and normal faults in the area. Some faults, e.g., the Bull Lake fault within the Leonia-Pine Creek fault system, appear to have had a period of thrusting which was followed by a period of normal faulting.

Lorenz (1984) suggests that the Lewis and Clark Line acted as a shear zone during the compressive regime of the Laramide orogeny. North of the Lewis and Clark Line, accommodation of the compressive forces was by thrusting with as much as 160 km (100 miles) of crustal shortening (Lorenz, 1984).

Rocky Mountain Trench.--Portions of the Rocky Mountain trench are included in the study area. The trench is a complex, north-northwest trending structural depression in the main part of the Rocky Mountains. In the SLAR imagery it is a topographic depression characterized by numerous drumlins and other glacial features.

However, some regional geophysical studies suggest that this structure is more complex that it's topographic expression. For example, a geophysical study by Crosby (1984) suggests that the Swan Valley is a half graben and is a branch of the Rocky Mountain trench. Differences in two regional geophysical studies suggest that there is some controversy over the subsurface structure. A regional cross-section by Boberg et al. (1989) shows the Rocky Mountain trench as a graben between the Whitefish fault and the Wigwam thrust. Yoos et al. (1991) show seismic lines across the trench with strata in the subsurface of the trench dipping to the east. Yoos et al. (1991) show the trench terminating against the Stryker fault on the east side.

Leonia-Pine Creek System—The Leonia-Pine Creek system of faults is the westernmost and includes the Leonia, Pine Creek (or O'Brian Creek), Savage Lake and Bull Lake faults. Several unnamed structures are also present. This system extends from the Idaho panhandle through the southwestern corner of the study area near Troy. It appears to terminate at the Hope fault system (Marvin et al., 1984).

Movement along the faults is complex and appears to be contradictory. Some faults, such as the Leonia, are described as high-angle thrusts (Johns, 1970); other major structures, e.g., the Pine Creek and Savage Lake faults, have been mapped as normal faults with the strata on the west downthrown (Johns, 1970). Johns (1970, p. 62-63) states that the Bull Lake fault originally may have been a thrust fault based on a wide zone of shearing and brecciation. However, renewed movement along the fault zone has been normal with the strata on the west side being down.

One possible explanation is that two or more periods of movement has occurred on many of the individual faults within the Leonia-Pine Creek system. The initial period of movement may have been thrusting in response to compression caused by the formation of an Andean type of arc in the area of the Nelson and Kanisku batholiths during the Laramide orogeny. Sears (2000) has suggested that a massive slab was thrust eastward during the Laramide orogeny. Later movement along the fault planes occurred as normal faulting with the west side down as an extensive tectonic regime developed (Burchfiel, 1981). Constenius (1996) suggests that the extensive tectonic regime is due to extensional collapse of the foreland fold and thrust belt. The change in tectonic regimes was associated with a change in direction of movement of the North American plate (Burchfiel, 1981) and the break-up of

the Juan de Fuca plate about 40 to 50 million years ago. A westward jump in the subduction zone to its present position occurred at about the same time. The Cascade Mountains started forming after the jump in the subduction zone.

Thompson Lakes-Pipe Creek System—The Thompson Lakes-Pipe Creek system includes the Thompson Lakes, Poole Lake, Pipe Creek, and Rainy Creek faults (Johns, 1959 and 1970). The SLAR imagery shows several unnamed branches and subsidiary structures. The Quartz Creek fault may also be part of this system; the radar imagery suggests that this fault merges with the Thompson Lakes system. The west-look SLAR imagery also suggests that the Snowshoe fault is part of the Quartz Creek structure. The structure extends from the Clark Fork River near Plains north-northwest to the Canadian border near Mt. Obermeyer and the town of Yaak.

The direction of movement on many of the faults within the Thompson Lakes system is uncertain in that both normal and reverse faults are present. For example the Thompson Lakes fault is normal and is downthrown on the west side (Johns, 1970). However, the Rainy Creek fault, which is a branch of the Thompson Lakes fault, is a high angle reverse structure. As with the Leonia-Pine Creek system, two separate periods of movement has occurred on this system (Sears, 2000). Constenius (1996) suggests that the extensive tectonic regime is due to extensional collapse of the foreland fold and thrust belt.

The relationship between the Thompson Lakes system and the Lewis and Clark Line (Montana Lineament) is uncertain. Several of the thrust faults in the Thompson Lakes system appear to terminate at the first northwest-trending structure that is part of the Lewis and Clark Line (Montana Lineament) (Marvin and Others, 1984) suggesting that the latter structure is dominant. However, other lineaments within the Thompson Lakes system appear to merge with structures in the Lewis and Clark Line between Plains and Moiese.

Pinkham-Dunsire System—The Pinkham-Dunsire thrust system occurs along the west side of the Rocky Mountain trench. Johns (1970) describes it as extending from the Little Bitterroot Lake to the Canadian Border. The Pinkham system occurs as a broad zone with multiple branches in the SLAR imagery (Fig. 3). Lineaments in the SLAR imagery extend the system southward to the Hog Heaven mining district and the Lake Mary Ronan area (Vice, 1984).

Data presented by Johns (1970) suggest that both the Pinkham and the Dunsire faults are high-angle reverse structures. Data from the ARCO/Marathon No. 1 Paul Gibbs well shows that the Pinkham thrust duplex consists of sheared and imbricated quartzites and diabase intrusive sills (Boberg et al., 1989). Post-well structural interpretation suggests that east of the No. 1. Paul Gibbs well, the Pinkham thrust splits into several high-angle thrust faults. Several lower Prichard gabbro or diabase sills are present throughout the sequence of Prichard rocks penetrated by the well and these igneous sills had affected the interpretation of the seismic data (Boberg et al., 1989).

Hog Heaven Mining District.--The Hog Heaven mining district is a small lead and precious metal district associated with a late Laramide volcanic complex that is located mainly in Sections 8, 16, 17, 20, 21, and 30, T. 25 N., R. 23 W.

The volcanic complex consists of a sequence of rhyodacite and porphyritic trachyandesite flows and ignimbrites, which is capped by the

Battle Butte latite and some trachyandesite flows (McAleer, 1971). The volcanics sit on Precambrian Belt sediments. The volcanic complex has been dated at 30.8 ± 2.4 million years old (Daniel and Berg, 1981).

BN had explored the area for geothermal energy because of the presence of the volcanics and its large block of land ownership in the area. During the exploration, several factors indicated that there was very little geothermal potential. One factor was the Mid-Tertiary age of the volcanics which suggested that little heat remained in the system (Duffield and Sass, 2003). A thermal infrared (TIR) survey was conducted over the area and found no indication of thermal springs or warm ground (Vice, 1978). The TIR imagery show some light gray spots indicating warm water but this is probably ground water coming to the surface. Geochemical data from surface springs in the area found slightly anomalous concentrations of Fluorine, Lithium, and Boron, which could be due to geothermal activity but could also be due to the volcanic rocks (Vice, 1978). Therefore, the Hog Heaven prospect was dropped because of the lack of significant indications of geothermal activity (Vice, 1978).

This volcanic complex is the only one associated with the thrust systems in Northwestern Montana and is somewhat of an enigma.

Whitefish System—The Whitefish fault system occurs on the east side of the Rocky Mountain Trench. This structure is described by Johns (1970) as extending from the Olney area to the Dickey Lake-Fortine area. However, lineaments visible in the SLAR imagery indicate that this structure and related structures extend to the town of Whitefish on the southeast and to the Canadian Border on the north-northwest (Vice, 1984). The SLAR imagery shows that several branches of the structure occur in the area between upper Whitefish Lake and Dickey Lake and in other areas (Vice, 1984).

As noted above, Boberg et al. (1989) shows the Whitefish fault on the west side of the Rocky Mountain trench and the Swan fault on the east side of the trench in their cross-section.

Data presented by Johns (1970) indicates that one part of the Whitefish system, the Stryker fault is normal, i.e., the west side is downthrown, which is consistent with seismic data showing that the system is a listric normal fault. Yoos et al. (1991) show both the Stryker and the Whitefish faults as downthrown on the west side.

Tuchuck System—The Tuchuck system occurs in the eastern part of the Whitefish Range and extends into the northern part of the Flathead Range. According to Johns (1970), this system can be extended from the northern part of the Flathead Range northward to the Canadian Border. The SLAR imagery suggests that several branches and subsidiary faults exist, particularly from Polebridge to the Canadian Border (Vice, 1984).

Johns (1970) suggests that the Tuchuck structure is a high-angle thrust fault. However, fault dips and stratigraphic displacements vary at different locations along the fault system, suggesting that it is a complex structure.

The SLAR imagery shows several northeast-trending lineaments in the Whitefish Range that are locally discontinuous and offset the Tuchuck fault, suggesting that differential movement has occurred on individual segments of the Tuchuck system (Vice, 1984).

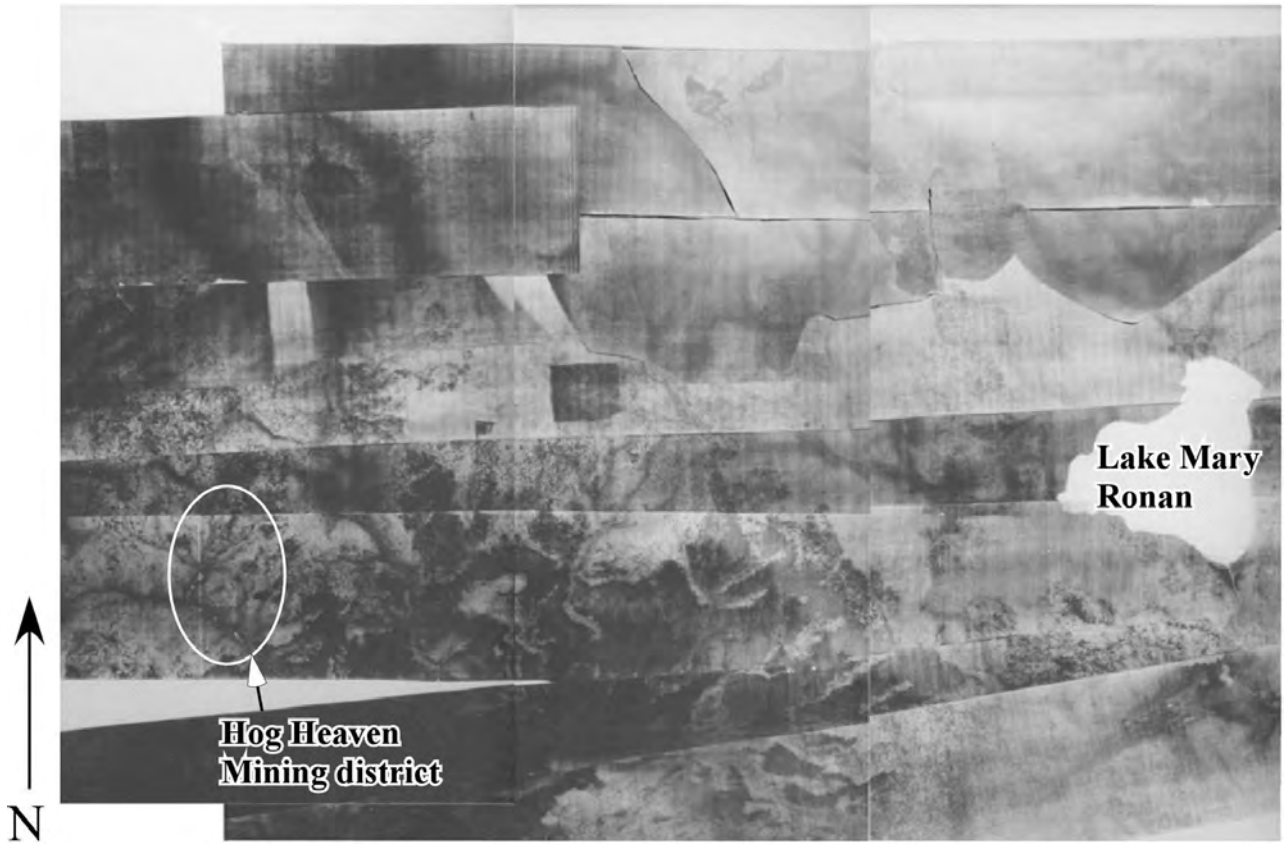

Figure 4. Thermal infrared imagery covering the Hog Heaven mining district and Lake Mary Ronan area. East-West flight directions. The thermal infrared scanner (Daedalus model 1210) recorded the data electronically and converted it to strips of grey-scale imagery that approximates a scale of 1:62,500. The TIR strips were assembled into the mosaic shown in figure 4. The survey was flown in the fall of 1976 at an elevation between 5000 and 6000 feet (Crowley Environmental & Planning Associates, Inc., 1982). The TIR imagery will be sent to the Montana Bureau of Mines and Geology where it will be made available to the public.

Summary and Conclusions

The structure of Northwestern Montana is complex. Five north- to north northwest-trending fault systems are visible in the SLAR imagery of Northwestern Montana. Johns (1970), Harrison and Others (1983) and other workers have mapped and located many of these major structures. However, the SLAR imagery suggests that each system contains many subsidiary and parallel structures suggesting that they are more complex than previously realized.

Data presented by Johns (1970) show that some of the faults are thrust systems and others are normal faults. Some of the faults, e.g., the Bull Lake fault, have had a complex history with an earlier period of thrusting followed by a later period of normal movement and block faulting. This change in type of faulting is consistent with the suggestion by Sears (2000) that the late Mesozoic and the Cenozoic tectonic history of Northwestern Montana underwent a compressive regime during the Laramide orogeny but changed to an extensive tectonic regime and erosion from Mid-Tertiary to the present. Constenius (1996) suggests that the extensive tectonic regime is due extensional collapse of the foreland fold and thrust belt.

Two different interpretations of the subsurface structure of the Rocky Mountain Trench based on regional seismic data are present in the literature. Boberg et al. (1989) shows the Whitefish fault on the west side of the Rocky Mountain Trench and the Wigwam thrust on the east side. However, Yoos et al. (1991) shows the Pinkham fault system on the west side of the trench and the Stryker fault on the east side.

Acknowledgements

The author wishes to thank a number of people for assistance in help in scanning the SLAR imagery and inserting it into this paper and in reviewing it, including Barbara Brazon. The author wishes to thank Lee Muroski and Larry Smith for reviewing this paper and making several useful suggestions.

The author wishes to thank Cenex and Burlington Northern for permission to use their data in this paper. These companies, Cenex and Burlington Resources, Inc., the successor to the minerals branch of Burlington Northern, have not participated in this study and do not endorse any views, statements, or conclusions made by the author.

References

Boberg, W.W., Frodesen, E.W., Lindecke, J.W., Hendrick, S.J., Rawson, R.R., and Spearing, D.R., 1989, Stratigraphy and tectonics of the Belt Basin of Western Montana: Evidence from the ARCO/Marathon No. 1 Paul Gibbs well, Flathead County: *in* French, D.E., and Grabb, R.F., eds., Geologic Resources of Montana: Montana Geological Society, 1989 Field Conference Guidebook: Montana Centennial Edition, vol. 1, p. 217-229.

Burchfiel, B.C., 1981, Structural evolution of Western North America and tectonics of marginal fold and thrust belts: Syllabus for AAPG continuing education course, Billings, Montana, February 27th.

Constenius, K.N., 1996, Late Paleogene extensional collapse of the Cordilleran foreland fold and thrust belt: Geological Society of America Bulletin, v. 108, p. 20-39.

Crosby, G.W., 1984, Structural-geophysical interpretation of Swan Valley, Montana: *in* McBane, J. Duncan, and Garrison, P. B., eds., Northwest Montana and Adjacent Canada: Montana Geological Society 1984 Field Conference and Symposium, p. 245-251.

Crowley Environmental & Planning Associates, Inc., 1982, Review of the BN-Meridian geothermal remote sensing program: Unpublished report

prepared for Meridian Land & Mineral Co., October, 26 p. plus 2 appendices.

Daniel, Faith, and Berg, R.B., 1981, Radiometric dates of rocks: Montana Bureau of Mines and Geology, Bulletin 114.

Duffield, W.A., and Sass, J.H., 2003, Geothermal energy-clean power from the Earth's heat: U.S. Geological Survey, Circular 1249, 36 p.

Erdmann, C.E., 1963, Petroleum: *in* Mineral and Water Resources of Montana: U.S. Senate Committee on Interior and Insular Affairs, Montana Bur. of Mines and Geology, Special Publication 28, p. 33-39.

Johns, W.M., 1970, Geology and mineral deposits of Lincoln and Flathead Counties, Montana: Montana Bur. of Mines and Geology, Bulletin 79.

Johns, W.M., 1959, Progress report on geologic investigations in the Kootenai-Flathead area, Northwest Montana: Montana Bur. of Mines and Geology, Bull. 12.

Lorenz, J.C., 1984, The function of the Lewis and Clark fault system during the Laramide orogeny: *in* McBane, J. Duncan, and Garrison, P.B., eds., Northwest Montana and Adjacent Canada: Montana Geological Society 1984 Field Conference and Symposium, p. 221-230.

Marvin, R.F., Zartman, R.E., Obradovich, J.D., and Harrison, J.E., 1984, Geochronometric and lead isotope data on samples from the Wallace 1˚ x 2˚ Quadrangle, Montana and Idaho: U.S. Geol. Survey Miscellaneous Field Studies Map MF-1354G.

McAleer, J.F., 1971, Geology map Hog Heaven mining district: Unpublished map of the Anaconda Company.

Moulton, Floyd, 1984, Oil and gas possibilities under the Precambrian Belt multiple thrust complex of Northwestern Montana and Northern Idaho: *in* McBane, J. Duncan, and Garrison, P.B., eds., Northwest Montana and Adjacent Canada: Montana Geological Society 1984 Field Conference and Symposium, p. 259-261.

Reynolds, M.W., 1979, Character and extent of basin-range faulting, Western Montana and East-Central Idaho: *in* Newman, G.W., and Goode, H.D., eds., Basin and Range Symposium: Rocky Mountain Association of Geologists and Utah Geological Association, p. 185-193.

Sabins, F.F., 1997, Remote Sensing: Principles and Interpretation: W. H. Freeman and Company, New York, Third Edition, 494 p.

Sears, J.W., 2000, Rotational kinematics of the Rocky Mountain thrust belt of Northern Montana: *in* Shalla, R.A., and Johnson, E.H., eds., Montana/Alberta thrust belt and adjacent foreland: Montana Geological Society, 50th Anniversary Symposium, p. 143-149.

Vice, D.H., 1984, A study of side-looking airborne radar imagery of Northwest Montana: Unpublished report prepared for Cenex, 9 p. plus maps.

Vice, D.H., 1978, A summary of the Hog Heaven geothermal prospect: Unpublished Burlington Northern memorandum to Mr. C.W. Jordan, March 2, 2 p.

Woodward, L.A., 1983, Structural geology of the Helena salient: A synopsis: *in* Smith, D.L., compiler, Guidebook of the fold and thrust belt, West-Central Montana: Montana Bur. of Mines and Geology, Special Publication 86, 98 p.

Witkind, I.J., 1977, Major active faults and seismicity in and near the Big Fork-Avon area, Missoula-Kalispell Region, Northwestern Montana: U.S. Geological Survey Miscellaneous Field Studies Map MF-923.

Yoos, T.R., Potter, C.J., Thigpen, J.L., and Brown, L.D., 1991, The Cordilleran foreland thrust belt in Northwestern Montana and Northern Idaho from COCORP and industry seismic reflection data: AAPG Bull., v. 75, no. 6, p.1089-1106.

A CASE FOR POST-100 MA FAULT BLOCK TILTING OF A CRETACEOUS LACCOLITH, BONNER COUNTY, IDAHO

Russell F. Burmester
Geology Department, Western Washington University, Bellingham, WA 98225
russb@wwu.edu

Reed S. Lewis
Idaho Geological Survey, University of Idaho, Moscow, ID 83844-3014
reedl@uidaho.edu

Abstract

East of the Purcell Trench in northern Idaho, most rocks of the Belt-Purcell Supergroup and rare overlying Cambrian strata dip east and are repeated across steep faults. Within the Cambrian strata are intrusions of granodiorite in at least three separate fault blocks. We propose that they are related as fault-repeated segments of a broad sill or laccolith, and use paleomagnetic methods to demonstrate that the faulting and tilt postdated intrusion. The most likely time for this deformation was during Eocene extension.

Introduction

Most layered rocks east of the Purcell Trench dip eastward. Northeast of Sandpoint these include the Eocene Sandpoint Conglomerate (Doughty and Price, 2000; Lewis et al., 2007), demonstrating that, at least there, some of the tilt was Eocene or later. Southeast of Sandpoint, however, the youngest layered rocks are Cambrian (fig. 1), which provides little constraint on when they were tilted. Cretaceous intrusions exposed in the area provide a possible constraint. Elsewhere, paleomagnetism has been used on plutons to document post-intrusion tilting (e.g., Marquis and Irving, 1990). Perhaps more interesting is the possible genetic relationship between these Cambrian-hosted igneous bodies. Of special interest are the granodiorite porphyry of Packsaddle Mountain and the granodiorite of Whiskey Rock (both Kgdp, fig. 1). Note that the northern exposures along the eastern shore labeled as Khgd were formerly part of the granodiorite of Whiskey Rock (Miller et al., 1999) but are not included here because only Kgdp is porphyritic. West of the lake, the Salee Creek pluton (Khgd in the southwest; Miller et al., 1999; Burmester et al., 2007) is coarser and not porphyritic. Yet all have hornblende in addition to biotite, narrow contact aureoles, and at least partial roofs of Cambrian Lakeview Limestone. The body across Packsaddle Mountain appears to be a sill or laccolith entirely within the Cambrian section with a floor of Rennie Shale (Lewis et al., 2008; IGS unpublished mapping of Minerva Peak and Packsaddle Mountain quadrangles). Previous mapping depicted these bodies as separate plutons (Harrison and Jobin, 1965) but we propose that they were a single laccolith or fat sill before being broken into separate tilted fault blocks.

The work undertaken here was to evaluate the tilted-sill hypothesis by measuring magnetic susceptibility and remanent magnetization. Results of these measurements can be used to test the hypothesis that the rocks were intruded parallel to horizontal contacts before they and the enclosing layered rocks were tilted (fig. 2). The Packsaddle Mountain exposure proved unsuitable for

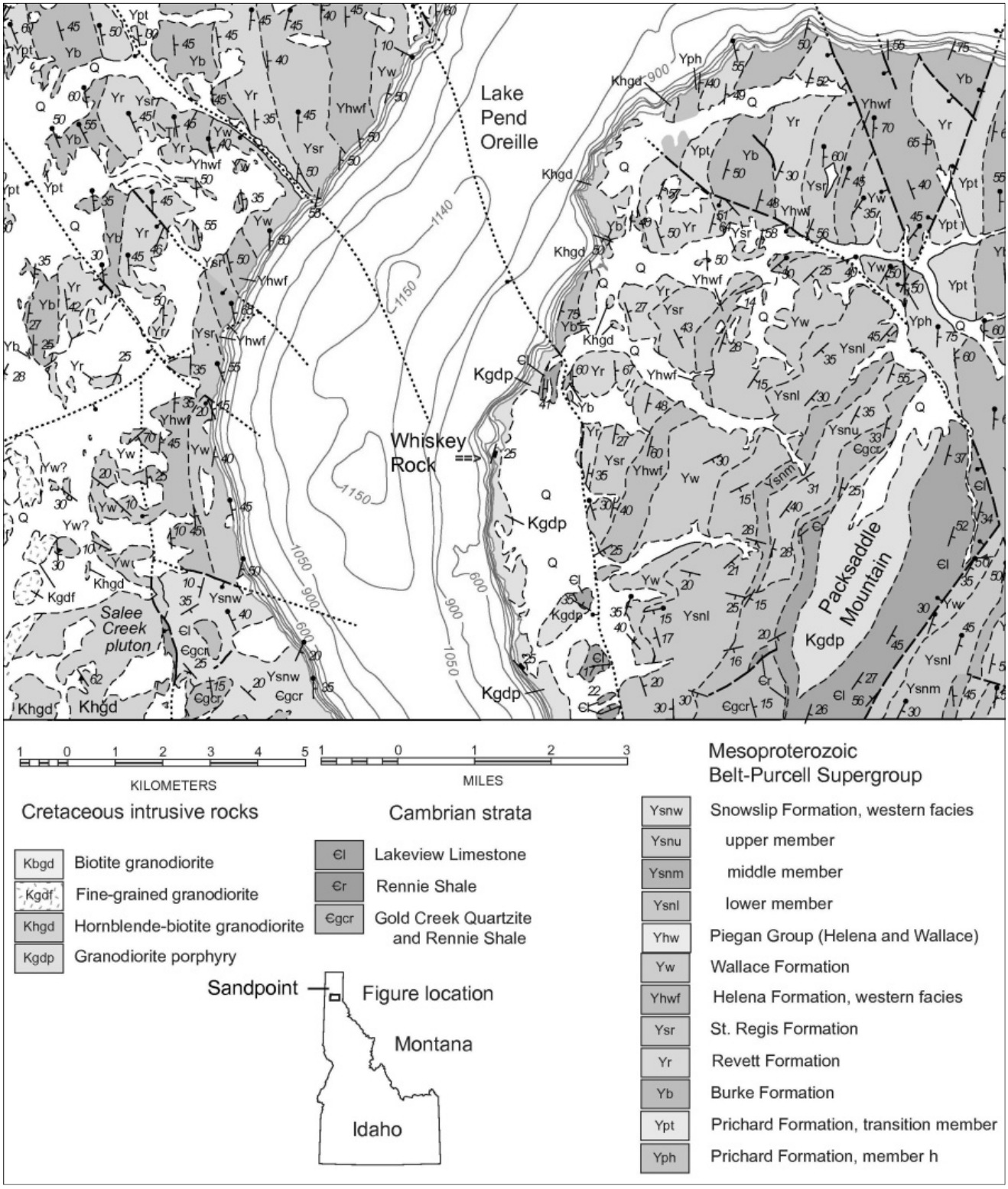

Figure 1: Geologic map across part of Lake Pend Orielle, Idhao, adapted from Lewis et al. (2008). Down to the southwest normal faults repeat the Cambrian section and intrusions within Kgdp of Packsaddle Mountain and Whiskey Rock, and Khgd of Salee Creek pluton that are interpreted to have been a single fat sill or laccolith before block faulting and tilting. Paleomagnetic results and age control are from Whiskey Rock.

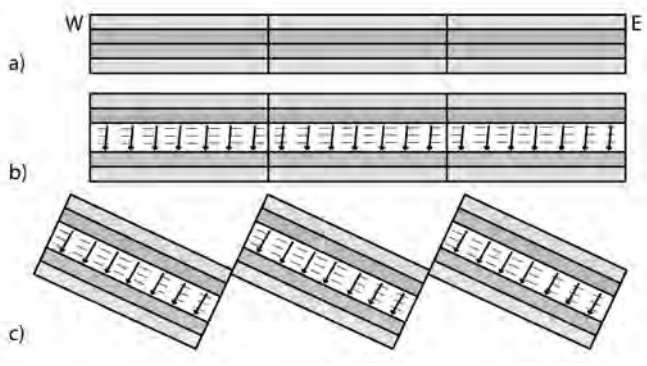

Figure 2: Cartoon of hypothesized history of the area, viewed north. a) Horizontal basal Cambrian strata unconformably on Snowslip Formation (bottom layer). b) Intrusion of magma as a sill in the Cambrian (dark) strata, and magnetization upon cooling below 580°C at 100 Ma. Arrows depict steeply down magnetization consistent with the Cretaceous magnetic field at this location; dashed lines represent flow fabric. c) Block faulting and tilt to the east that shallows the magnetization, and extends this crust westward.

paleomagnetic sampling because the only rocks reasonably in place are at the peak where there is a high likelihood of lightning strike remagnetization. Samples of the Salee Creek pluton did not retain a useful remanent magnetization, probably due to slow cooling and deep weathering. Rocks along the east shore of Lake Pend Orielle are suitable, but the only location with road access is Whiskey Rock State Park. Sampling was less extensive than desired, but the results prove to be useful if not robust for this test. Furthermore, a sample from the same location yielded a weighted $^{206}Pb/^{238}U$ age from laser ablation inductively coupled plasma mass spectrometry (LA-ICPMS) of 100.1 ± 1.3 Ma (Richard Gaschnig, written communication, 2009). The fine-grained groundmass of the porphyry suggests rapid cooling and retention of useful remanent magnetization of that age.

Methods

Fairly standard methods were used throughout. These include collecting oriented samples of joint blocks spanning about 8 m (25 feet) of shoreline, coring those blocks in the lab and cutting cores into specimens using nonmagnetic core barrel and saw blade. Specimens were measured on an AGICO KLY-3A spinning susceptometer to allow calculation of anisotropy of magnetic susceptibility (AMS). Calculation used bootams.exe and plotams.exe from Tauxe (1998). Hysteresis parameters and Curie temperature for the magnetic minerals were measured on a Princeton Measurements Corporation Model 3900 vibrating sample magnetometer. Remanent magnetization was measured with a 2-G 755R DC-SQUID magnetometer. Demagnetization started with low temperature treatment in liquid nitrogen in a low magnetic field environment to reduce the contribution from large magnetite grains (e.g., Housen et al., 2003). Subsequent thermal demagnetization used an ASC TD-48SC oven with an argon atmosphere to retard oxidation of grains on specimen surfaces. Analysis of remanence used visual examination of demagnetization paths on orthogonal projections (Zijderveld, 1967), principal component analysis (PCA, Kirschvink, 1980) for least-squares line and plane fitting, and boot_di.exe, plot_di.exe and lnp.exe programs (Tauxe, 1998) to calculate and plot mean directions. Many of these programs rely on bootstrap methods (Tauxe et al., 1991), which allow statistical testing of paleomagnetic data that are not Fisherian (Fisher, 1953) distributed. The low number samples in this study preclude testing for Fisher distribution. Traditional tests using Fisher parameters were not employed because their use on non-Fisherian distributions could lead to erroneous conclusions. Reference directions are fairly straightforward. The age of the rock sampled falls within a period of little apparent polar wander for North America (130-90 Ma; Beck and Housen, 2003) and within the Creta-

ceous Superchron (C34, 118-83 Ma; Gradstein et al., 1994) when the magnetic field polarity was constant and normal.

Results

Magnetic Susceptibility

Susceptibility maximum, intermediate, and minimum axes are shown in Figure 3 as squares, triangles, and circles, respectively. Susceptibility minima are well clustered 25° west of vertically down (270.2°, 64.8°) while the maxima are north-northeast as part of a magnetic foliation girdle with strike and dip of 0.2° and 25.2°. This pattern is consistent with emplacement between floor and roof rocks dipping 25° east, or into flat-lying strata that were later tilted 25° east. Comparison with attitudes of enclosing strata is not straightforward. The best choice might be from the Gold Creek Quartzite underlying the intrusion northwest of Packsaddle Mountain. The mean of seven attitudes (from Harrison and Jobin, 1965) has strike and dip of 18° and 25.6°, close to the attitude of the magnetic foliation. The steeper attitudes from fewer observations in roof rocks of Lakeview Limestone north of Whiskey Rock State Park (approximately 46°) and northeast of Packsaddle Mountain (about 39°) could be due to bulging above the intrusion, consistent with it being a laccolith. Attitudes of both Paleozoic and Mesoproterozoic strata farther south are too varied to help define a regional attitude.

Rock Magnetism

The narrow hysteresis loop and low coercivity of remanence of a typical sample (fig. 4) are typical of multidomain magnetite. Relatively high saturation magnetization and the ratio of saturation remanence to it, however, suggest presence of 5-10% single domain grains with shape anisotropy (Dunlop, 2002). The single inflection in the smooth heating and cooling curves (fig. 5) is consistent with magnetite being the only magnetic mineral present. The indicated Curie temperature is about 10° lower than that of a pure magnetite standard run subsequently to check the thermocouple calibration. This lower temperature can be explained by replacing of a few percent of the iron in the magnetite lattice by titanium. Similarity of shapes of the two curves demonstrates that there was no major change to the magnetite when heated in inert helium atmosphere. Therefore, it is expected that thermal demagnetization in a similarly inert (argon) atmosphere would not alter the magnetite.

Remanent Magnetization

Thermal demagnetization of remanent magnetization produced clear if somewhat irregular curvilinear paths that ended with straight line segments that trend toward the origin (fig. 6). Almost half of the magnetization was removed in the first treatment with liquid nitrogen (77 K), and two thirds with 6 additional cold treatments (second 77) and heating to 105°C. This magnetization likely resided in the coarser, multidomain magnetite grains. The components of magnetization removed at low temperatures were somewhat scattered but tended to be more northerly and steeper than higher temperature components. Only above 540°C did heating reduce the magnetization without changing direction. The mean of magnetizations left after each thermal step moved progressively westward until about 520°C (Table 1; fig. 7a). The overall mean for the high temperature remanence was calculated in three ways: from the vectors removed over the interval ~520-560° C (free), over that range but with the mean vector constrained to go through the origin (anchored), and from the intersection of the planes defined by the curvilinear demagnetization paths and the origin. The coincidence

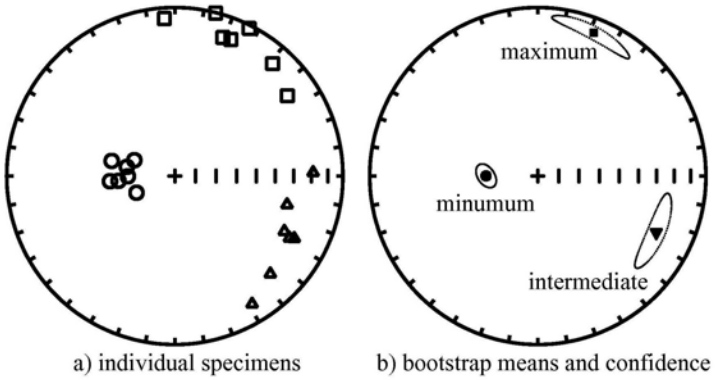

Figure 3: Equal area projections, in geographic (present) coordinates, of maximum (squares) intermediate (triangles) and minimum (circles) susceptibility axes for a) individual specimens from Whiskey Rock, and b) their bootstrap means and 95% confidence regions. Minimum near 270°, 65° (declination, inclination) is 25° from vertical. Generated using plotams.exe from Tauxe (1998).

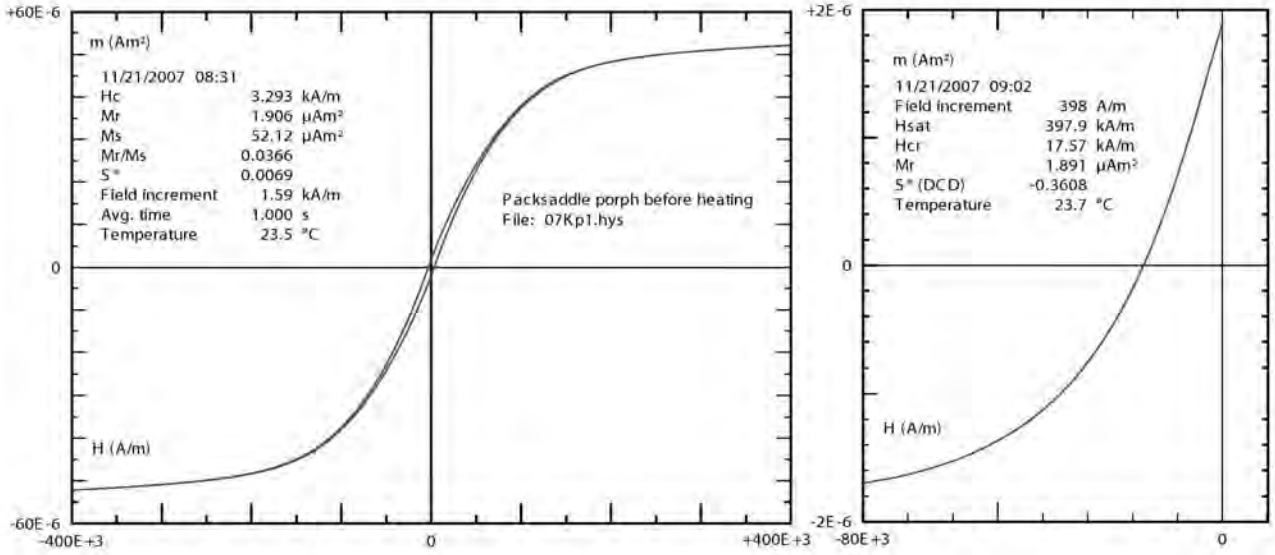

Figure 4: Hysteresis and back-field demagnetization plots. Narrow hysteresis curve suggests that coarse-grained magnetite is the dominant magnetic mineral.

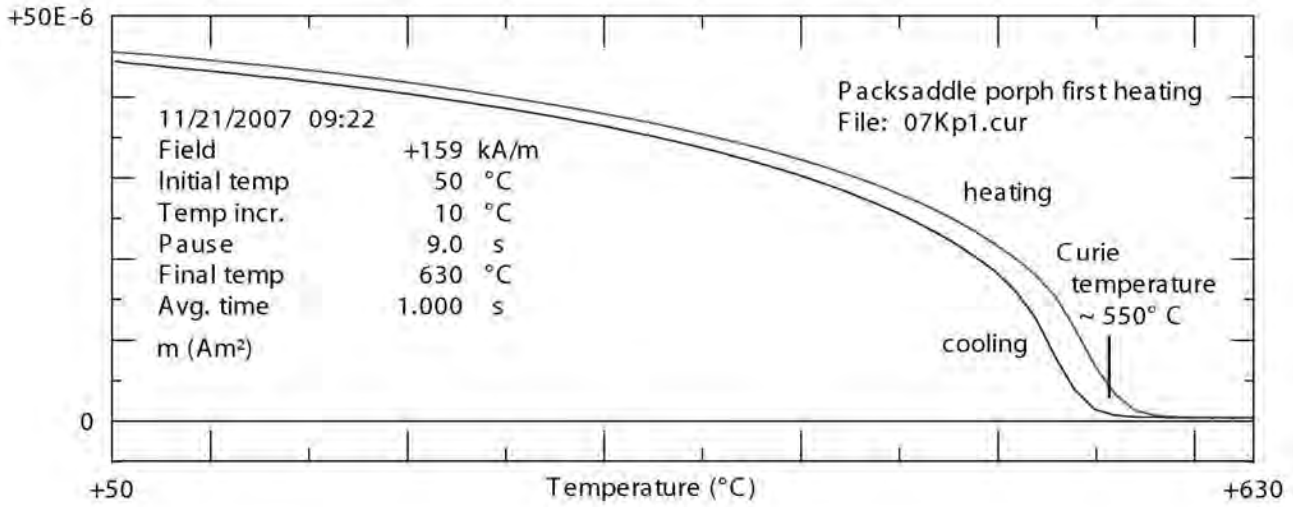

Figure 5: Change in saturation magnetization with heating and cooling. Cooling curve is displaced to the left because the temperature of the sample lags behind the temperature of the thermocouple. Shape of the curves is consistent with a single magnetic mineral, and their similarity suggests that there was no change to the magnetic mineral due to heating in the inert (helium) atmosphere. Curie temperature is about 10°C below that of a pure magnetite standard, suggesting a small content of TiO_2 (e.g., Akimoto, 1957, *in* Nagata, 1961).

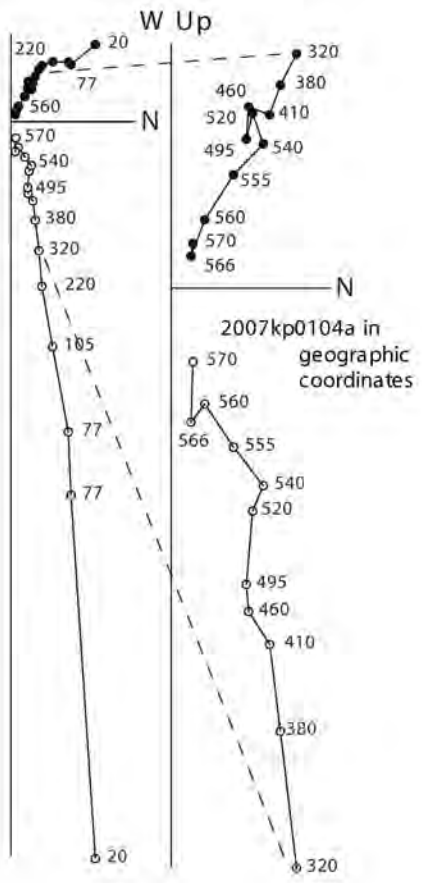

Figure 6 (left): Orthogonal projections of demagnetization path on horizontal (solid symbols) and S-N vertical plane (open symbols). Labels indicate temperature to which specimens were heated before being cooled and remanence measured. Remanence removed by treatment in liquid nitrogen (points labeled 77) probably resided in multidomain magnetite. Initial path is steeper and more northerly than later trends. High temperature path is enlarged on the right. Last segment, 540-570, trends toward the origin of the plot, consistent with it being the sole remaining magnetic component and the original magnetization.

Figure 7 (below): Equal area projections of mean directions. a) shows progressive change of measurements at individual demagnetization levels. b) compares means of free and anchored lines fit to demagnetization data spanning 520-560°C with the intersection of planes fit 520-560°C. The higher precision of the means of anchored lines makes it more useful as an estimate of the 100 Ma magnetic field. c) compares the anchored line mean direction with ones expected for Cretaceous magnetizations. The one rotated clockwise 30° posits post 100 Ma rotation of the Purcell anticlinorium (Price and Sears, 2000). The mean of anchored lines is near, but 7.5° shy of where the Cretaceous paleomagnetic field would appear in the rocks if they had only been tilted from an originally horizontal AMS fabric. If the rocks had been rotated 30° clockwise before tilting, the discrepancy is 4° but in the opposite direction. Within these uncertainties, both are consistent with intrusion of the magma into (nearly) horizontal strata forming a contact-parallel flow fabric followed by magnetization after solidification, then tilting about 19° east or rotating then tilting 27° east. The low temperature magnetization (105 in a) is an overprint probably acquired in an Eocene or later field after tilting.

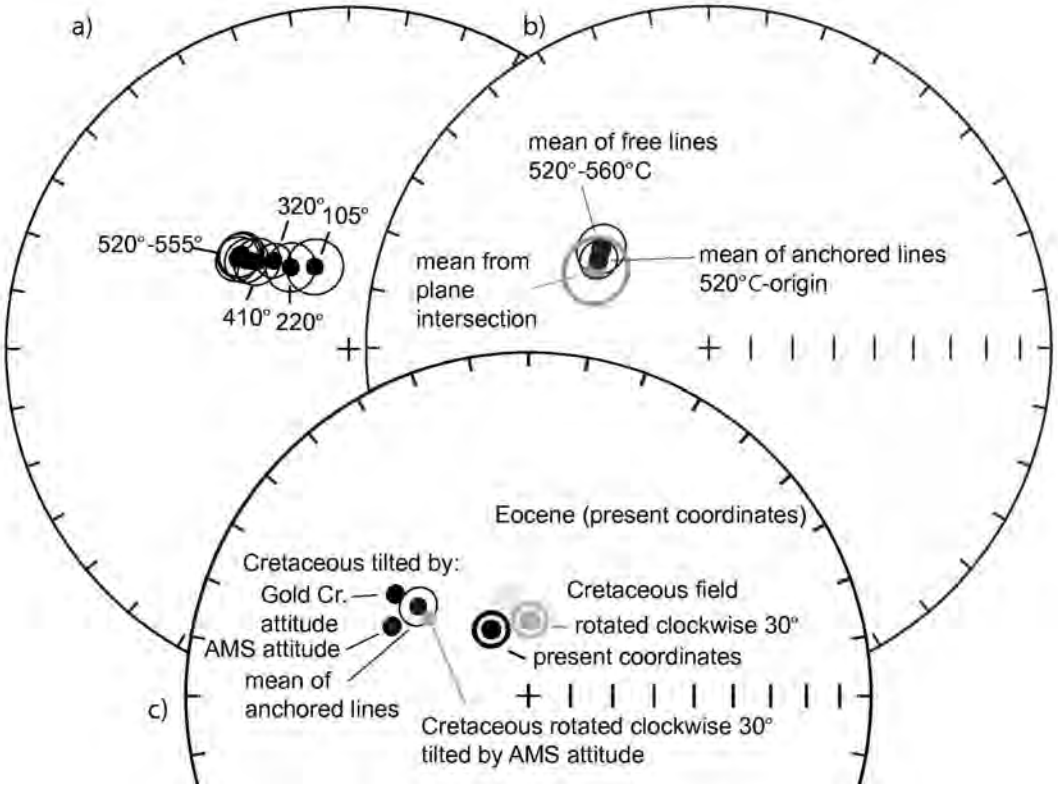

of these means (fig. 7b) suggests that they are unbiased by the low temperature component. Since the anchored mean is central and has the tightest confidence region, it is taken as the best estimate the direction of the magnetic field at 100 Ma in the intrusion's present orientation.

Interpretation

Figure 7c compares the anchored line mean direction with directions expected for Cretaceous and Eocene paleomagnetic fields. The Eocene and Cretaceous fields are close to the low temperature magnetization (105; fig 7a), which is consistent with the strong overprint being acquired in a normal polarity field in the intrusion's present orientation sometime during or after Late Cretaceous. However, the high temperature direction is much different. This difference can be explained by tilting of the magnetized rock package. Three options are shown to illustrate the Cretaceous remanence expected if the measured magnetic fabric or the average bedding of the Gold Creek Quartzite had been horizontal at 100 Ma. The mean of anchored lines is close to these, although it supports less tilt from the Cretaceous reference in present coordinates. In contrast, more tilt is implied if the rock package had rotated 30° clockwise (Price and Sears, 2000) after magnetization but before tilting.

Why is there a discrepancy between the high temperature direction and the tilt-corrected Cretaceous field direction? One explanation is that these results might not average paleomagnetic secular variation so do not record the Cretaceous axial dipole field. Another factor may be that the high temperature directions are still biased steep and east by the overprint. Also possible is that the AMS fabric was not parallel to the bounding strata. Flow along a contact tends to imbricate the magnetic fabric the same way currents in water imbricate platy cobbles in a river (Knight and Walker, 1988). But this might be small as we could guess that the maximum susceptibility direction reflects the direction of flow north-northeast or south-southwest, so east-west imbrication error would be small. It is also plausible that there was some earlier deformation such that the enclosing strata were not horizontal when intruded. About 7° tilt to the east before or during intrusion but before cooling through magnetite's Curie temperature would erase the discrepancy if there were no pre-tilting rotation. But, if there were such rotation, the discrepancy is smaller but has the opposite sense.

However these discrepancies are small potatoes; all or the bulk of the tilting was after intrusion. Restoration of these tilted fault blocks so the Cambrian strata are horizontal and continuous makes at least the Whiskey Rock and Packsaddle Mountain bodies of granodiorite contiguous, which is consistent with them and probably the Salee Creek pluton, too, being parts of a single concordant intrusion. The greater lateral extent of the fault blocks after tilting in this model (fig. 2c) than before (fig. 2b) is consistent with tilting during Eocene extension. Although results presented here only constrain tilting to post 100 Ma, the most likely time seems to be coincident with deposition and tilting of the Sandpoint Conglomerate to the north at about 47 Ma (Doughty and Price, 2000).

Acknowledgements

Field work was supported by the STATEMAP program in 2007. We express our gratitude to the Pacific Northwest Paleomagnetism Laboratory (http://pnpl.geol.wwu.edu/index.html) for use of the equipment.

Table 1. Mean and expected directions

Temperature	Lower	Upper	Dec	Inc	N	R	k	a-95
	105		337.7	68.8	7	6.944	107.0	5.9
	220		324.7	66.1	7	6.952	124.2	5.4
	320		319.7	62.2	7	6.971	204.6	4.2
	380		316.8	60.3	7	6.946	110.6	5.8
	410		313.6	59.7	7	6.962	158.1	4.8
	460		310.9	57.5	7	6.961	154.5	4.9
	495		311.8	58.2	7	6.968	188.6	4.4
	520		310.6	55.4	7	6.942	104.2	5.9
	540		311.5	55.6	7	6.939	98.1	6.1
	555		309.1	55.6	7	6.945	108.5	5.8
	560		298.4	55.5	7	6.896	57.8	8.0
	566		312.7	58.5	7	6.721	21.5	13.3
	570		290.8	71.1	7	6.286	8.4	22.1
free lines	520	570	312.7	54.8	6	5.868	37.9	11.0
anchored lines	520	570	308.9	56.1	7	6.955	131.9	5.3
planes	520	570	304.5	57.1	7	6.973	92.5	7.7
Cretaceous								
in situ			331.9	72.2	20	19.950	377.3	1.7
rotated 30°			1.9	72.2				
tilt in situ to AMS horizontal			296.8	53.3				
tilt rotated to AMS horizontal			307.8	60.1				
tilt in situ to bedding flat			307.3	49.7				
Eocene			348.6	66.0				2.8

Notes:

Dec and Inc are declination and inclination of mean direction calculated from N unit vectors whose resultant R is used to calculate Fisher (1953) precision parameter k and semi-angle of a cone of 95% confidence a-95.

Cretaceous and Eocene field directions calculated for sample location using poles in Beck and Housen (2003).

Sample location: 48.04876° N latitude; 116.45555° W longitude, NAD 27

References

Beck, M.E., Jr., and Housen, B.A., 2003, Absolute velocity of North America during the Mesozoic from paleomagnetic data: Tectonophysics, v. 377, p. 33-54.

Burmester, R.F., Lewis, R.S., McFaddan, M.D., Breckenridge, R.M., Miller, D.M., and Miller, F.K., 2007, Geologic map of the Cocolalla quadrangle, Bonner County, Idaho: Idaho Geologic Survey Digital Web Map, DWM-91.

Doughty, P.T., and Price, R.A., 2000, Geology of the Purcell Trench rift valley and Sandpoint Conglomerate: Eocene en echelon normal faulting and synrift sedimentation along the eastern flank of the Priest River metamorphic complex, northern Idaho: Geological Society of America Bulletin, v. 112, p. 1356-1374.

Dunlop, D.J., 2002, Theory and application of the Day plot (Mrs/Ms versus Hcr/Hc) 1. Theoretical curves and tests using titanomagnetite data: J. of Geophysical Research B, v. 107, p. 2056, doi: 10.1029/2001JB00486, EPM 4-1 to 4-22.

Fisher, R.A., 1953, Dispersion on a sphere: Proceedings of the Royal Society of London, Series A, 217, p. 295-305.

Gradstein, F.M., Agterberg, F.P., Ogg, J.G., Hardenbol, J., van Veen, P., Thierry, J., and Huang, Z.-H., 1994, A Mesozoic time scale: J. of Geophysical Research, v. 99, p. 24,051–24,074.

Harrison, J.E., and. Jobin, D.A., 1965, Geologic map of the Packsaddle Mtn. quadrangle, Idaho: U.S. Geological Survey Geological Quadrangle Map GQ‑375, scale 1:62,500.

Housen, B.A., Beck, M.E., Jr., Burmester, R.F., Fawcett, T., Petro, G., Sargent, R., Addis, K., Curtis, K., Ladd, J., Liner, N., Molitor, B., Montgomery, T., Mynatt, I., Palmer, B., Tucker, D., and White, I., 2003, Paleomagnetism of the Mount Stuart Batholith revisited again; what has been learned since 1972?: American J. Science, v. 303, p. 263-299.

Kirschvink, J., 1980, The least-squares line and plane and the analysis of paleomagnetic data: Geophysical J. Royal Astronomical Society, v. 62, p. 699-718.

Knight, M.D., and Walker, G.P.L., 1988, Magma flow directions in dikes of the Koolau Complex, Oahu, determined from magnetic fabric studies: J. of Geophysical Research, v. 93, p. 4301–4319.

Lewis, R.S., Burmester, R.F., and Breckenridge, R.M., 2007, Geologic map of the Elmira quadrangle, Bonner County, Idaho: Idaho Geologic Survey Digital Web Map, DWM-90.

Lewis, R.S., Burmester, R.F., Breckenridge, R.M., McFaddan, M.D., and Phillips, W.M., 2008, Preliminary geologic map of the Sandpoint 30- x 60-minute quadrangle, Idaho and Montana, and the Idaho Part of the Chewelah 30- x 60-minute quadrangle: Idaho Geologic Survey Digital Web Map, DWM-94.

Marquis, G., and Irving, E., 1990, Observing tilts in midcrustal rocks by paleomagnetism: Examples from southeast British Columbia: Tectonics, v. 9, p. 925-934.

Miller, F.K., Burmester, R.F., Powell, R.E., Miller, D.M., and Derkey, P.D., 1999, Digital geologic map of the Sandpoint 1- by 2-degree quadrangle, Washington, Idaho, and Montana: U.S. Geological Survey Open-File Report 99-0144.

Nagata, T., 1961, Rock Magnetism: Maruzen Co., Tokyo, 360 p.

Price, R.A., and Sears, J.W., 2000, A preliminary palinspastic map of the Mesoproterozoic Belt-Purcell Supergroup, Canada and USA: Implications for the tectonic setting and structural evolution of the Purcell Anticlinorium and the Sullivan deposit: *in* Lydon, J.W., Höy, T., Slack, J.F., and Knapp, M.E. eds., The Geological Environment of the Sullivan Deposit, British Columbia: Geological Association of Canada, Mineral Deposits Division, Special Publication No. 1, p. 61-81.

Tauxe, L., 1998, Paleomagnetic Principles and Practice, Kluwer Academic Publishing, Dordrecht, 299 p.

Tauxe, L., Kylstra, N., and Constable, C., 1991, Bootstrap statistics for paleomagnetic data: J. of Geophysical Research, v. 96, p. 11,723-11,740.

Zijderveld, J.D.A., 1967, A. C. demagnetization of rocks: Analysis of results: *in* Collinson, D.W., Creer, K.M., and Runcorn, S.K., eds., Methods in Palaeomagnetism: Elsevier, Amsterdam, New York., p. 254–286.

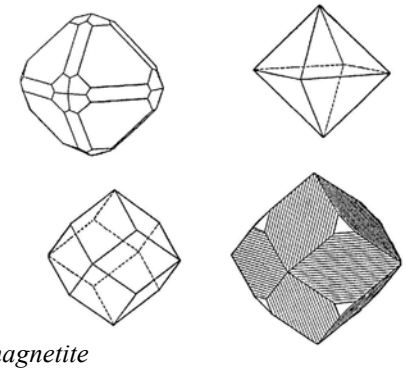

magnetite

RESULTS FROM HIGH RESOLUTION GRAVITY SURVEYS NEAR FLATHEAD LAKE, MONTANA

Jason R. Braden
ExxonMobil, Exploration Geologist, Houston, TX
jason.r.braden@exxonmobil.com

Michael H. Hofmann
Department of Geosciences, The University of Montana, Missoula, MT
michael.hofmann@umontana.edu

ABSTRACT

Collection of multiple high resolution gravity surveys near Flathead Lake, in the Flathead and Mission Valleys, reveals new information about the sedimentary fill and basin geometries. Each survey line contained between 25 and 36 data points and was conducted from west to east, perpendicular to the strike direction of the main structural elements. 2D modeling of the gravity suggests ~900m of sedimentary fill at the northern end of Flathead Lake and upwards of 1200m of sediment just south of the lake. Best results were obtained by using a multi-layered density model for the sedimentary fill instead of assuming a single layered homogenous basin fill sequence. In general, the multi-layered model increased depth to bedrock in all locations. Modeling efforts also verified the subsurface locations of previously mapped faults, such as the Mission Fault on the eastern margin of the basin. The study also revealed a series of new potential faults, in particular along the western margin of the basin. All faults mapped in this survey have normal movement, usually down to the west along the eastern margin and down to the east closer to the western valley margin.

INTRODUCTION

Over the past few decades, the Flathead and Mission Valleys in northwestern Montana have emerged as an exceptional natural laboratory for gaining a better understanding of the neotectonic history of the Mission Fault system (e.g. Stickney, 1980; Ostenaa et al., 1995; Lageson and Stickney, 2000; Hofmann et al., 2006a), and for studying the late Pleistocene and Holocene climate history of the region (e.g. Levish, 1997; Smith, 2004; Hofmann et al., 2006b; Hofmann and Hendrix, 2010).

Most of these studies focused on the interpretation of the Pleistocene and Holocene valley fill sediments but largely did not include detailed analysis of bedrock geometries and structures in these valleys. This is, in part, due to the lack of existing data sets pertinent to the analysis of bedrock geometry and the position of structural elements below this thick valley fill. In one of the few geophysical studies focusing on bedrock geometries, LaPoint (1971) interpreted a north/south trending gravity low as a result of basin subsidence along the Mission Fault. Bedrock profiles, under the Polson moraine, were interpreted by the same author to consist of a series of small horst and graben structures; obtaining a maximum depth of valley fill along this profile to be slightly more than 910m. Most other conclusions about the position of structural elements and the resulting valley geometries, however, are either drawn from the evaluation of focal points of recent seismicity (e.g. Stickney, 1980; Lageson and Stick-

ney, 2000), trenching studies of young valley fill deposits (e.g. Ostenaa et al., 1995), or interpretation of shallow seismic reflection data from Flathead Lake (Kogan, 1980; Hofmann et al., 2006a).

To fill this gap and to help advance the understanding of the geologic history of the Flathead and Mission valleys we obtained a number of high resolution gravity surveys located immediately south and north of Flathead Lake. Preliminary results from this study show that the depth to bedrock north of the lake is at ~ 900m below the valley surface and even deeper, at ~1200m, immediately south of the lake. Both of these depths exceed those of previous interpretations (LaPoint, 1971; Smith, 2000) and provide new insights about the total subsidence in these valleys. This high resolution gravity data also helped to identify the position of bedrock faults in the basin that have previously not been mapped.

GEOLOGIC SETTING

Structural Setting

The study area is located in the southern Flathead and northern Mission valleys, adjacent to Flathead Lake, Montana. Flathead Valley extents for ~90km from the southern shores of Flathead Lake to the north and is between 15 to 25km-wide, while the Mission Valley extends from the lake ~50km to the south and is ~25–30km-wide. These valleys have been interpreted to occupy the southern end of the linear northwest-southeast trending Rocky Mountain Trench (Leech, 1966) and are part of the Intermountain Seismic Belt (ISB). The ISB defines a belt of high seismicity that extends from the Flathead Lake Region south through western Montana, eastern Idaho, northwestern Wyoming, central Utah, and northernmost Arizona, and has a rich history of active seismicity, as well as a significant prehistoric record of seismicity (Stickney et al., 2000). Pleistocene and Holocene faults in the ISB typically are range-bounding normal faults that display evidence of recurrent, discrete, surface displacements of up to several meters during individual seismic events. Within the study area, geomorphically well-expressed fault scarps have been documented as offsetting Pleistocene and Holocene sediments onshore as well as offshore in Flathead Lake (Ostenaa et al., 1995; Hofmann et al., 2006a).

Many of these Quaternary north-south trending extensional faults in the northern Basin and Range Province are closely related to the traces of older, mainly Mesozoic compressional faults (Constenius, 1996). After a period of thrusting and deformation during the late Mesozoic Sevier orogeny (74-59 Ma; Sears, 2001) many surficial thrust faults were reactivated as extensional faults during the early Paleocene (e.g. Constenius, 1996).

Valley Fill

The main fill sequence in the Mission and Flathead Valleys consists of Paleogene, Neogene, and Quaternary deposits. Geophysical investigations and interpretation of borehole log data has indicated the presence of upwards of 1500m of basin fill, 600m of which are Paleogene and Neogene material, north of the study area (Alden, 1953; Smith, 2000). There, Paleogene and Neogene deposits are described as brown and orange, medium to coarse grained pebbly sandstone, well-rounded pebble and cobble conglomerate of the Kishenehn Formation and Paola gravel (Constenius, 1996). Constenius (1996) additionally describes the sandstone and conglomeratic beds having channelized and erosional bases; locally infilling fractures of the Mesoproterozoic Belt Supergroup rock, the

sedimentary basement in the Mission and Flathead Valleys, respectively. Closer to the study area, unconsolidated and consolidated Paleogene and Neogene strata have been described in the Flathead Valley west and north of the lake (Smith, 2004), and Braden (2006) mapped similar Paleogene deposits near Kerr dam just south of the lake.

The majority of the valley fill in the study area is, however, related to the rich Pleistocene glacial history. During the last glacial maximum the study area was located near the southern terminus of the Flathead Lobe of the Cordilleran Ice Sheet. Related sediments include ice-contact deposits, widespread glaciofluvial deposits, local eolian deposits, and glaciolacustrine deposits associated with glacial Lake Missoula (Pardee, 1910, 1942; Davis, 1920; Nobles, 1952; Alden, 1953; Ostenaa et al., 1995; Levish, 1997; Hofmann and Hendrix, 2004; Smith, 2004). Locally overlying these Pleistocene sediments are Holocene fluvial, alluvial, and eolian deposits. The thickness of these deposits is highly variable, but exceeds 150m in water wells just north of the lake (Smith, 2000). Results from seismic reflection data from Flathead Lake suggest that the lake contains Quaternary strata in excess of 160 m below the water bottom (Wold, 1982; Hofmann et al., 2006b; Hofmann and Hendrix, 2010).

METHODS AND LIMITATIONS

Gravity Survey

Three linear gravity surveys were collected, one at the northern end and two at the southern end of Flathead Lake (fig. 1). For each of these surveys a Scientrex CG3 gravimeter, with a measurement resolution of 0.005 milligals (mGal) was utilized. Additionally a combination of a handheld Garmin and a Trimble Pathfinder PRO XRS mapping-

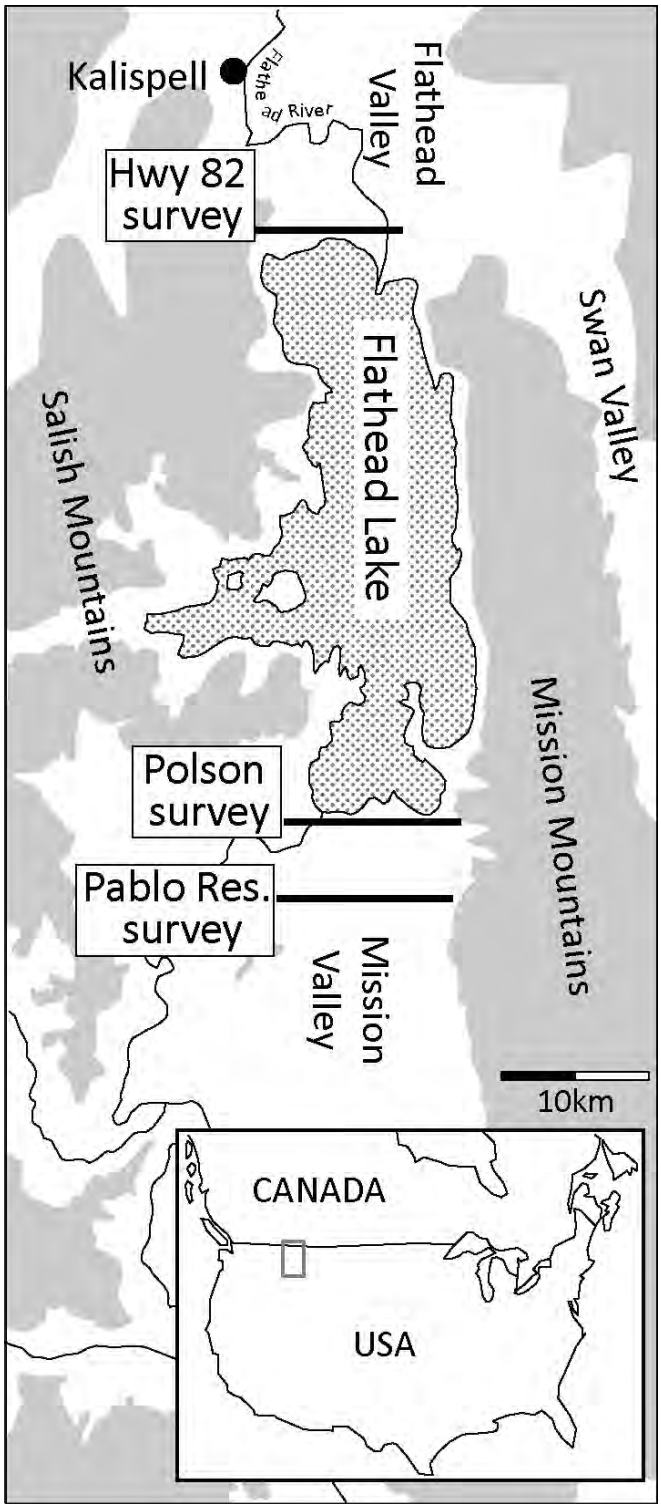

Figure 1: Map of the Flathead Lake region of northwest Montana showing the locations of the three gravity surveys: Highway 82 at the north end of the lake, Polson and Pablo Reservoir surveys at the southern end of the lake.

grade global positioning systems were used to determine gravity station location and elevation. At each gravity station multiple measurements were recorded via the devices to ensure data quality, and minimize errors. A base station was employed in each survey for determining the tidal drift curve. The surveys were tied to the gravity station located in the geophysics laboratory (Clapp Building) on the campus of the University of Montana with a verified absolute gravity value of 980,432.210 mGal.

The following corrections are customarily applied to gravity data or commonly referred to as 'gravity reduction:' Earth tides, instrumental drift, latitude, free air, Bouguer, and terrain. Prior to the study the magnitude of instrumental drift had been determined and, though slight, were applied to the data. Based upon the measurements taken from reacquiring the field base-station throughout the course of the survey a tidal curve was determined and applied to the recorded data. For further corrections to the gravity data, a standard crustal density of 2.67g/cm^3 was used along with the 1967 Geodetics Reference System Formula for determining the theoretical gravity value. The free air correction was calculated by +0.3086h, where h is the height above the geoid (Blakely, 1995). Calculation of the Bouguer slab correction used +0.11195h that approximates $2\pi G\rho h$, where h is the height above the geoid (Blakely, 1995).

The final portion of the gravity reduction was the calculation of the terrain correction. Modification of the gravity data due to topographic undulations surrounding a gravity station was identified by Hayford and Bowie (1912). Over the last century refinements have been made to this laborious but significant calculation most notably early on by Bullard (1936) and Hammer (1939). Bullard (1936) first applied terrain corrections out to a distance of 1½° or 166.735km, and this has become standard practice. More recent improvements as stated by Nowell (1999) have gained detailed understanding of the necessity to carefully carry out these corrections, and be aware of potential errors in the final Complete Bouguer Anomaly (CBA). This study utilized computer software based on the original Hammer charts and digital elevation models (DEMs) to calculate terrain corrections.

The final CBA values were then compared to the gravity map of the state of Montana. The CBA for the state of Montana is maintained by the United States Geological Survey (USGS). Data complied to form the map were obtained from the National Geophysical Data Center (from unclassified Department of Defense data), the USGS, and from a number of university thesis and dissertation studies (McCafferty et al., 1998). Approximately 35,000 data points in and around the state were used to generate the CBA map for Montana and of those points 45 lie near to or along this study's survey lines. Comparison of the datasets results in very good correlation between the free air and CBA gravity anomaly measurements with typical variances in the range of 1–2%.

To establish depth to basement the models used residual gravity values which were determined by subtracting the CBA from a regional gravity gradient. In order to find the slope of the regional gravity a linear trend was fit to the first and last survey stations. These two stations, as designed in conducting the survey, were taken on bedrock outcrops near the starting and ending points of the line of section. LaPoint (1971) seemingly took this approach, which is useful for comparing modeling results.

Modeling Process

The primary efforts of the modeling of the gravity data were to 1) estimate the depth to sedimentary basement (determine sediment thickness) and 2) identify potential fault locations. 2D models were built using a computer software package which utilizes standard procedures and Talwani-type polygons to calculate the computed gravity signal (Talwani et al., 1959).

Initial models for each of the surveys were built with a single layer, homogenous valley fill above the sedimentary basement. Belt Supergroup rock, the sedimentary basement in the study area, consists primarily of quartzites and argillites. The density of similar Precambrian rock used in previous work in western Montana range from 2.6 to 2.9g/cm^3 (LaPoint, 1971; Constenius, 1988; Kleinkopf, 1997; Nyquest, 2001; Harrison, 2004; Stalker, 2004). For this study, a constant density value of 2.72g/cm^3 was used to model the basement. To model the lower density valley fill we chose a constant density contrast of 0.55 g/cm^3.

For our final model we chose to model a total of four polygons above the sedimentary basement to account for the complex sedimentary fill history in these valleys. As stated previously in this paper the presence of Paleogene and Neogene strata has been described in the region of the study area. This indicates the likelihood that such sediment is present at depth in the basins; therefore, are included in the model as the base sediment package. Constenius (1988) estimated the density of the Paleogene and Neogene sediments in the Kishenehn Basin ranges from 2.2 to 2.4g/cm^3. In the absence of any other measurements, we adapted a similar value for our model. The three other polygons included in the models represent generic sedimentary packages associated with Quaternary glacial, fluvial, and lacustrine deposits of varying ages and sedimentary densities.

Once each beginning model was generated, several iterations of the gravity inversion modeling were undertaken. To constrain the models we searched the Groundwater Information Center (GWIC) maintained by the Montana Bureau of Mines and Geology for water wells drilled near or along the surveys. Several wells, within a couple hundred meters of the study lines, were identified and reported general driller lithology descriptions. Some of these wells had encountered bedrock when drilled and were used to directly control the modeled depth to basement. Analysis of other nearby wells suggested gross sediment packages that might indicate boundaries between modeled units.

Limitations

A concern of gravity modeling is the impact of large bodies of water on the resulting gravity readings and terrain corrections. Water bodies will cause the gravity values to be measured or calculated low which in turn causes and over estimation of the depth of bedrock. Studies have shown the variable impact of large bodies of water (lakes, seas, or ocean) or glacial fields on the terrain corrections (Bullard, 1936; Reilly, 1972; Steinhauser et al., 1990; Nowell, 1994; Nowell, 1999). A gravity survey collected on a coastal area in eastern Iceland provides a good example of the minimal to significant effects. Nowell (1994) examined the net effect of calculating the terrain corrections to sea level versus the sea bed at various distances and elevations. Stations located along the coast near sea level, where the water depth was ~100m at a distance of 14 to 22km from shore, were impacted the least with up to 45 μGals (0.045mGals), or less than 2% net effect in terrain correction when calculated at

sea level versus the sea bed (Nowell, 1994). In contrast, stations located in more inland locations and at significantly higher elevations (700m versus 20m) the net effect of calculating the terrain correction to the sea bed was under 3%, but this translates into ~300μGals (0.3mGals) (Nowell, 1994).

Flathead Lake water depths approach 112m at the maximum, with a large portion of the lake on the eastern margin with 80–100m water depths, and a lake average of ~50m. Considering the gravity station locations and elevation in reference to the lake in comparison to the study by Nowell (1994) the water effects are interpreted to be minimal. However, several points along the Polson and Pablo surveys are ~100m above the typical water surface elevation, and a couple stations are 200 to 300m higher.

GRAVITY SURVEYS

Highway 82 Survey

This survey line consists of 25 survey points located along Highway 82, starting in the west at the junction of Highway 82 and 93 and extending to just east of the Flathead River, covering a distance of approximately 10km (Table 1; fig. 1).

Calculated residual gravity values range from 0 to -13 mGal, indicating low density fill across the survey section (figs. 2, 5). The highest residual gravity values mark the location of bedrock outcrops at the eastern and the western end of the line respectively. The lowest residual gravity values were recorded between 5–6.5km to the east from the survey starting point and mark the area with the potentially thickest low density valley fill. Most significant change in residual gravity is near the eastern end of the survey where the signal appears to be a gradual decrease from -2 to -13 mGal over a distance of ~2km. This is in difference to the western margin where the drop in residual gravity occurs over a longer distance (~5km) and includes a series of steps (areas of more consistent residual gravity), the most noticeable between 1–2km from the starting point of the survey.

Polson Survey

This second survey line is located at the southern end of Flathead Lake partially running through the town of Polson, along 7th Ave/Hillcrest Dr. and extending to the east to the Mission Mountains along Highway 35 (fig. 1). The survey consists of 34 survey points, starting near a bedrock outcrop slightly west of the Polson Airport, and terminates on Hellroaring Creek Tr. near the base of the Mission Mountains (Table 1).

Calculated residual gravities along this survey line range from 0 to -16 mGal, indicating low density fill across the survey section and a greater depth to bedrock than along the northern end of Flathead Lake (figs. 3, 6). The residual gravity data shows a strong asymmetry with an area of rapidly decrease residual gravity from -3 mGal to -16 mGal

Survey Name	No. of Stations	Length	Avg. Spacing	Elevation	FAA (mgals)	CBA (mgals)	Residual (mgals)
Highway 82	25	10.1km	0.4km	883-904m	-46 to -62	-146 to -160	0 to -13
Polson	34	13.4km	0.35km	891-1174m	-13 to -56	-135 to -154	0 to -16
Pablo Reservoir	36	11.7km	0.33km	970-1033m	-25 to -41	-135 to -149	0 to -13

Table1: General data for the three gravity surveys collected, where elevation is meters above sea level, FAA = Free Air Anomaly and CBA = Complete Bouguer Anomaly.

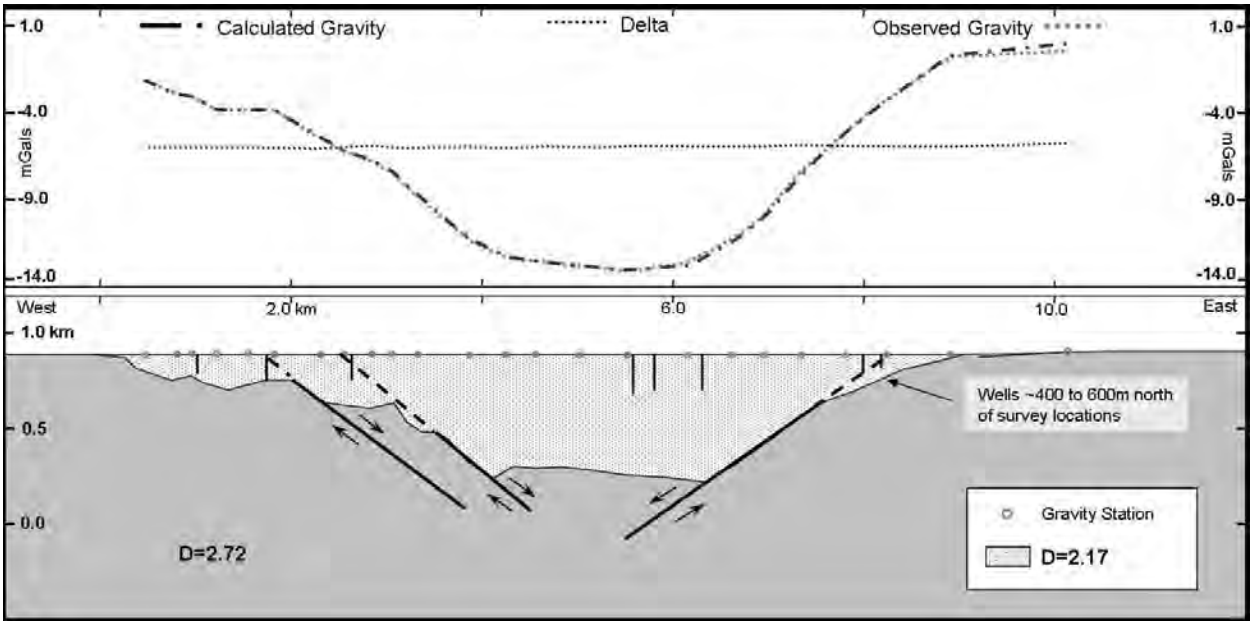

Figure 2: Highway 82 single sedimentary polygon model using a density contrast of 0.55g/cm^3. Vertical black lines in the model represent depth-scaled water wells projected into the plane of the survey. Maximum depth to basement is ~600m.

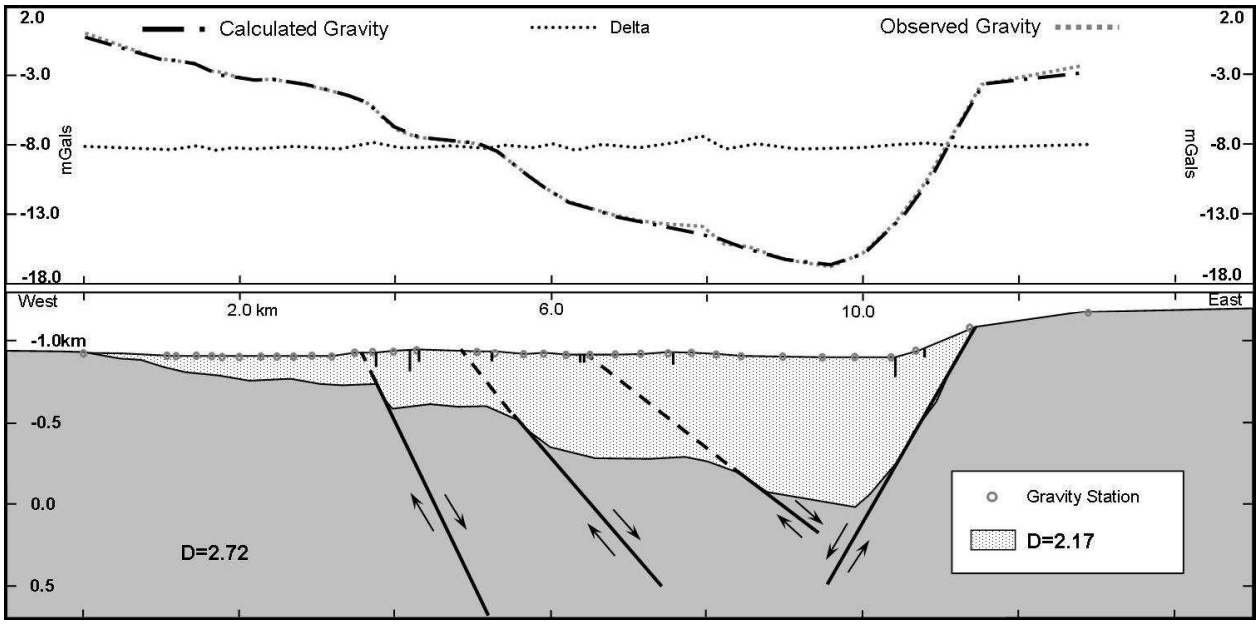

Figure 3: Polson single sedimentary polygon model using a density contrast of 0.55g/cm^3. Vertical black lines in the model represent depth-scaled water wells projected into the plane of the survey. Maximum depth to basement is ~800m.

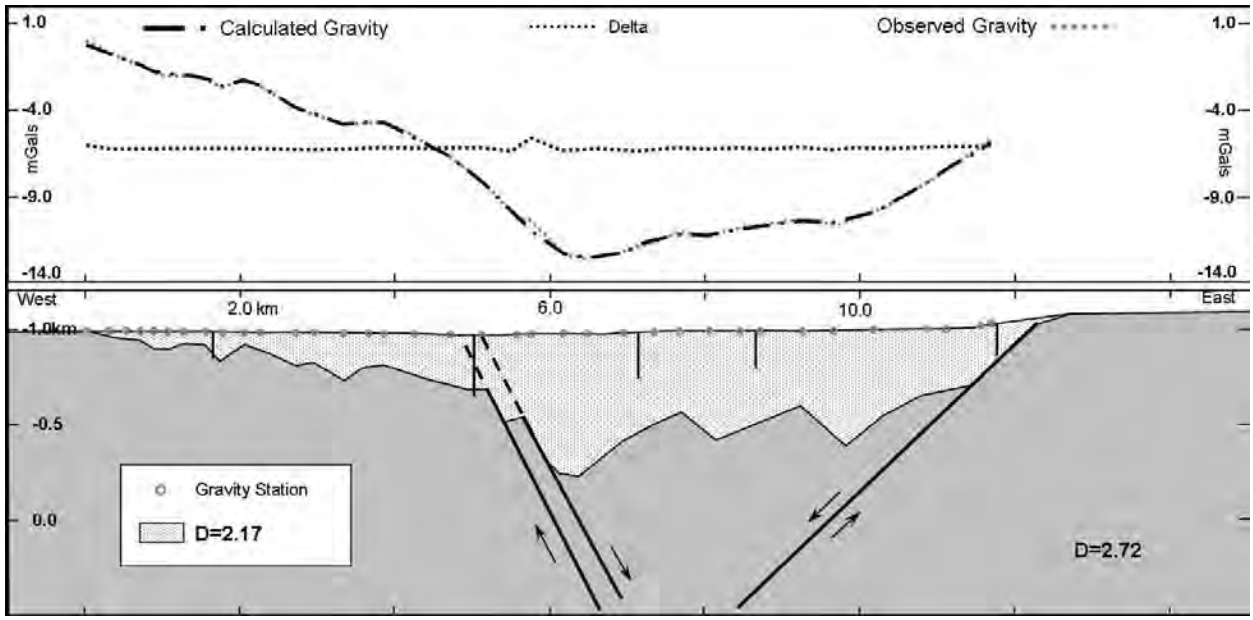

Figure 4: Pablo Reservoir single sedimentary polygon model using a density contrast of 0.55g/cm^3. Vertical black lines represent depth-scaled water wells projected into the plane of the survey. Maximum depth to basement is ~700m.

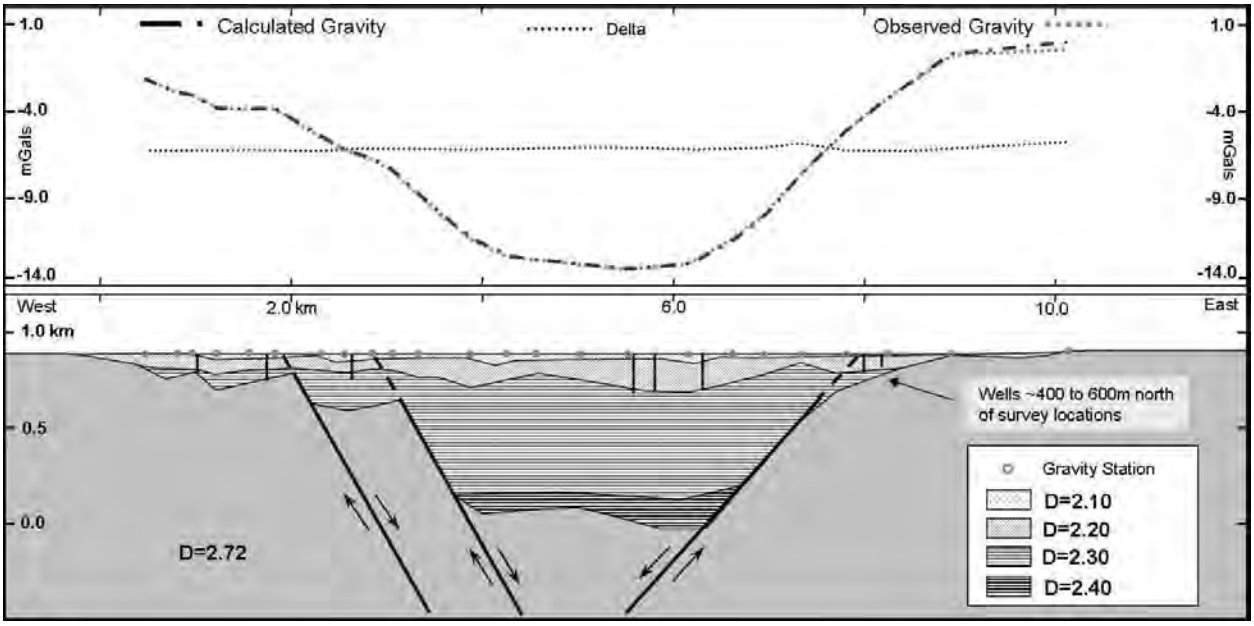

Figure 5: Highway 82 final multi-polygon model using 4 sedimentary units of differing densities. Vertical black lines represent depth-scales water wells projected into the plane of the survey. The Mission Fault in on the east and the two western faults are associated with the Kalispell-Finley Point and Table Bay Faults. Maximum depth to basement is 880m near the 6.0km marker.

over a distance of only 1km marking the eastern margin of the basin and a more gently dipping slope of increasing residual gravity to the west. The highest residual gravity values are at -16 mGal about 9–10km to the east of the survey starting point. The change in residual gravity from the starting point in the west to the lowest measured residual gravity over the distance of 9km is not gradual but interrupted by sections of almost consistent residual gravity values. A first step is begins 3–4km from the starting point with a consistent residual gravity reading of ~-3 mGal; a second is between 4–5km with residual gravities almost unchanged at -8 mGal; and a third is between 7–8km with a residual gravity value around -13 mGal.

Pablo Reservoir Survey

The third survey line is located approximately 5km south of the Polson survey starting in the west at the Valley View Hills along North Reservoir Rd and extends to the Mission Mountains along Minesinger Tr on the east (fig. 1; Table 1). Unlike the other two surveys the most eastern point of the 12km-long, 36-station survey was not taken on a bedrock exposure due to limited land access, posing some initial concerns about the model accuracy. To mitigate this potential reason for inaccuracy we compared our data to gravity data for the state of Montana, and in conjunction with values measured in the Polson survey determined an estimated CBA value. This process resulted in residual gravity values similar to those observed in the Polson survey and those of LaPoint (1971), building confidence in the survey results.

The resulting residual gravity profile displays a range of values from 0 to -13 mGal along a profile that undulates (figs. 4, 7). In contrast to the others, this profile has a much gentler drop in gradient along its eastern margin. Values decrease from -4 mGal near the eastern end of the line to -13 mGal in the center of the line (6km). A similar decrease over the exact same distance of 6km was observed on the western end of the survey. Several steps in the residual gravity profile are present.

HOW MUCH SEDIMENT FILLS THE VALLEY?

Previous interpretations suggest maximum depths to sedimentary basement of approximately 450–600m (1500 – 2000 ft) just north of Flathead Lake near the Highway 82 survey line and 240–300m (800–1000 ft) close to the two southern surveys (Smith, 2000). In a first modeling step we attempted to match this interpretation by using a single density contrast of 0.55g/cm^3 between the Belt Supergroup rock and sedimentary fill in the basin. This approach resulted in a maximum depth to bedrock of 600m, within the range of this previous study, for the northern line (fig. 2). However for the southern surveys a much greater depth to bedrock (~ 800m for the Polson survey, ~ 700m for the Pablo survey) resulted (fig. 3, 4). In order to match the shallower bedrock depth in the southern lines an increase in density contrast is required. Such an increase, however, seems to be unreasonable, because results from a linear gravity survey over the western portion of the Polson moraine indicate that the best fit between observed gravity curve and shallow bedrock encountered in a nearby well can be achieved by using a single density value of 2.35g/cm^3 (Braden, 2006) and density is expected to increase with depth.

Our modeled depth to bedrock in a single density model is, however, closer to results from previous gravity work in the area (Decker, 1968; LaPoint, 1971). These authors found a north/south trending gravity low as a result of a sediment-filled basin caused by the Mission Fault along the eastern side of the valley. The maximum depth to bedrock was calculated to range between 910m (3000 ft)

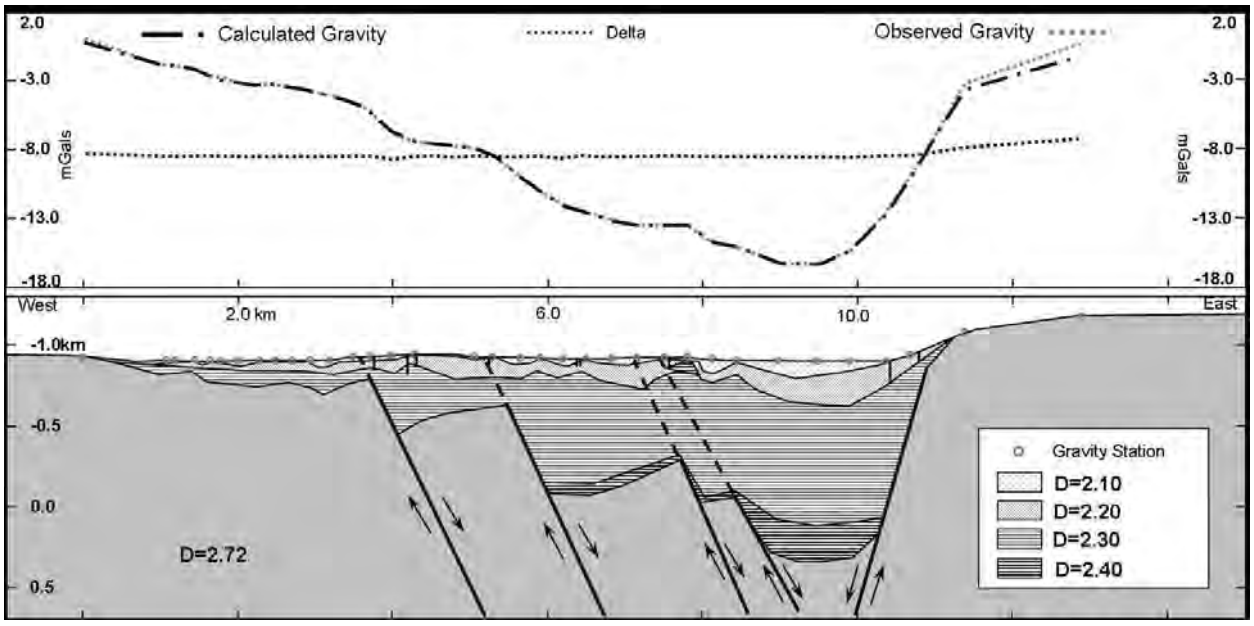

Figure 6: Polson final multi-polygon model using 4 sedimentary units of differing densities. Vertical black lines represent water wells projected into the plane of the survey. The Mission Fault is on the eastern margin of the basin. Other east-dipping faults have not been previously identified via surface mapping. Maximum depth to basement is 1200m near the 10km marker.

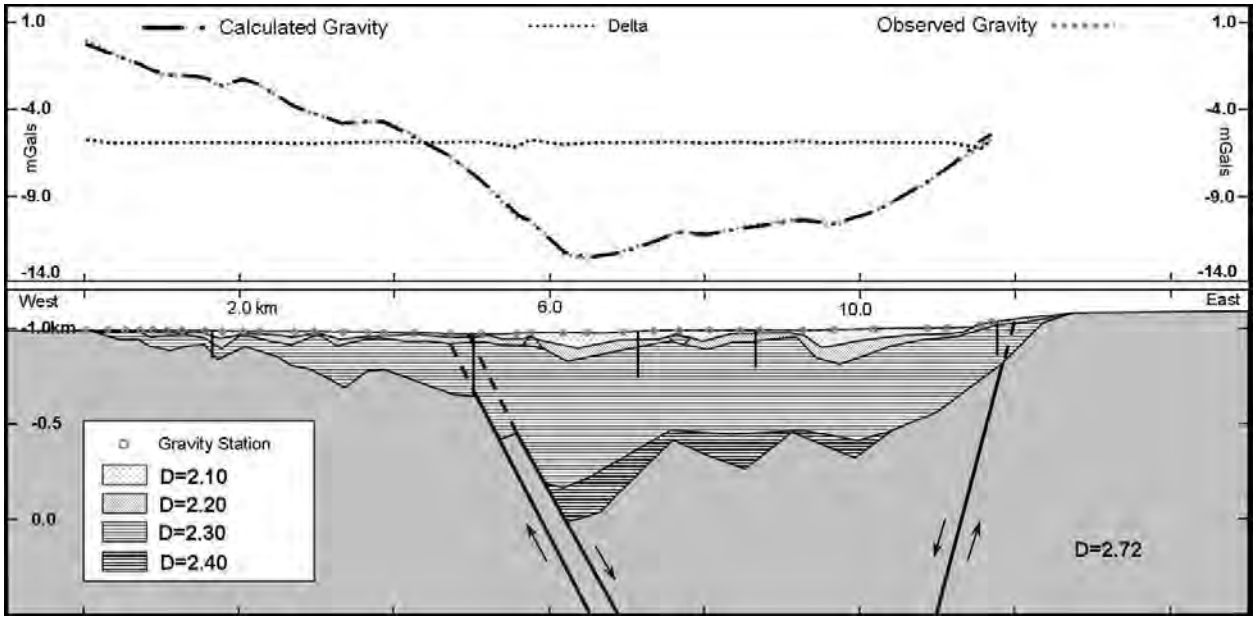

Figure 7: Pablo Reservoir multi-polygon model using 4 sedimentary units of differing densities. Vertical black lines represent water wells projected into the plane of the survey. The estimated position of the Mission Fault is on the eastern margin of the basin, based on the positioning of Hofmann et al., (2006a). East-dipping faults near the center of the survey have no been previously identified via surface mapping. Maximum depth to basement is 950m near the 6km marker.

and 1370m (4500 ft) near and at the location of the two southern surveys, depending on the applied regional corrections (Decker, 1968; LaPoint, 1971).

A one-layer homogenous valley fill is an unreasonably simplistic model because the basin contains different Paleogene/Neogene and Quaternary deposits. To address this expected fill heterogeneity we created a multi-layered model and assigned each sediment polygon unique density values. During the modeling process the initial three-polygon model was adjusted by adding a fourth polygon at the shallowest level. The assigned densities are, from deepest to shallowest, in the valley fill sequence 2.4g/cm^3, 2.3g/cm^3, 2.2g/cm^3, and 2.1g/cm^3 respectively. Lithology logs from multiple groundwater wells were used to constrain the vertical extent of these polygons in the shallow subsurface and to help estimate densities. These more complex models resulted in optimal match to available bedrock constraints, mainly in form of logs from water wells, and generally greater depth to bedrock than in any of the previous models.

The final model for the Highway 82 section shows a maximum depth to bedrock of 880m (~2900ft), just north of the northernmost tip of Flathead Lake (fig. 5). Constraints for this model come from four water wells that encountered bedrock in the shallower parts along the survey line and were used to verify results (Table 2). Results from the Polson survey also were constraint by water well logs. A water well located about 2.5km south of the survey, just west of Highway 93 encountered bedrock near 510m (1672 ft). Extrapolating this well northward the location would be near the center of the line, at the approximate position of the Highway 35 and 93 junction. Further to the east of this location, the maximum depth to basement was calculated at ~1200m (3940 ft) (fig. 6). Along the Pablo Reservoir survey line the deepest portion of the basin, as indicated by this model, has shifted toward the west compared to the Polson line just 5km to the north. At this point, the maximum depth to bedrock in our multi-layered model is 950m (3120 ft) (fig. 7). A groundwater well located 200m north of the survey line and about 2km from the survey start point encountered bedrock at 138m, matching very closely our modeled depth from the gravity data (Table 2). As previously mentioned, a well drilled 2.5 km to the north of the survey line encountered bedrock at 510m (1672 ft). Considering the out-of-the-plane projection of the depth from the well, and the variability that could exist the bedrock there is good agreement with the model. Four other wells near the line of section did not drill bedrock but were used for adjusting the sedimentary polygons based on the potential gross packages interpreted from lithology descriptions.

LOCATION OF BEDROCK FAULTS

Focus of this study was to understand both the total valley fill sequence and to map fault locations as revealed from modeled bedrock profiles. Previous studies have shown the great complexity of the fault framework in the area (e.g. LaPoint, 1971; Stickney, 1980; Hofmann et al., 2006a). Comparing the fault traces interpreted from our bedrock model along Highway 82 to these previous studies, there is reasonable agreement in the projection of the interpreted bedrock fault planes to the present land surface (fig. 8). According to these previous researchers there are two segments to the Mission Fault crossing the Highway 82 survey line in a N-S direction. Our gravity survey did not extend far enough east to intersect the eastern strand of the Mission Fault, but clearly identified the western of the two segments (fig. 5). Along the western part of our survey, we recognize two bedrock highs. We interpret these shoulders in the gravity profile to represent rotational bedrock blocks bound by easterly dipping normal

Survey Name	GWIC Number	Depth of Well	Bedrock Depth
Highway 82	258354	116m/380ft	102m/334ft
	241112	143m/469ft	142m/466ft
	243705	136m/445ft	n/a
	80740	207m/679ft	n/a
	207798	152m/500ft	99m/323ft
	257291	256m/840ft	71m/234ft
	80742	192m/629ft	n/a
	237283	195m/640ft	n/a
Polson	131954	68m/224ft	n/a
	76907	54m/177ft	n/a
	206420	55m/182ft	n/a
	251634	79m/260ft	n/a
	253927	98m/320ft	n/a
	255485	54m/177ft	n/a
	207059	61m/200ft	n/a
	76825	126m/415ft	n/a
	76925	134m/440ft	n/a
	261128	701m/2300ft	510m/1672ft
Pablo Reservoir	77005	244m/800ft	n/a
	212210	329m/1080ft	n/a
	172465	180m/590ft	n/a
	254807	201m/660ft	n/a
	188088	146m/480ft	139m/455ft
	261128	701m/2300ft	510m/1672ft

Table 2: The Groundwater Information Center, maintained by the Montana Bureau of Mines and Geology, was searched for information to help constrain the models. The information from these wells was incorporated into the construction of the models.

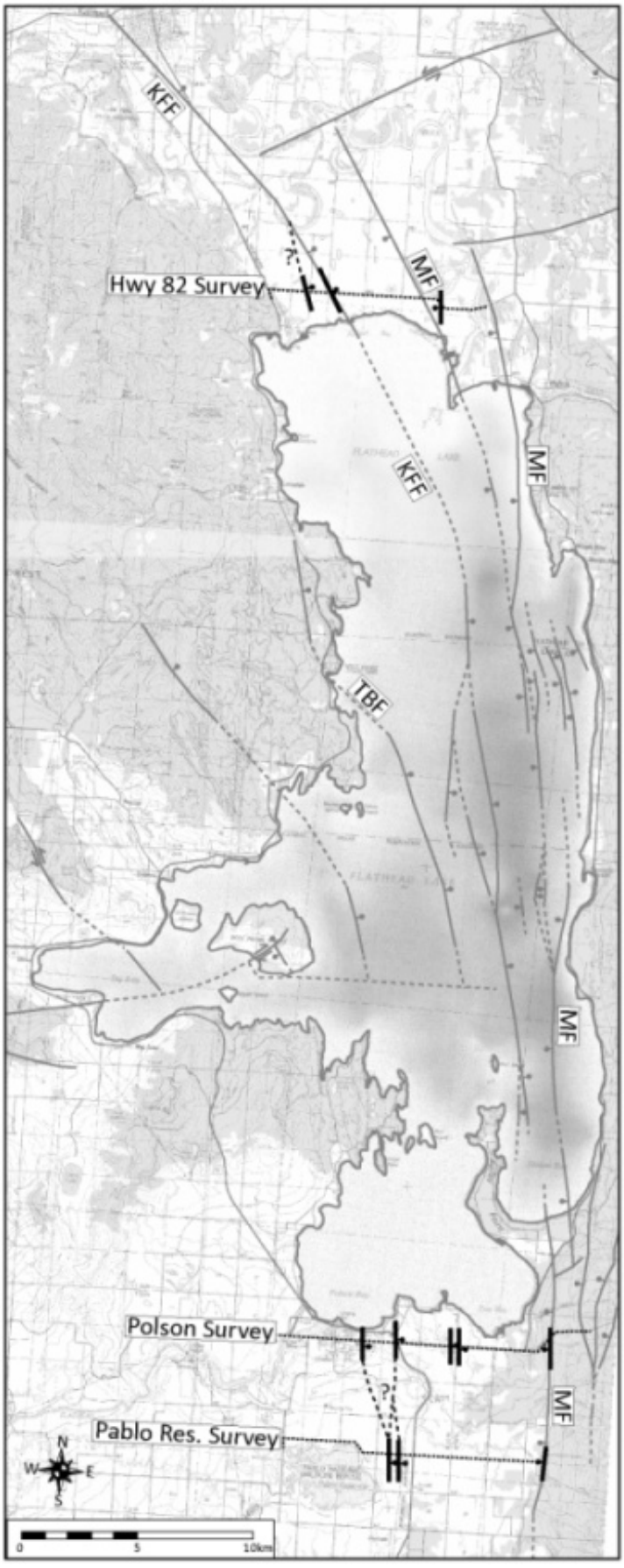

faults. One of those matches the position of the Kalispell-Finley Point Fault (KFF) on the western side of the basin. The second fault on the western side of the basin has not been mapped previously, but could be the northern extension of the Table Bay Fault (TBF) or another splay of the KFF (fig. 8).

Similar to the Highway 82 model, the refined gravity survey along the Polson transect did not just result in a deeper than previously thought depth to bedrock, but also gives way to interpret additional faults in the area. LaPoint (1971, 1973) interpreted the bedrock geometry to be constructed of multiple faults in horst and graben structures. However, the gravity signal indicates continued increasing basin depth from west to east toward the position of the Mission Fault suggesting continued down dropping basement. The frequency of the gravity signal is decreasing which also supports the interpretation of the deepening of the basement structure from west to east. Comparable to the structures interpreted in the Highway 82 model, a series of four bedrock shoulders have been modeled and are interpreted to be rotational bedrock blocks bounded by east dipping normal faults (fig. 6). Other than in the gravity interpretation models by LaPoint (1971) these faults have not been included on geologic maps of this area (fig. 8). The lack of recognition of these faults most likely can be attributed to the absence of evidence of faulting at the surface as shown in the maps by Hofmann and Hendrix

Figure 8: Map of fault traces in the southern Flathead and northern Mission valleys. Black faults are faults mapped in this study, gray fault traces are faults previously mapped by LaPoint, 1971; Stickney, 1980; Harrison et al., 1986; Ostenaa et al., 1995; Hofmann and Hendrix, 2004; Hofmann et al., 2006a. In particular the faults mapped in the southern part (Polson survey and Pablo reservoir survey) have not been previously recognized. Their extent to the north and south respectively are unknown. MF=Mission Fault; KFF=Kalispell-Finley Point Fault. Map modified from Hofmann et al., 2006.

(2004) and Braden (2006). If the fault planes are projected to the modern surface their alignment with near shore topographic features along Polson Bay suggesting a potential relationship. Further to the east of these faults a single strand of the Mission Fault has been clearly identified and the surface projection of the fault plane corresponds well with the mapped location by Hofmann and Hendrix (2004).

The Pablo Reservoir survey allows for fault interpretations. An important caveat is that no land access was available to the area where the Mission Fault crops out, thus this model cannot be used to clearly define that fault plane. Though the main bounding fault on the eastern edge of the basin has not been delineated, the remaining bedrock geometries suggest the location of other faults (fig. 7). In the central portion of this survey, the bedrock geometries suggest that the two westernmost faults identified in the Polson survey have converged. An alternate possibility is the westernmost fault on the Polson line has lost displacement, and a secondary splay formed near the remaining fault. While the Mission Fault is not clearly defined in the eastern part of the model, which could have implications on the geometries of the nearby bedrock, the basement is shallower by a few hundred meters compared to the Polson model. The interpreted structural style could indicate two rotational fault blocks with west dipping bounding normal faults, potentially related to the Mission Fault. However, previous studies (Harrison et al., 1986; Osteena et al., 1995; Hofmann and Hendrix, 2004; Hofmann et al., 2006a) have indicated the Mission Fault is a single fault strand south of Flathead Lake and becomes a multiple segment fault system northward (fig. 8). Another interesting relationship is that while the Mission Fault is a north-south striking feature, in the proximity of this survey line, the fault profile does bend to the west. Further investigations on resolving the Mission Fault along this line will be needed to help understand these bedrock geometries.

CONCLUSIONS

Results from a multi-line gravity survey in the Mission and Flathead Valleys provide new insight into the valley-fill history of these extensional basins. The surveys collected in this study have had standard processing and modeling approaches applied to the data. In difference to previous gravity surveys, we added a number of polygons with different densities to model the complex valley fills composed of a series of Paleogene/ Neogene and Quaternary sediments. Preliminary results indicate a thicker package of sediment filling the basins and more fault complexity than shown on previous studies. Along the survey at the northern extreme of Flathead Lake, the modeled depth to basement reaches 880m; while just south of the lake the basin fill is as thick as 1200m. The valleys are bounded on the eastern side by at least one strand of the Mission Fault system, a major range bounding normal fault. In contrast, we interpret multiple, previously unrecognized faults on the western margins. Either a fault associated with the Kalispell-Finley Point Fault or Table Bay Fault has been identified at the western end along the northern gravity survey. Multiple faults, which have not been previously documented along the southern end of the lake, may be expressed as topographic features along the shores of Polson Bay.

Further detailed investigations or refinement of interpretations in the Flathead Lake region should consider the water body effect on the gravity readings and 2D modeling efforts in order to minimize errors. Gravity modeling supplies an open-ended solution; however, by incorporating geologic knowledge of the region and constraints the resulting sensitivities can be limited.

ACKNOWLEDGEMENTS

We would like to thank the Confederated Salish and Kootenai Tribes for access to tribal lands to conduct this study. Braden extends additional thanks to the University of Montana (Dr. Steven Sheriff and Dr. Marc Hendrix) for use of the geophysical and GPS tools for collection of the data. We appreciate review comments by Larry Smith that helped to improve this manuscript.

REFERENCES

Alden, W.C., 1953, Physiography and glacial geology of western Montana and adjacent areas: U.S. Geological Survey Professional Paper 231, 200 p.

Blakely, R., 1995, Potential theory in gravity and magnetic applications: Cambridge Univ. Press, 441 p.

Braden, J.R., 2006, History of syn-glacial and post-glacial sedimentation at the former terminus of the Flathead Ice Lobe near Polson, MT: M.S. thesis, University of Montana, Missoula, 100 p.

Bullard, E.C., 1936, Gravity measurements in East Africa: Philosophical Transactions of the Royal Society, London, 235, p. 445–534.

Constenius, K.N., 1988, Structural configuration of the Kishenehn Basin delineated by geophysical methods, northwestern Montana and southern British Columbia: The Mountain Geologist, v. 25, p. 13-28.

Constenius, K.N., 1996, Late Paleogene extensional collapse of the Cordilleran foreland fold and thrust belt: Geological Society of America Bulletin, v. 108, p. 20-39.

Davis, W.M., 1920, Features of glacial origin in Montana and Idaho: Annals of the Association of American Geographers, p. 75–148.

Decker, G.L., 1968, Preliminary report on the geology, geochemistry and sedimentology of Flathead Lake, northwestern Montana: M.S. Thesis, University of Montana, Missoula, Montana, 91 p.

Hammer, S., 1939, Terrain corrections for gravimeter stations: Geophysics, v. 4, p. 184-194.

Harrison, J.E., Cressman, E.R., and Whipple, J.W., 1986, Geologic and structure maps of the Kalispell 1ºx2º quadrangle, Montana, Alberta, and British Columbia: USGS Miscellaneous Investigations Series Map I-2267, scale 1:250,000.

Harrison, N., 2004, Gravity, radar and seismic investigations to help determine geologic, hydrologic, and biologic relations in the Nyack valley, Northwestern Montana: M.S. Thesis, University of Montana, Missoula.

Hayford, J.F., and Bowie, W., 1912, The effect of topography and isostatic compensation upon the intensity of gravity: U.S. Coast and Geodetic Survey Special Publication No. 10, Washington, DC.

Hofmann, M.H., and Hendrix, M.S., 2004, Geologic map of the East Bay 7.5' quadrangle, northwest Montana: Montana Bureau of Mines and Geology Open-File Report 496, scale 1:24,000.

Hofmann, M.H., and Hendrix, M.S., 2010, Depositional processes and the inferred history of ice-margin retreat associated with the deglaciation of the Cordilleran Ice Sheet: The sedimentary record from Flathead Lake, northwest Montana, USA: Sedimentary Geology 223, p. 61-74.

Hofmann, M.H., Hendrix, M.S., Sperazza, M., and Moore, J.N., 2006a, Neotectonic evolution and fault geometry change along a major extensional fault system in the Mission and Flathead Valleys, NW Montana: Journal of Structural Geology 28, p. 1244-1260.

Hofmann, M.H., Hendrix, M.S., Moore, J.N., and Sperazza, M., 2006b, Late Pleistocene and Holocene depositional history of sediments in Flathead Lake, Montana: evidence from high-resolution seismic reflection interpretation: Sedimentary Geology 184, p. 111-131.

Kleinkopf, M. D., 1997, Geophysical interpretations of the Libby thrust belt, Northwestern Mon-

tana: U.S. Geological Survey Professional Paper 1546, 32 p.

Kogan, J., 1980, A seismic sub-bottom profiling study of recent sedimentation in Flathead Lake, Montana: M.S. thesis, University of Montana, Missoula, 98 p.

Lageson, D.R., and Stickney, M.C., 2000, Seismotectonics of northwest Montana, USA: *in* Schalla, R.A., and Johnson, E.H., eds., Montana Geological Society 50th Anniversary Symposium, Montana/Alberta Thrust Belt and Adjacent Foreland: Montana Geological Society, Billings, p. 109–126.

LaPoint, D.J., 1971, Geology and geophysics of the Southwestern Flathead Lake region, Montana: M.S. thesis, University of Montana, Missoula, 110 p.

LaPoint, D.J., 1973, Gravity survey and geology of the Flathead Lake region, Montana: Northwest Geology, v. 2, p. 13-20.

Leech, G.B., 1966, The Rocky Mountain Trench: Geological Survey of Canada Paper, p. 307-329.

Levish, D.R., 1997, Late Pleistocene sedimentation in glacial Lake Missoula and revised glacial history of the Flathead lobe of the Cordilleran ice sheet, Mission Valley, Montana: Ph.D. dissertation, University of Colorado, Boulder, 191 p.

McCafferty, A., Bankey, V., and Brenner, K.C., 1998, Montana aeromagnetic and gravity maps and data: U.S. Geological Survey Open File Report 98-333, http://pubs.usgs.gov/of/1998/ofr-98-0333/index.html

Nobles, L.H., 1952, Glacial geology of the Mission Valley, western Montana: Ph.D. dissertation, Harvard University, 125 p.

Nowell, D.A.G., 1994, Gravity studies of two silicic volcanic complexes: M. Phil. thesis, The Open University, Milton Keynes, 193 p.

Nowell, D.A.G., 1999, Gravity terrain corrections – An overview: Journal of Applied Geophysics, v. 42, p. 117-134.

Nyquest, D., 2001, A bedrock model of the Hellgate Canyon and Bandmann Flats area, Montana through constrained inversion of gravity data: M.S. thesis, University of Montana, Missoula, 186 p.

Ostenaa, D.A., Levish, D.R., and Klinger, R.E., 1995, Mission Fault study: U.S. Bureau of Reclamation Seismotectonic Report 94-8.

Pardee, J.T., 1910, The glacial Lake Missoula: Journal of Geology, v. 18, p. 376–386.

Pardee, J.T., 1942, Unusual currents in glacial Lake Missoula: Geological Society of America Bulletin, v. 53, p. 569–600.

Reilly, W.I., 1972, New Zealand gravity map series: New Zealand Journal of Geology and Geophysics, v. 15, p. 3–15.

Sears, J.W., 2001, Emplacement and denudation history of the Lewis-Eldorado-Hoadley thrust slab in the northern Montana Cordillera, USA: Implications for steady-state orogenic processes: American Journal of Science, v. 301, p. 359-373.

Smith, L.N., 2000, Altitude of and depth to the bedrock surface in the Flathead Lake Area, Flathead and Lake counties, Montana: Montana Bureau of Mines and Geology Groundwater Assessment Atlas 2, Map 7, scale 1:150,000.

Smith, L.N., 2004, Late Pleistocene stratigraphy and implications for deglaciation and subglacial processes of the Flathead Lobe of the Cordilleran Ice Sheet, Flathead Valley,

Montana, USA: Sedimentary Geology, v. 165, p. 295-332.

Stalker, J., 2004, Seismic and gravity investigation of sediment depth, bedrock topography and faulting in the Tertiary Drummond-Hall Basin, western Montana: M.S. thesis, University of Montana, Missoula, 63 p.

Steinhauser, P., Meurers, B., and Ruess, D., 1990, Gravity investigations in mountainous areas: Exploration Geophysics, v. 21, p. 161–168.

Stickney, M.C., 1980, Seismicity and gravity studies of faulting in the Kalispell Valley, northwest Montana: M.S. thesis, University of Montana, Missoula, 82 p.

Stickney, M.C., Haller, K.M., and Machette, M.N., 2000, Quaternary faults and seismicity in western Montana: Montana Bureau of Mines and Geology Special Publication 114.

Talwani, M., Worzel, J.L., and Landisman, M., 1959, Rapid gravity computations for two-dimensional bodies with application to the Mendocino submarine fracture zone: J. Geophysical Research, v. 64, p. 49–59.

Wold, R.J., 1982, Seismic reflection study of Flathead Lake, Montana: U.S. Geological Survey Miscellaneous Field Studies Map MF-1433, scale 1:117,647.

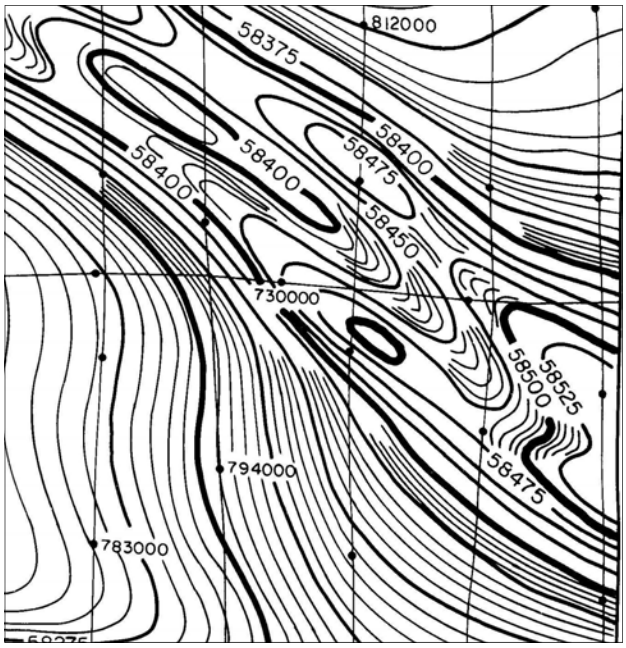
812000
58375
58400
58475
58400
58400
58450
730000
58500
58525
58475
794000
783000

NEW DISPLAY OF THE 1970 FLATHEAD LAKE SEISMIC DATA

Robert W. Lankston
Geoscience Integrations, 1861 35th St. Missoula, MT 59801
rlankston@geogrations.com

Abstract

The seismic data collected on Flathead Lake in 1970 employed recording components that were common for bathymetry and sub-bottom profiling during that era. That particular seismic system, however, was embellished to provide data recording on analog magnetic tape. Data from about 60 km of the 200 km of the original survey have survived on tape. The analog data on tape were digitized and then displayed in seismic section form using color-coded amplitudes. The original data had been displayed in a facsimile format with dots to indicate only those amplitudes above a set threshold, not actual waveforms. The color displays brought out subtleties not previously recognized in the facsimile images.

The success of the initial display of the recovered data invited the application of modern digital processes to reduce multiple reflections and noise phases introduced by the air gun source. While attenuation of the multiples has not been particularly successful to date, bubble oscillations and the first phase of the bubble wave train have been successfully attenuated.

Introduction

In the summer of 1970, Richard Wold, on the faculty of the University of Wisconsin-Milwaukee, and Gary Crosby, a faculty member at the University of Montana, joined forces to conduct a seismic survey on Flathead Lake in northwest Montana. Unfortunately, no report on the survey, such as a thesis or dissertation, gave operational details of the program, and Wold's (1982) paper gave only a few highlights of field operations. Much of the information on the survey presented in the next few paragraphs has been gleaned from communications with people who were familiar with the survey or similar surveys of that time. After 40 years, though, some memories are fading, and details are missing. Some statements are the author's own conjecture.

The project may have been funded, in part, by the Office of Naval Research (ONR), which supported Wold's experiments with marine seismic systems. A snippet of data from Line E of the Flathead Lake survey appears in Figures 4, 6, and 7 in an obscure report to the ONR (Wold, 1976).

In the late 1960's, Wold and his technician, Ronald Friedel, assembled a seismic system for surveying lakes using components readily available in those days. According to Friedel (2011), the basic system was used to survey part of Lake Michigan (1968), Great Salt Lake and Green Bay (1969), Flathead Lake (1970), Bear Lake (1971), and Yellowstone Lake (1972 and 1973). The heart of the system was gear commonly employed for bathymetric work and sub-bottom profiling (Simpkin, 2007). The usual recording medium was a facsimile-style of chart recorder on which the chart paper was "burned" by the electrical current flowing through a stylus whenever the received seismic signal exceeded a set threshold. Each pass of the stylus over the chart paper was equivalent to one seismic trace. While the closely spaced stylus

passes gave an image of the subsurface, it did not record the actual seismic waveforms.

What made my new analysis of the 1970 data possible is the fact that the data were recorded on magnetic tape as well as the traditional chart paper. Not all surveys of that era used magnetic recording. For example, the survey of Lake Tahoe reported by Hyne et al. (1972) did not use magnetic recording.

By 1970, analog recording had been common in the petroleum industry for almost 20 years, and digital recording was rapidly replacing the analog technology. However, the Wold-Friedel system did not use petroleum industry technology for magnetic recording. Instead, they used a reel-to-reel stereo unit of the day that would have been more at home in the audio-visual (AV) laboratory or the music department of a university than on a seismic survey boat (Hess, 2006). Unfortunately, the technical details of the seismic recording system, such as dynamic range, availability of filters and automatic gain control (AGC), whether or not synchronization pulses were recorded, and other details have been lost.

The energy source was a Pneumatic Acoustical Repeater (PAR) "10 in 3"—later called air guns—made by Bolt Technologies. This size of source is still in regular use for surveys in shallow water.

The Flathead Lake survey was conducted over a period of about a week in August 1970, and about 200 km (120 mi) of line were traversed. Line locations were measured by theodolite and sextant methods. According to Wold (1982), some post-acquisition processing was applied to the data on magnetic tape. However, he does not detail the processing. Assuming that the processing was all analog, it was probably limited to bandpass filtering and AGC. Wold's (1976) report to the ONR includes concerns with designing time varying analog operators such as AGC and filters.

The surviving paper seismic sections from the 1970 Flathead Lake survey at the University of Montana include the original field recordings and images from some type of redisplay of the recorded data. These are possibly products from the processing that Wold mentioned in his 1982 paper, and are available for view in the K. Ross Toole Archive of the Mike and Maureen Mansfield Library at the University of Montana. The paper sections have been scanned and will be available on-line sometime in the summer of 2011 through the digital collections website at the University of Montana library. The archive also holds a paper copy of an apparently unpublished bathymetric map that was prepared by Silverman et al. (1971). The map shows Silverman's bathymetry survey lines and the 1970 Wold-Crosby seismic survey lines. An image of the map will also be available on the university website.

An analog tape labeled "Flathead Lake" was discovered at the US Geological Survey library at Woods Hole in 2006. The tale of that discovery and the conversion of the data from its analog form to digital .wav files was reported by Lankston (2007). Additional details of field operations and the recovery of the data are presented at http://www.geogrations.com/Academic/Flathead/History/History1.html.

Figure 1 shows the locations of the six lines of data that are on the tape. This paper describes efforts to generate new images of the subsurface from data recorded along those six lines. The results, in general, show geologic details that were not seen in the facsimile displays of 40 years ago.

The Digital Data

Based on a photograph provided by Richard Wold (2006), the data were recorded on a common studio or audio hobbyist stereo tape recorder. The machine used quarter-inch tape. The tape that was discovered in the USGS library, however, is 0.5 in wide indicating that it is some derivative of the field tape(s). Whether the archive tape includes simple copies of the field data or whether it records the output of some stage of processing is not known. Whatever the case, after transcription from analog to digital form, the data can be displayed with modern seismic imaging tools to show details that were just not available in the original paper recordings.

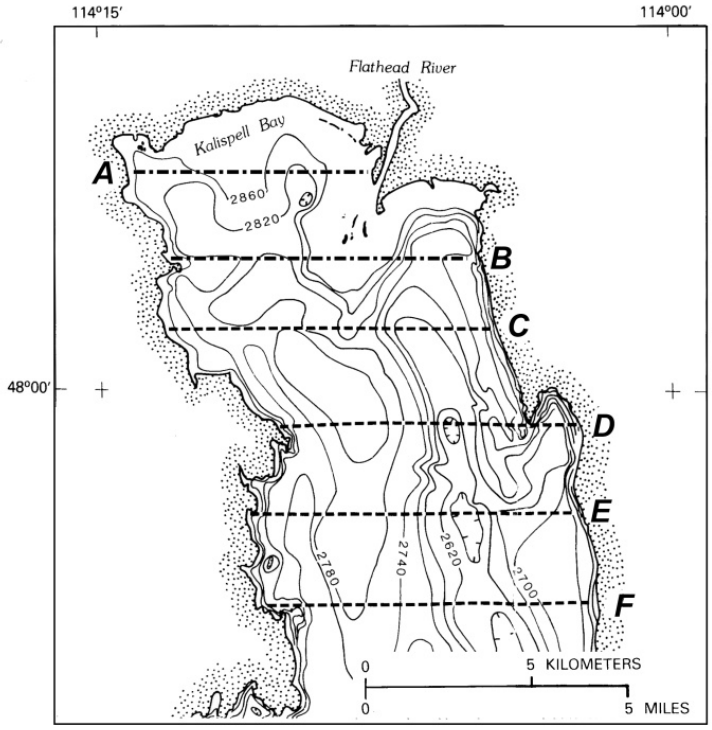

Figure 1. Locations of lines with digital data (after Wold, 1982). This is the northern half of Wold's map showing the locations of the lines that he used in his interpretation (dashed lines). His report shows the seismic data for Line F displayed in the facsimile style. The locations for Lines A and B (dot dash lines) were transcribed from the Silverman et al. (1971) map. Bathymetric contours are in feet. Wold credits the bathymetry to Kogan (1980), however, Kogan's source was the Silverman et al. (1971) map.

Unexpected Color Stripes

Converting the data from their trace-streaming format in the digital image of the analog tape to a digital format recognized by modern seismic processing and display software required some custom programming. Once reformatted, the traces were plotted with color-coded amplitudes using a blue-white-red color scheme. The plot of the (presumably) raw traces showed distinct red and blue bands or stripes across the sections (Fig. 2a). These are the result of the compressions and rarefactions of the air bubble released by the gun as the bubble oscillated during its ascent in the water.

A monochrome analog to these color bands was not seen in the original facsimile displays for two reasons. First, the blue bands, the ones relating to negative signal amplitudes would not have been displayed at all. Second, the red bands, from the positive signals, would have been manifested only as a dot. All dots were the same, i.e., they carried no amplitude information other than the indication that a signal exceeded a threshold value.

Paul Chelminski (2011) mentioned that Wold attenuated air bubble noise like this with analog highpass filtering, probably during data acquisition. Highpass filtering worked reasonably well for attenuating the bubble oscillations in the case of the Flathead Lake data. However, the color striping did not seem to be truly band-limited, and a different approach was chosen for attenuating this phenomenon.

The process began with summing all of the traces in a seismic line. In this stacking proc-

ess, the components of the striping added constructively while the more randomly arriving geologic signals added to zero, at least, in principle. The normalized, stacked trace was then subtracted from all of the traces in the line. Figure 2b shows the result of the stack and subtract process. Some alternatives to this process might yield better results, but they were not investigated. For example, instead of summing all of the traces in a line to create a single stacked trace, the stacked trace could consist of some number (n) of traces adjacent to each side of the input trace. However, defining an optimum n might be difficult because the necessary randomness of the geologic signals would be reduced, leading to a higher number of constructively summed seismic reflection signals. This means that more of the desired seismic signal would be removed along with the unwanted signal during the subtraction process.

In Line F (Fig. 2) as with all of the other lines, the striping pattern seems to trail off at the start of the line, the west (left) end in the case of Line F. The origin of this is not known. It might be related to the air pressure that was available to the source, or it might be related to the depth of the source changing as the boat came up to speed at the start of the line. Bandpass filtering was somewhat more effective than the stack and subtract process in removing the striping in these line startup segments. Summing over a set of localized traces might have been an effective tactic in these line start segments.

Bubble Pulse Removal

The next issue addressed was removal of the first phase of the bubble pulse. The first phase of the bubble pulse in this survey occurs at 26 ms after primary reflections like the water bottom and the tentatively-interpreted Precambrian Belt floor of the basin. Wold (1982) interpreted the latest strong reflection as acoustic basement and equated that with the Belt "bedrock". However, the present redisplay of the data has allowed that interpretation scheme to be questioned. In some locations, that acoustic basement might represent the top of the Tertiary section or a surface related to Bull Lake glaciation (Hofmann, 2011) suggesting that the actual bedrock floor of the basin is not seen in the new sections except at the western and eastern ends of the seismic lines.

Whatever the geologic explanation, the bubble pulse is easily visible after the strong reflections, and one can, therefore, expect that it follows the weaker reflections, also. The time delay between the primary and the "ghost" reflection is 26 ms, which is consistent with data on air gun source wavelets provided by Paul Chelminski (2011). For sources discharged at depths of one meter or less, the first pulse of the bubble wavetrain occurs 25-30 ms after the primary pulse. A photograph provided by Richard Wold (2006) shows the pontoon from which the air gun was suspended. The photo suggests that the gun was suspended less than 1 m below the surface.

The bubble pulse phase is clear even in the small image in Figure 2b. It can be easily traced as a relatively bright red event following the water bottom reflection between shotpoints 240 and 520. Experiments to remove this phase with classical gapped deconvolution were not successful.

As noted above, the Wold-Friedel seismic system was employed in a study at Yellowstone Lake. Otis et al. (1977) gave some details of the Yellowstone Lake survey, e.g., 4 s shot intervals and a 9 km/h (5.6 mi/h) boat speed. This agreed with the shot interval on the Flathead Lake archive tape and the apparent boat speed given the shot interval time, the number of traces in a line, and the line

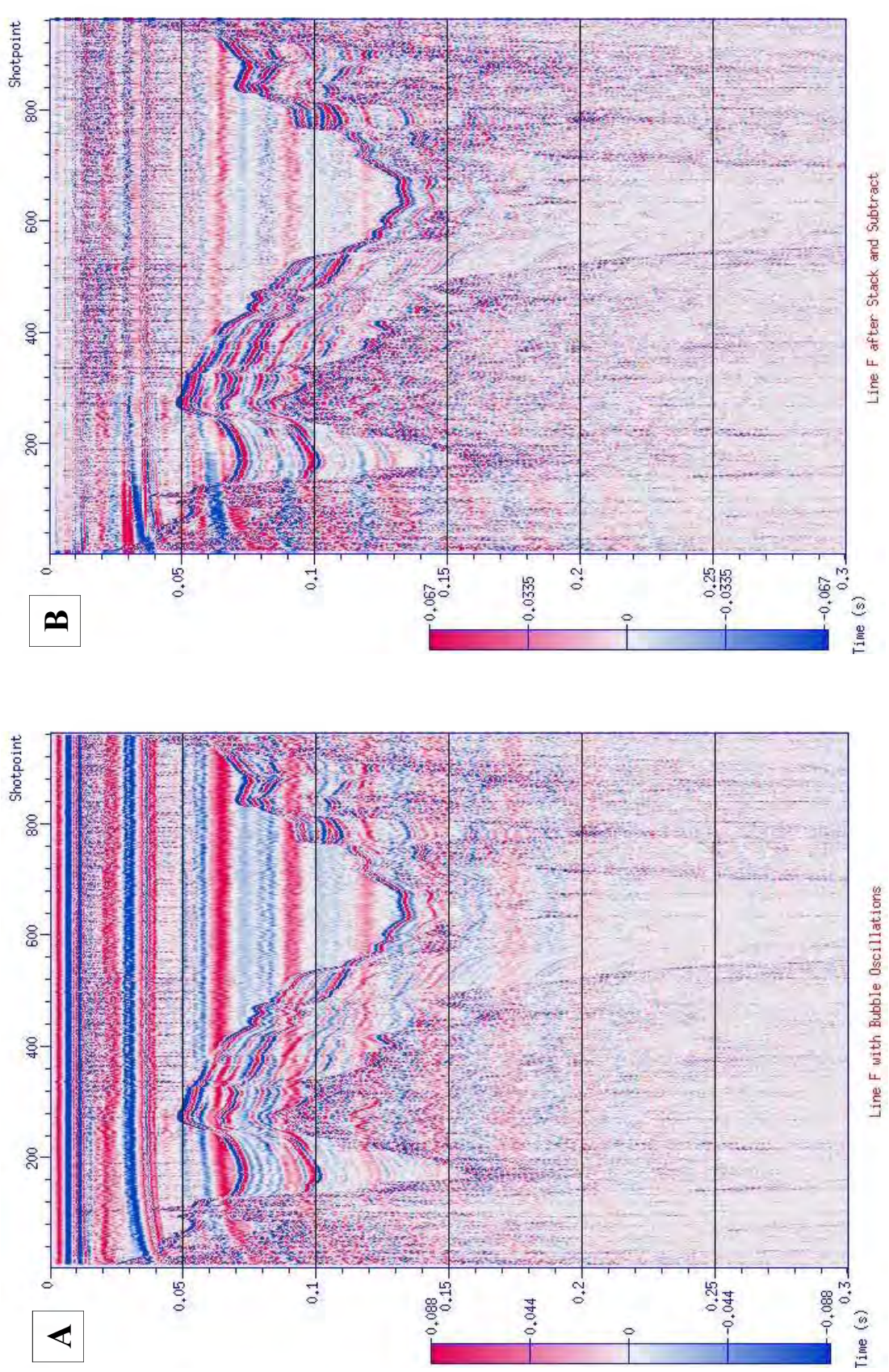

Figure 2. Line F. Both images are plotted west (left) to east (right). The shotpoint interval is nominally 10 m. The color bars indicate that red is positive amplitude and that blue is negative amplitude. (A) Raw data with horizontal bands of red and blue caused by bubble oscillations. (B) Data after removal of oscillations with the stack and subtract process described in the text. The bubble pulse that follows the strong water bottom reflection by 26 ms is the red event clearly visible across much of the line.

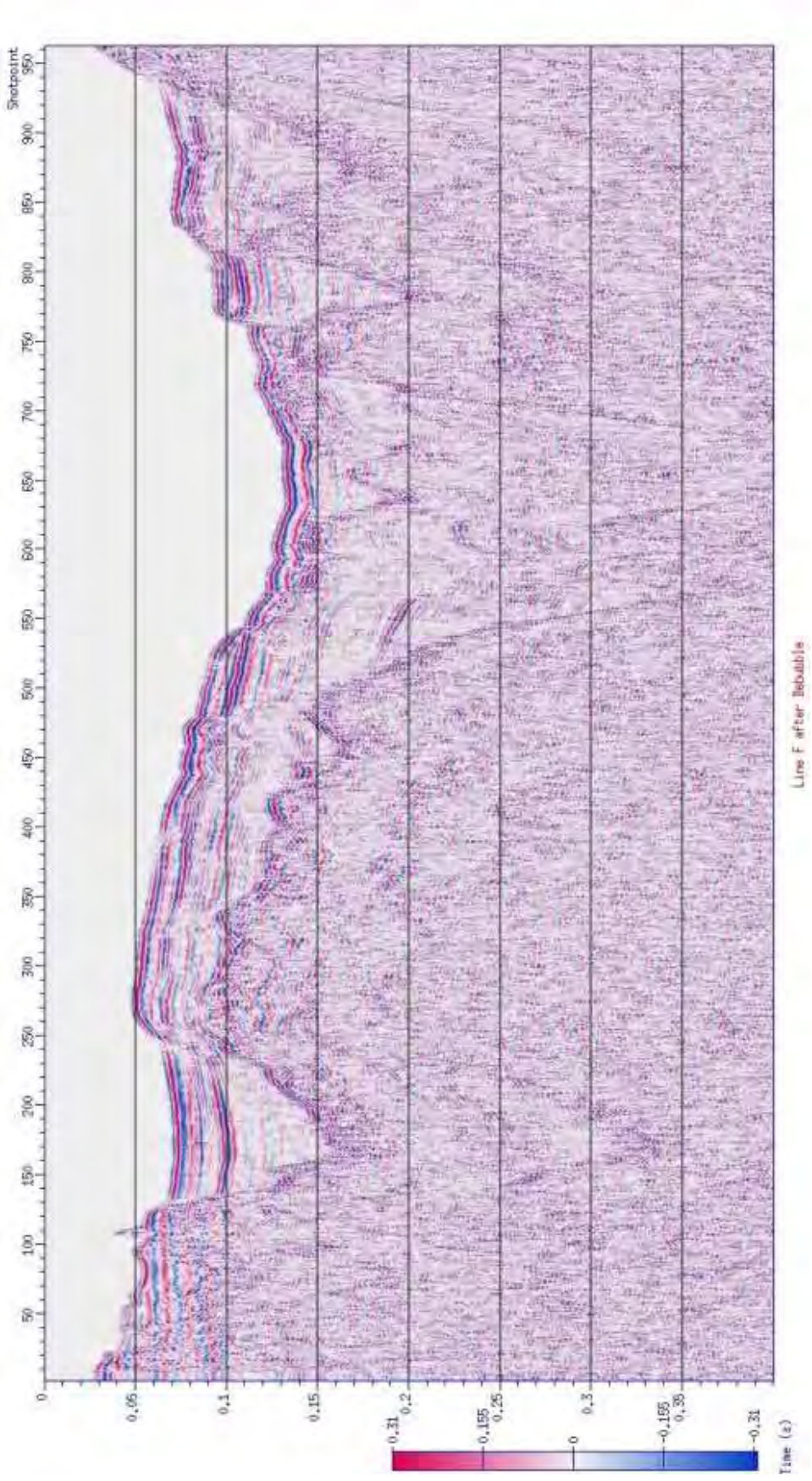

Figure 3. Line F after removal of the bubble pulse. The bubble event that was obvious in Figure 2b is significantly attenuated. Vertical exaggeration is approximately 25x.

length scaled from the Wold (1982) map. The 4 s shot interval and the nominal 9 km/h boat speed yields reflection points spaced at 10 m intervals.

In addition to the operational details, Otis et al. (1977) mentioned the bubble pulse issue and stated that they attenuated that phase using homomorphic deconvolution, which was described in detail in Otis and Smith (1977).

The homomorphic process appeared to work fairly well on the Flathead Lake data. It seems to be dependent on the number of traces used in the summation in the frequency domain. Lines C, D, E, and F, which each have about 1000 traces, showed better results than Line A, which has less than 400 traces. Because the process depends on a stacking process analogous to that used to remove the bubble oscillations, albeit in the frequency domain, one would expect the process to work better with more traces so that the random contributions to the air gun wavelet by the geologic reflections add to zero.

Figure 3 is an image of Line F after removal of the bubble pulse. Some vestiges of the bubble phase that followed the water bottom reflection can still be seen, but it is largely gone, which suggests that particular noise phase is no longer following the lower amplitude reflections.

Water bottom multiples are a serious problem in about half of Line C and parts of Line B. Like the bubble pulse, even where the water bottom multiple is not as obstructive as in the Line C case, it is still causing some degradation to true geologic events. Unfortunately, efforts to attenuate the water bottom multiples using gapped deconvolution have not produced dramatic results to date.

The Results Package

Images of the results of the three main processing stages described here can be viewed in the poster display at the 2011 TRGS field conference. Digital files of the raw data in SEG-Y format can be requested from the author via email (rlankston@geogrations.com).

Summary

Richard Wold's insightful integration of magnetic tape recording into an otherwise standard sub-bottom profiling system that generated only paper charts yielded some data that survived from the 1970 Flathead Lake seismic survey. Those data can be displayed with modern tools. By being able to display color-coded amplitudes, geologic details that were not rendered in the displays generated in the 1970's can be seen. With the data in digital form, reflections can be enhanced through filtering, gain functions, and various forms of deconvolution. Key events, such as the water bottom reflection, can be timed. For example, the arrival time of the water bottom reflection can be trivially doubled to make a new surface that shows the expected arrival time of the water bottom multiple. A phase arriving at that time in the seismic section is, therefore, suspect. It could be a primary reflection, but it might be a multiple. This technique was particularly useful in verifying the bubble pulse phase. In the case of the bubble pulse, the water bottom reflection time was increased by 26 ms, and that new surface was plotted on the sections.

Finally, with these few seismic images of the section below Flathead Lake, one might wonder what details could be extracted from data recorded with today's instruments. Positioning with GPS would be virtually absolute compared to the theodolite and sextant methods used in 1970. Multichannel recording would provide data from which multiple re-

flections could be more easily removed through CMP stacking or other multichannel process, and the velocity analysis for CMP stacking would provide more accurate estimates of the depths to reflectors below the lake bottom.

Acknowledgements

I am grateful to many people for helping me to reconstruct the story of the 1970 Flathead Lake seismic survey. Communications with Ronald Friedel, Peter Simpkin, and Paul Chelminski are noted in the references and were most informative. Richard Wold's photographs helped me to visualize some aspects of the field operations and provided insight during the analog to digital transcription. John Stockwell of Colorado School of Mines provided significant mentoring on the use of Seismic Unix (SU), and he did a lot of new programming in early 2011 to provide stable routines for the homomorphic deconvolution process. Michael Hofmann's belief that the new displays would be valuable in resolving structural and stratigraphic details in the basin helped to keep my enthusiasm up through tedious hours of experimentation with parameter settings. Debbie Smith (MBMG) reviewed the manuscript.

References

Chelminski, P., 2011, personal correspondence.

Friedel, R., 2011, personal correspondence.

Hess, R.L., 2006, personal correspondence.

Hofmann, M., 2011, personal communication.

Hyne, N.J., Chelminski, P., Court, J.E., Gorsline, D.S., and Goldman, C.R., 1972, Quaternary History of Lake Tahoe, California-Nevada: Geological Society of America Bulletin, v. 83, p. 1435.

Kogan, J., 1980, A seismic sub-bottom profiling study of recent sedimentation in Flathead Lake, Montana: M.S. thesis, University of Montana, Missoula.

Lankston, R.W., 2007, Revisiting the 1970 Flathead Lake seismic survey: The Leading Edge, v. 26, p. 1058.

Otis, R.M, and Smith, R.B., 1977, Homomorphic deconvolution by log spectral averaging: Geophysics, v. 43, p. 1146.

Otis, R.M, Smith, R.B., and Wold, R.J, 1977, Geophysical surveys of Yellowstone Lake, Wyoming: J. of Geophysical Research, v. 82, p. 3705.

Simpkin, P., 2007, personal correspondence.

Silverman, A., Pevear, D., and Prahl, S., 1971, Bathymetry of Flathead Lake: unpublished map available at Mansfield Library, University of Montana, Missoula.

Wold, R. J., 1976, Marine geophysical instrumentation: final report for period 1 April 1970 thru 30 June 1976: US Office of Naval Research.

Wold, R. J, 1982, Reflection study of Flathead Lake, Montana: U.S. Geological Survey Miscellaneous Field Study MF-1433.

Wold, R. J., 2006, Personal photographs of field operations and equipment: unpublished, available to view at http://www.geogrations.com/Academic/Flathead/History/History1.html.

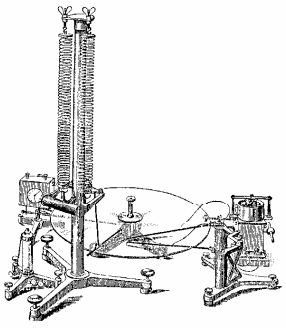

STREAM TERRACES ALONG THE CLARK FORK RIVER FROM NINEMILE TO THE FLATHEAD RIVER, MONTANA

Larry N. Smith, Shannon Wilson, and Shawn Christensen
Department of Geological Engineering, Montana Tech of the University of Montana
1300 W. Park St., Butte, MT 59701 • lsmith@mtech.edu

Introduction

Downstream from the Missoula Valley, the Clark Fork River has incised through glaciolacustrine and alluvial sediments and bedrock to form a series of narrow-canyon and wide-valley reaches. Silty lake-bottom deposits from of the most recent stand of Glacial Lake Missoula directly underlie high benches above the river. They silty, glaciolacustrine deposits are known as the "Lake Missoula beds" (after Langton, 1935), and they are characterized by rolling topography, which is most obvious in the areas where trees have been cleared for agriculture. Below the benches and above the Clark Fork River are many stream terraces, which record previous positions of the stream valley floors.

Stream terraces can provide evidence of the history of, and mechanisms affecting, downcutting over time. Terraces are commonly thought to be either paired or unpaired. Paired terraces correlate locally across the valley floors and sometimes great distances upstream and downstream. Paired terraces are thought to form during relatively long periods of stability interrupted by relatively short periods of downcutting along a stream profile, and represent the remnants of the same flood plain or valley floor. In contrast, unpaired terraces have no corresponding terrace on the opposite side of the valley, and are difficult to correlate up or downstream. They suggest that the river was downcutting at the same time as it was shifting across the valley, leaving behind remnants of valley floors at various altitudes. Quaternary stratigraphy (Smith, 2006) and geologic mapping have been performed along the Clark Fork River from Missoula to Paradise (Lonn and McFaddan, 1999; Lonn and Smith, 2005; Lonn and others, 2007), however detailed mapping or correlation of stream terraces along the Clark Fork River has not been done. Previous geologic maps have grouped stream terraces at various heights above the river into a single unit.

The purpose of this study was to:

Portray the distribution and number of stream terrace levels below, and possibly above, outcrops of the Lake Missoula beds along a portion of the Clark Fork River (fig. 1)

Correlate terraces, if possible, and determine whether they are either parallel to or diverge from the modern channel

Interpret the downcutting history by represented by the terraces

Methods

This study focused on mapping the altitude and dimensions of each stream terrace along the Clark Fork River; the locations were then transposed onto a longitudinal valley profile. Black and white stereo pairs were obtained from the repository at the Montana Bureau of Mines and Geology in Butte, MT. Various flight lines were available for portions of the study area, from about five km west of Huson, MT to about

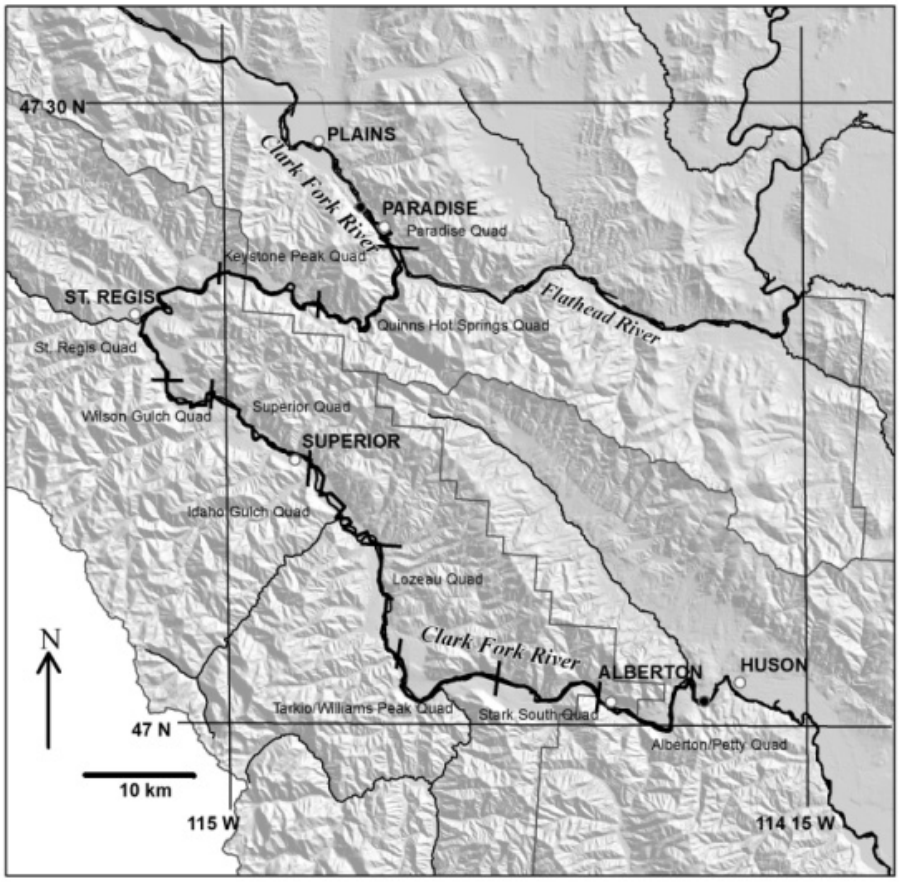

Figure 1. The Clark Fork River study reach is shown by a heavy black line along the river from near Huson to Paradise. Locations of quadrangles and their boundaries indicated by short black lines; base is a hillshaded SRTM digital elevation model.

two km west of Paradise, MT (fig. 1). Source flight lines include: GS-VAI (8/5/1955 and 10/16/1954) at a scale of 1:47,200 and DYR-1DD (9/19/1963) at a scale of 1:24,000. These photos were used in stereo to identify the mapping units. The mapping units were either plotted directly onto 7½-minute topographic quadrangle maps, or digitized using ESRI's ArcMap software.

By interpreting air photos, about twice the number of stream terraces were identified that had been included on previous maps (Lonn and McFaddan, 1999; Lonn and Smith, 2005; Lonn and others, 2007). Not only were more terraces mapped, but terrace levels at different altitudes could be differentiated. Previously mapped terraces typically have a few meters of fluvial sediments above an erosional bench (or strath) (Lonn and others, 2007; Smith, 2006); some landforms are locally stripped of sediment; and fewer still are "fill terraces", where the terrace is underlain by 10's of meters of sediment, especially in the area downstream of Superior. Areas that appeared to be routinely flooded, with recognizable channel topography, were all near the contemporary stream level and were interpreted to be modern floodplains, and not stream terraces.

In order to locate stream terraces on the stereo photographs, we used abrupt changes in the topography—either an active or ancient cut bank—to denote terrace boundaries. Changes in vegetation, such as tree lines at terrace boundaries, were useful in some areas. Human modification of terraces is common, obscuring the original surface and making mapping difficult in some places. Transportation corridors for the Burlington Northern Santa Fe tracks and Interstate 90 were built on this system of terraces, and local terrace remnants were excavated during their construction. In these areas the natural edges of the terraces had to be inferred. Stream terraces are characteristically planar, so relatively flat areas were interpreted to be terraces.

An axial valley profile along the Clark Fork River was plotted in ArcMap using digital elevation model topographic data (SRTM, 30 m horizontal grid data, from http://eros.usgs.gov/). The profiles generated from ArcMap 3DAnalyst were placed in Microsoft Paint and stream terraces and river levels were identified. Although it roughly followed the river valley, the line of profile was locally drawn to intersect terraces, thus expanding the horizontal dimension. Later, the profile was horizontally compressed so that it represented down-valley gradients. The river level was drawn by connecting the lowest portions of the profile. The positions of the Lake Missoula beds and a few other mapped features were projected onto the profile. The total length and path along the river is illustrated in Figure 1.

Results

Lake Missoula beds

The Lake Missoula beds along the Clark Fork have been mapped previously (Lonn and Smith, 2005; Lonn and others, 2007). The range in altitudes of the deposits shown on Figure 2 represents the upper and lower positions of the deposits in local areas. These wide ranges are due to not only thickness of the beds, but to the draping of silts across the valley sides. The ranges represent uncertainty in the altitude of the valley bottom where. The lake bed deposits range in altitude from 915 m near Huson, MT, to 815 m near St. Regis, and 760 m near Paradise, MT. There are reaches where deposits are uncommon, such as between St. Regis to Paradise, due to the narrowness of the Clark Fork River canyon. Between Paradise and Huson, the Lake Missoula beds are at higher altitudes than the stream terraces. In the Paradise area, near the confluence of the Clark Fork and Flathead rivers, the lakebeds are close to the level of the modern stream.

Terraces

Stream terraces are variably preserved in the Clark Fork River canyon. Some wider reaches of the valley contain as many as three distinct levels of stream terraces that can be correlated for downstream distances over 5 km, as shown on the Lozeau, Tarkio/Williams Peak, Alberton, and Stark South 7 ½-minute quadrangles (fig. 2). In contrast, the narrower canyon reaches developed on bedrock of the Belt Supergroup, for example in the Lozeau and Keystone Peak 7½ minute quadrangles, have limited stream terrace preservation.

Stream terraces thus far recognized along the Clark Fork River are almost all located below the altitude of the Lake Missoula beds, which represent the valley grade prior to the last draining of Glacial Lake Missoula. The altitudes of some terrace remnants overlap the lowest estimated level of the Lake Missoula beds in the reaches between Alberton and Superior. The positions of the terraces show that they were downcut into the Lake Missoula deposits, or into the bedrock underlying the lake bed (fig. 2). Correlations of distinct terrace levels are problematic. As shown on Figure 2, the terrace remnants span the entire vertical distance between the modern stream level and the Lake Missoula beds. Distinct terrace altitudes extend downstream for distances of less than 10 km.

Scabland and other indicators of catastrophic discharge

Scabland topography was mapped on the bedrock surface at a few places near the Clark Fork River, but they were not included on the previous geologic maps (Lonn and Smith, 2005; Lonn and others, 2007). Four locations with scabland landscapes are shown on Figure 2. Scabland topography is

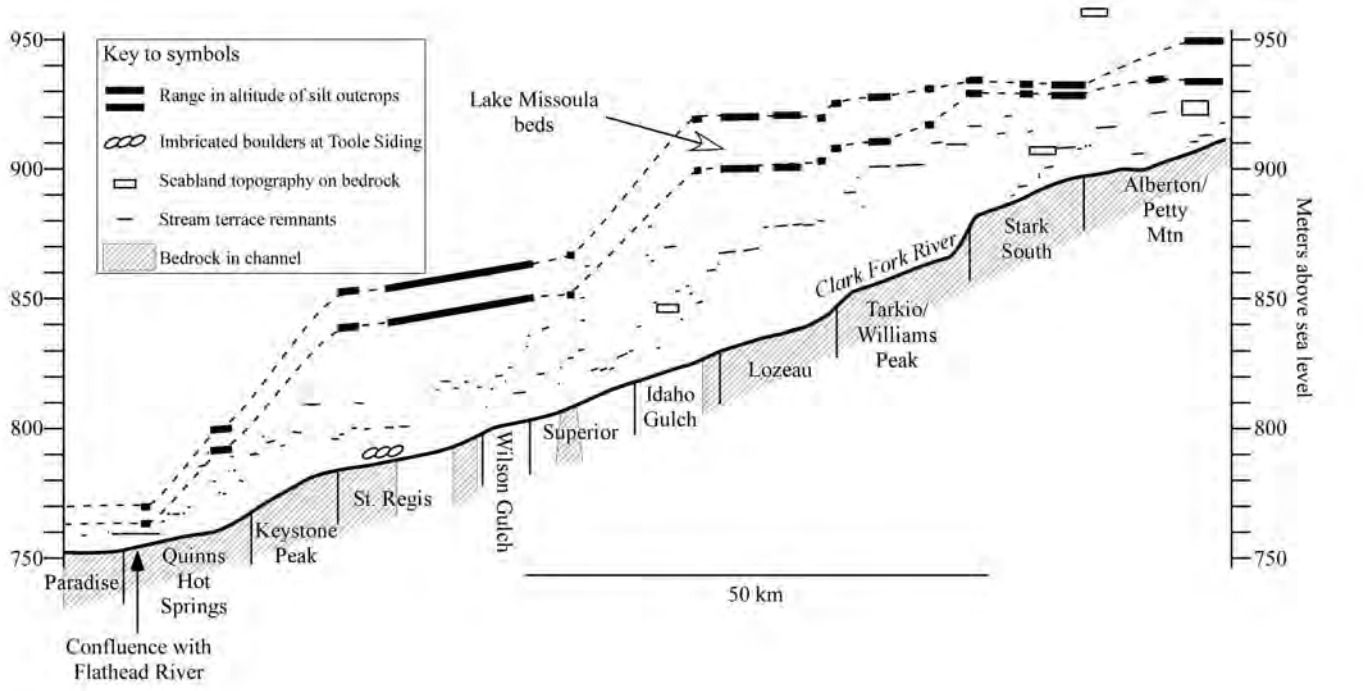

Figure 2. Vertically exaggerated longitudinal profile of the Clark Fork River valley from near Ninemile to near Paradise, MT showing an irregular canyon reach of the river. Former valley bottoms are shown by the position of Lake Missoula bed silts and remnants of stream terraces (short black lines above the Clark Fork River). The positions of important deposits or erosional features and where the stream is on bedrock are shown; the borders of USGS 7½-minute quadrangles are shown beneath the stream profile.

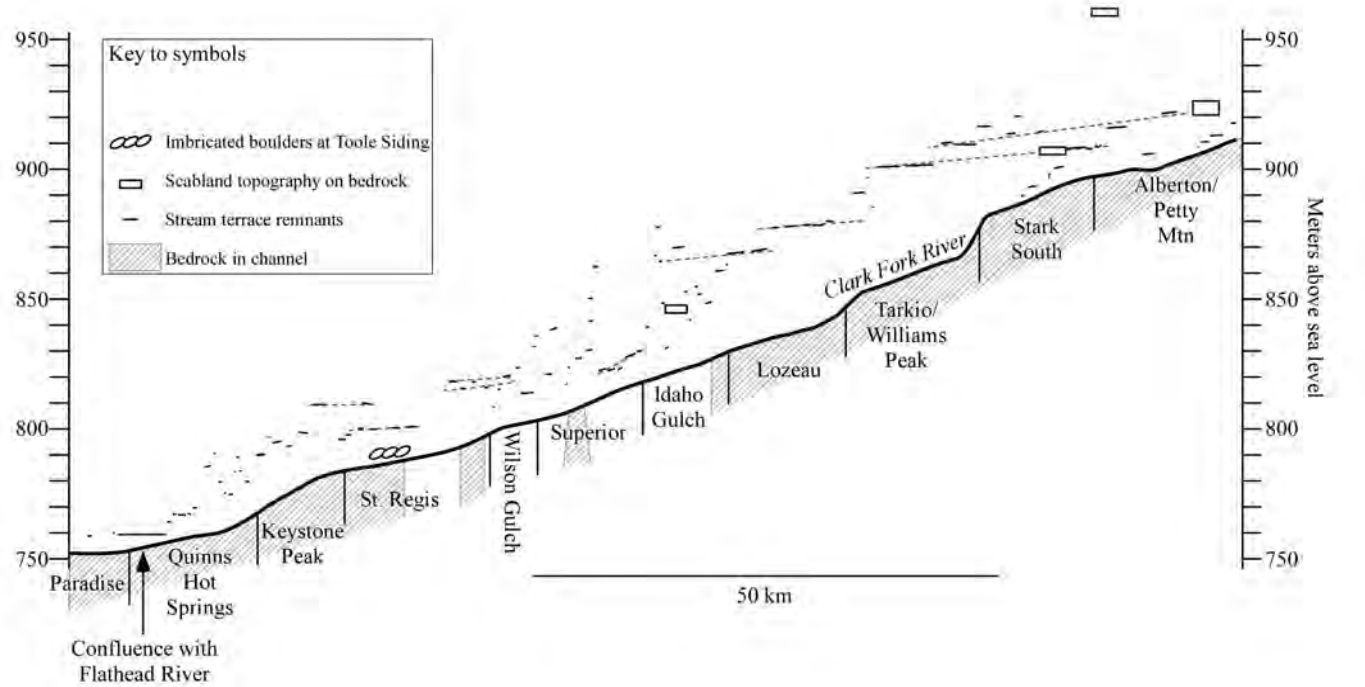

Figure 3. Longitudinal valley profile that shows correlation scheme number 2, where the slopes of terrace remnants are assumed to be important and remnants can be correlated for short distances in the upper reaches. See text for explanation.

distinguished by internally drained, jagged depressions formed by vertical plucking of resistant bedrock. It was first recognized in Washington State where it developed on basalt flows. Its formation is attributed to high velocity flows that produce extremely high vertical forces on the bed (Bretz, 1969).

At the Toole Siding downstream from St. Regis, there is an accumulation of 2–6 m-diameter boulders from above the railroad tracks to river level (fig. 2). Some of the boulders are in place and imbricated, at a distance of about 10 m above the river. These boulders must have been deposited during catastrophic drainage of the glacial lake (Smith, 2006).

Discussion

The Lake Missoula beds illustrate the position of the last lake bottom about 13,000 years ago (Pardee, 1910, 1942; Smith, 2006). Since all of the Clark Fork River terraces are below this level, they must have been formed in the last 13,000 years. Canyon width is a major factor affecting the preservation of stream terraces and Lake Missoula beds. In areas where the canyon floor is broad, the larger terrace remnants were preserved (shown as the longer lines in fig. 2). In areas where the canyon floor is narrow, the terraces either did not develop or have been eroded away. In these narrow sections of the canyon, the Clark Fork River flows over bedrock, and terraces and Lake Missoula beds are rare.

Terrace correlation schemes

Terraces cannot be uniquely correlated based on topographic position alone; however, we propose three correlation schemes that may explain patterns in the terraces shown in Figure 2.

Scheme one is based on the assumption that the distribution of terraces is essentially random, and the terraces cannot be correlated. This scheme requires that the terraces are unpaired, implies that the downcutting occurred throughout the study reach at essentially the same time, and that there were no periods of stability on either local or regional scales.

Scheme two (shown in Figure 3) recognizes similar slopes and heights of terrace remnants over distances of 10 to ~25 km. This concept assumes that the portrayed downstream slopes of individual terrace remnants are significant and form a pattern. Just as in scheme 1, the terrace levels cannot be correlated throughout the study reach; however, local correlations can be made. It suggests that there were periods of relative stability primarily in the upstream reaches of the canyon system, and that these valley gradients were less than the present gradient of the Clark Fork River (upstream half of fig. 3a). The best examples of these patterns are between the Lozeau and Alberton/Petty Mountain quadrangles where large terrace remnants appear to be co-linear in valley profile, and are subparallel to the valley floor represented by the Lake Missoula beds (figs. 2 and 3). The inability to correlate terrace levels in the reach downstream of the Lozeau quadrangle suggests that this reach was unstable, and that downcutting may have been continuous. As downcutting progressed, the higher stream gradient migrated upstream.

Figure 4 illustrates another scheme that recognizes apparent groupings of terrace remnants, in this case the correlated terraces individually diverge in an upstream direction from the modern stream profile. Four, to possibly six, sets of terraces can be correlated based on this scheme, which assumes that the downstream slopes of individual terrace remnants are not significant because

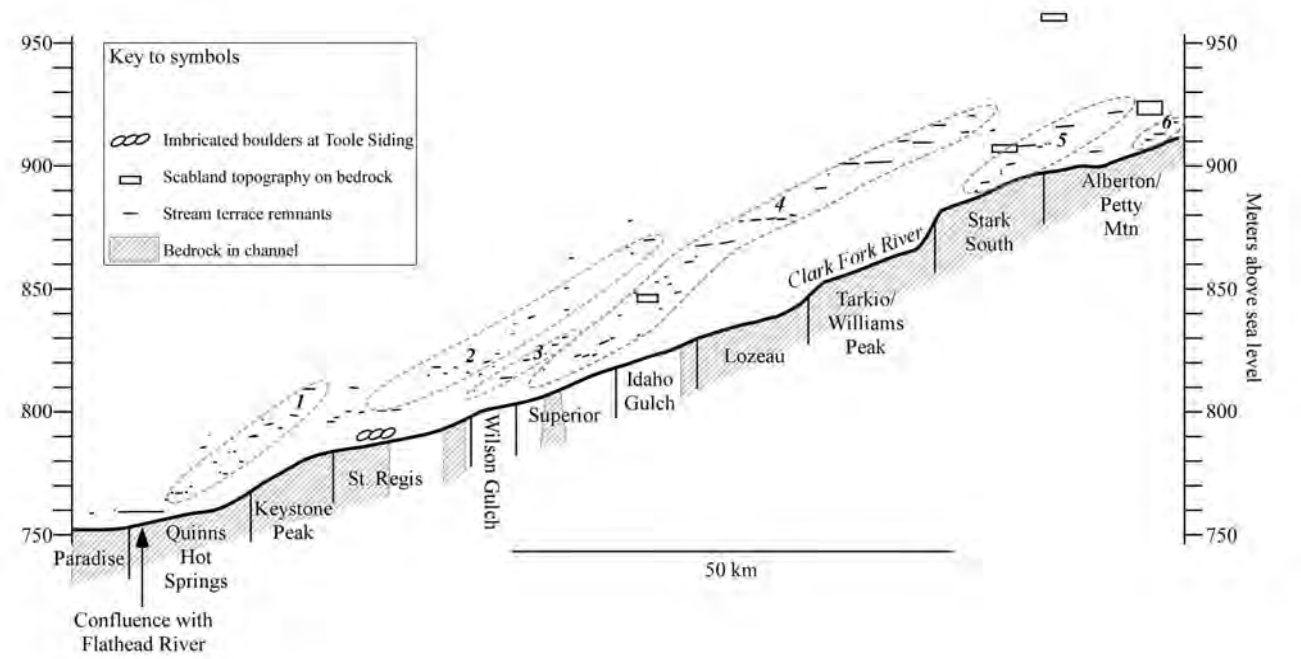

Figure 4. Longitudinal valley profile that shows correlation scheme number 3, where the groupings of terrace remnants are assumed to be important. See text for explanation.

they do not accurately portray the valley profile. Rather, the terrace groupings shown in Figure 4 are better representations of valley profiles. These problems could be explained by the difficulty in projecting remnants to the plane of section from different sides of the river, inclusion of depositional surfaces and those stripped of sediment, and that the longitudinal slopes may have had an irregular, step-like profile.

The correlations shown in Figure 4 can be described as follows. Terrace set 1 projects to near the modern stream level near the confluence of the Flathead and Clark Fork rivers; sets 2, 3, and 4 begin near the upstream end of a steep reach near St. Regis; and sets 5 and 6 are near a steep reach of the valley in the Stark South and Alberton/Petty Mountain quadrangles (fig. 4). The valley profiles of these terrace sets are nearly parallel to the lake bottom profile represented by the Lake Missoula beds in the lower half of the study reach. These correlations suggest that downcutting through the Lake Missoula beds occurred by a series of knickpoint recessional events. That is, set 1 is the oldest and farthest downstream. It was initiated by base-level lowering. Sets 2–6 then developed sequentially in an upstream direction as the river cut down to its current level. Under this correlation scheme, the terrace sets decrease in age from 1–6, and each represent a period of some stability during downcutting of its particular reach.

Timing of terrace development

No age control exists, other than the stratigraphic argument that all of the terraces are younger than the Lake Missoula beds. However, the occurrence and position of scabland erosional features and imbricated boulders at and near modern river level provide significant constraints on the timing of incision and terrace development. Estimation of flow velocities needed to produce scablands and imbricated boulders show that they could only

be formed during catastrophic drainage of Glacial Lake Missoula (Baker, 1973; Alho and others, 2010). The occurrence of large boulders in the Clark Fork River at Toole Siding indicate that no significant downcutting of the river has occurred in this area since the last drainage took place. Additionally, the three areas of scabland topography below the level of the Lake Missoula beds in the Idaho Gulch, Stark South, and Alberton/ Petty Mountain quadrangles (fig. 2) show that the Clark Fork has not cut down more than 15-20 m since the last lake drained (Smith, 2006). Thus, downcutting and terrace formation was essentially completed in the days to weeks it took for the lake to drain.

Refinement of terrace correlation will increase our understanding of how the catastrophic draining took place. For instance, the periodically retreating knickpoint scheme (fig. 4) suggests terrace formation during times of relative stability was interspersed with times of rapid erosion and knickpoint retreat. Unsteady retreat could be explained by complex draining of the glacial lake, as water is backed up behind constrictions and flow is routed differently as controlled by the complex bathymetry of the lake basin (e.g. Alho and others, 2010).

Conclusions

The black and white stereo pairs used in this study revealed numerous remnants of stream terraces along the Clark Fork River. The stream terraces are better developed (and preserved) in areas where the canyon floor is broad, and smaller and less evident where the canyon is narrower. All recognized terraces are at or below the level of the Lake Missoula beds, and they have all developed since the last draining of Glacial Lake Missoula, about 13,000 years ago.

The terraces are distributed either randomly or in a complex pattern along the reach from Ninemile to Paradise (depending on correlation schemes). The terraces do not represent sets of simple terraces indicative of periodic downcutting along the study reach. Given just geomorphic position, the terraces may be random and non-correlative, or they could be correlated in different ways. Two possible correlation schemes discussed in this paper, which cannot be proven or disproven given the present data, result in divergent upstream and divergent downstream patterns over parts of the study reach. Outcrops of imbricated boulders and scablands indicate most of the terraces formed during draining of the last Glacial Lake Missoula, possibly in a time period of a few days.

Further work will need to be done to test each of these three different correlation schemes. Correlation of the cut surfaces below terrace deposits may prove to be more useful to distinguish subtleties. Additionally, relative or numerical age-dating of surfaces and sediments may support or disprove stratigraphic arguments and geomorphic correlation schemes proposed here.

Acknowledgements

Drainage basin mapping and measurements were carried out as part of the 2011 Photogeology and Geomorphology class at Montana Tech. Computer facilities and software licenses provided by Montana Tech were critical to project completion. The manuscript benefited from a detailed review by Marie Garsjo.

References

Alho, P., Baker, V., and Smith, L.N., 2010, Paleohydraulic reconstruction of the largest Glacial Lake Missoula draining(s): Quaternary Science Reviews, v. 29, p. 3067-3078.

Baker, V.R., 1973, Paleohydrology and sedimentology of Lake Missoula flooding in Eastern Washington: Geological Society of America Special Paper 144, p. 1-79.

Bretz, J.H., 1969, The Lake Missoula floods and the Channeled Scabland: Journal of Geology, v. 77, p. 505-543.

Langton, C.M., 1935, Geology of the northeastern part of the Idaho Batholith and adjacent region in Montana: Journal of Geology, v. 43, p. 27-60.

Lonn, J.D., and McFaddan, M.D., 1999, Geologic map of the Wallace 30′ × 60′ quadrangle: Montana Bureau of Mines and Geology Open-File Report 388, scale 1:100,000.

Lonn, J.D., and Smith, L.N., 2005, Geologic map of the Tarkio and Lozeau 7.5′ quadrangles, western Montana: Montana Bureau of Mines and Geology Open-File Report 516, scale 1:24,000.

Lonn, J.D., Smith, L.N., and McCullloch, R.B., 2007, Geologic map of the Plains 30' x 60' quadrangle, western Montana: Montana Bureau of Mines and Geology Open-File Report 554, 43 p., scale 1:100,000.

Pardee, J.T., 1910, The glacial Lake Missoula, Montana: Journal of Geology, v. 18, p. 376-386.

Pardee, J.T., 1942, Unusual currents in glacial Lake Missoula, Montana: Geological Society of America Bulletin, v. 53, p. 1569-1599.

Smith, L.N., 2006, Stratigraphic evidence for multiple drainings of glacial Lake Missoula along the Clark Fork River, Montana, USA: Quaternary Research, v. 66, p. 311-322.

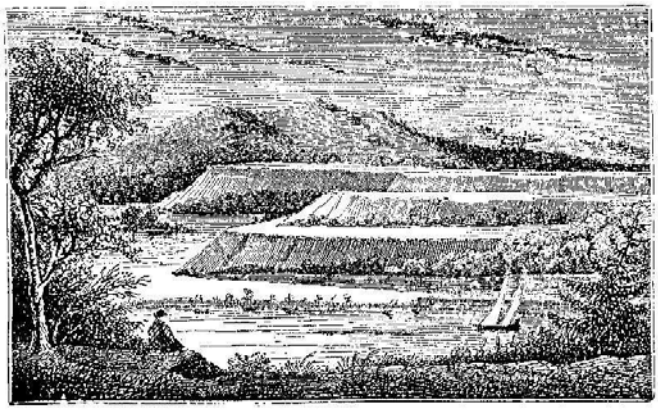

THE ALBERTON-FRENCHTOWN SEISMIC ZONE

Michael Stickney
Montana Bureau of Mines and Geology, Butte, MT 59701
mstickney@mtech.edu

The Alberton-Frenchtown seismic zone (AFSZ) is a recently recognized zone of seismicity in west-central Montana along the western margin of the Intermountain Seismic Belt (Stickney and Bartholomew, 1987; Smith and Arabasz, 1991). The AFSZ lies within the Lewis and Clark zone, an ancient 400 km-long, WNW-trending zone of faulting and deformation that extends from the Helena, MT area to Coeur d'Alene, ID, which includes 12 major faults with up to 28 km of right-lateral displacement (Wallace et al., 1990) since early Tertiary (Sears and Hendrix, 2004). Small- to moderate-magnitude earthquakes associated with the Intermountain Seismic Belt occur throughout the eastern half of the Lewis and Clark zone between Missoula and Helena, but are not obviously associated with mapped Lewis and Clark zone faults. In contrast, the western half of the Lewis and Clark zone, west of Missoula

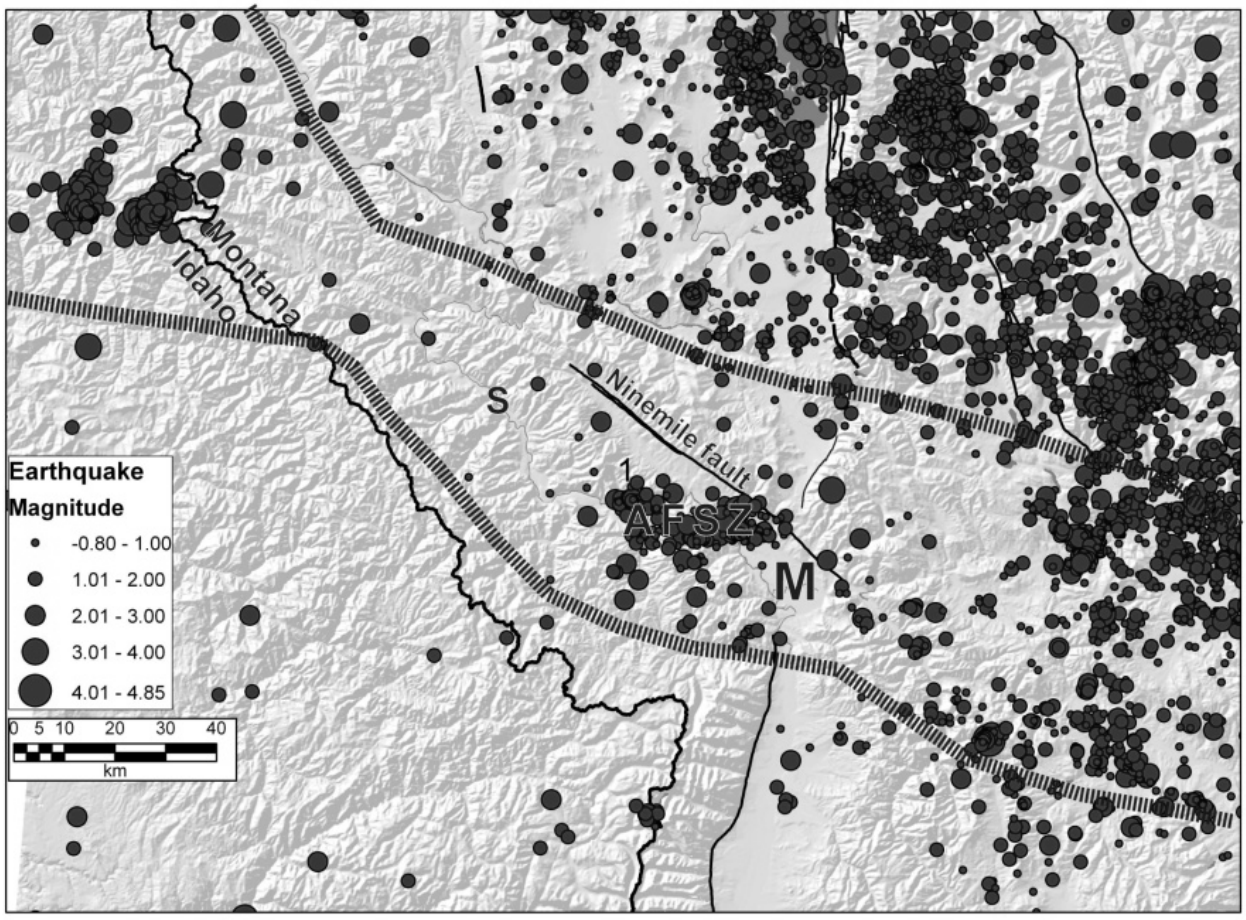

Figure 1. Earthquake epicenters from the Montana Regional Seismograph Network and Quaternary faults for west-central Montana. The Alberton-Frenchtown seismic zone (AFSZ) is the prominent cluster of seismicity northwest of Missoula (M). "S" indicates the town of Superior. The Lewis and Clark zone lies between the dotted lines.

has exhibited rather low levels of seismicity in recent decades with two exceptions: seismic events near the MT-ID border primarily—but not exclusively—associated with deep underground mining in the Coeur d'Alene mining district (Sprenke et al., 1991), and the AFSZ just west of Missoula.

Hypocenter locations of AFSZ earthquakes were not well resolved until additional seismograph stations of the Montana regional seismic network provided reliable coverage of the Lewis and Clark zone in western Montana in 2000. This improved seismic monitoring coverage has revealed the AFSZ as an elongate cluster of seismicity extending from the Ninemile fault just east of Frenchtown approximately 35 km westward to the vicinity of Alberton, with a north-south dimension of about 10 km (fig. 1). The long axis of the eastern two-thirds of the AFSZ trends about 20° south of west and appears to terminate against, and form a 55° angle with, the Ninemile fault. The western end of the AFSZ includes a concentration of epicenters near Alberton that lies 5-10 km to the north of the N70°E-S70°W-trend formed by the eastern two-thirds of the AFSZ.

The AFSZ is composed of 191 events that have occurred since 1983 with magnitudes ranging from -0.1 to 3.1 (fig. 2). Only 40 of these earthquakes occurred prior to 2000. Montana regional seismic network coverage prior to mid 2000 was inadequate to completely detect and locate smaller ($M < 2.0$) earthquakes in the AFSZ, but improved monitoring coverage after this date lowered the detection threshold to magnitude 0.8 (fig. 3). The rate of occurrence of magnitude 2.0 and larger earthquakes throughout the period is fairly uniform, suggesting complete detection and reporting of earthquakes above this magnitude level since 1983 (fig. 2).

One hundred seventeen AFSZ earthquakes have well-resolved hypocenters (horizontal and vertical uncertainties $\leq$ 2.0 km). For these earthquakes, the most frequent hypocenter depth is 13 km below the surface and 56 percent occur 5 to 10 km deep (fig. 4), which is similar to most other regions of the Intermountain Seismic Belt in western Montana. No reliably located earthquake hypocenters occurred deeper than 20 km.

Sufficient P-wave first-motions were recorded for 11 AFSZ earthquakes plus two nearby earthquakes to determine fault-plane solutions. For AFSZ earthquakes, five

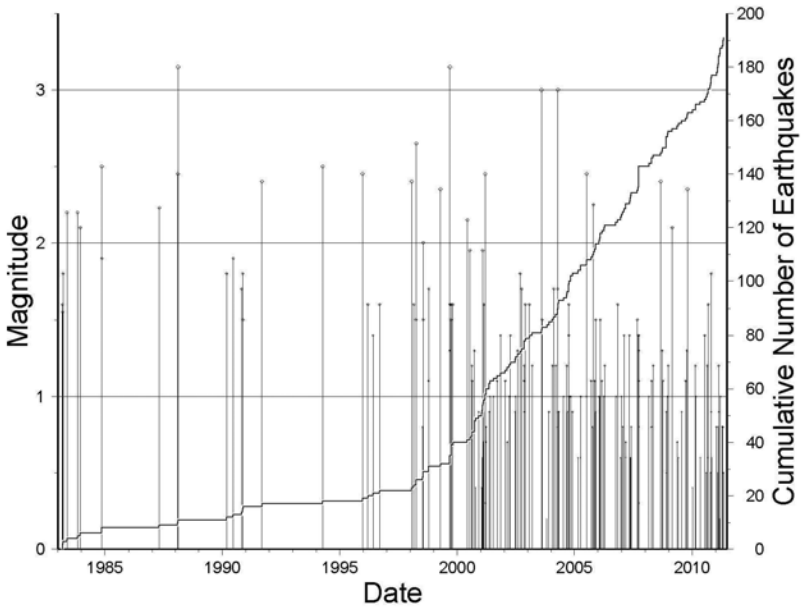

Figure 2. Magnitudes (left axis) and dates of occurrence of earthquakes in the Alberton-Frenchtown seismic zone. Also plotted is the cumulative number of earthquakes (stair step line labeled on right axis) versus time. The number of earthquakes detected and located increased dramatically as a direct consequence of improved seismic monitoring coverage in beginning in 2000.

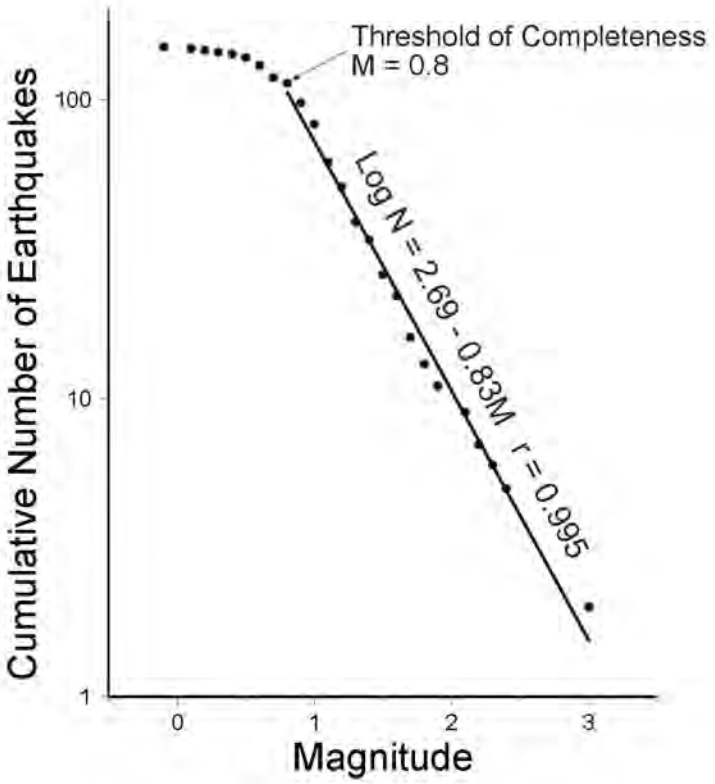

Figure 3. Cumulative number of earthquakes versus magnitude for Alberton-Frenchtown seismic zone earthquakes from June 7, 2000 to May 5, 2011. The line segment is a least squares fit to the data points between magnitude 0.8 and 3.1 satisfying the equation: Log N = 2.69 - 0.83 M, where N is the number of earthquakes with magnitude greater than or equal to M. The correlation coefficient for the least squares fit is -0.995.

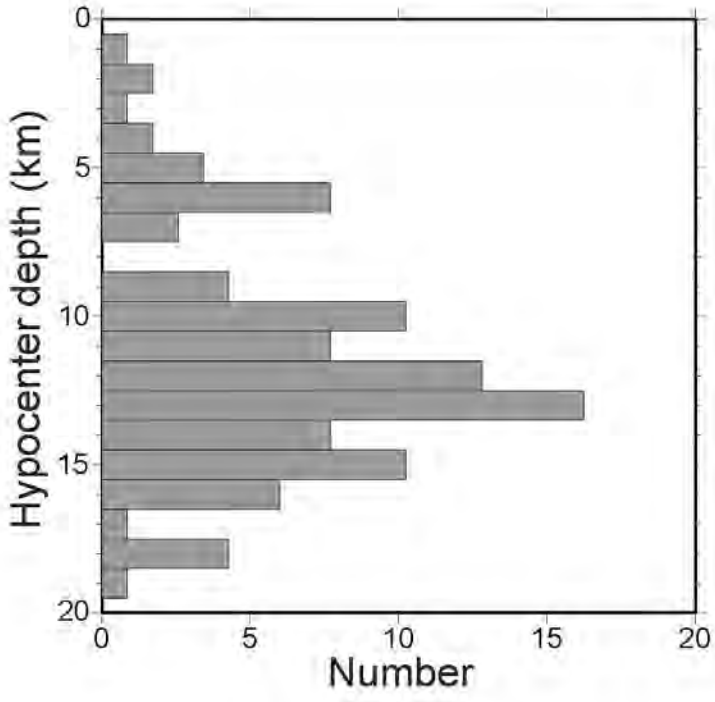

Figure 4. Histogram of hypocenter depths for 117 well-located Alberton-Frenchtown seismic zone earthquakes (horizontal and vertical uncertainties of hypocenter ≤2 km). Fifty-six percent of these earthquakes occurred between 5 and 10 km below the surface.

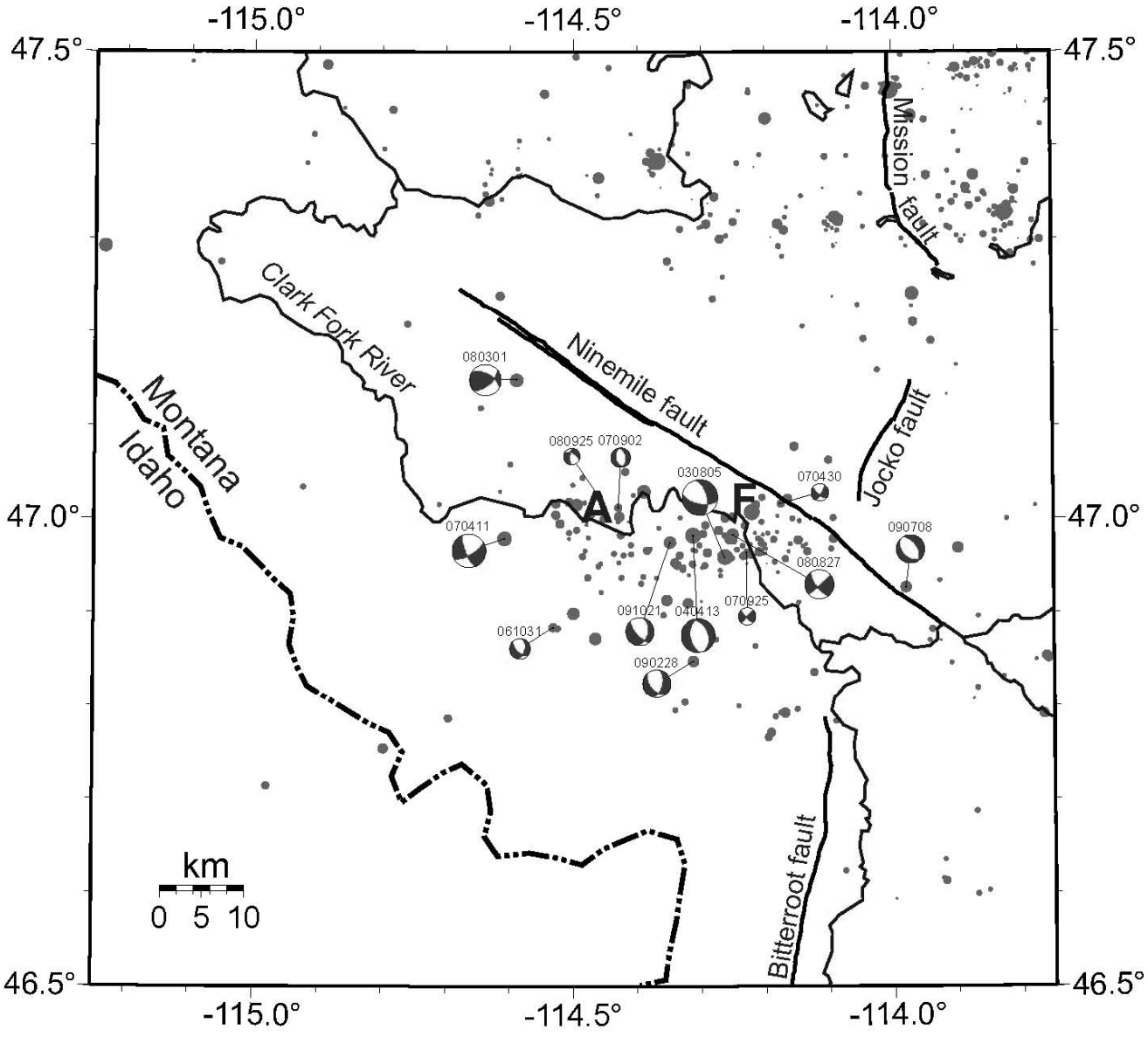

Figure 5. Fault-plane solutions for 13 earthquakes in and adjacent to the Alberton-Frenchtown seismic zone shown as lower hemisphere, equal area projections with shaded areas representing compressional quadrants. The size of the fault-plane solution is proportional to the earthquake's magnitude and labels represent the year (last two digits), month and day of occurrence. Quaternary faults are labeled. Grey dots are earthquake epicenters (scaled to magnitude) determined from the Montana Regional Seismograph Network since 1982 with horizontal epicentral uncertainty less than 5 km (most have uncertainties less than 1 km). "A" indicates Alberton, "F" indicates Frenchtown.

fault-plane solutions indicate normal faulting and six fault-plane solutions indicate strike-slip faulting (fig. 5); none of these solutions show pure normal or strike-slip faulting, instead, all are oblique combinations of both types. The four fault-plane solutions at the east end of the AFSZ, closest to Frenchtown and the Ninemile fault exhibit predominately strike-slip movement. There is no compelling evidence to suggest that any of these four events occurred at depth along the Ninemile fault, although the 60° south-dipping, east-west-trending nodal plane for event 030805 (fig. 5) does project from the hypocenter up to the surface near the trace of the Ninemile fault. The Ninemile fault apparently dips south (Haller, 1996) but its subsurface attitude is poorly known and the straight surface trace suggests a very steep dip. Several fault-plane solutions indicate normal faulting on northerly trending faults between Alberton and Frenchtown but these small earthquakes are not obviously related to any structures indicated on 1:500,000 scale geologic maps. The fact that normal fault-plane solutions with northerly trending nodal planes lie within a westerly trending seismic zone indicates that multiple faults at depth are responsible for the AFSZ seismicity.

East of the AFSZ, a fault-plane solution for event 090708 (fig. 5), which occurred north of Missoula within 1 km of the Ninemile fault, indicates normal slip on a northwest-trending fault at a depth of 14.6 ± 0.6 km below the surface. Despite the proximity of this epicenter to the Ninemile fault trace, the depth of the hypocenter together with the sense of slip indicate that this magnitude 2.2 earthquake did not occur along the Ninemile fault at depth. To the northwest of the AFSZ, earthquake 080301 (fig. 5) occurred in the upper part of the Ninemile drainage, about 5 km southwest of the Ninemile fault, in a region of very sparse seismicity and has a well-constrained hypocenter depth of 14.5 ± 0.5 km. The fault-plane solution for this magnitude 2.5 earthquake is the only one of the 13 for this region that indicates oblique-reverse slip; the nodal plane that strikes parallel to the Ninemile fault dips 56° to the northeast and therefore cannot be associated with the Ninemile fault at depth. As with most other seismically active regions of western Montana where recent seismicity cannot be confidently associated with the nearby Quaternary faults, available evidence indicates that AFSZ earthquakes do not occur along the Ninemile fault.

The conical best fit to T-axis orientations (representing σ_3, the least principle stress) for the 13 fault-plane solutions lies at an azimuth 258 degrees with a nearly horizontal attitude (fig. 6). This average T-axis orientation is similar to that observed in other areas of western Montana (Stickney and Bartholomew, 1987) and lies at an angle of 47° to the 305° average strike of the Ninemile fault. Thus, existing tectonic stress directions inferred from fault-plane solutions in the western Lewis and Clark zone are compatible with continued dextral slip on the Ninemile fault. P-axis orientations (representing σ_1, the maximum principle stress) form a weakly defined belt ranging from north to south (fig. 6). A cylindrical best fit to the P-axis orientations has a poorly defined, maximum dip of 50° with an azimuth of 355°. This larger range in P-axis orientations, as compared to T-axis orientations, reflects the variety of strike-slip to normal faulting mechanisms, which all have a relatively uniform T-axis (extension) direction.

The reason for the clustered seismicity in the AFSZ in an otherwise relatively aseismic western Lewis and Clark zone remains unknown. No significant historic earthquakes have occurred within the AFSZ and

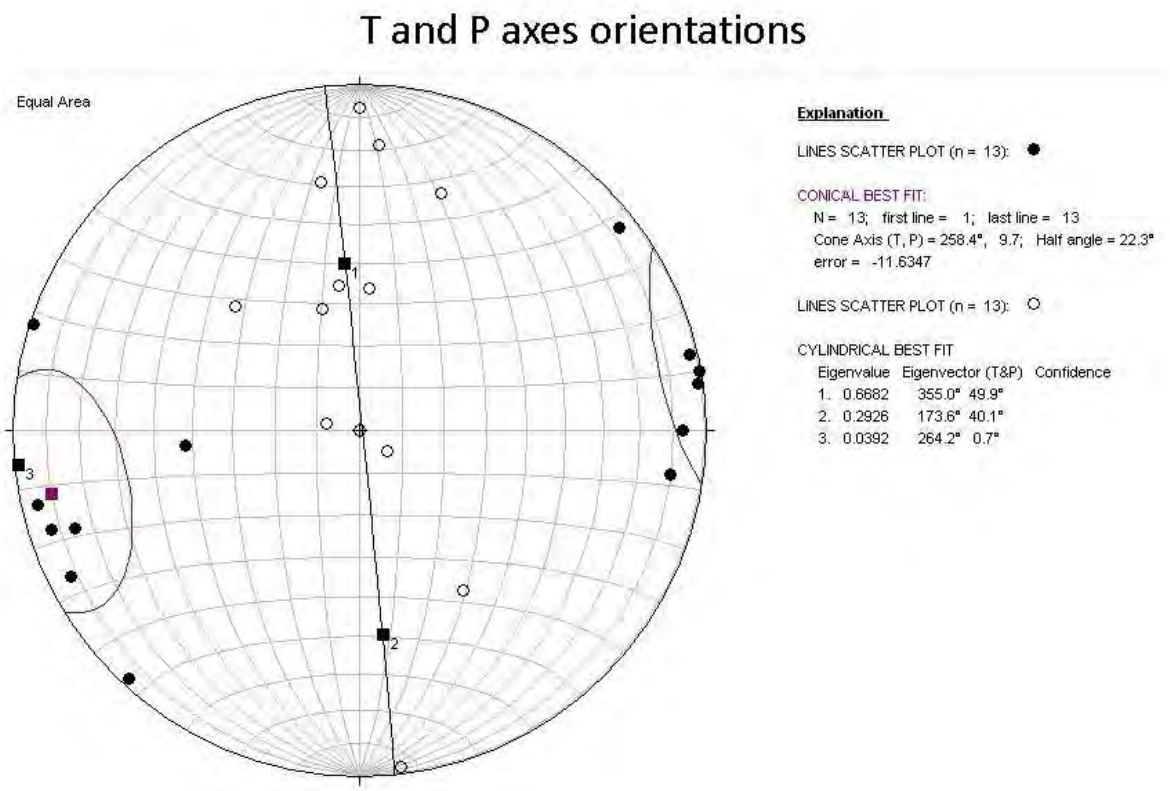

Figure 6. T-axis (solid circles) and P- axis (open circles) orientations from fault-plane solutions in and adjacent to the Alberton-Frenchtown seismic zone plotted on a lower hemisphere, equal area stereo projection. The unlabeled square surrounded by small circle is the conical best fit to the T-axis distribution. The great circle (northerly trending line) is the cylindrical best fit to the P-axis distribution with square labeled 1 representing the average maximum compressional direction and the square labeled 3 representing the average minimum compressional direction, which agrees well with the best fit to the T-axis orientations.

Magnitude	Observed Number/Year	Predicted Number/Year	Return Time (years)
1.0	7.6	6.7	0.15
1.5	2.4	2.6	0.39
2.0	0.83	0.98	1.02
2.5	0.23	0.35	2.7
3.0		0.14	7.0
3.5		0.055	18.2
4.0		0.021	47.4
4.5		0.0081	123.
5.0		0.0031	323.
5.5		0.0012	841.
6.0		0.00046	2195.
6.5		0.00017	5725.

Table 1. Annual observed and predicted numbers of earthquakes and return times (inverse of the annual predicted number) based on the recurrence equation developed for earthquakes from June 7, 2000 to May 5, 2011 (10.91 years) for the Alberton-Frenchtown seismic zone (see fig. 3).

the largest recent earthquakes have barely exceeded magnitude 3.0. A recurrence analysis (Table 1) for earthquakes since 2000 (when seismic monitoring coverage improved) suggests that if seismicity rates remain similar to what has occurred over the past 10.9 years, an earthquake up to magnitude 4.0 may occur once in a 47 year period and a magnitude 5.0 may occur once in a 323 year period. Although moderate by regional standards, earthquakes in the magnitude 4 to 5 range could adversely impact transportation corridors and lifelines through steep terrain in the vicinity of the AFSZ and should be considered in seismic hazard evaluations and emergency response planning.

Acknowledgements

This work benefited from reviews by Colleen Elliot and Debbie Smith, both with the Montana Bureau of Mines and Geology, and comments by the editor. The Generic Mapping Tools software package (Wessel and Smith, 1991) was used to create Figures 2–5. StereoWin software freely provided by Richard Allmendinger, http://www.geo.cornell.edu/geology/faculty/RWA/OldPrograms.htm, accessed 06/01/2011, was used to create Figure 6.

References

Haller, K.M., compiler, 1996, Fault number 705, Ninemile fault, in Quaternary fault and fold database of the United States: U.S. Geological Survey website, http://earthquakes.usgs.gov/regional/qfaults, accessed 05/24/2011 07:47 AM.

Sears, J.W., and Hendrix, M.S., 2004, Lewis and Clark line and the rotational origin of the Alberta and Helena salients, North American Cordillera: Geological Society of America Special Paper 383, p. 173-186.

Smith, R.B., and Arabasz, W.J., 1991, Seismicity of the Intermountain Seismic Belt: *in* Slemmons, D.B, Engdahl, E.R., Zoback, M.D., and Blackwell, D.D., eds., Neotectonics of North America: Geological Society of America, Decade of North American Geology Map Volume 1.

Sprenke, K.F., Stickney, M.C., Dodge, D.A. and Hammond, W.R., 1991, Seismicity and tectonic stress in the Coeur d'Alene mining district: Bulletin of the Seismological Society of America, v. 81, p. 1145-1156.

Stickney, M.C., and Bartholomew, M.J., 1987, Seismicity and Late Quaternary faulting of the northern Basin and Range Province, Montana and Idaho: Bulletin of the Seismological Society of America, v. 77, p. 1602-1625.

Wallace, C.A., Lidke, D.J., and Schmidt, R.G., 1990, Faults of the central part of the Lewis and Clark line and fragmentation of the late Cretaceous foreland basin in west-central Montana: Geological Society of America Bulletin, v. 102, p. 1021-1037.

Wessel, P., and Smith, W.H.F., 1991, Free software helps map and display data: EOS, v. 72, p. 441-446.

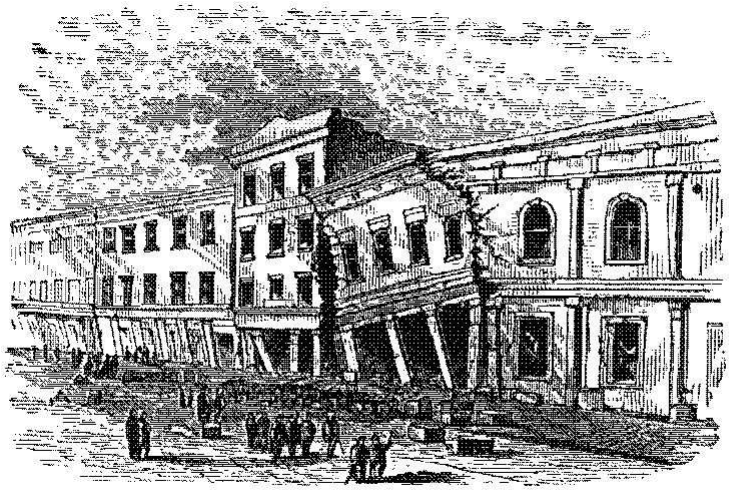

ALBERTON BRECCIA AND LANDSLIDE: A FIELD TRIP TO EXAMINE ENIGMATIC LANDFORMS IN THE CLARK FORK RIVER CORRIDOR

Bruce E. Cox
Geologist, Missoula, MT 59801

Introduction

Cambrian and Mesoproterozoic rocks are complexly faulted along the Clark Fork River corridor near Alberton Montana. Previous mapping by Wells (1974) and Lonn et al. (2007) provides the regional geologic framework for the current examination. Local bedrock consists of Proterozoic metasedimentary rocks and diabase (sill?) thrust northward over Cambrian Hasmark dolomite along the splays and principal ramp of the Lothrop fault zone (fig. 1). The thrust package is cut by high-angle WNW normal and/or strike slip faults parallel to the Lewis and Clark Lineament and subsequently by NNE-trending strike slip faults; the later trend becomes increasingly more distinct southward into the Fish Creek drainage. The faulted terrane at Alberton is locally overlain by Quaternary Glacial Lake Missoula silts and, in turn, by the rock debris of one or more landslides.

Landslide

The Alberton landslide (fig. 2) is dramatically exposed at the west edge of town between the water tank and town dump. The landform is 2/3 mile in plan length and consists of a steep chute-like headwall, a broad medial lobe and a tapering toe that extends to the edge of I-90. Landslide debris ranges from cobble-sized clasts to boulders the size of a small house. Mapping to date indicates that all debris is light-to-medium grey micritic dolomite (Hasmark Fm.) of which approximately 90% is angular, monolithologic clast-supported breccia and 10% is unbrecciated and thick bedded dolomite.

Breccia

All breccia clasts in the landslide cobbles and boulders are Cambrian dolomite with minor inclusions of stratiform chert. The breccia matrix appears to be fine-grained carbonate (re)crystallized at the clast margins plus minor local travertine +/- banded silica. Regardless of size, the clasts are angular and randomly oriented. Mylonitic or coarser shear fabrics were not observed.

In-place breccia is exposed along the landslide headwall above 3900 feet elevation and in the SW-plunging gulch 500 feet east from the landslide margin (figs. 3 to 6). Thick bedded dolomite in these exposures shows a progression from shattered to brecciated rock toward NE-trending fracture zones. Brecciated dolomite is locally flanked by unbroken dolomitic strata across steeply dipping fracture surfaces (figs. 7 and 8).

Wild Speculation

The overall geologic context suggests that dolomite breccia developed during the Eocene along a zone of NNE-trending strike slip faulting that has been mapped as far south as the west flank of the Lolo Hot Springs batholith (Lewis, 1998). Local expression of this strike-slip domain includes right-lateral stratigraphic offsets, fault-parallel dike swarms and, at Alberton, a polygonal collapse feature (negative flower structure?). A rectangular, downthrown block of Hasmark dolomite mapped by Wells (1974) further suggests this strike-slip mechanism.

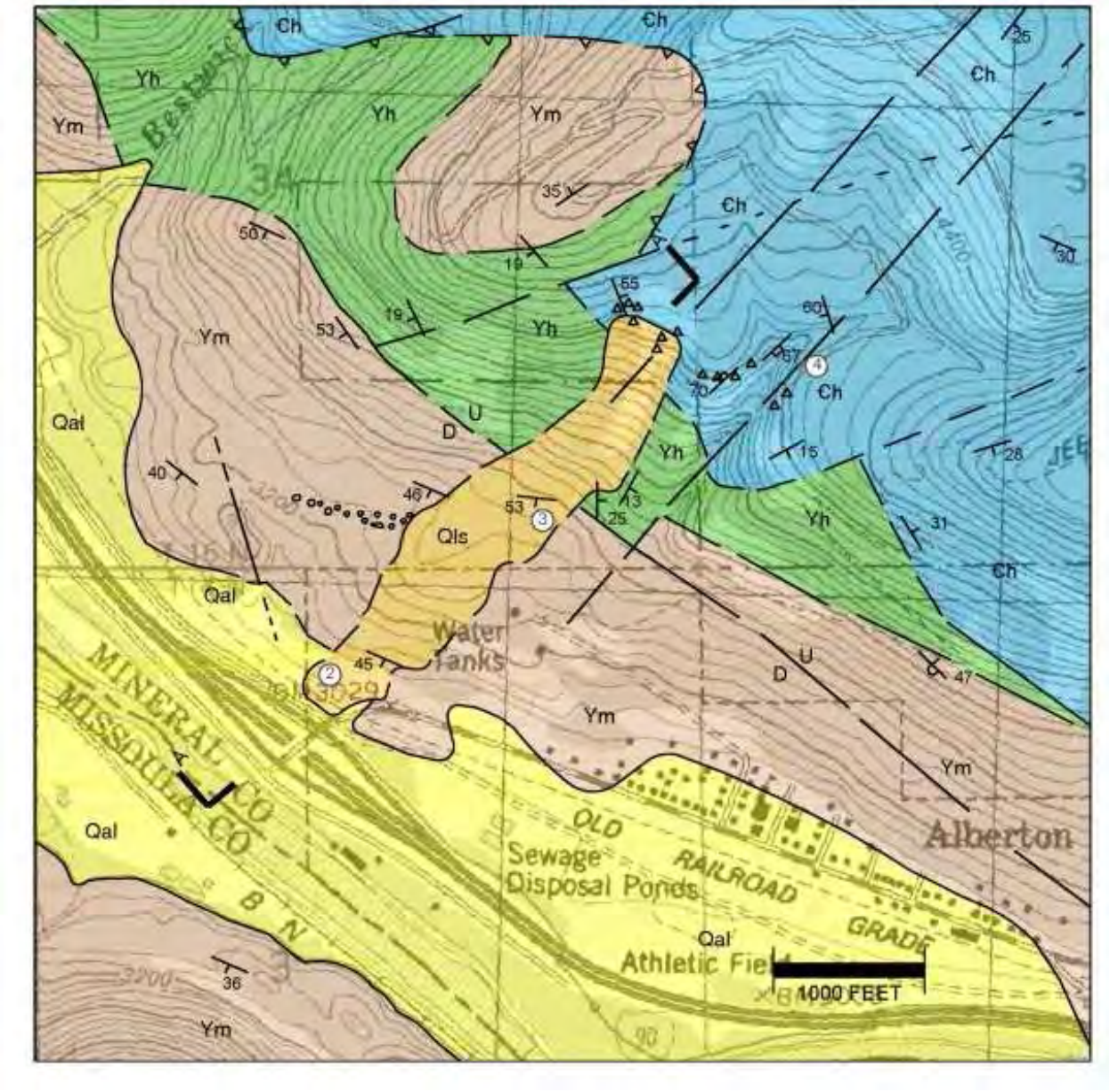

Figure 1 - Geologic map of the Alberton landslide, Mineral County, Montana. Geology compiled from mapping of Wells (1974), Lonn et al. (2007) and Cox (2011 unpublished mapping). Qal = alluvium, Qls = landslide debris, Ql = Quaternary Glacial Lake Missoula – silts and sand, Ch = Cambrian Hasmark Formation – dolomite, Csh = Silver Hill Formation – limestone and shale, Cf = Flathead Sandstone, Ym = Missoula Group – quartzite, siltstone and argillite, Yh = Helena Formation – calcareous siltstone and argillite, triangles = brecciated dolomite, ovals = boulder train, circled numbers = field trip stops.

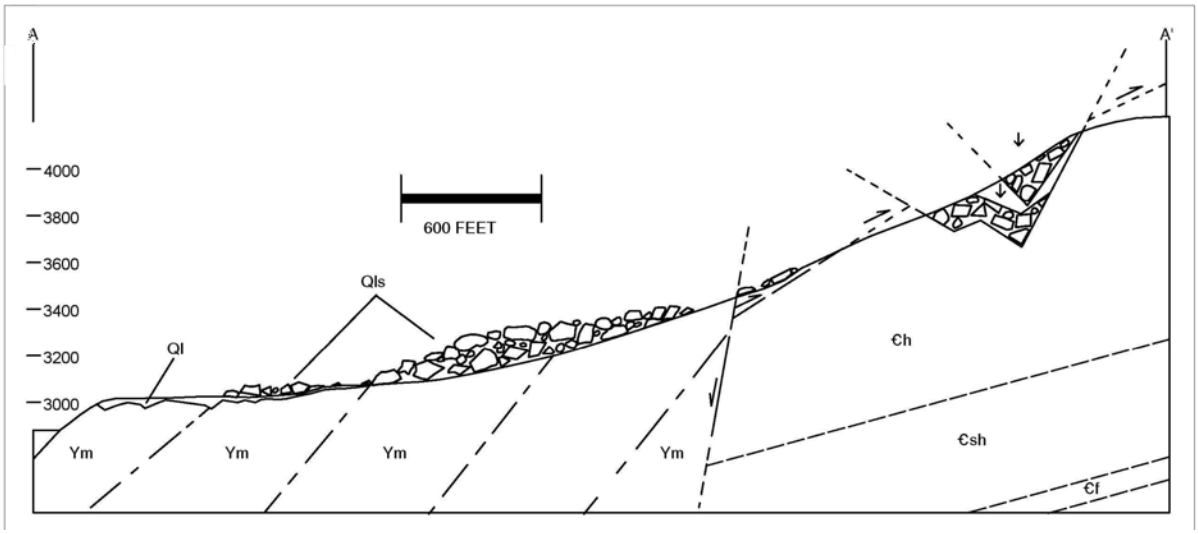

Figure 2 - Schematic cross-section / cartoon through Alberton landslide. Waxy green argillite subcrop (Yh?) is exposed along the lower reach of the landslide headwall, suggesting that the landslide slipped along the sole of the Lothrup thrust.

Figure 3 - Outcrops of brecciated Hasmark Formation dolomite at the canyon rim above Alberton. The dark grey-weathering clast at the left side crest of the outcrop is ~5 ft long; view is west from Stop 4.

Figure 4 - Knobs of brecciated dolomite near the headwall of the Alberton landslide. The middle knob is ~20 ft high, view is northwest. The forested hillslope on the skyline is underlain by Helena Formation argillite and siltstone.

Another curious landform is the narrow train of breccia boulders which extends westward from the main landslide mass (fig. 1). These boulders might have been plucked from the landslide during a Glacial Lake Missoula flood event, be the erosional remnant of a once much wider landslide deposit or be evidence of delicate work by extraterrestrial intelligence.

ROAD LOG

Leave Superior and drive east on I-90 to the Alberton Exit 75 (~28 miles). Set odometer to 0.0 at head of east-bound ramp.

1.8 Cross Clark Fork of the Columbia River ("CFR").

2.3 to 5.5 Driving on terrace gravels. Note higher gravel bench north of the highway.

6.2 Cross CFR. Roadcuts east of the bridge expose terrace gravels of uniform size.

9.7 to 9.8 Glacial Lake Missoula silts in roadcuts.

10.2 I-90 Rest Area (optional stop).

11.0 Cross CFR.

11.8 Roadcuts expose subcrop of Proterozoic mudstone.

12.2 to 12.5 Highway cuts through Quaternary gravel capped by Lake Missoula silts.

13.0 to 13.7 Hummocky topography both sides of highway. Glacial Lake Missoula flood megaripples?

13.9 Pine-covered conical hill north of the interstate. (Optional Stop from the Tarkio Exit on return to Superior. Visiting this hill requires the landowners' permission to cross the pasture.)

14.1 Tarkio Exit.

14.5 to 15.0 Roadcut to north is a thick sequence of coarse gravel.

18.5 Ridge rising to the northeast exposes Missoula Group rocks.

18.8 Cross CFR.

19.2 Fish Creek Exit 66.

20.8 Downstream terminus of deposit of large boulders.

21.3 STOP 1. Park on the highway shoulder, watch for eastbound traffic and walk across highway to examine boulder field. I-90 roadcuts locally show boulders atop lake silts which in turn lay on terrace gravel. Two questions for discussion - where is the bedrock source of these boulders and how were they deposited here? Return to vehicles, pull carefully onto the highway and proceed east to Alberton.

STOP 1

22.8 Cross CFR.

26.3 South-dipping Missoula Group outcrops (left) are underlain by splays of the Lothrup fault zone. Note isolated remnants of flat-lying Glacial Lake Missoula silts.

27.6 Alberton Exit 75. Exit I-90. Boulders in toe of Alberton landslide visible to the north as you exit. Cross over I-90 and bear east on the frontage road toward town. At the "Entering Alberton" sign, make a left / U-turn into Posio Lane which heads west into the Alberton Dump.

28.0 Alberton Landslide at the Alberton Dump.

Figure 5 - Brecciated Hasmark dolomite at the canyon rim; clipboard for scale.

Figure 6 (below) - Flexure (?) in clast within breccia; pen for scale.

Figure 7 - High-angle, NE-striking fractures at the southeast margin of brecciated Hasmark dolomite; photo taken ~ 700 ft SSW from Stop 4.

STOP 2 STOP 2. Examine Hasmark dolomite boulders and landform of the Alberton landslide and relationships with underlying lake sediments and Proterozoic bedrock. Depending on condition of the dirt roads, we may be able to venture further north into the landslide boulder field (STOP 3).

Return to I-90 (Exit 75), reset odometer to zero and turn west into the north side frontage road (do not re-enter I-90).

0.7 Turn right (north) under the log arch onto Waterhill Road (landowner permission required to travel roads beyond this point). The next 3.5 miles requires a 4WD vehicle; drivers are cautioned to turn wheels into the cutface and set parking brakes at any stops.

0.8 Turn right at cul de sac and follow dirt road into Bestwick Gulch.

0.9 Gravel pit in colluvium on right.

1.2 Locked gate of Plum Creek Timberlands. South-dipping Proterozoic sedimentary rocks exposed in the canyon wall. These calcareous siltstones and argillites were called Helena Formation by Wells (1974) and Shepard Formation (Ysh) by Lonn et al. (2007). As the road climbs Bestwick Gulch, the first switchback is on the sole of the Lothrop fault zone (reverse displacement - Y Missoula Group over C Hasmark dolomite). Climbing to the second switchback, we are back in Missoula Group rocks.

1.8 Cross west plunging gulch which traces the sole of the Lothrop fault. For the next mile, roadcuts expose subcrop and bedrock of Cambrian Hasmark dolomite plus local blocks of brecciated carbonate.

2.2 Road turns south along contour (4040 ft

Figure 8 - Breccia in fault contact (?) with thick beds of the parent dolomite; clipboard for scale.

elev.), crossing the toe of another suspect landslide.

2.4 Turn right at "Y" intersection.

2.9 Switchback in Missoula Group subcrop.

3.4 Roadcut at ridge nose exposes west-dipping Ym hematitic siltstone.

3.5 Crossing fault in gulch; limonitic soils grading to float of Cambrian carbonates.

3.9 Hasmark dolomite with breccia developed along fractures.

STOP 3 4.0 Stop 3. End of road traverse. From this point, walk 200 yards southwest to examine cliff outcrops of brecciated Hasmark dolomite. A traverse 700 yards west-northwest provides views of the landslide headwall plus shallow outcrops and hoodoos of brecciated dolomite.

Return to vehicles and proceed carefully down Bestwick Gulch to the Alberton frontage road.
Leave Alberton and head west toward Superior on I-90. Reset odometer to zero at head of west-bound ramp.

13.5 Tarkio Exit. Optional Stop 5. Walking traverse to a very curious conical hill at south margin of the Tarkio bench.

After exiting interstate, take north frontage road westward to the first ranch house, the home of Walt and Jackie Robb. Walk across their pasture to examine the hill (~ 1/8 mile).

End of field trip.

Acknowledgements

Many thanks to Peter Mejstrick, Ted Antonioli, Tim Zeiser, and Candee Schweitzer for their candid observations and help in the field. Larry Johnson provided some nifty orthophotos and much help with drafting Figures 1 & 2. Road access to the upper outcrops was graciously granted by Lee Johnson of Alberton and Art Pencek of Plum Creek Timberlands. We traveled the Alberton Dump roads courtesy of Joe Hansen, caretaker and Mayor. This road log is dedicated to Ruby, my sweet and faithful friend and travel companion.

References

Lewis, R.S., 1998, Geologic map of the Missoula West 30' x 60' quadrangle: Montana Bureau of Mines and Geology Open-File Report MBMG 373, scale 1:100,000.

Lonn, J.D., Smith, L.N., and McCulloch, R.B., 2007, Geologic map of the Plains 30' x 60' quadrangle: Montana Bureau of Mines and Geology Open-File Report MBMG 554, scale 1:100,000.

Wells, J.D., 1974, Geologic map of the Alberton quadrangle, Missoula, Sanders, and Mineral counties, Montana: U.S. Geological Survey Quadrangle Map GQ-1157, scale 1:62,500.

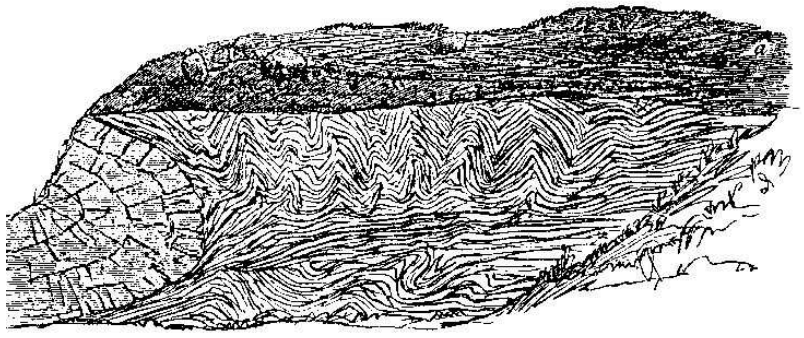

WALLACE FORMATION BRECCIAS EXPOSED ALONG TROUT CREEK, MINERAL COUNTY, MONTANA

Dave Godlewski
Tech Cominco, Spokane, WA

This somewhat informal, half-day field trip will be to accessible locations where distinctive sedimentary breccias in the Wallace Formation of the Belt Supergroup are exposed. These outcrops were some of those studied by Godlewski (1980). Below is a copy of the abstract from his thesis.

Origin and Classification of the Middle Wallace Breccias

"In three drainages flowing northeast off the Bitterroot divide in westernmost Montana near the town of Superior, Montana are excellent outcrops of the middle Wallace breccias (Precambrian V, Belt Supergroup) and attendant soft sediment deformation. These outcrops were studied and their parts classified in detail using an empiric scheme that grouped the elements of soft sediment deformation (soft sediment folds, faults, breccia packages, and open void spaces) into regimes that reflect upon genesis and led to a proposed origin for the unit of subaqueous slumping. In this classification, deformational structures are grouped into three categories which represent the strain inferred in their formation, i.e. 1) T-regime, which shows extension of the sediment surface and which is characterized by the creation of open voids on all scales (slump scars, clastic dikes, surface cracks); 2) C-regime, which displays compression of the sediment surface (folds of varying brittleness and overturn, soft sediment thrusts); 3} P-regime, which shows a lack of sediment cohesion and competency (breccias, load structures, current structures) .

The importance of the above defined scheme is that deformation structures, while ambiguous when observed individually, are placed into sets of similarly formed structures which define dynamic regimes. These regimes, then, can be used to interpret the geologic history of a deformed unit at a single outcrop based upon geologic relationships such as crosscutting or superposition. In addition, by placing the individual localities into a broader stratigraphic framework in which single stratigraphic horizons can be delineated, the relative position of that outcrop on the original slope can be inferred by the abundance of one regime's structures over another. On an idealized slope, T-regime structures should be most prevalent on the slope itself at or near the slump's origin. As the slump moves down the slope frictional resistance between the slumping mass and the slope surface will cause the toe of the slump to slow relative to the tail thereby superposing C-regime structures ,over any other structures in the slump sheet. The effects of frictional resistance will be most important at the base of the slope and therefore the C-regime structures will be indicative of that area. Finally, the P-regime structures, lacking internal competence, will flow for great distances beyond the slope proper, kept in suspension by internal turbulence to finally come to rest on the slope apron or basin floor."

References

Godlewski, D.W., 1980, Origin and classification of the middle Wallace breccias: M.S. thesis, University of Montana, Missoula, 108 p.

Lonn, J.D., and McFaddan, M.D., 1999, Geologic map of the Montana part of the Wallace 30' x 60' quadrangle: Montana Bureau of Mines and Geology Open-File Report MBMG 388, 16 p., scale 1:100,000.

Lonn, J.D., Smith, L.N., and McCulloch, R.B., 2007, Geologic map of the Plains 30'x60' quadrangle, western Montana: Montana Bureau of Mines and Geology Open-File Report 554, scale 1:100,000.

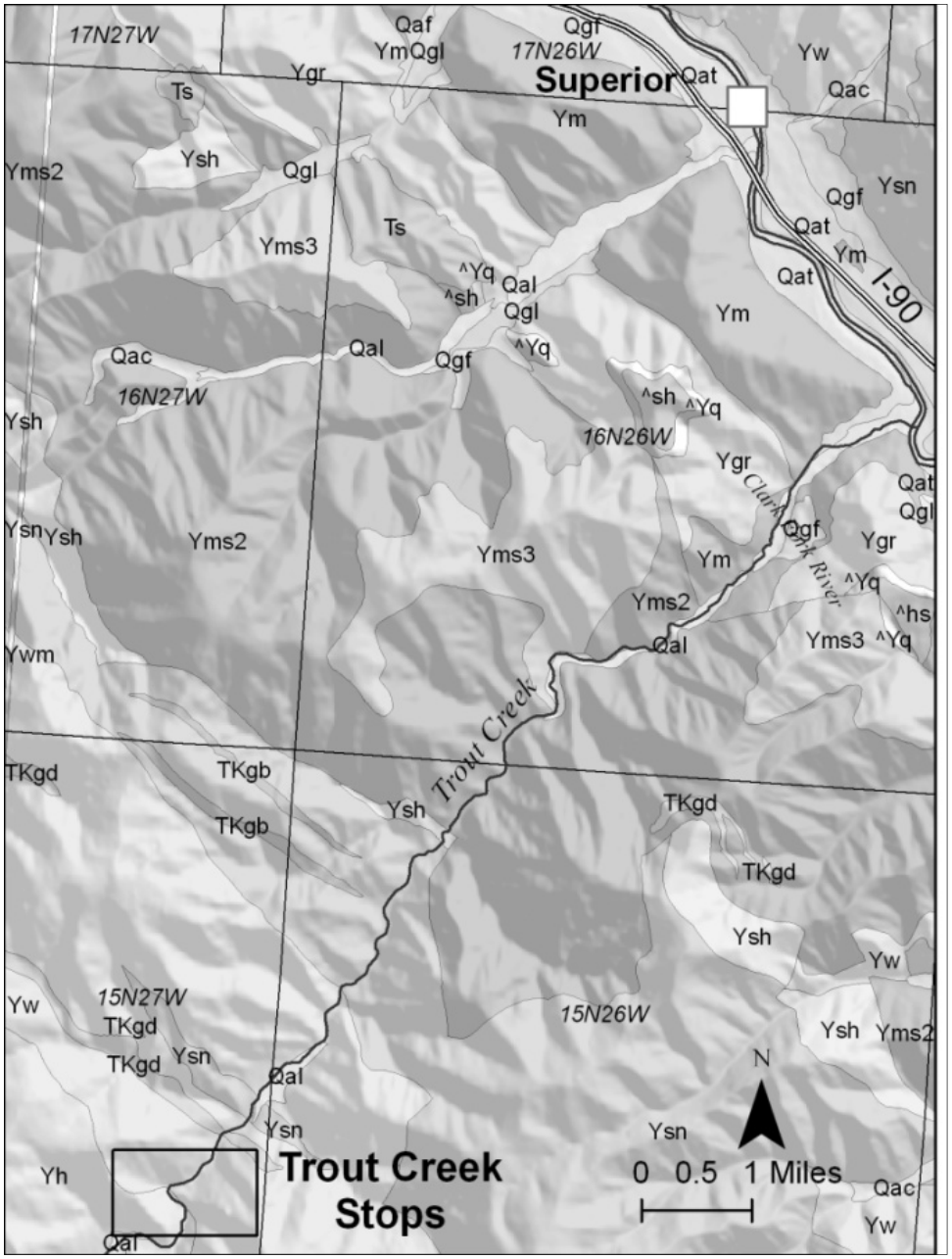

Figure 1. Location and geologic map of the field trip stops along Trout Creek. Relevant geologic units include Yh – Helena Formation, Yw – Wallace Formation, Ysn – Snowslip Formation, TKgd – Tertiary or Cretaceous granodiorite; Qal – Quaternary alluvium; modified from Lonn and McFaddan (1999) and Lonn et al. (2007).

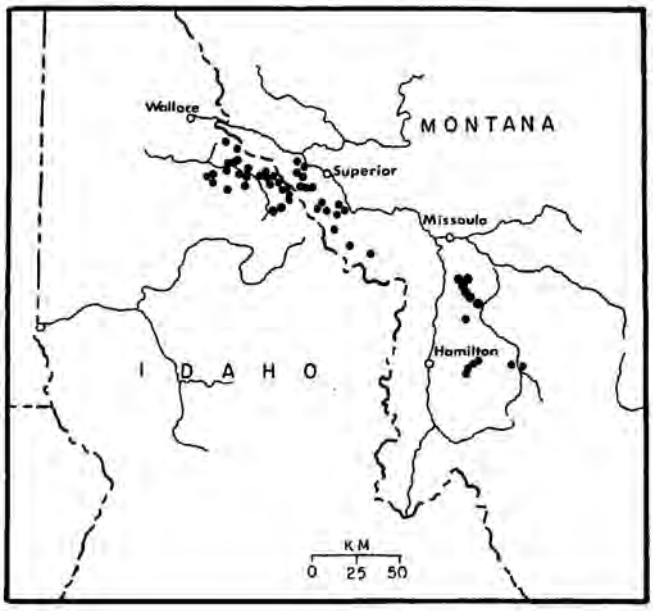

Figure 2. Map showing known locations of breccias in the Wallace Formation (from Godlewski, 1980).

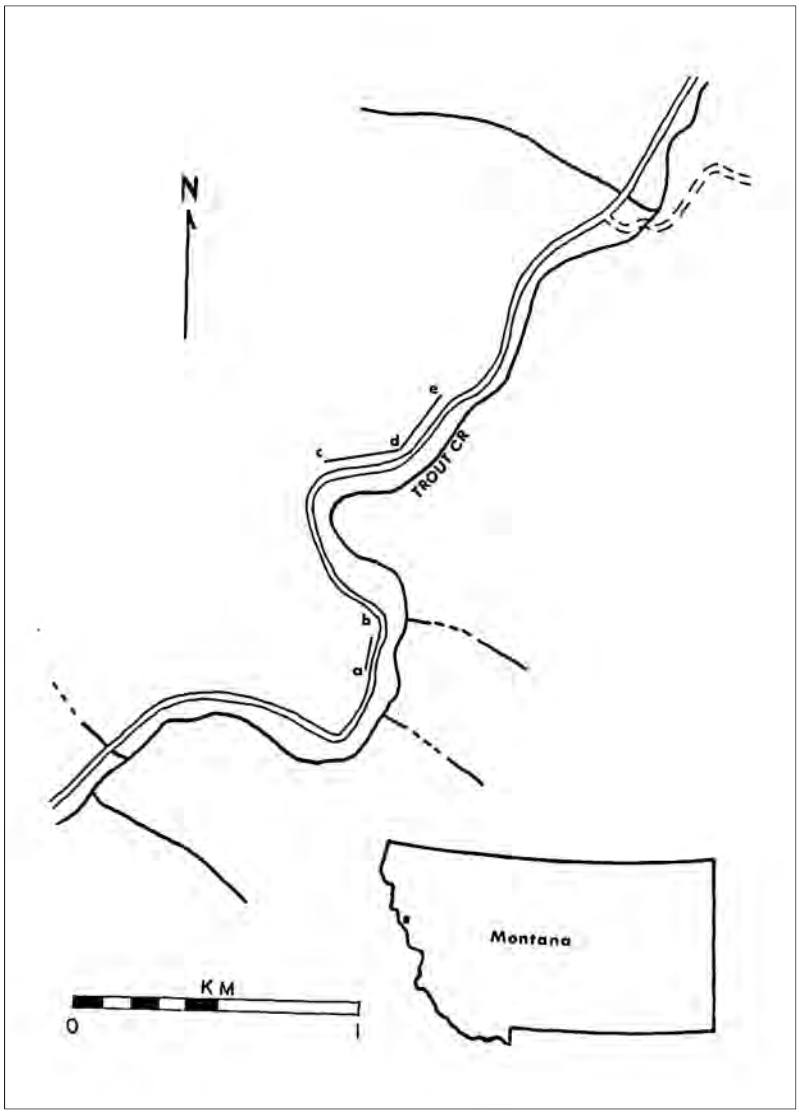

Figure 3, Map of the Trout Creek study area, showing locations of outcrop sketches shown in Figure 4 (from Godlewski, 1980).

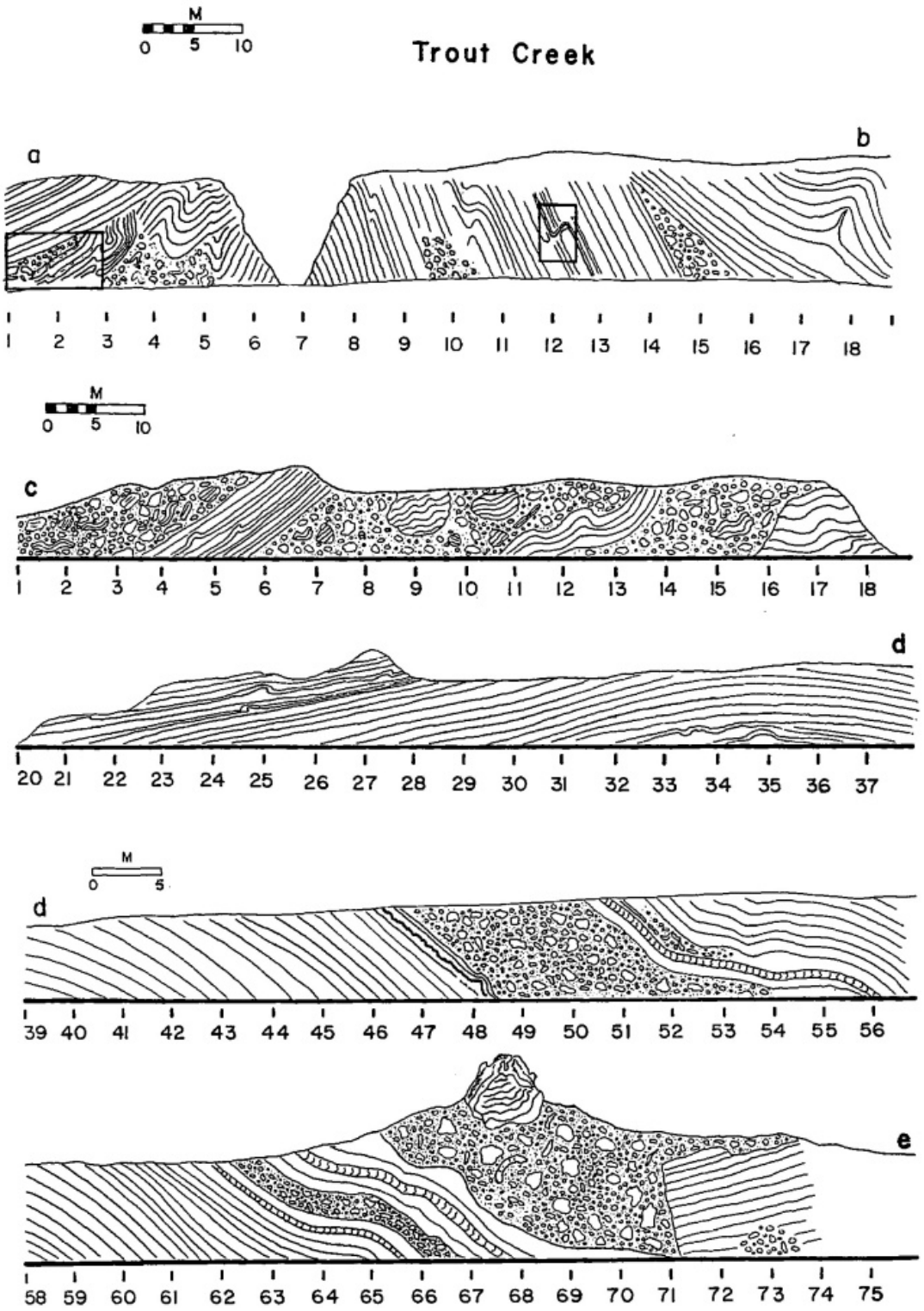

Figure 4. Sketches of outcrop intervals a–b, c–d, and d–e (from Godlewski, 1980).

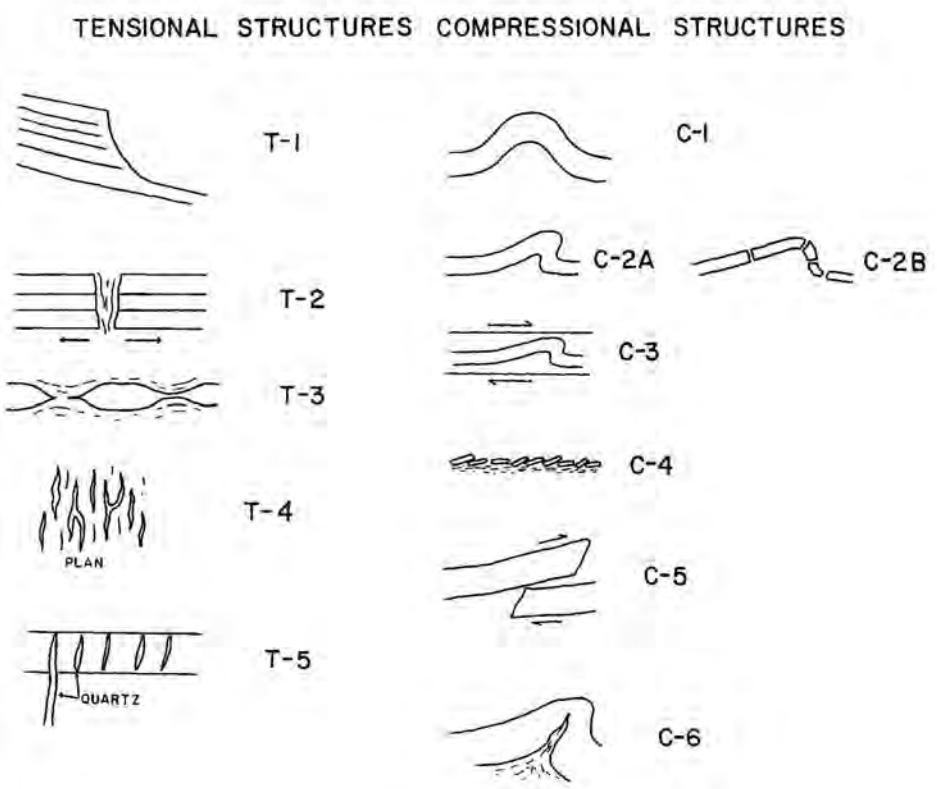

Figure 5. Diagram of tensional (t-regime) and compressional (c-regime) structures recognized in the sedimentary breccias (from Godlewski, 1980).

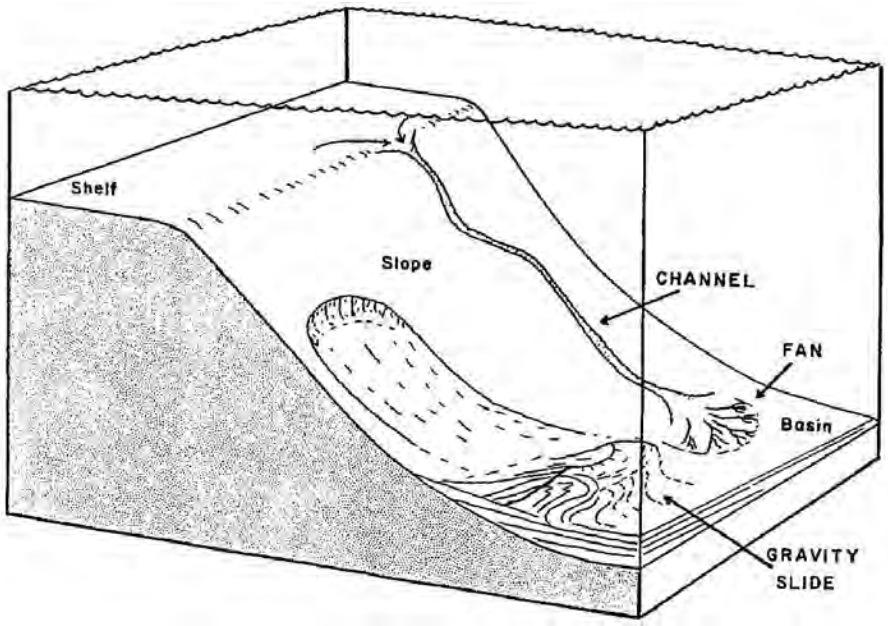

Figure 6. Model of middle Wallace sedimentation in the area of the breccias. Sediment is transported into the basin via slope channels as low density, low velocity sand flows. Periodic earthquake shocks dislodge sheets of sediment as gravity slides, which come to rest at the base of the slope. Breccias, generated by slumping, continue beyond the base of the slope as high-density debris flows (from Godlewski, 1980).

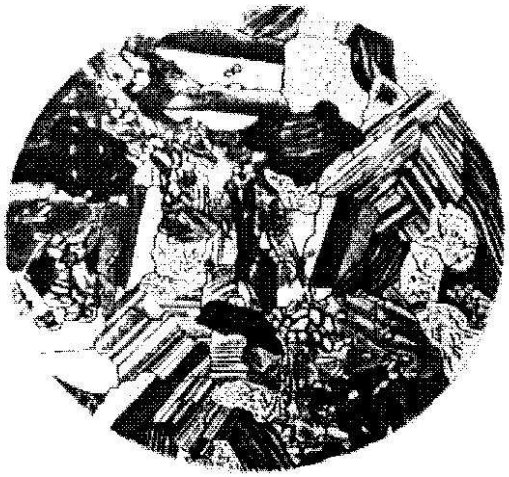

BEDROCK STRUCTURE OF THE LEWIS AND CLARK LINE AND MIOCENE DIVERSION OF THE CLARK FORK RIVER: FIELD GUIDE FROM SUPERIOR TO PARADISE, WESTERN MONTANA

J.W. Sears
University of Montana, Missoula MT 59812

Introduction

The Lewis and Clark Line (LCL) trends ESE for 800 km, from northwestern Washington to central Montana (Harrison et al., 1974; Wallace et al., 1990; Vuke et al., 2007). This crustal-scale transverse structure experienced major left-lateral shear during the Late Cretaceous-late Paleocene Laramide orogeny, followed by right-lateral extension during the Eocene and Miocene (Sears and Hendrix, 2004). The field trip route traverses a deeply exposed part of the Mesoproterozoic Belt basin along the LCL (Harrison, 1972; Link et al., 1993; Evans et al., 2000).

Between Superior and Paradise, Montana, the route crosses the deeply incised Terror shear zone of the LCL (Lonn et al., 2007). Structural plunge and large-scale extensional dissection permit the reconstruction of a crustal-scale cross-section of this Laramide feature as it may have existed in Late Cretaceous time (Fig. 1). The cross-section exhibits a compressional flower structure in which deep levels have been extruded upwards and outwards. The flower structure was squeezed between two major blocks of the Belt basin as they rotated clockwise during Laramide collisions (Sears, 1988, 1994, 2007). The rocks east of the Ninemile fault overrode a 15 km basement ramp at the edge of the Belt basin. The basement ramp subsided under the load of the thrust slab, but rebounded upon conclusion of thrusting, and erosion and tectonic denudation exposed the deep section in the footwall of the resulting Ninemile fault (Sears, 2001).

The main phase of extension occurred during the Eocene in concert with the exhumation of metamorphic core complexes that link along the LCL (Hyndman, 1980; Coney and Harms, 1984; Hyndman et al., 1988; Janecke, 1994; Constenius, 1996; Foster and Fanning, 1997). A second phase of extension occurred during the Late Oligocene to Middle Miocene, when the LCL acted as a transfer zone for extension in SW Montana. The second phase re-arranged drainage patterns in SW and west-central Montana (Sears, 2010).

The cross-section indicates some 20 km of cumulative, down-to-the-SW normal displacement on the Ninemile, Osborn, Boyd Mountain, and Tin Cup faults in the area of the field trip. The SW half of the cross-section is inspired from Lonn et al. (2007). The heavy dashed lines in Figure 1 indicate the modern ground levels shown on their cross-section, and part of the underlying geology is from their section. The heavy dashed lines approximate the route of the field trip across the LCL. Thus, we will see contrasting structural and stratigraphic levels as we transect the fault blocks. Note the schematic locations of the field trip stops on the figure.

I constructed the section to undo the Eocene and Miocene extensional faulting. The

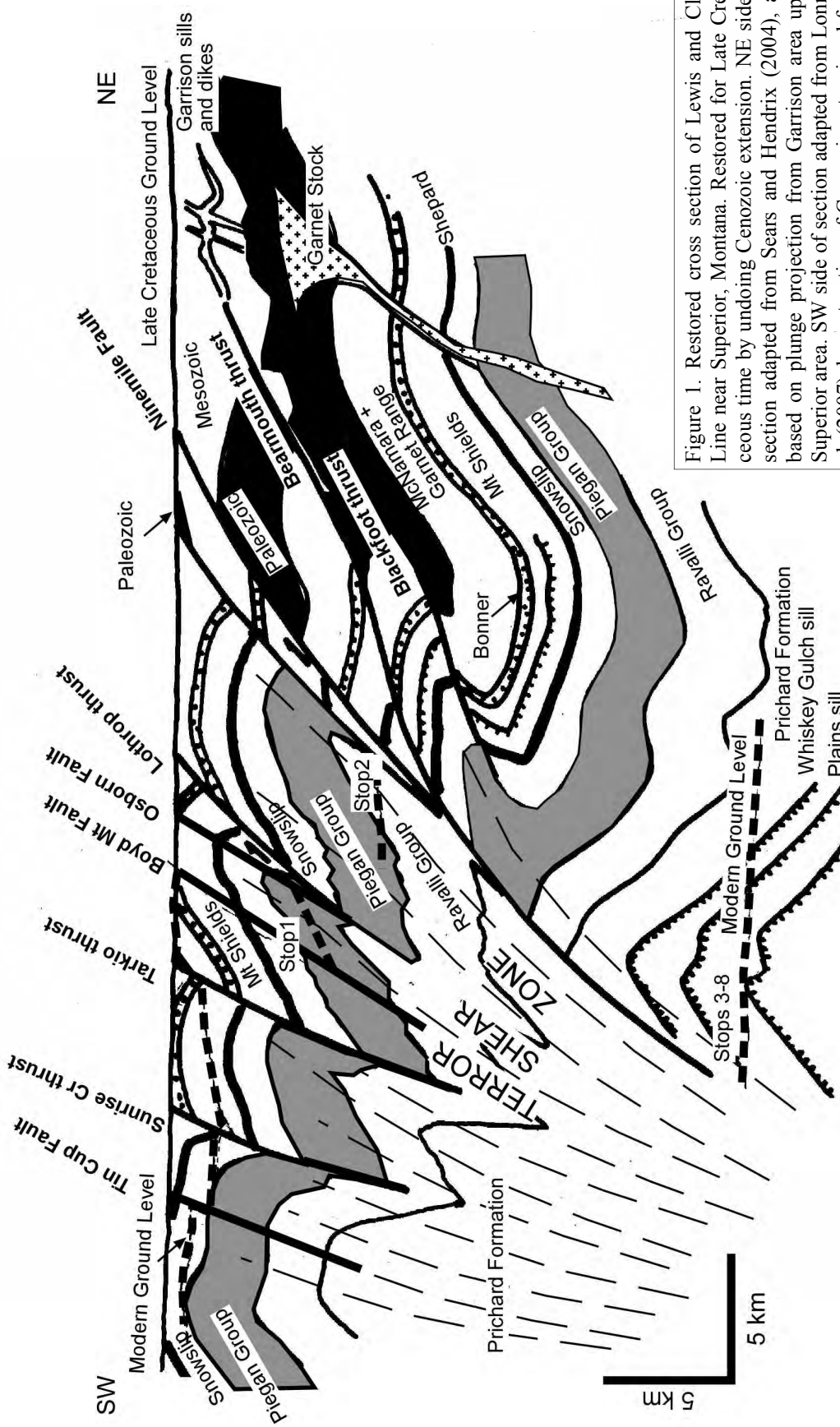

Figure 1. Restored cross section of Lewis and Clark Line near Superior, Montana. Restored for Late Cretaceous time by undoing Cenozoic extension. NE side of section adapted from Sears and Hendrix (2004), and based on plunge projection from Garrison area up to Superior area. SW side of section adapted from Lonn et al. (2007), by restoration of Cenozoic extensional faults relative to NE side of section. Heavy dashed lines indicate restored positions of modern ground surface near Superior from Lonn et al. (2007) cross-section. Note restoration of 15 km of throw of modern ground surface on Ninemile fault, SW side down.

restoration accounts for not only the minimum stratigraphic separations across the normal faults, but also for reactivation of thrust structures that significantly uplifted blocks of the Terror shear zone prior to the Cenozoic extension.

The scale of extension is comparable to the Eocene extension of the Bitterroot, Clearwater, and other metamorphic core complexes that are linked by the LCL (Hyndman et al., 1988; Foster and Fanning, 1997). The relatively cold footwall of the Ninemile fault reflects a typical continental geotherm, in contrast with magma-enhanced geotherms characteristic of the core complexes.

An en echelon series of SE-plunging half-grabens overprint the LCL across western Montana (Vuke et al., 2007). These include the Tarkio, Missoula-Ninemile, Arlee, Potomac, Greenough, Ovando, and Helena grabens. Broad valleys occupy the SE ends of these grabens, where thick Cenozoic deposits are preserved. Bedrock emerges toward their NW ends, where brecciated fault zones control steep valleys. The Cenozoic deposits of the grabens indicate that the Eocene faults were reactivated in Late Oligocene to Early Miocene. In several grabens, Eocene volcanics and fossiliferous Late Oligocene beds are tilted and overlain with angular unconformity by horizontal Middle Miocene fluvial gravel. A fluvial terrace can be traced through bedrock gorges between the grabens, showing that the modern drainages were established by Middle Miocene time (Sears 2009).

The Middle Miocene bedrock terrace is commonly displayed about 80 m in elevation above the Clark Fork and Bitterroot River (Sears, 2009, 2010). The terrace is dated to Middle Miocene near Garrison and near Drummond, because fossiliferous beds of Arikareean age are cut by the terrace, and fossiliferous fluvial beds of Barstovian age overlie the terrace (Rasmussen, 1969). Along the LCL near Missoula, steeply tilted beds dated as young as Oligocene underlie the terrace (Sears et al., 2010). Fossiliferous Miocene fluvial beds overlie it near Stevensville. The terrace is well expressed along the St. Regis cutoff, where the Clark Fork meanders in a Pleistocene canyon cut through the terrace.

However, the terrace appears to be missing along the Flathead and Jocko Rivers. Rather, Eocene paleovalleys are directly incised by the Pleistocene valleys with no intermediate terrace. Miocene faulting along the LCL evidently diverted the river from its Eocene course until rejoining it in Paradise.

Eocene-Oligocene drainage followed the Bitterroot Valley on the margin of the Bitterroot core complex, and may have passed through a gap in the Boundary Divide Range at Evaro Hill to link into the Flathead River drainage. The diverted Clark Fork cut Alberton Gorge across the uptilted edge of the Ninemile block to enter the Tarkio graben. It followed the Boyd Mountain fault zone to St. Regis, where it cut back across the Ninemile block to the Ninemile fault zone, which it followed SW for 15 km. The Clark Fork then cut across the Boundary Divide to link into a broad Eocene valley along the Hope fault (Yin and Oertel, 1995).

Where the river cuts across bedrock blocks, steep canyons give good outcrops of the structure and stratigraphy of the Belt Supergroup along the LCL. On this field trip, in addition to tracing the course of the Clark Fork, we will observe Laramide structures of the Terror shear zone and Plains anticline (Lonn et al., 2007). We will observe Belt Supergroup units, including the Prichard Formation and its sills, and the Ravalli

and Piegan groups. Winston (1991) interpreted the Belt Supergroup as the deposit of an intracratonic basin. His interpretation may generate discussion.

Part of the field guide presented here is adapted from longer field trips along the LCL by Sears et al. (1989, 2010), and Winston et al. (2003).

FIELD GUIDE

The field guide is generally keyed to highway mileposts to simplify locations of geologic features. GPS co-ordinates are given for most stops. Figure 2 shows the route of the field trip and the locations of the stops on a geologic base map.

Begin at Mineral County Courthouse in Superior. Proceed north and cross Clark Fork River. Turn right on Mullan Road. Go about 0.2 mi and stop beside large road cuts above river.

STOP 1 STOP1. 11TPN60055/29170. Road cuts on Mullan Road north of Superior. Park on shoulder above river.

Clark Fork River valley follows Boyd Mountain fault, one of the major strands of the LCL. Here it places McNamara Formation of upper Missoula Group, south of the river, against Wallace Formation of Piegan Group, north of the river. The fault has approximately 5.5 km of down-to-the-SW throw.

At this stop, the footwall of the Boyd Mountain fault exposes part of the Terror shear zone (Lonn et al., 2007), in the vertically-extruded core of the LCL flower structure. Note SW-directed thrust faults and shear fabrics.

RETURN through Superior and take I-90 west, toward Couer d'Alene.

MP 44. Brecciated McNamara Formation, Missoula Group, across river to left. The brecciation resulted from brittle Eocene and Miocene movement on the Boyd Mountain fault that overprinted the LCL flower structure. Miocene terrace cuts across McNamara and Garnet Range formations and is well-displayed for next 10 miles.

TAKE EXIT 33 toward St. Regis. Turn right on Montana Highway 135, toward Plains.

MP 0.5 Ravalli Group quartzites form low outcrop on left. Long ridge on left is truncated by Miocene terrace.

MP 2. Steeply-dipping Ravalli Group white quartzites crop out on left. These rocks were swept upward in the Terror shear zone. Large road cut shows open folds of bedding plunging to the SE. Miocene terrace on left.

MP 2.5. Cross trace of Osburn fault, one of the major dextral-normal, Eocene and Miocene faults of the LCL. It continues west to the Couer d'Alene district in Idaho. The brecciated fault zones control the placement of valleys along the LCL. Approximate center of Cretaceous-Paleocene Terror shear zone.

MP 3.5. Trace of Butler Gulch fault, which has 2 km of apparent dextral offset.

MP 4. Steeply-dipping, sheared Revett quartzite beds on the north in a tight fold along the LCL.

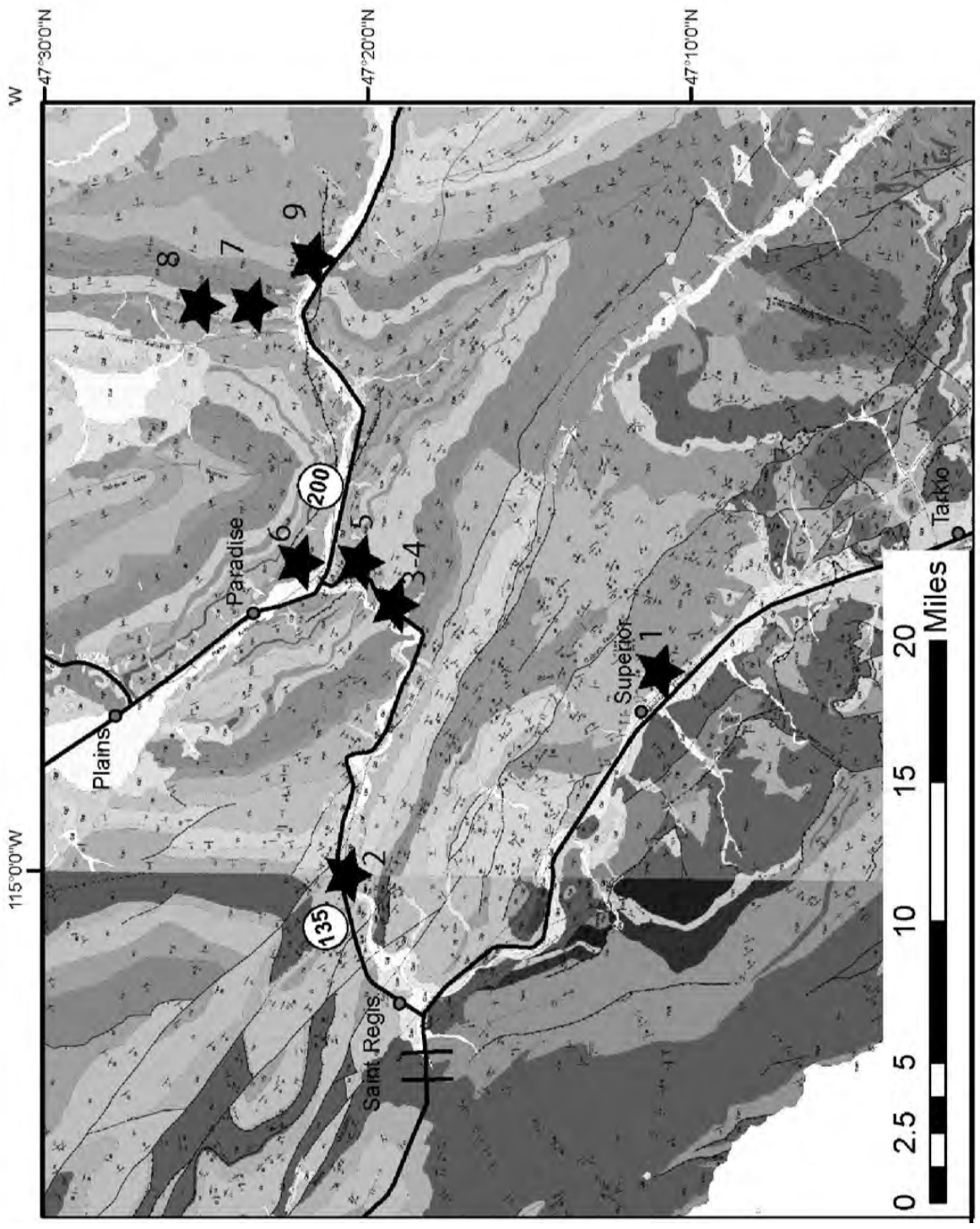

Figure 2. Map of field trip stops. Geological patterns from Lonn and McFaddan (1999) and Lonn et al. (2007).

STOP 2 MP 4.5. STOP 2. 11T PN 49354/43555. Pull over to large parking area on left side of road. The power lines cross the road and are visible from the stop.

St. Regis Formation of the Ravalli Group on the NE side of the Terror shear zone (Lonn et al., 2007). Bedding and ripple marks are preserved in vertical tabular quartzite beds and thin argillite couples and couplets.

CONTINUE east on Highway 135.

MP 7.5. Cross Sanders County Line. Large trough crossbeds in the Revett Quartzite are exposed in the roadcuts on the right near County line. This was a field trip stop for 2000 GSA meeting out of Missoula (White, 2000).

MP 10. Dolan Flats. Approximate trace of Thompson Pass Fault, which splays from the Ninemile Fault, one of the major Eocene-Miocene strands of the LCL.

MP 10.5. Cross Ninemile Fault and enter Prichard Formation, the oldest exposed part of the Belt Supergroup. This is the SW side of the Lewis-Eldorado-Hoadley thrust slab (Price and Sears, 2000).

MP 11. Good view of Railroad Bridge. Shiny phyllites on left are highly sheared Prichard Formation. Yin and Oertel (1995) studied the strain of these rocks. River meanders incise Miocene terrace for next 8 miles.

MP 13-16. Begin long traverse across SW limb of Plains anticline exposing 7-km thick section of Prichard and its mafic sills, with the base not exposed (Cressman, 1989). Note flat-irons of bedding planes in rusty-weathering Prichard Members 'G and F' across river in canyon walls.

MP 17.5. STOP 3. Park on left in large pull-out. Diabase sill in Prichard F. This **STOP 3** sill may be part of the 780 Ma "Gunbarrel Large Igneous Province", which has been mapped from Wyoming to the NW Territories of Canada. The sill appears to feed upwards into a dike/sill swarm which gave a 780 Ma U-Pb zircon age near Missoula (Burtis et al., 2007). Here the sill exhibits brittle quartz-filled tension gashes, and has been retrograded near its margins, due to Cretaceous-Paleocene effects on the flank of the Plains anticline.

MP 18. Siegel Creek Road. This rough road leads to the Ninemile Valley along the Clark Fork-Ninemile fault.

MP 18.5. STOP 4. 11T PN 65930/42792. Good pull-**STOP 4** off parking area on left, beside Clark Fork River, just west of Camp Bighorn. Tourist informational signs at parking area include one about Prichard Formation! Good exposures along river and across highway.

Prichard E on SW flank of Plains anticline. Prichard E is 800 m thick and represents the first shoaling interval in the Prichard Formation. Ripples and mudcracks on bedding planes may be the desiccated tops of sheet floods that crossed exposed mud flats. This unit yielded detrital zircons with an age range 1.6-1.5 Ga, suggesting a possible source area in Australia (Ross and Villeneuve., 2003). The Belt basin collapsed back into deep water after deposition of this unit. The collapse was accompanied by sill injection, mud diapirism, soft-sediment deformation, and exhalation of sedimentary exhalative (SEDEX) deposits. A syn-depositional fault intruded by soft-sediment breccia paralleled the Lewis and

Clark line in this region. The point source of the Prichard appears to have shifted northward at the time of the basin collapse, and built a new delta lobe for the Prichard Member G and middle Aldridge Formation (Cressman, 1989; Sears et al., 1998) .

CONTINUE on Montana Highway 135.

STOP 5 MP 19. STOP 5. 11T PN 67057/44286. Quinn Hot Springs. Plains sill. Pull off to right and park in café parking lot. Walk behind tourist cabins to old adit in Plains sill hidden in bushes.

Poage et al. (2000) studied the petrography of the Plains sill in detail. The Plains sill is a 150-300 m thick hornblende-diabase with thick granophyric caps. At this location, the sill is 220 m thick, intrudes Prichard Member D, and lacks the granophyre cap. Granophyre is best developed where the sill intrudes Prichard Member E. Mafic parts are high-iron tholeiites with mixed oceanic to continental affinities. There is no evidence for primary clinopyroxene in the sill. Hornblende is high-temperature and probably magmatic, but has undergone alteration to low-temperature hornblende in upper parts of the sill. Plagioclase is variably altered to epidote. The granophyre appears to be magmatic, perhaps due to sediment contamination, and migrated up-dip along synsedimentary structures. It has been U-Pb dated at 1469 Ma (Sears et al., 1998). It is vesicular and also contains miarolitic cavities. It was hydrated by absorption of water from the wet sediments that it intruded. It produced interference structures with the sediments, indicating intrusion into wet sediments. These include granosediments and ovoid structures indicative of boiling. This indicates that the sill injected at relatively low pressure, below the critical pressure for water. It intruded during basin collapse at the Prichard Member E-F boundary. It varies in thickness and stratigraphic position, and mapping indicates that the sill crossed an active normal fault that was injected with soft-sediment breccia dikes. Thick granophyre accumulated along fold hinge zones that were likely related to normal faulting. Mud volcanoes in the F member are probably correlative with the Sullivan SEDEX body in British Columbia (Lydon, 2000).

CONTINUE on Montana Highway 135.

MP 21. Cross Paradise sill, intruded into Prichard A-B boundary.

MP 21.5. STOP 6. Lower Prichard Formation and sills. **STOP 6**

The lowest part of the Prichard Formation is exposed here in the core of the Paradise anticline. Cressman (1989) defined the Prichard A member to include those turbidites underlying the prominent Paradise sill visible to the north in the columnar-jointed cliff across the Flathead River. The Paradise sill was intruded after sediment consolidation and yielded a U-Pb age of 1457 Ma (Sears et al., 1998). Although it was hydrated and autometamorphosed to amphibolite gabbro, it did not produce soft-sediment interference textures with the host rocks. The Prichard A is a rusty-weathering silty turbidite. It has biotite, chlorite, and garnet porphyroblasts indicative of burial metamorphism, probably augmented by heat flow from the mafic sills. A conventional K-Ar date of 1330 Ma from biotite porphyroblasts from the upper Prichard Formation (Obradovich and Peterman, 1968) may record cooling of the section through the biotite blocking-temperature.

The bedrock terrace cut on the Paradise sill on the north side of the Flathead River may be a remnant of the Middle Miocene paleovalley floor. The terrace continues NW to Plains. Similar terraces occur at that relative height above many of the Clark Fork tributaries, and in several localities are dated to Middle Miocene. To the NW, the Clark Fork follows the Hope Fault, one of the major strands of the LCL. The Hope fault had large-scale extensional displacement in the Eocene and linked Eocene core complexes of northern Washington and Idaho with those of western Montana. Early to Middle Miocene faulting may have diverted the Clark Fork through Alberton Gorge and the St. Regis cut-off to this point, where it rejoined its original, broad Eocene valley. The deep canyon of the Clark Fork to the SW of this stop (which we just passed through) may have been cut during the Late Oligocene-Early Miocene down to the elevation of the Middle Miocene terraces.

CONTINUE on MT 135.

Junction Highway 200. Turn right toward Ravalli.

MP 91. Long road cuts of rusty-weathering Prichard Member B run parallel to strike.

MP 92. Cross Seepay Creek. Axial trace of the large Seepay Creek anticline trends southeast down this valley. Deepest exposed part of Prichard, Member A, is in core of this anticline. On north side of river is the Paradise sill in the hinge zone of the anticline.

MP 93. Gently-dipping, columnar-jointed Paradise sill on north side of river intrudes the boundary of Prichard members A and B. This sill dated as 1457 +/-2 Ma by U-Pb on magmatic zircon (Sears et al., 1998).

MP 94. Intersection of Highway 382. Turn left toward Hot Springs. Cross Flathead River.

MP 2. STOP 6.11T PN 83391/51684. Park on shoulder on right.

Vertical beds of Prichard E with dewatering structures and ripple marks. This is the east limb of the north-trending Camas Prairie anticline, one of the folds of the Purcell anticlinorium. The structural trends bend abruptly from southeasterly along the Lewis and Clark line to northerly in the LEH slab.

Continue north on Highway 382.

MP 3. STOP 7.11T PN 83012/52800. Park on shoulder.

STOP 7

Vertical Prichard E member with Plains sill. The contact displays soft-sediment deformation features indicating that the sill injected syndepositionally.

RETURN to Montana Highway 200, continue east.

MP 96. STOP 8. 11T PN 83938/48186. Park in large lot on north side of road, walk back to west to see outcrop.

STOP 8

On west side of outcrop is an exposure of vertical Whiskey Gulch sill and its basal intrusive contact on east limb of Camas Prairie anticline. It intrudes Prichard member F, and is a marker unit that can be traced around the Perma culmination. We suggest that the Green Mountain dike and other en echelon dikes that cut the Burke and Revett formations may branch from this sill, and that this sill therefore post-dates deposition of the Revett Formation. Recent U-Pb dates of 780 Ma

on zircon from sills exposed farther to the east (Burtis et al., 2007) suggest that this sill-dike system corresponds to Neoproterozoic Windermere rifting. The dike swarm sub-parallels the LCL, indicating Neoproterozoic reactivation of the LCL.

END OF FIELD GUIDE.

REFERENCES

Burtis, E.W., Sears, J.W., and Chamberlain, K.R., 2007, Age and Petrology of Neoproterozoic Intrusions in the Northern Rocky Mountains, U.S.A.: Correlation with the Gunbarrel Magmatic Event: *in* Link, P.K. and Lewis, R., eds., Proterozoic geology of western North America and Siberia: SEPM Special Paper 86.

Coney, P.J., and Harms, T.A., 1984, Cordilleran metamorphic core complexes; Cenozoic extensional relics of Mesozoic compression: Geology, v. 12, p. 550-554.

Constenius, K.N., 1996, Late Paleogene extensional collapse of the Cordilleran foreland fold and thrust belt: Geological Society of America Bulletin, v. 108, p. 20-39.

Cressman, E. R., 1989, Reconnaissance stratigraphy of the Prichard Formation (Middle Proterozoic) near Plains, Sanders County, Montana: U.S. Geological Survey Professional Paper 1490, 80 p.

Evans, K.V., Aleinikoff, J.N., Obradovich, J.D., and Fanning, C.M., 2000, SHRIMP U-Pb geochronology of volcanic rocks, Belt Supergroup, western Montana: Evidence for rapid deposition of sedimentary strata: Canadian Journal of Earth Sciences, v. 37, p. 1287-1300.

Foster, D.A., and Fanning, M., 1997, Geochronology of the northern Idaho batholith and the Bitterroot metamorphic core complex: Magmatism preceding and contemporaneous with extension: Geological Society of America Bulletin, v. 109, p. 379-394.

Harrison, J.E., 1972, Precambrian Belt basin of the northwestern United States, its geometry, sedimentation, and copper occurrences: Geological Society of America Bulletin, v. 83, p. 1215-1240.

Harrison, J.E., Griggs, A.B., and Wells, J.D., 1974, Tectonic features of the Precambrian Belt basin and their influence on post-Belt structures: U.S. Geological Survey Professional Paper 866, 15 p.

Hyndman, D.W., Alt, D., and Sears, J.W., 1988, Post-Archean metamorphic and tectonic evolution of western Montana and northern Idaho: *in* Ernst, W.G., ed., Metamorphism and crustal evolution of the western United States: Prentice-Hall, N.J., Rubey Volume VII, p. 332-361.

Hyndman, D.W., 1980, Bitterroot dome-Sapphire tectonic block, an example of a plutonic core-gneiss-dome complex with its detached suprastructure: *in* Crittenden, M.D., Coney, P.J., and Davis, G.H., eds., Cordilleran core complexes: Geological Society of America Memoir 153, p. 427-443.

Janecke, S.U., 1994, Sedimentation and paleogeography of an Eocene to Oligocene rift zone, Idaho and Montana: Geological Society of America Bulletin, v. 106, p. 1083-1095.

Link, P.K., Christie-Blick, N., Devlin, W.J., Elston, D.P., Horodyski, R.J., Levy, M., Miller, J.M.G., Pearson, R.C., Prave, A., Stewart, J.H., Winston, D., Wright, L.A., and Wrucke, C.T., 1993, Middle and Late Proterozoic stratified rocks of the western United States Cordillera, Colorado Plateau, and Basin and Range Province: *in* Reed., J., Sims, P., Houston, R.S., Rankin, D.W., Link, P.K., Van Schmus, W.R., and Bickford, M.E., eds., Precambrian: Conterminous United States: Geological Society of America Decade of North American Geology Series, v. C-3, p. 474-690.

Lonn, J.D., and McFaddan, M.D., 1999, Geologic map of the Montana part of the Wallace 30' x 60' quadrangle: Montana Bureau of Mines and Geology Open-File Report MBMG 388, 16 p., scale 1:100,000.

Lonn, J.D., Smith, L.N., and McCulloch, R.B., 2007, Geologic map of the Plains 30' x 60' quadrangle, western Montana: Montana Bureau of Mines and Geology Open-File Report 554, 43 p., scale 1:100,000.

Lydon, J.W., 2000, A synopsis of the current understanding of the geological environment of the Sullivan deposit: *in* Lydon, J.W., Höy, T., Slack, J.F., and Knapp, M.E., eds., The Geological Environment of the Sullivan Deposit, British Columbia: Geological Association of Canada, Mineral Deposits Division Special Publication 1, p. 12-31.

Obradovich, J.D., and Peterman, Z.E., 1968, Geochronology of the Belt series, Montana: Canadian Journal of Earth Sciences, v. 5, p. 737-747.

Poage, M.A., Hyndman, D.W., and Sears, J.W., 2000, Petrology, geochemistry, and diabase-granophyre relations of a thick basaltic sill emplaced into wet sediments, western Montana: Canadian Journal of Earth Sciences, v. 37, p. 1109-1119.

Price, R.A., and Sears, J.W., 2000, A preliminary palinspastic map of the Mesoproterozoic Belt-Purcell Supergroup, Canada and USA: Implications for the tectonic setting and structural evolution of the Purcell anticlinorium and the Sullivan deposit: *in* Lydon, J.W., ed., The Sullivan deposit and its geological environment: Geological Survey of Canada, p. 61-81.

Rasmussen, D., 1969, Late Cenozoic geology of the Cabbage Patch area, Granite and Powell Counties, Montana: Ph.D. thesis, University of Montana, Missoula, 188 p.

Ross, G.M., and Villeneuve, M., 2003, Provenance of the Mesoproterozoic (1.45 Ga) Belt basin (western North America): Another piece in the pre-Rodinia paleogeographic puzzle: Geological Society of America, Bulletin, v. 115, p. 1191-1217.

Sears, J.W., 1988, Two major thrust slabs in the west-central Montana Cordillera: *in* Schmidt, C., and Perry, W.J., eds., Interactions of the Rocky Mountain Foreland and the Cordilleran Thrust Belt, Geological Society of America, Memoir 171, p. 165-170.

Sears, J.W., 1994, Thrust rotation of the Belt basin, Canada and United States: Northwest Geology, v. 23, p. 81-92.

Sears, J.W., 2001, Emplacement and denudation history of the Lewis-Eldorado-Hoadley thrust slab in the northern Montana Cordillera, USA: Implications for steady-state orogenic processes: American Journal of Science, p. 359-373.

Sears, J.W., 2007, Belt-Purcell basin: Keystone of the Rocky Mountain fold-and-thrust belt, United States and Canada: *in* Sears, J.W., Harms. T.A., and Evenchick, C.A., eds., Whence the Mountains? Inquiries into the Evolution of Orogenic Systems: A Volume in Honor of Raymond A. Price: Geological Society of America Special Paper 433, p. 147-166.

Sears, J.W., 2009, Straths as tectonic timelines and baselines: Example from southwest Montana: Northwest Geology, v. 38, p. 35-39.

Sears, J.W., 2010, Lost lakes and re-arranged rivers: Neotectonic disruption of the Middle Miocene Big Hole River basin, SW Montana: Northwest Geology, v. 39, p. 113-121.

Sears, J.W., Weiss, C.P., Reynolds, P.H., and Griffin, J.H., 1989, A structural section through a 25-km-thick thrust plate in west-central Montana: A field trip from Paradise to Garrison: *in* Chamberlain, V.E., Breckenridge, R.M., and Bonnichsen, B., eds., Guidebook to the Geology of Northern and Western Idaho and Surrounding Area: Idaho Geological Survey Bulletin 28, p. 87-102.

Sears, J.W., Chamberlain, K.R., and Buckley, S.N., 1998, Structural and U-Pb geochronologic evidence for 1.47 Ga rifting event in the Belt basin, western Montana: Canadian Journal of Earth Sciences, v. 35, p. 467-475.

Sears, J.W., and Hendrix, M., 2004, Lewis and Clark line and the rotational origin of the Alberta and Helena salients, North American Cordillera: *in* Sussman, A., and Weil, A., eds., Orogenic curvature: Geological Society of America Special Paper, p. 383, p. 173-186.

Sears, J.W., MacDonald, C., and Lonn, J., 2010, Lewis and Clark Line, Montana: Tectonic evolution of a crustal-scale flower structure in the Rocky Mountains: *in* Morgan, L.A., and Quane, S.L., eds., Through the generations: Geologic and anthropogenic field excursions in the Rocky Mountains from modern to ancient: Geological Society of America, Field Guide 18, p. 1-20.

Vuke, S.M., Porter, K.P., Lonn, J.D., and Lopez, D.A., 2007, Geologic map of Montana: Montana Bureau of Mines and Geology Geologic Map 62, scale 1: 500,000.

Wallace, C.A., Lidke, D.J., and Schmidt, R.G., 1990, Faults of the Lewis and Clark line and fragmentation of the Late Cretaceous foreland basin in west-central Montana: Geological Society of America Bulletin, v. 102, p. 1021-1037.

Winston, D., 1991. Evidence for intracratonic, fluvial, and lacustrine settings of Middle to Late Proterozoic basins of western U.S.A.: *in* Gower, C.F., Rivers, T., and Ryan, B., eds., Mid-Proterozoic Laurentia-Baltica: Geological Association of Canada Special Paper 38, p. 535-564.

Winston, D., Sears, J.W., and Lonn, J.D., 2003, Road log, field trip #1, Belt Symposium IV: Missoula-Ravalli-Perma-St. Regis-Alberton-Missoula, Montana: Northwest Geology, v. 32, p. 1-17.

White, B.G., 2000, Coeur d'Alene mining district: Product of preconcentrated source deposits and tectonism within the Lewis and Clark line: *in* Roberts, S., and Winston, D., eds., Geological field trips, western Montana and adjacent areas: Geological Society of America, Rocky Mountain section meeting, Missoula: University of Montana, Missoula, p. 95- 101.

Yin, A., and Oertel, G., 1995, Strain analysis of the Ninemile fault zone, western Montana: Insights into multiply deformed regions: Tectonophysics, v. 247, p. 133-143.

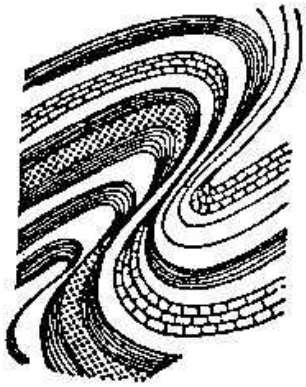

BELT ROCKS AND STRUCTURES OF THE LEWIS AND CLARK LINE IN ALBERTON GORGE, WESTERN MONTANA: A RIVER LOG

Jeff Lonn
Montana Bureau of Mines and Geology, 1300 W. Park St., Butte, MT 59701 • jlonn@mtech.edu

INTRODUCTION

Near Huson the Clark Fork River leaves the wide Missoula-Ninemile Valley to slice a deep canyon west through the mountains and across the structural grain of the Lewis and Clark Line. Between Cyr and Tarkio it has cut a narrow inner gorge in the valley bottom that reveals the underlying bedrock geology. Here, in Alberton Gorge (fig. 1), also known as Cyr Canyon, the Clark Fork has polished beautiful examples of Belt Supergroup sedimentary features and exposed complex faults and folds characteristic of the Lewis and Clark Line. On this trip, we will float 10 miles through Class II and III rapids to view these fantastic examples of Belt geology.

Although whitewater boaters do not consider Alberton Gorge to be a difficult run, it should not be attempted by those without whitewater experience or suitable whitewater craft. Numerous fatalities have occurred along this stretch, and the high flows and cold water temperatures of spring should be avoided. This trip is scheduled for late July, when water temperatures average about 70^{o} F with flows of 1500 to 4000 cubic feet per second (cfs).

This river log is a revision of a field guide written for the 2001 Tobacco Root Geological Society's annual field conference (Lonn, 2001). In the 10 years since that first trip, tremendous advances have been made in the understanding Belt stratigraphy and the Lewis and Clark Line, both locally (Lonn and Smith, 2005, 2006; Lonn et al., 2007) and regionally (Burmester and Lewis, 2003; Winston, 2007; Sears and Hendrix, 2004; Sears et al., 2010; Lonn et al., 2010). This field guide incorporates new concepts from that work.

REGIONAL GEOLOGY

Numerous geologic maps cover this region (Campbell, 1960; Hall, 1968; Wells, 1974; Lonn, 1984; Harrison et al., 1986; Winston and Lonn, 1988; Lewis, 1998b; Lonn and McFaddan, 1999; Lonn and Smith, 2005, 2006; Lonn et al., 2007), but many offer contrasting and conflicting interpretations of both the stratigraphy and structure. Mapping completed since 2001 by the Montana Bureau of Mines and Geology has resolved most of these controversies.

Stratigraphy

Bedrock exposed in Alberton Gorge belongs to the Mesoproterozoic Belt Supergroup, an immensely thick sequence (more than 8 miles, or 13 km, thick!) of weakly metamorphosed sedimentary rocks about 1.4 billion years old. Alberton Gorge contains exposures of the Belt section from the Wallace to the Mount Shields Formations (fig. 2), representing about 12,000 feet (3,692 m) of the Belt Supergroup stratigraphic section. Because most Belt rocks are mixtures of siliciclastic fine-grained arenite, siltstone, and claystone, and color is affected by diagenesis and metamorphism, conventional descriptions based on color, grain size, and composition are inadequate. Winston (1986b) has addressed this problem by devising a system of sediment types that do successfully delineate Belt units (fig. 3). The trip provides participants with the opportunity to observe beau-

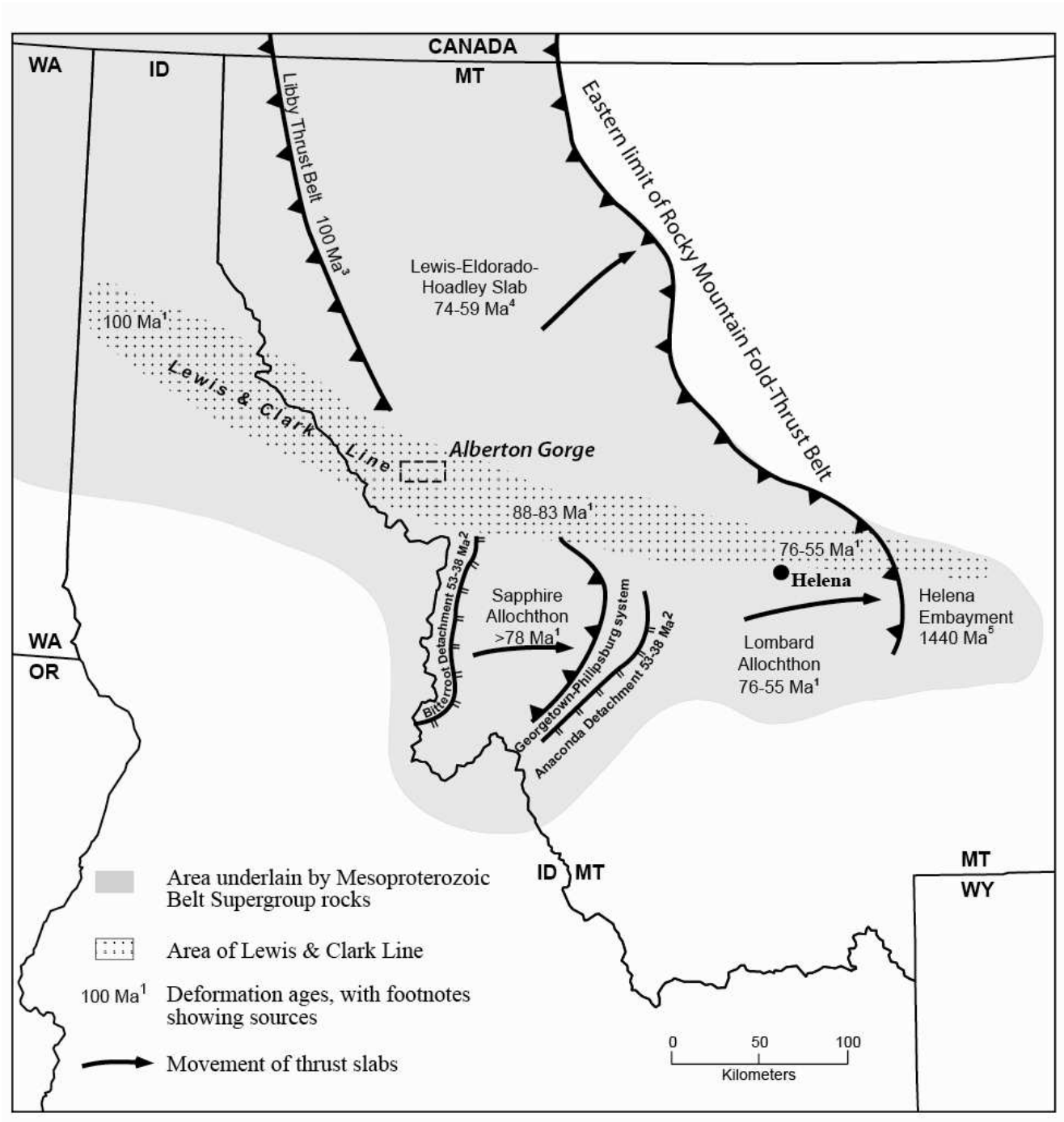

Figure 1. Location of Alberton Gorge with respect to major structural features of western Montana. Data sources for ages of structures: [1]Sears and Hendrix (2004); [2]Foster et al. (2007); [3]Harrison and Cressman (1993); [4]Sears (2001); [5]Elston et al. (2002).

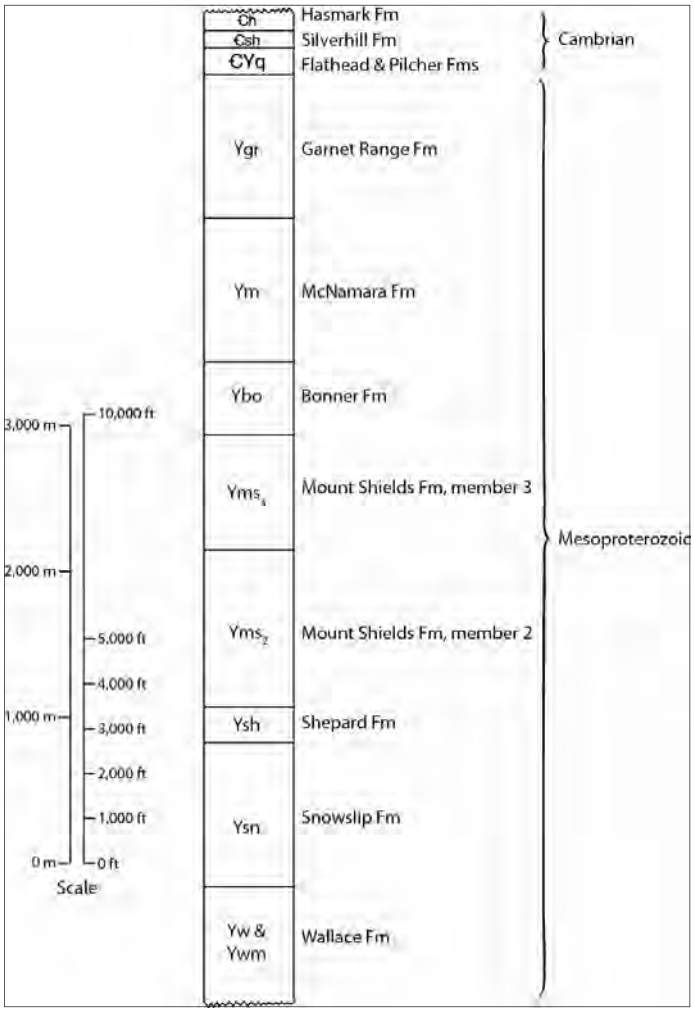

Figure 2. Stratigraphic section for Alberton Gorge area geologic map (fig. 4). Unit thicknesses drawn approximately to scale.

tiful river-polished examples of diagnostic sediment types and to discuss what the sedimentary features indicate about the environments of deposition.

Unusual lithologies in the Snowslip Formation have produced a great deal of confusion in mapping this region. A 500-foot-thick quartzite interval at the top of the Snowslip was misidentified by Campbell (1960) and Harrison et al. (1986) in several localities. And a carbonate-rich zone beneath the Snowslip quartzite appears on Harrison et al.'s (1986) map as lower Wallace Formation. Assignment of these rocks to a normal stratigraphic sequence significantly simplifies the structural complexity depicted on earlier maps. We will view these atypical Snowslip facies along the river.

Unconsolidated Quaternary deposits cover the bedrock, forming the rim of the inner gorge and the flat valley floor above. These are mostly bouldery glacial flood gravels deposited during the catastrophic draining of Glacial Lake Missoula that occurred several times during the Pleistocene Ice Ages. Lake Missoula was held back by a dam of glacial ice in northern Idaho, and when the glacial dam burst, as it did several times, tremendous volumes of water, perhaps 200 million cubic feet per second (cfs), rushed through this narrow valley, tumbling enormous boulders and scouring the valley sides down to bare rock. The resulting deposits are poorly sorted mixtures of sand, gravel, and huge boulders, and we will view them at the put-in as well as in the sides of the inner gorge. They form the flat floor of the main valley, suggesting that the inner gorge has been cut since the last flood about 15,000 years ago.

Structure

This trip crosses part of the Lewis and Clark Line (LCL), a wide, 800-km-long, WNW-striking zone of faults and folds that transects the more northerly structural grain of the northern Rockies (fig. 1). It extends from the Coeur d'Alene mining district southeastward to Missoula, to north of Helena, and onward to the Helena Embayment of the Belt Basin. Because it coincides with the Helena Embayment and also with facies and thickness changes in the Belt units farther west, most workers agree that Precambrian structure had some influence on the LCL's geometry, although the details of this Precambrian structure are contested (Hobbs et al., 1965; Harrison et al., 1974;

SEDIMENT TYPE	SEDIMENTARY STRUCTURES	DESCRIPTION	DEPOSITIONAL PROCESSES
CROSSBEDDED SAND		Coarse- to fine-grained, crossbedded, feldspathic sand, beds 10 to 150 cm thick.	Channeled flood and sheetflood transport and deposition.
FLAT-LAMINATED SAND		Medium- to fine-grained flat-laminated sand, climbing ripples, mudchips, beds 10 to 150 cm thick.	Sheetflood transport and deposition.
DISCONTINUOUS LAYER	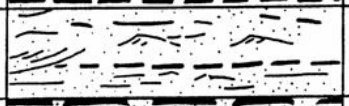	Fine sand to silt lenses in mud layers, occasional mudchip concentrations.	Waning flood and intermittent flow transport and deposition.
MUDCRACKED EVEN COUPLE		Even, mudcracked, graded fine sand and silt-to-mud layers 3 to 10 cm thick.	Sheetflood transport and deposition.
MUDCRACKED EVEN COUPLET		Even, mudcracked, graded, fine sand and stlt-to-mud layers 0.3 to 3 cm thick.	Sheetflood flow across exposed mudflats followed by deceleration, suspension settleout and desiccation.
MUDCRACKED LENTICULAR COUPLET		Oscillation-rippled fine sand and silt lenses, capped by clay laminae, cut by mudcracks.	Wave transport of fine sand and silt, followed by clay settleout and desiccation.
MUDCRACKED MUD		Mud layers up to 2 cm thick, cut by mud-filled mudcracks.	Suspended load transport across dried playa floors, followed by submergence and desiccation.
MICROLAMINA		Interlayered or graded silt and clay laminations less than 0.3 cm thick.	Alternating silt and clay suspension settleout.
COARSE SAND AND INTRACLAST		Coarse- to fine-grained, sand and flat clasts, crossbedded and imbrecated at various angles.	Transport of coarse sand grains and scoured clasts by breaking waves.
CARBONATE MUD		Micrite and dolomicrite without detectable siliciclastic laminations.	Aragonite or calcite precipitation, in places followed by dolomitization.
UNCRACKED LENTICULAR COUPLET		Oscillation-rippled fine sand and silt lenses, capped by clay laminae, cracked and uncracked.	Wave transport of fine sand and silt, followed by suspension settleout.
UNDULATING COUPLET		Graded to sharply bounded silt-to-clay couplets that thicken and thin across outcrops in a gently wavy or undulating manner.	Episodic deposition of silt by small storm waves, possibly limited in size by shallow depth, followed by suspension settleout.
PINCH-AND-SWELL COUPLET		Graded fine sand to dark mud layers with undulating scoured and loaded bases, 0.3 to 3 cm thick.	Episodic erosion by storm waves, deposition of hummocks, which loaded into underlying mud, followed by mud settleout.
PINCH-AND-SWELL COUPLE		Graded fine sand to dark mud layers with undulating scoured and loaded bases >3 cm thick.	Episodic erosion by storm waves, deposition of hummocks, which loaded into underlying mud, followed by mud settleout.
MUDDY GRADED SAND		Graded structureless or plane-laminated, dark muddy sand beds.	Turbidiy flow transport and deposition.
UNCRACKED EVEN COUPLET	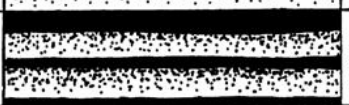	Even, uncracked graded silt-to-clay couplets 0.3 to 3 cm thick.	Episodic suspension transport and settleout.
PLANE-LAMINATED SILT AND CLAY		Even, sharply bounded, silt and clay interlaminations.	Alternating silt and clay transport and settleout.

Figure 3. Belt sediment types of Winston (1986b).

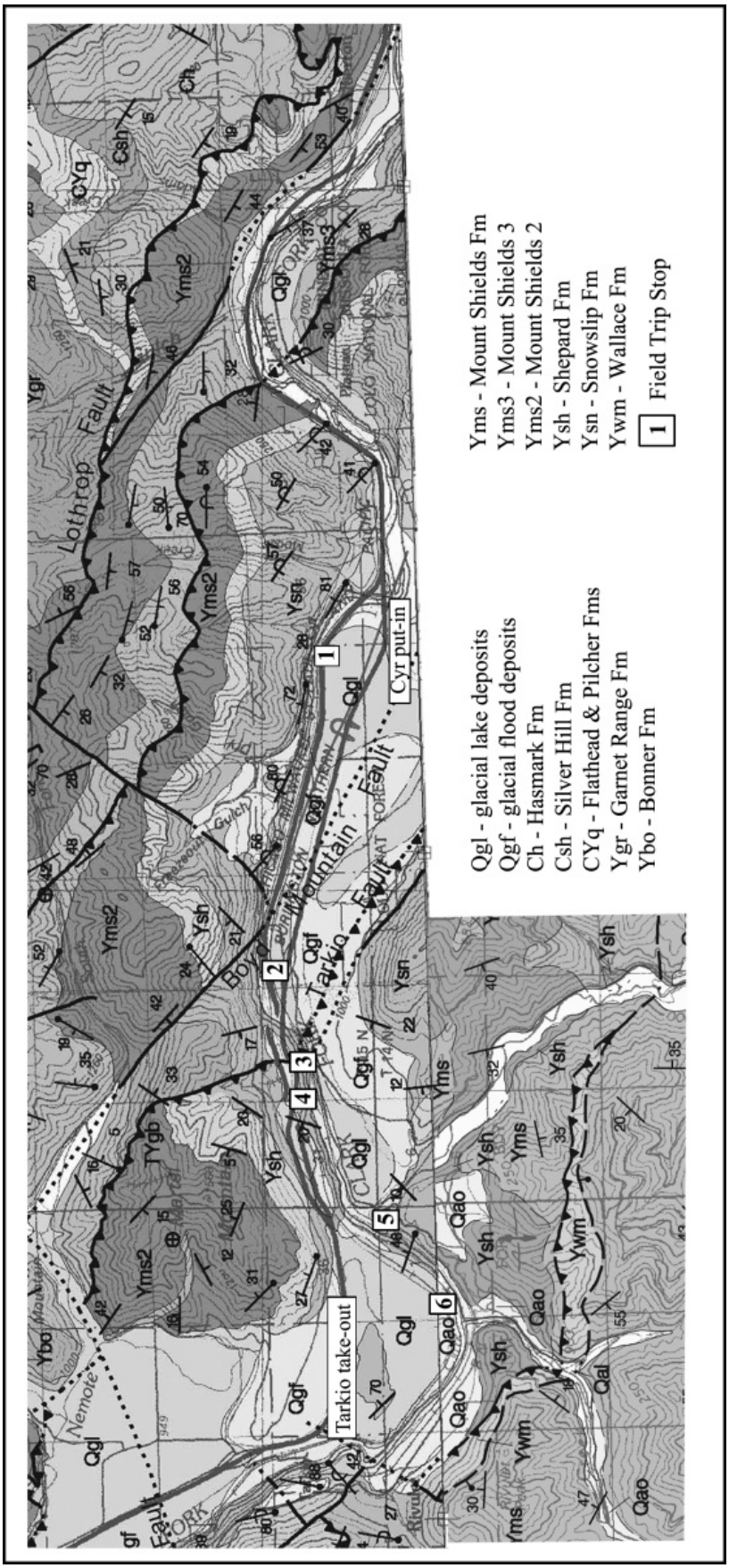

Figure 4. Geologic map of field trip area (from Lonn et al., 2007; Lewis, 1998b). Numbered stops along the river are shown; scale 1:100,000.

Reynolds, 1977; Winston, 1986a; Leach et al., 1988; Sears and Hendrix, 2004). Indeed, documented Precambrian structures along the LCL are rare, and in the Superior and Alberton Gorge areas (fig. 4), all the structures that define the LCL are Cretaceous and Cenozoic in age.

Although the original definition of the line (Billingsley and Locke, 1941) was based on geography controlled by Cenozoic strike-slip and normal faults rather than contractile features, most subsequent workers have concluded that Cretaceous compressive or transpressive structures are an important component of the LCL (Smith, 1965; Lorenz, 1984; Hyndman et al., 1988; Griffin, 1989; Wallace et al., 1990; Reid et al., 1993, 1995; White, 1993; Yin et al., 1993; Yin and Oertel, 1995; Sears and Clements, 2000; Burmester and Lewis, 2003; Sears and Hendrix, 2004; Lonn et al., 2007, 2010; Sears et al., 2010). Subsequent Cenozoic extension and/or right-lateral shear (Hobbs et al., 1965; Reynolds, 1979; Harrison et al., 1974; Bennett and Venkatakrishnan, 1982; Sheriff et al., 1984; Winston, 1986a; Doughty and Sheriff, 1992; Yin et al., 1993; Yin and Oertel, 1995; Lonn and McFaddan, 1999; Lonn et al., 2007, 2010) superimposed high angle normal and dextral faults that roughly parallel and obscure the compressional features.

The LCL appears to be a long-lived feature. It forms the southern boundaries of the Cretaceous Libby thrust belt/Purcell Anticlinorium and Late Cretaceous to Paleocene Lewis-Eldorado-Hoadley slab, and it forms the northern boundaries of the Mesoproterozoic Helena Embayment of the Belt Basin, the Late Cretaceous Sapphire Allochthon, the Late Cretaceous to Paleocene Lombard allochthon, and the Eocene Bitterroot and Anaconda metamorphic core complexes (fig. 1). In the Alberton Gorge area, the LCL has been shown to post-date the 100-million-year-old north-trending folds and reverse faults of the Libby thrust belt and Purcell Anticlinorium (Lonn et al., 2007).

Sears and Hendrix (2004) interpreted the LCL as a Cretaceous flower structure that developed in response to sinistral transpression. Flower structures develop in areas of transpression, or oblique convergence, where shortening and strike-slip displacement occur simultaneously. In flower structures, material at depth is squeezed plastically upward along near-vertical ductile structures that fan outward and dip more gently at higher structural levels (fig. 5). Because the LCL plunges southeastward, deeper structural levels with near vertical ductile structures are exposed along the western part of the line, from the Coeur D'Alene mining district to the Superior area, and more gently dipping, brittle structures are exposed southeastward from Superior (fig. 6). The Alberton Gorge area lies within the lower reaches of the brit-

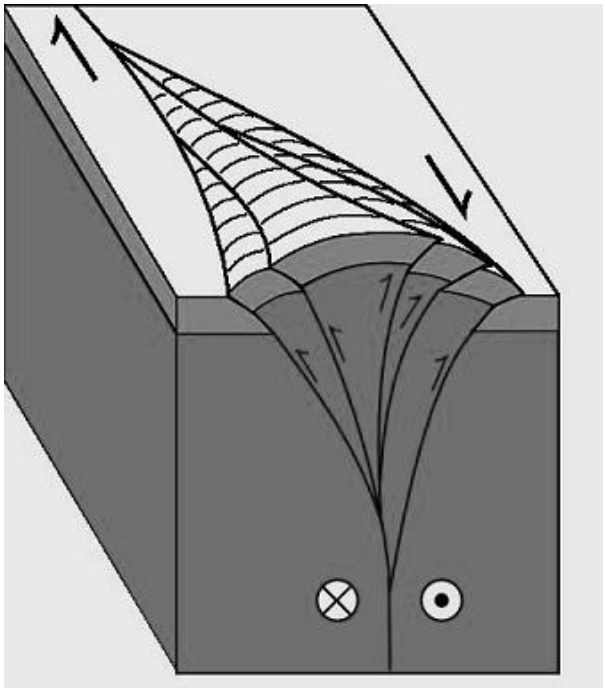

Figure 5. Simplified block diagram of a positive flower structure (from Wikipedia).

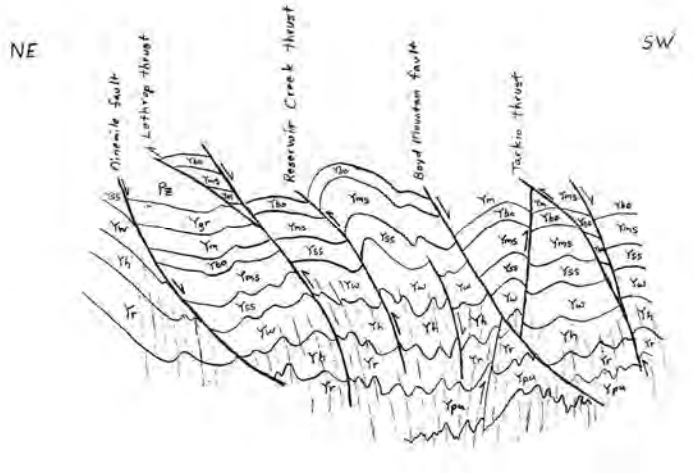

Figure 6. Sketch of downplunge projection of the LCL in the Alberton Gorge area modeled as a flower structure after Sears and Hendrix (2004). Light lines depict steep foliation at depth where material was squeezed plastically upward. Tarkio and Lothrop fault systems are interpreted as Cretaceous extraction faults (Frotzheim et al., 2006), while the Ninemile and Boyd Mountain faults are shown as cross-cutting Cenozoic normal faults.

tle domain, and displays contractile structures that include zones of WNW-striking, anastomosing reverse and normal faults, WNW-trending folds, some of which are overturned to the NE, and steeply south-dipping, WNW-striking cleavage (figs. 4, 6). In the anastomosing fault zones, south-dipping reverse and normal faults define lozenges or wedges of older strata caught between blocks of younger strata. A wedge of older rock is typically flanked by a south-dipping reverse fault on its north side and a sub-parallel, south-dipping normal fault to its south (fig. 7). This fault geometry is common along the LCL and it has been explained by extensional reactivation of pre-existing reverse faults (fig. 7a; Lewis, 1998c) or by out-of-sequence thrusting (Wallace, 1987; Lidke et al., 1988). However, this geometry may also result when a wedge of rock is extruded or extracted be-

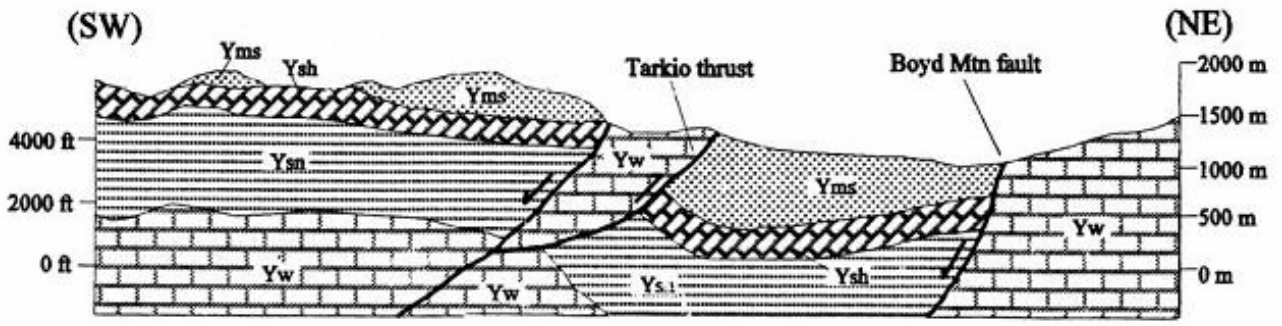

Figure 7. Two processes that can form parallel and anastomosing normal and reverse faults, common along the LCL: a) Extensional reactivation of a pre-existing reverse fault (from Lewis, 1998c). b) Horizontal contraction generating synchronous reverse and normal faults through an extrusion or extraction process. This type of normal fault has been termed a "shortening-induced normal fault" (Ring and Glodny, 2010); modified from Reid et al. (1995).

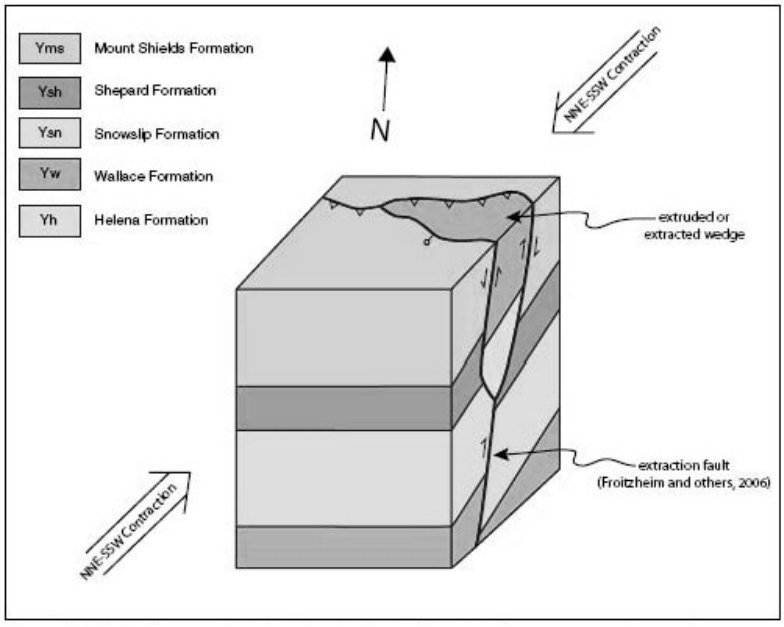

tween two coeval faults with opposite shear sense (fig. 7b; Froitzheim et al., 2006) as has been proposed for the deeper, western segments of the LCL (Wavra et al., 1994; Reid et al., 1993, 1995; Lonn et al., 2007). In other words, these wedges may have been squeezed upward like bars of soap by horizontal contraction. In the classic flower structure model, the vertical structures at depth diverge upward to dip in both directions, but along this part of the LCL, most faults dip SW and most folds verge NE. However, these wedges may still represent "flowers", but ones that droop to the northeast instead of standing straight up (figs. 6, 7b).

Regional map patterns suggest that left-lateral shear accompanied the Cretaceous NE-SW contraction, but left-lateral faults are difficult to document. This may be because the strike-slip movement was partitioned into narrow bands that have been obscured by the later Tertiary normal/dextral faults, or because the left-lateral movement was broadly distributed across the LCL as a zone of ductile shear expressed by sets of NW-striking en echelon folds that are especially evident east of Missoula (Lonn et al., 2010) and by the north-trending folds that have been bent eastward in a left-lateral sense near Plains and Dixon (Lonn et al., 2007).

The WNW-striking transpressive structures are cut by steep N to NE-striking faults. Some of these are associated with N-S-trending overturned folds, suggesting that they too are reverse faults (Lonn et al., 2010).

A series of Cenozoic WNW-trending normal and dextral faults then cut and reactivated the earlier structures. These appear to have developed during Tertiary extensional tectonism, and are represented by the Boyd Mountain fault. Some normal faults parallel and have probably reactivated the Cretaceous reverse faults, resulting in map patterns that mimic those of the extraction faults described above, but that instead were formed by two superimposed tectonic regimes (Lewis, 1998c). Both Cretaceous shortening-induced normal faults (Ring and Glodny, 2010) and Tertiary extensional normal faults probably occur along the LCL, and they are very difficult to tell apart (fig.7).

A right-lateral component to the Tertiary movement has also been documented along the LCL (Hobbs et al., 1965; Wallace et al., 1990; Lonn and McFaddan, 1999). The relationships of the right-lateral normal faults along the LCL to other Tertiary extensional structures, such as the Anaconda and Bitterroot metamorphic core complexes, are uncertain.

Tertiary extension is also responsible for the formation of near-horizontal kink folds (fig. 8) along the western part of the LCL (White, 1993, 2000; White et al., 2000; Lonn et al., 2007) and of related (?) low-angle normal faults documented in the Superior to Alberton area (Lewis, 1998b; Lonn et al., 2007). These may have formed prior to the high-angle Tertiary structures described above.

The complex structural history of this area might be summarized as follows (also see fig. 1):

D_1; 100 Ma: E-W horizontal shortening, producing the NNW-striking Libby thrust belt and NNW-trending folds of the Purcell Anticlinorium.

D_2; 80-100 Ma: Sinistral transpression along the LCL, producing simultaneous NNE-SSW shortening and left-lateral shear, resulting in a positive flower structure.

D_3; 75?-50? Ma: Extension producing sub-

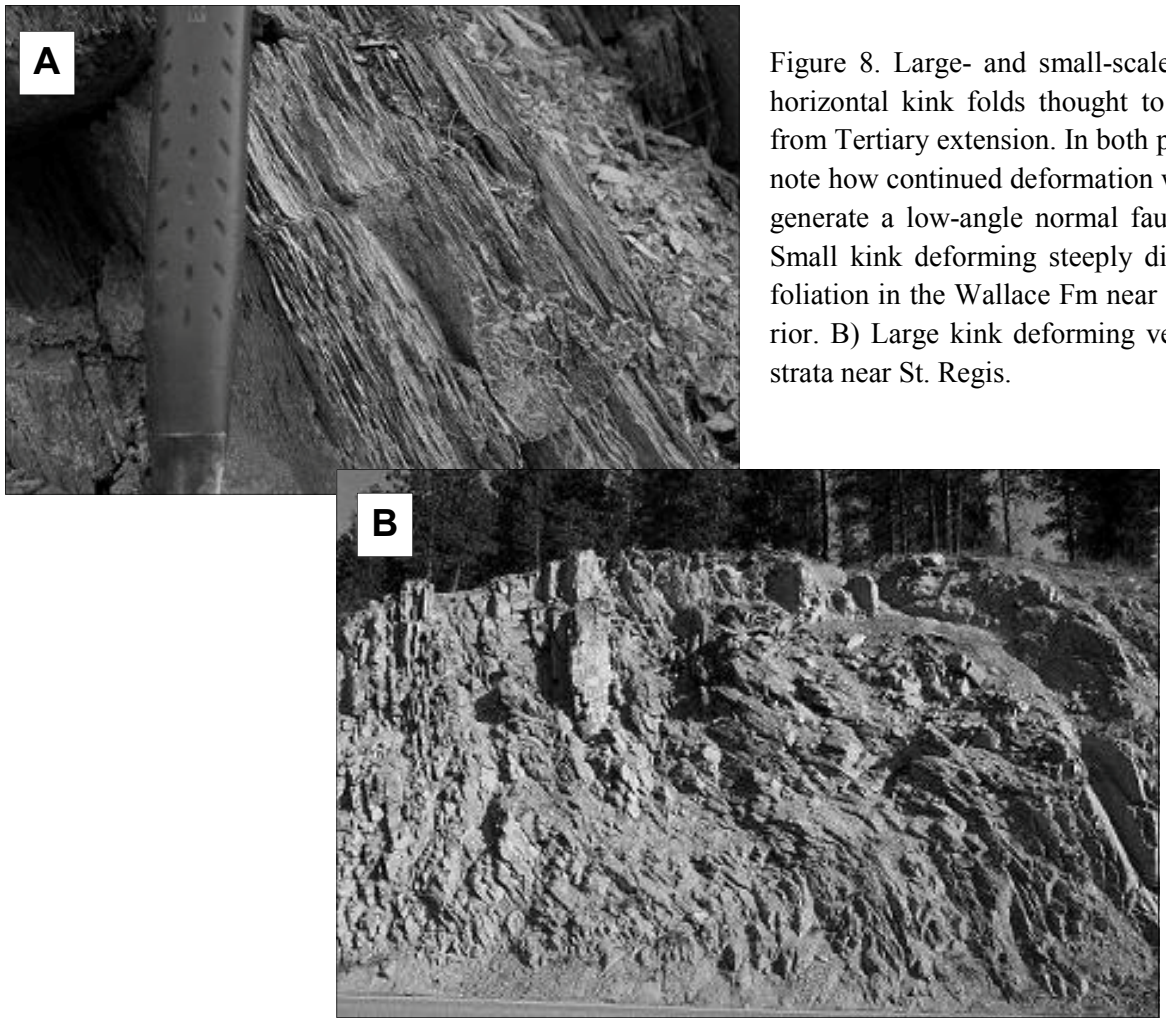

Figure 8. Large- and small-scale sub-horizontal kink folds thought to form from Tertiary extension. In both photos note how continued deformation would generate a low-angle normal fault. A) Small kink deforming steeply dipping foliation in the Wallace Fm near Superior. B) Large kink deforming vertical strata near St. Regis.

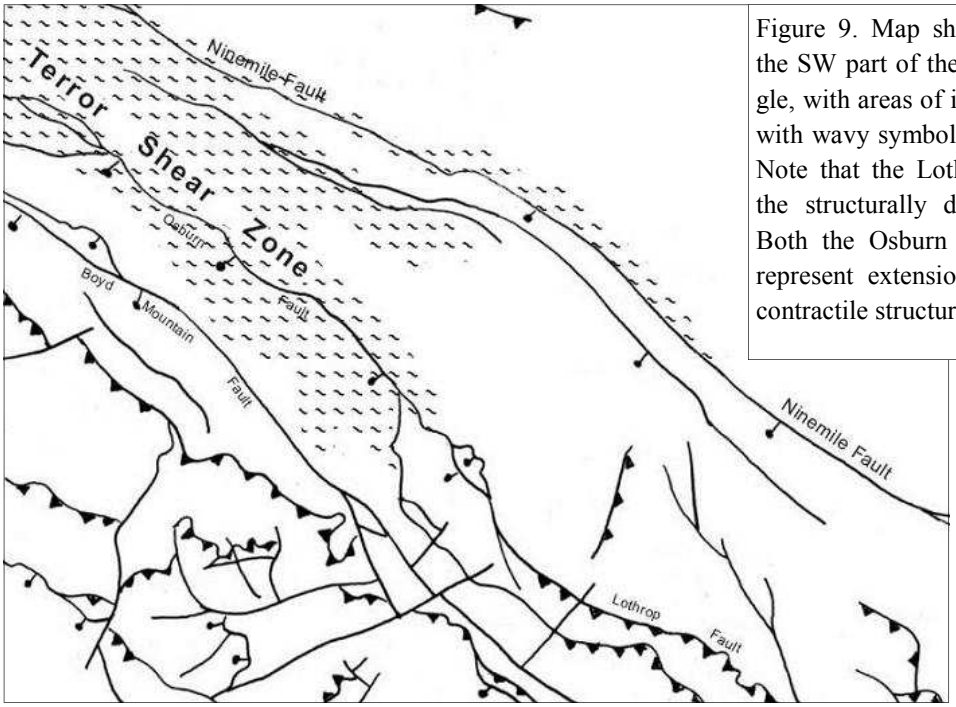

Figure 9. Map showing major structures in the SW part of the Plains 30' x 60' quadrangle, with areas of intense ductile shear shown with wavy symbols (from Lonn et al., 2007). Note that the Lothrop fault traces NW into the structurally deeper Terror shear zone. Both the Osburn and Ninemile faults may represent extensional reactivation of earlier contractile structures.

horizontal kink folds and low-angle normal faults.

D_4; 55 Ma-present?: Dextral transtension, producing high-angle normal faults and right-lateral strike-slip faults that parallel and obscure the D_2 structures.

Obviously, Alberton Gorge and the Superior region have had an extremely complex structural history. Participants on this trip have the opportunity to view examples of many of the structures described above, and offer their own conclusions.

THE FIELD TRIP

River Access

To reach the put in from Superior, take I-90 east for 19 miles to the Fish Creek exit. The wide valley between Superior and Tarkio is developed along the Tertiary Boyd Mountain fault, which we will cross on the river trip. Get off at Fish Creek, turn left and proceed 0.3 miles across a railroad crossing to a stop sign. Turn right and travel 3.3 miles to a road junction just before a bridge across the Clark Fork. Turn right, into the Cyr River Access.

To reach the take-out, backtrack from Cyr to the Fish Creek exit, take I-90 west for 5 miles to the Tarkio exit, turn left under the interstate, then left again, following the signs 1 mile to the Tarkio Fishing Access.

River Log

Begin the trip at the Cyr River Access. We will put in here, but first walk up the gentle, grassy slope at west end of the parking lot for an overview of the geology (fig. 4). The wide valley surrounding you is developed along the Boyd Mountain Fault, a major Tertiary northwest-striking normal fault that cuts obliquely across the river canyon. We will cross its trace downriver. To the southeast, the massive mountain topped by a lookout is Plateau Point, underlain by southwest dipping, overturned Missoula Group and Wallace Formation beds in the lower, east limb of the Reservoir Creek anticline. The rocks were first folded in response to Cretaceous/ Paleocene compression, and then broke in a forelimb thrust, the Reservoir Creek thrust, exposed on the east side of Plateau Point. This style of deformation is common along the LCL: thrusts are steeply dipping and often break from huge overturned folds.

Beyond Plateau Point and out of sight, just above the town of Alberton, is another northeast directed thrust, the Lothrop thrust (fig. 4). The Lothrop thrust brings Proterozoic Shepard Formation up over Cambrian Hasmark Formation and exemplifies another common structural style of this area. Behind (southwest of) and closely paralleling the thrust is a southwest-dipping normal fault that probably merges with the Lothrop thrust at depth. Lewis (1998b, 1998c) found this structural style, that is, normal faults developed behind and parallel to thrust faults, to be common in the area. As discussed previously, this geometry was formed either by Tertiary reactivation of the Cretaceous thrust, or by the simultaneous formation of reverse and normal faults bounding an extruded or extracted wedge (fig. 7). The Lothrop fault system passes northwest (up-plunge, to deeper structural levels) into the Osburn fault near Superior and more importantly, into the Terror shear zone (fig. 9). The Terror shear zone, named by Reid et al. (1993) in the Coeur D'Alene mining district, is a ductile Cretaceous contractional structure characterized by an intense zone of steeply SW-dipping mylonitic foliation (average N60°W 62°SW) with steep downdip lineations (average 60° S52°W) (Lonn et al., 2007). The lineation rakes 0-20° west of the dip line, suggesting mostly dip-slip movement with a minor com-

Figure 10. Structural styles representative of deeper levels of the LCL exposed to the WNW of Alberton Gorge near St. Regis. Above: A) Steep folds with a prominent axial plane foliation. Below: B) Steep mylonitic foliation with downdip lineations.

ponent of left lateral movement. Thus, shortening across the Lothrop fault was accommodated at deeper structural levels by ductile deformation within the Terror shear zone (figs. 6, 10), whereas the Osburn fault is a Cenozoic dextral-normal fault superimposed on these earlier fabrics.

The flat surface on which you are standing is littered with huge sub-angular boulders deposited by floodwaters during the drainings of Glacial Lake Missoula.

Walk across the road to the unloading area, where the Montana Department of Fish, Wildlife, and Parks has thoughtfully placed boulders (although some are upside down!) that provide great examples of Belt sedimentary structures and sediment types. We will spend some time discussing them.

Walk down the boat ramp and launch. This is River Mile (RM) 0.0. Across the river, under the bridge, are more Pleistocene flood deposits deposited during the drainings of Glacial Lake Missoula. Note the poor sorting of clasts.

Below is a large, calm pool with a bedrock outcrop at its lower end on river right at RM 0.2. Boaters use the terms "right" and "left" in reference to downstream views, so this outcrop is on river right. The outcrop is in the uppermost part of the Wallace Formation, striking downriver (northwest) with a near vertical dip. Stratigraphic "up" is to the northeast (river right), and the rocks are on the forelimb of the Reservoir Creek anticline, whose axis parallels the river for the next couple of miles. Notice the small scale folds of probable tectonic origin, common in the relatively incompetent, carbonate-rich Wallace Formation. A stop here would show that the undulating couplet sediment type predominates, formed by the action of storm waves in the shallow Belt Sea. The Clark Fork turns abruptly left and passes through a riffle caused by ledges of Wallace. The river continues through a long calm section, and then enters another riffle.

STOP 1 is at a small beach on river right near the top of this riffle (RM 1.2). **STOP 1**
Watch out for poison ivy! The outcrop above the beach contains diagnostic undulating and pinch-and-swell couplets of the Wallace Formation. Tan-weathering, dolomitic, fine-grained quartzite and siltite beds commonly grade upward into black argillite. The sand beds thicken and thin across the outcrop, have sharp bases, and are loaded and sometimes cut into the underlying argillite. Note the prominent "gutter" of fine sand. Has it

been compacted into the underlying black argillite or does it fill a scour channel? Look carefully for molar tooth structures (calcite) present in the carbonate mud sediment type, and for ptygmatic or "crinkle" cracks. These cracks formed subaqueously by wave action in soupy mud (Winston, 2008). Unlike desiccation cracks, they are discontinuous, do not intersect, and have a squiggly, contorted form in cross section.

Winston (1986b) interpreted the features of the Wallace to record relatively higher stands or deeper parts of the Belt Sea, but with water still shallow enough to allow storm waves to reach the bottom. Storm waves first reworked and deposited the sand beds in hummocky crossbeds, and then the mud settled out of suspension.

The blocks of green mudcracked float probably rolled down from the stratigraphically and topographically higher Snowslip Formation, although desiccation mudcracks do occur uncommonly in the Wallace.

Put in and run through the long riffle below. Just below the riffle a striking sequence of vertical beds comes into view. These are again outcrops of Wallace Formation, but sedimentary features are somewhat obscured by bedding-parallel shears. As we proceed downstream, we are also going slightly down-section, and the cliffs flanking the Ledge and Cliffside I rapids on the right are also composed of Wallace.

Proceed through Cliffside I rapid (RM 2.1) to the top of its clone, Cliffside II (RM 2.6). The cliffs flanking Cliffside II are still Wallace in structural continuity with that of the beginning of the trip. Here the rocks strike downriver and are overturned in the northeast limb of the Reservoir Creek anticline. However, downstream, directly on line with the strike of these beds, are gently dipping green and tan rocks that are clearly different.

Cliffside II rapid (RM 2.7). Below these rapids, rocks that are folded and broken, with gouge developed, suggest a northeast-striking fault that drops gently dipping Snowslip Formation down to the northwest (downstream). The fault truncates the overturned Reservoir Creek anticline and associated thrust. Overturned beds associated with some NE-striking faults suggest that they are reverse faults. If this is a reverse fault, it is west-directed. On river right, in the long calm section below the sharp left turn are nice exposures of tan and green dolomitic microlaminae characteristic of the lowermost Snowslip Formation.

The gougy, colorful, green and purple rocks that appear downstream represent more typical Snowslip Formation, but are crushed and brecciated along the Boyd Mountain fault. These rocks are characterized by mudcracked even couplets, and the mudcracks and red colors here will contrast with the unusual Snowslip lithologies we will see later in the day. The purple cliffs at the downstream end of this straight, calm section of river are Mount Shields Formation member 3 on the other side of the Boyd Mountain fault.

Cross the trace of the Boyd Mountain Fault (RM 3.3). The Boyd Mountain fault is a major northwest-striking, down-to-the-southwest normal fault. Stratigraphic displacement here is at least 4000 feet (1219 m), but it varies greatly along the strike of the fault. Is this because there has been some strike-slip movement? The Boyd Mountain Fault can be followed for almost 10 miles (16 km) to the southeast and 40 miles (64 km) northwest, where it merges with the Osburn Fault. Tertiary fluvial gravel in its hanging wall near St. Regis is tilted into the fault (Lonn and McFaddan, 1999), indicating listric movement. Around Superior, it is evident that rocks in the foot wall (NE side) of the Boyd

Mountain fault are much more intensely cleaved than are rocks in the hanging wall. This relationship extends to the Coeur d'Alene mining district, where the Osburn Fault bounds the different domains (Reid et al., 1993; Wallace and Hosterman, 1956; Campbell, 1960; Hobbs et al., 1965; Lonn and McFaddan, 1999).The intensely cleaved zone is the Terror shear zone. Both the Boyd Mountain and Osburn faults are interpreted as Tertiary dextral/normal faults, and their northeast sides represent significantly lower structural levels now exposed by extension.

RM 3.5-4.1. Pass beneath the purple cliffs, a spectacular exposure of Mount Shields member 3. Note the alternating green and red beds, and also that some of the green beds pass laterally into red beds, showing that color is not always a primary sedimentary feature and should not be used to differentiate Belt formations!

STOP 2 STOP 2 is at the outcrop below the Sandy Beach river access (RM 3.9) on river left. The outcrop is located between the two beaches. If this popular spot is crowded, an alternative outcrop on the left at a small beach (RM 4.1) just downstream shows the same features. This is Mount Shields member 3, characterized by even couplets and couples, and also contains abundant lenticular couplets, flat-laminated sand, discontinuous layer sediment type, microlaminae, both current and oscillation ripple marks, desiccation cracks, and salt casts. Winston (1986b) interpreted much of the Mount Shields 3 as recording sheetflood deposition across sandflats at the toes of alluvial aprons. Sand and silt were deposited first, and then clay settled out as the water ponded in a flat, playa lake environment. The lake then shrank to expose the mud, causing cracks to develop before the next flood arrived.

Continue downstream under the Triple Bridges (there are actually four bridges) and through Triple Bridges rapid (RM 4.25), where Mount Shields 3 constricts the river. Hordes of kayakers normally play the waves here.

The next portion of the trip duplicates Stop 3 of Winston and Lonn (1988). On that trip, participants scrambled into the canyon from above, endangering themselves and each other with slips, falls, and rolling boulders. Floating the river is a better way to travel, wouldn't you agree?

Pull into the eddy formed by the first isolated outcrop on the right downstream from Triple Bridges, and view the geology from the boat (RM 4.6). This is west-dipping Mount Shields member 3 capped by a thin layer of tan-weathering dolomitic rock, not unusual for the Mount Shields 3. Far to the northwest, in the Clark Fork Quadrangle, the Mount Shields 3 passes into a lacustrine carbonate unit mapped by Harrison and Jobin (1963) as Striped Peak member 2. Farther up on the outcrop the rocks are sheared and shattered; they, in turn, are topped by rocks that appear distinctly different, and indeed they are. The top of the outcrop is Wallace Formation, verified by viewing the distinctive black and tan lithology across the river downstream. The Wallace here has been thrust over Mount Shields 3 by the Tarkio thrust mid-way up the outcrop. Here the Tarkio thrust displays at least 6000 feet (1829 m) of stratigraphic offset. The thrust plane itself is well exposed a few hundred feet downstream.

STOP 3 STOP 3. Split Rock rapid (RM 4.7) and the giant mid-river boulder are formed along the sole of the Tarkio thrust. Run the rapid right of the boulder and land on the gravel bar below, river right. The best exposure of the fault is at the edge of the gravel

bar. Boulders of Wallace Formation are set in a foliated matrix containing smaller, rounded quartzite and Wallace clasts, creating a mylonitic appearance. In thin section, the matrix is not foliated, but it does contain grains of strained, broken quartz with undulose extinction and twinned dolomite crystals. Deformation along the Tarkio thrust apparently involved both ductile and brittle processes.

Lewis (1998b) was able to follow the Tarkio thrust for 10 miles (16 km) southeast and discovered the parallel normal fault that formed behind (southwest of) it. A thin sliver of Wallace is caught between the two faults. This sliver can be found north of the river as well, but farther north, near the Martel Mountain ridge crest, the fault traces merge and Wallace Formation is no longer exposed (fig. 4). So, like the Lothrop thrust, the Tarkio thrust could be interpreted as an extraction fault, or as a reactivated thrust that slid back. The trace of the normal fault probably crosses the river just downstream in the covered interval, because the next outcrops you see downriver are of Snowslip Formation.

Continue downriver through the narrow constriction that forms Tumbleweed rapid (RM 4.9), a strong Class III at most flows. Smooth, sculpted gorge walls below Tumbleweed rapid are green- and tan- weathering, dolomitic, couplet-scale beds of the Snowslip Formation.

STOP 4

STOP 4 is on the right, below the glassy "Surfer Joe" waves (RM 5.1). Sediment types represented here are mostly dolomitic, uncracked varieties of even and lenticular couplets. Note the lenticular couplets near the water line that have been deformed by compaction. Walk up the inclined bedding surfaces for good exposures of even and lenticular couplets, best viewed by splashing a bucket of water on them. Desiccation cracks and mud chips are uncommon, but straight-crested oscillation ripples are present. You may find some microlaminae. Although participants on the 2001 trip thought that these rocks belonged to the Shepard Formation, they are now thought to be part of the unusual carbonate-rich facies of the Snowslip. Downstream we will see that they grade up into quartzite of the uppermost Snowslip. This dolomite-rich Snowslip is restricted to the Tarkio area. In this area all sediment types in the Snowslip are dolomite-rich, including the flat-laminated sands and the mudcracked even couplets, suggesting that the dolomite is not a primary sedimentary feature but perhaps a result of diagenesis.

Pull over to the stack on the right in the wide calm spot where the dip of the rocks flattens (RM 5.2). Splash water on these outcrops to see red even couplets and couples, flat laminated sand, and discontinuous layer sediment types. Downstream, and upsection, the rocks get coarser-grained and thicker bedded.

Run through Boateater rapid, so named for the fearsome holes that develop during high flows, and look at the rocks on the left in the long calm section below (RM 5.4-5.6). We are now in an interval of thick quartzite beds mostly of the even couple and flat laminated sand sediment types. The Snowslip's type section in Glacier National Park contains few such beds, and is dominated by red and green mudcracked even and lenticular couplets. The interval here closely resembles the Mount Shields member 2, but a climb up the cliffs of Martel Mountain less than 0.5 miles (0.8 km) to the north reveals that these quartzite beds grade upward into unmistakable Shepard Formation and then into Mount Shields 2 at the top of the mountain (fig. 4). Lewis (1998a,b) also described sandy intervals in the Snowslip at locations 12 miles (20 km) southeast of here and also in the Sapphire Mountains.

Assignment of this interval to the Mount Shields 2 resulted in overly complex structural interpretations (Harrison et al., 1986). However, like the Mount Shields 2, these beds probably reflect deposition by sheetfloods on the middle and distal parts of alluvial aprons (Winston 1986b, 2000).

Exit the constricted gorge via Fang rapid (RM 5.6) with its large, violent surfing wave and attendant gaggle of kayakers, and run another rapid with an enormous boulder on the right (RM 5.9). Downriver are more Snowslip outcrops that appear to be internally deformed. A long section without bedrock outcrops follows and continues through a long riffle. Bedrock again appears just past the kayaker's take-out on the right (RM 6.4).

These upstream-dipping (north-dipping) outcrops above Fish Creek were mapped as Shepard Formation (fig. 4; Lewis, 1998b), but have been reinterpreted as carbonate-rich Snowslip. Some deformation is apparent, including NE-striking fault gouge and a possible WNW-trending fault with little apparent offset just above the mouth of the creek. Faults are ubiquitous in this region, but perhaps only those with documented stratigraphic offset should be mapped.

Less than a mile (1.6 km) to the south, a significant fault, the Rivulet thrust, has been mapped (Lewis, 1998b), and it parallels the river on the left for the next 2 miles (3.2 km). Like the Tarkio thrust, this one has Wallace Formation in its hanging wall and is closely backed by a normal fault. Both faults appear to dip gently (<30°) south. Is the pair the result of thrust reactivation, or did they move simultaneously? Several low-angle normal faults have been mapped to the west and northwest (Lewis, 1998b; Lonn et al., 2007) in the hanging wall of the Rivulet thrust.

Land on the left just below the mouth of Fish Creek (RM 6.7) for STOP 5.

STOP 5

Here, beautiful white sand ripples are exposed in lenticular couplets, and good examples of the microlamina sediment type are present. Most beds are dolomitic or calcareous. Green and tan-weathering, dolomitic micro-couplets are characteristic of the Shepard Formation, but are also present in the Snowslip. Microlamina or microcouplets in the Belt are enigmatic; their stratigraphic positions in cycles of the Helena and Wallace Formations indicate that they formed in very shallow water (Winston, 1993). Possibly they were deposited either on wind set-up flats, where wind blew shallow water onto the mud flats surrounding the Belt sea, or maybe they represent wind-blown silt from nearby exposed playa flats (Winston, 1993, and personal communication, 2001).

This outcrop is now interpreted as Snowslip Formation that is structurally continuous with that upstream and downstream. Placing it in the Shepard Formation requires a fault, as yet unrecognized. In the area between here and Superior, Harrison et al. (1986) mistakenly mapped this interval as lower Wallace Formation (Helena Formation in the new nomenclature [Winston, 2007]), which resulted in some complicated structural interpretations.

Continue downstream and downsection, through the rapids created by the huge midstream boulders (RM 6.8). Lithologies here represent good Snowslip Formation, although the unusually high dolomite content is evident from the tan color of the beds. The railroad cut far above the river on the left indicates some structural complications, possibly related to the Rivulet thrust.

STOP 6 is at the last outcrop on the right just above Rock Creek (RM 7.5). The

STOP 6

outcrop contains beautiful examples of "starved ripples" in lenticular couplets, and also some undulating couplets, both characteristic of the Snowslip Formation.

Continue past the mouth of Rock Creek (RM 7.6), and its grove of small Western Red Cedars. For the next mile the river has exposed mostly glaciofluvial deposits and a few ratty outcrops deemed Snowslip. On the right bank at about RM 8.6 are some iron-stained, brecciated outcrops along one of the many faults in the Rivulet area.

The rocky bluff that finally appears ahead on river left (RM 9.2) is composed of deformed Wallace Formation. The chaotic bedding here is interpreted to be the result of tectonic rather than soft sediment deformation. Slump features such as sedimentary breccia and soft sediment folds are extensively developed in the Wallace as a result of syndepositional faulting (Wallace et al., 1976; Godlewski, 1980; Winston, 1986a), but only at stratigraphic levels lower than this. We are probably very near the top of the Wallace Formation here, although faulting in the immediate area is complex and unresolved.

Continue around the corner through fast water to the Tarkio take-out on the right (RM 9.5). Outcrops across the river are beds of north-striking, near-vertical Wallace near its upper contact with the Snowslip to the east (right). Vertical cliffs rise directly out of the water in the Tarkio Gorge downstream, but the water is calm and has not polished the rocks; instead the rocks are covered in lichen, obscuring the geology.

Drive up through glaciofluvial deposits to the interstate highway. The Quartz-Nemote Creek flats here near the Tarkio exit are underlain by Glacial Lake Missoula silt beds, which are commonly preserved in wide sections of the valley above and below constrictions, where quieter water presumably prevailed during the drainings of Lake Missoula. The gravels in the high road cut along the interstate to the right were deposited on a great point bar (Harrison et al., 1986; Alt, 2000) during the Lake Missoula floods. During those floods, more than 200 million cfs passed this point (estimated from Pardee's [1942] calculations). That would have been a river trip! For comparison, historic peak flow has been near 70,000 cfs, most recently in 1997.

End of trip.

REFERENCES

Alt, D., 2000, The catastrophic drainage of Glacial Lake Missoula: *in* Roberts, Sheila, and Winston, Don, eds., Geologic field trips, western Montana and adjacent areas: Rocky Mountain Section of the Geological Society of America, University of Montana, p. 31-39.

Bennett, E.H., and Venkatakrishnan, R., 1982, A palinspastic reconstruction of the Coeur d'Alene mining district based on ore deposits and structural data: Economic Geology, v. 77, p. 1851-1866.

Billingsley, P., and Locke, A., 1941, Structure and ore deposits in the continental framework: American Institute of Mining and Metallurgical Engineers Transactions, v. 144, p. 9-59.

Burmester, R.F., and Lewis, R.S., 2003, Counterclockwise rotation of the Packsaddle syncline is consistent with regional sinistral transpression across north-central Idaho: Northwest Geology, v. 32, p. 147-159.

Campbell, A.B., 1960, Geology and mineral deposits of the St. Regis-Superior area, Mineral County, Montana: U.S. Geological Survey Bulletin 1082-I, p. A1-A33, scale 1:62,500.

Doughty, P.T., and Sheriff, S.D., 1992, Paleomagnetic evidence for en echelon crustal extension and crustal rotations in western Montana and Idaho: Tectonics, v. 11, p. 663-671.

Elston, D.P., Enkin, R.J., Baker, J., and Kisilevsky, D.K., 2002, Tightening the Belt: Paleomagnetic-stratigraphic constraints on deposition, correlation, and deformation of the Middle Proterozoic strata (1.4 Ga) Belt-Purcell Supergroup, United States and Canada: Geological Society of America Bulletin, v. 114, p. 619-638.

Foster, D.A., Doughty, P.T., Kalakay, T.J., Fanning, C.M., Coyner, S., Grice, W.C., and Vogl, J., 2007, Kinematics and timing of exhumation of metamorphic core complexes along the Lewis and Clark fault zone, northern Rocky Mountains, USA: Geological Society of America Special Paper 434, p. 207-232.

Froitzheim, N., Pleuger, J., and Nagel, T.J., 2006, Extraction faults: Journal of Structural Geology, v. 28, p. 1388-1395.

Godlewski, D.W., 1980, Origin and classification of the middle Wallace breccias: M.S. thesis, Missoula, University of Montana, 108 p.

Griffin, J.H., 1989, Structural style in a left lateral thrust ramp zone, Bearmouth, Montana: M.S. thesis, Missoula, University of Montana, 68 p., scale 1:24,000.

Hall, F.W., 1968, Bedrock geology, north half of Missoula 30' quadrangle, Montana: Ph.D. dissertation, Missoula, University of Montana, 253 p., scale 1:48,000.

Harrison, J.E., and Cressman, E.R., 1993, Geology of the Libby thrust belt of northwestern Montana and its implications to regional tectonics: U.S. Geological Survey Professional Paper 1524, 42 p., scale 1:125,000.

Harrison, J.E., and Jobin, D.A., 1963, Geology of the Clark Fork quadrangle, Idaho-Montana: U.S. Geological Survey Bulletin 1141-K, 38 p.

Harrison, J.E., Griggs, A.B., and Wells, J.D., 1974, Tectonic features of the Precambrian Belt basin and their influence on post Belt structures: U.S. Geological Survey Professional Paper 86, 15 p.

Harrison, J.E., Griggs, A.B., and Wells, J.D., 1986, Geologic and structure maps of the Wallace 1º x 2º quadrangle, Montana and Idaho: U.S. Geological Survey Miscellaneous Investigations Map I-1509-A, scale 1:250,000.

Hobbs, S.W., Griggs, A.B., Wallace, R.E., and Campbell, A.B., 1965, Geology of the Coeur d'Alene district, Shoshone County, Idaho: U.S. Geological Survey Professional Paper 478, 139 p., scale 1:24,000.

Hyndman, D.W., Alt, David, and Sears, J.W., 1988, Post-Archean metamorphic and tectonic evolution of western Montana and northern Idaho: *in* Ernst, W.G., ed., Metamorphism and crustal evolution in the western conterminous U.S. (Rubey Volume VII): Englewood Cliffs, New Jersey, Prentice-Hall, p. 332-361.

Leach, D.L., Landis, G.P., and Hofstra, A.H., 1988, Metamorphic origin of the Coeur d'Alene base and precious metal veins in the Belt basin, Idaho and Montana: Geology, v. 16, p. 122-125.

Lewis, R.S., 1998a, Geologic map of the Butte 1º x 2º quadrangle, Montana: Montana Bureau of Mines and Geology Open-File Report 363, 16 p., scale 1:250,000.

Lewis, R.S., 1998b, Geologic map of the Montana part of the Missoula West 30' x 60' quadrangle: Montana Bureau of Mines and Geology Open-File Report 373, scale 1:100,000.

Lewis, R.S., 1998c, Stratigraphy and structure of the lower Missoula Group in the Butte 1º x 2º and Missoula West 30' x 60' quadrangles, Montana: Northwest Geology, v. 28, p. 1-14.

Lidke, D.J., Wallace, C.A., Zarske, S.E., MacLeod, N.S., and Broeker, L.D., 1988, Geologic map of the Welcome Creek Wilderness and vicinity, Granite, Missoula, and Ravalli Counties, Montana: U.S. Geological Survey Miscellaneous Field Studies Map MF-1620-B, scale 1:50,000.

Lonn, J., 1984, Structural geology of the Tarkio area, Mineral County, Montana: M.S. thesis, Missoula, University of Montana, 51 p.

Lonn, J., 2001, Floater's guide to the Belt rocks of Alberton Gorge, western Montana: Northwest Geology, v. 31, p. 1-17, scale 1:100,000.

Lonn, J.D., and McFaddan, M.D., 1999, Geologic map of the Montana part of the Wallace 30' x 60' quadrangle: Montana Bureau of Mines and Geology Open-File Report 388, 16 p., scale 1:100,000.

Lonn, J.D., and Smith, L.N., 2005, Geologic map of the Tarkio and Lozeau 7.5' quadrangles, western Montana: Montana Bureau of Mines and Geology Open-File Report 516, 17 p., scale 1:24,000.

Lonn, J.D., and Smith, L.N., 2006, Geologic map of the Stark South 7.5' quadrangle, western Montana: Montana Bureau of Mines and Geology Open-File Report 531, 16 p., scale 1:24,000.

Lonn, J.D., Smith, L.N., and McCulloch, R.B., 2007, Geologic map of the Plains 30'x60' quadrangle, western Montana: Montana Bureau of Mines and Geology Open-File Report 554, scale 1:100,000.

Lonn, J.D., McDonald, C., Sears, J.W., and Smith, L.N., 2010, Geologic map of the Missoula East 30' x 60' quadrangle, western Montana: Montana Bureau of Mines and Geology Open-File Report 593, 2 sheets, scale 1:100,000.

Lorenz, J.C., 1984, Function of the Lewis and Clark fault system during the Laramide orogeny: *in* Northwest Montana and Adjacent Canada: Montana Geological Society 1984 Field Conference Guidebook, p. 221-230.

Pardee, J.T., 1942, Unusual currents in Glacial Lake Missoula, Montana: Geological Society of America Bulletin, v. 53, p. 1569-1600.

Reid, R.R., Bond, W.D., Hayden, T.J., and, Wavra, C.S., 1993, Structural analysis and ore controls in the Coeur d'Alene mining district, Idaho: U.S. Geological Survey Open-File Report 93-235, 66 p.

Reid, R.R., Wavra, C.S., and Bond, W.D., 1995, Constriction fracture flow: A mechanism for fault and vein formation in the Coeur d'Alene district, Idaho: Economic Geology, v. 90, p. 81-87.

Reynolds, M.W., 1977, Character and significance of deformation at the east end of the Lewis and Clark line, Montana: Geological Society of America, Rocky Mountain Section, Abstracts with Program, v. 9, p. 758.

Ring, U., and Glodny, J., 2010, No need for lithospheric extension for exhuming (U)HP rocks by normal faulting: Journal of the Geological Society, v. 167, p. 225-228.

Sears, J.W., 2001, Emplacement and depositional history of the Lewis-Eldorado-Hoadley thrust slab in the northern Montana Cordillera, USA: Implications for steady-state orogenic processes: American Journal of Science, v. 301, p. 359-373.

Sears, J.W., and Clements, P.S., 2000, Geometry and kinematics of the Blackfoot thrust fault and Lewis and Clark Line, Bonner, Montana: *in* Roberts, Sheila, and Winston, Don, eds., Geologic Field Trips, Western Montana and Adjacent Areas: Rocky Mountain Section, Geological Society of America, p. 123-130.

Sears, J.W., and Hendrix, M., 2004, Lewis and Clark line and the rotational origin of the Alberta and Helena salients, North American Cordillera: *in* Sussman, A.J., and Weil, A.B., eds., Orogenic Curvature: Integrating Paleomagnetic and Structural Analyses: Geological Society of America Special Paper 383, p. 173-186.

Sears, J.W., McDonald, C., and Lonn, J., 2010, Lewis and Clark Line, Montana: Tectonic evolution of a crustal-scale flower structure in the Rocky Mountains: *in* Morgan, L.A., and Quane, S.L., eds., Through the Generations: Geologic and Anthropogenic Field Excursions in the Rocky Mountains from Modern to Ancient: Geological Society of America Field Guide, v. 18, p. 1-20.

Sheriff, S.D., Sears, J.W., and Moore, J.N., 1984, Montana's Lewis and Clark fault zone: an intracratonic transform fault system: Geological Society of America Abstracts with Programs, v. 16, no. 6, p. 653-654.

Smith, J.G., 1965, Fundamental transcurrent faulting in the northern Rocky Mountains: American Association of Petroleum Geologists Bulletin, v. 49, p. 1398-1409.

Wallace, C.A., 1987, Generalized geologic map of the Butte 1º x 2º quadrangle, Montana: U.S. Geological Survey Miscellaneous Field Studies Map MF-1925, scale 1:250,000.

Wallace, R.E., and Hosterman, J.W., 1956, Reconnaissance geology of western Mineral County, Montana: U.S. Geological Survey Bulletin 1027, p. 575-612, scale 1:62,500.

Wallace, C.A., Harrison, J.E., Klepper, M.R., and Wells, J.D., 1976, Carbonate sedimentary breccias in the Wallace Formation (Belt Supergroup), Idaho and Montana, and their paleogeographic significance: Geological Society of America Abstracts with Programs, v. 8, p. 1159.

Wallace, C.A., Lidke, D.J., and Schmidt, R.G., 1990, Faults of the central part of the Lewis and Clark Line and fragmentation of the Late Cretaceous foreland basin in west-central Montana: Geological Society of America Bulletin, v. 102, p. 1021-1037.

Wavra, C.S., Bond, W.D., and Reid, R.R., 1994, Evidence from the Sunshine mine for dip-slip movement during Coeur d'Alene district mineralization: Economic Geology, v. 89, 515-527.

Wells, J.D., 1974, Geologic map of the Alberton quadrangle, Missoula, Sanders, and Mineral Counties, Montana: U.S. Geological Survey Geologic Quadrangle Map GQ-1157, scale 1:62,500.

White, B.G., 1993, Diverse tectonism in the Coeur D'Alene mining district, Idaho: *in* Berg, R.B., ed., Belt Symposium III: Montana Bureau of Mines and Geology Special Publication 112, p. 245-265.

White, B.G., 2000, Coeur d'Alene mining district: Product of preconcentrated source deposits and tectonism within the Lewis and Clark Line: *in* Roberts, S.M., ed., Belt Supergroup: A guide to Proterozoic rocks of western Montana and adjacent areas: Montana Bureau of Mines and Geology Special Publication 94, p. 95-101.

White, B.G., Winston, D., and Lange, I., 2000, The Lewis and Clark Line and the Coeur d'Alene mining district: *in* Roberts, S.M., ed., Belt Supergroup: A guide to Proterozoic rocks of western Montana and adjacent areas: Montana Bureau of Mines and Geology Special Publication 94, p. 103-121.

Winston, D., 1986a, Sedimentation and tectonics of the Middle Proterozoic Belt basin, and their influence on Phanerozoic compression and extension in western Montana and northern Idaho: *in* Peterson, J.A., ed., Paleotectonics and Sedimentation in the Rocky Mountain Region, United States: American Association of Petroleum Geologists Memoir 41, p. 87-118.

Winston, D., 1986b, Sedimentology of the Ravalli Group, middle Belt carbonate, and Missoula Group, middle Proterozoic Belt Supergroup, tectonics of the Belt Basin, Montana, Idaho, and Washington: *in* Roberts, Sheila, ed., Belt Supergroup: A guide to Proterozoic rocks of western Montana and adjacent areas: Montana Bureau of Mines and Geology Special Publication 94, p. 85-124.

Winston, D., 1993, Lacustrine cycles in the Helena and Wallace Formations, middle Proterozoic Belt Supergroup, western Montana: *in* Berg, R.B., ed., Belt Symposium III: Montana Bureau of Mines and Geology Special Publication 112, p. 70-86.

Winston, D., 2000, Belt stratigraphy, sedimentology, and structure in the vicinity of the Coeur d'Alene Mining District: *in* Roberts, Sheila, and Winston, Don, eds., Geologic field trips, western Montana and adjacent areas: Rocky Mountain Section of the Geological Society of America, University of Montana, p. 85-94.

Winston, D., 2007, Revised stratigraphy and depositional history of the Helena and Wallace Formations, mid-Proterozoic Piegan Group, Belt Supergroup, Montana and Idaho, U.S.A.: *in* Link, P.K., and Lewis, R.S., eds., Proterozoic geology of western North America and Siberia: Society for Sedimentary Geology, v. 86, p. 65-100.

Winston, D., 2008, Crinkle cracks: sub-aqueous sand-filled contorted cracks in mud formed by waves: International Geological Congress, Abstracts, v. 33, Abstract 1339320.

Winston, D., and Lonn, J., 1988, Road log No. 1: Structural geology and Belt stratigraphy of the Tarkio area, Montana: *in* Weidman, R.M., ed., Guidebook of the greater Missoula area: Tobacco Root Geological Society 13th Annual Field Conference, Missoula, Montana, 1-34.

Yin, A., and Oertel, G., 1995, Strain analysis of the Ninemile fault zone, western Montana: Insights into multiply deformed regions: Tectonophysics, v. 247, p. 133-143.

Yin, A., Fillipone, J.A., Harrison, M., Sample, J.A., and Gehrels, G.E., 1993, Fault kinematics of the western Lewis and Clark Line in northern Idaho and northwestern Montana: Implications for possible mechanisms of Mesozoic arc separation: *in* Berg, R.B., ed., Belt Symposium III: Montana Bureau of Mines and Geology Special Publication 112, p. 244-25.

SEDIMENTARY RECORD OF GLACIAL LAKE MISSOULA ALONG THE CLARK FORK RIVER FROM NINEMILE TO THE FLATHEAD RIVER, MONTANA

Larry N. Smith
Department of Geological Engineering, Montana Tech of the University of Montana
1300 W. Park St., Butte, MT 59701 • lsmith@mtech.edu

Introduction

Glacial Lake Missoula (GLM) formed by repeated blocking of the Clark Fork River by the Purcell Trench Lobe of the Cordilleran ice sheet near the present state boundary between Idaho and Montana (fig. 1; Pardee, 1910; Breckenridge, 1989). Multiple failures of a succession of ice dams released water across the Channeled Scabland tract of the northwestern US, carving the now famous landforms (Bretz, 1969; Baker, 1973). Like any mountainous reservoir, the impoundment had many subbasins defined by drainage basins tributary to the Clark Fork River (fig. 1). The northern subbasins, the Flathead River and lower Clark Fork area, held an immense amount of water in comparison to the southern subbasins, the Bitterroot Valley, the Missoula Valley, and the Clark Fork River above Missoula.

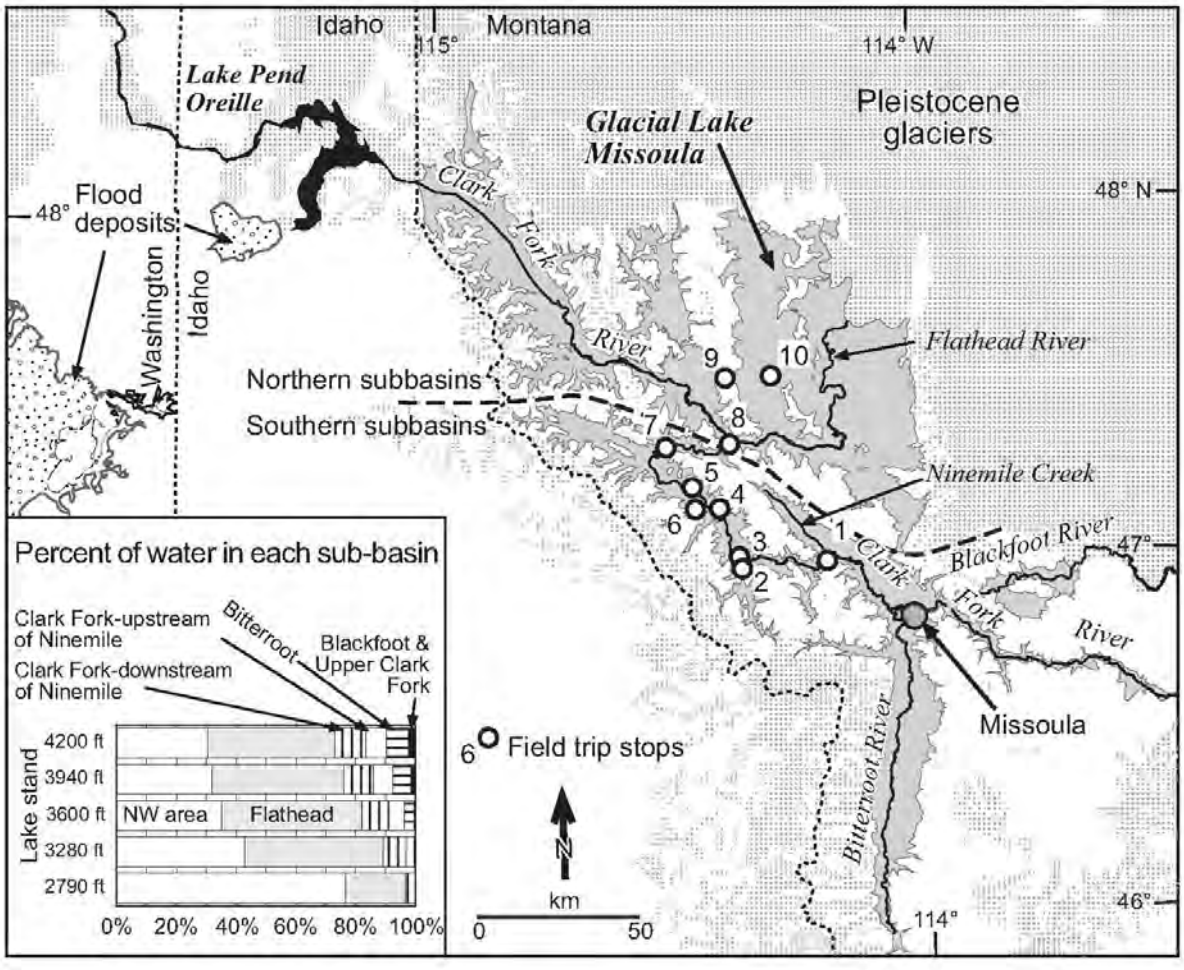

Figure 1. Location map, route for Glacial Lake Missoula field trip, and relative volumes of subbasins of glacial Lake Missoula at different lake-level stands (modified from Smith, 2006).

The original studies of the stratigraphy and geomorphic features formed by rapid lake drainage focused in the northern subbasins, in the areas east and west of Plains, MT (Pardee, 1910, 1942). Most subsequent work on the lake deposits and landforms has concentrated on the area downstream of the Clark Fork's confluence with the Flathead River (Baker, 1973; Breckenridge, 1989; Alho et al., 2010). Alternatively, this field trip road log focuses on sedimentary deposits and landforms preserved along the Clark Fork River upstream of its confluence with the Flathead River.

The purpose of this field trip is to view and discuss sedimentary sections and geomorphic features along the Clark Fork River including the Ninemile area, Alberton Gorge, Superior, St. Regis, and the canyon south of Paradise, MT. The area where Ninemile Creek enters the Clark Fork upstream of Alberton Gorge is the location of an exceptionally well-exposed and accessible section of glaciolacustrine silt. This section has been studied repeatedly and referenced in many works on the Channeled Scablands (Alt and Chambers, 1970; Chambers, 1971, 1984; Waitt, 1980, 1985; Fritz and Smith, 1993; Shaw et al., 1999, 2000; Atwater et al., 2000; Booth et al., 2004). Deposits of glaciolacustrine silt throughout the lake basin, correlative to the Ninemile section, were called the "Lake Missoula beds" by Langton (1935). On this field trip, we will look at some exposures of the Lake Missoula beds, but also at gravelly alluvium that lies below the silts and records catastrophic drainage of multiple stands of GLM. The field relationships show at least two episodes of lake filling and lake draining. Deposits and erosional features show discharges from the earlier lake stands were greater than the final lake stand (Pardee, 1942; Chambers, 1971; Smith, 2006).

Route and Road Log

The field trip will start from Superior, MT, and travel SE on I-90 to the Ninemile area. We will then travel downstream on the freeway and frontage roads to near Paradise, near the confluence of the Flathead and Clark Fork rivers. If there is time, some may make additional stops at Rainbow Lake and Camas Prairie late in the afternoon.

Mile 0—Enter the eastbound lane of I-90 and travel about 43 miles to the Ninemile Road, Exit 82. Along the way, you can observe the following features:

Miles 9-14—Flat to "rolling topography" is developed on top of the Lake Missoula beds There is a bridge over Clark Fork River at 11 miles. The rolling topography is especially evident east of the freeway in the half mile before Tarkio, Exit 61, at mile 14.

Mile 14-14.5—The Tarkio gravel bar makes up the northeastern embankment of the freeway. Note the rounded gravel in the road cuts—this is an eroded cross section of an immense bedform.

Mile 18.5—Bridge over the Clark Fork River.

Mile 19-22—You are driving along a gravel bar parallel to the valley, that is locally overlain by Lake Missoula beds.

Mile 22.5—Bridge over the Clark Fork at Cyr. Note the series of stream terraces cut into older deposits on the south side of the river. The wooded ridge due south of the valley is a 300-ft-high gravelly "eddy bar" deposited where the valley widened downstream of the narrow Cyr canyon.

Mile 34—As you cross over the Clark Fork River, you will climb to an impressive ex-

posure of the Ninemile section of the Lake Missoula beds. The section in the westbound lane is an excellent place to study the sediments, but the traffic on the interstate makes it a hazardous stop for a field trip. We will look at the sediments on the old highway. At the eastern edge of the outcrop along I-90, the silty section rests on gravelly alluvium that, unfortunately, is not exposed at Stop 1.

Mile 35—Exit I-90 at Exit 82 onto Ninemile Road. Travel north about 0.5 mile and pull over on the shoulder.

STOP 1

STOP 1. Ninemile section (47º 01' 28" N, 114º 22' 50" W, 3,190 ft)

The Ninemile section of Lake Missoula beds is exposed here on the south-facing road cut. Things to note at this outcrop:

The striking cyclic pattern of bedding

The overall lithology of the sediments, what defines the bedding surfaces and how much of the section is sand, silt, or clay.

Is there any evidence for scouring or exposure (desiccation or soil development) of the sediment?

This set of outcrops has long been recognized as an example of lake-bottom sedimentation in GLM. Published studies began with Dave Alt and his master's student Richard Chambers from the University of Montana (Alt and Chambers, 1970; Chambers, 1971, 1984). The laminations of silt and clay have been interpreted as varves (Alt and Chambers, 1970; Chambers, 1971, 1984; Waitt, 1980, 1985; Fritz and Smith, 1993; Levish, 1997). Different geologists have interpreted the depositional environments of the cross-stratified sand differently:

Shallow-water, high-energy currents generated by the complete drainage of GLM (Alt and Chambers, 1970; Curry, 1977; Waitt, 1980, 1985; Atwater et al., 2000).

Currents or lake-level fluctuations in a shallow lake (Chambers, 1971, 1984; Fritz and Smith, 1993).

Currents deep within the lake (Shaw et al., 1999, 2000)

The rhythmic character of the bedding is so striking and the bed count such that workers in central Washington have also correlated the sand and silt/clay "couplets" with episodic flooding, reestablishment of the lake, and lake-bottom sedimentation (Waitt, 1985; Atwater, 1986; Atwater et al., 2000). Something to keep in mind on the field trip is, if the rhythmic character of the Lake Missoula beds is due to filling and draining cycles of the lake, those cycles should be correlative to other deposits within the lake basin.

Take in the western view from the overlook to discuss the maximum altitude of the lake surface (~4,200 ft), bedrock, and occurrence of scabland features in the river valley (~3,100-3,150 ft). The river level has an altitude of about 3,000 ft; and the top of the Lake Missoula beds is about 3,200 ft (fig. 2). Note the hill slopes composed of bare bedrock. Lake drainage stripped the soil off the slopes, but typically on the outside (concave) bends within the canyon reaches. Keep this observation in mind as we trace the flow downstream.

Continue about five miles west on the Frontage road and get back on I-90. Travel about 16 miles and take Exit 61 toward Tarkio. Pass under the freeway towards the Tarkio Fishing Access Site, turn left at about 0.8

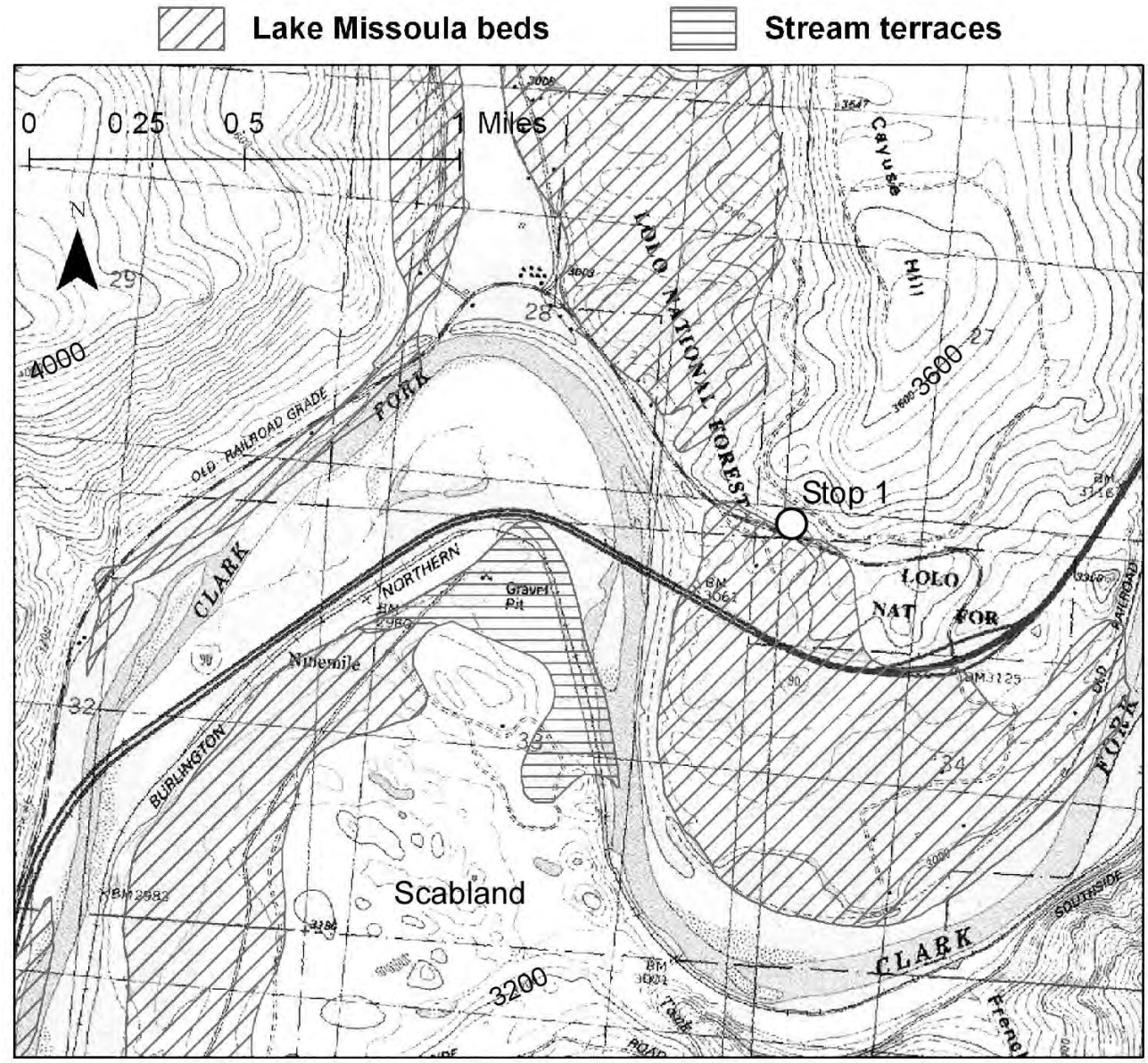

Figure 2. Geologic map of the area near Stop 1.

miles, and continue on the old rail grade. Travel ~0.3 miles to a wide spot near a driveway on the right.

STOP 2a

STOP 2a. Tarkio rail cut exposure (47º 00' 36" N, 114º 44' 11" W, 2,930 ft)

The cut along the rail grade near Tarkio exposes large-scale cross stratification developed in granule- to boulder-sized gravel capped by Lake Missoula beds (fig. 3). A syndepositional slump occurred in the gravel, with minor movement and soft-sediment deformation in the silt beds. Things to notice at this site:

Large-scale cross stratification is oriented downstream.

The contact at the base of the Lake Missoula beds must represent a transgressive sequence where alluvial deposits are overlain by lake-bed deposits.

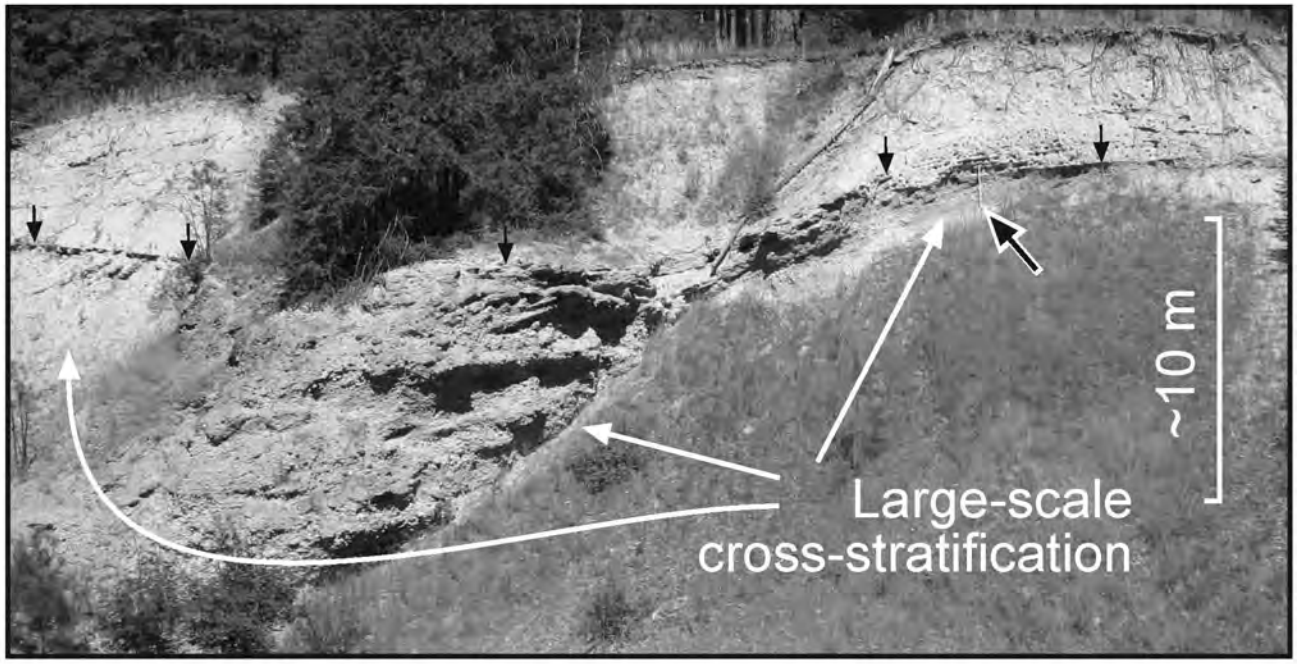

Figure 3. Photograph of gravelly alluvium with large-scale cross stratification overlain by Lake Missoula silts at Stop 2a; black arrows show contact between gravels and silts; 5 ft measuring staff at black and white arrow (modified from Smith, 2006).

Bedding in Lake Missoula beds does not appear to be as rhythmic as at Stop 1.

Return to the road that goes down to the river, park in the parking lot at the fishing access site.

STOP 2b

Stop 2b. Tarkio Fishing access site (47º 00' 53" N, 114º 47' 20" W, 2,790 ft)

Note the large boulders at the site—which must have come out of the nearby gravels. The largest clasts were likely moved by extremely high-energy flows. Their source area, whether near or far, is not known.

Return the same way, go under the freeway, travel northeast, about 1 mile, turn to the north on Nemote Creek Road, and travel about 0.5 mile to the crest of the low hills. Pull off on side of the road.

STOP 3

Stop 3. Rolling topography on Lake Missoula beds (47º 01' 57" N, 114º 44' 05" W, 3,120 ft)

The roads traverse the upper surface of the Lake Missoula beds. Note the topography on the surface. The east-west trending crests and troughs of the landforms in this area have been interpreted to be north-oriented (down valley) dunes that developed during high-energy drainage events (Alt, 2001, p. 76-77). Aerial-photo interpretation of this region suggests that this area contains networks of dry paleovalleys that have been incised into the Lake Missoula beds (fig. 4).

Key features to observe about the drainage basins developed on the Lake Missoula beds are:

Most of the drainages do not have active streams; if they do, the streams are underfit in much larger valleys

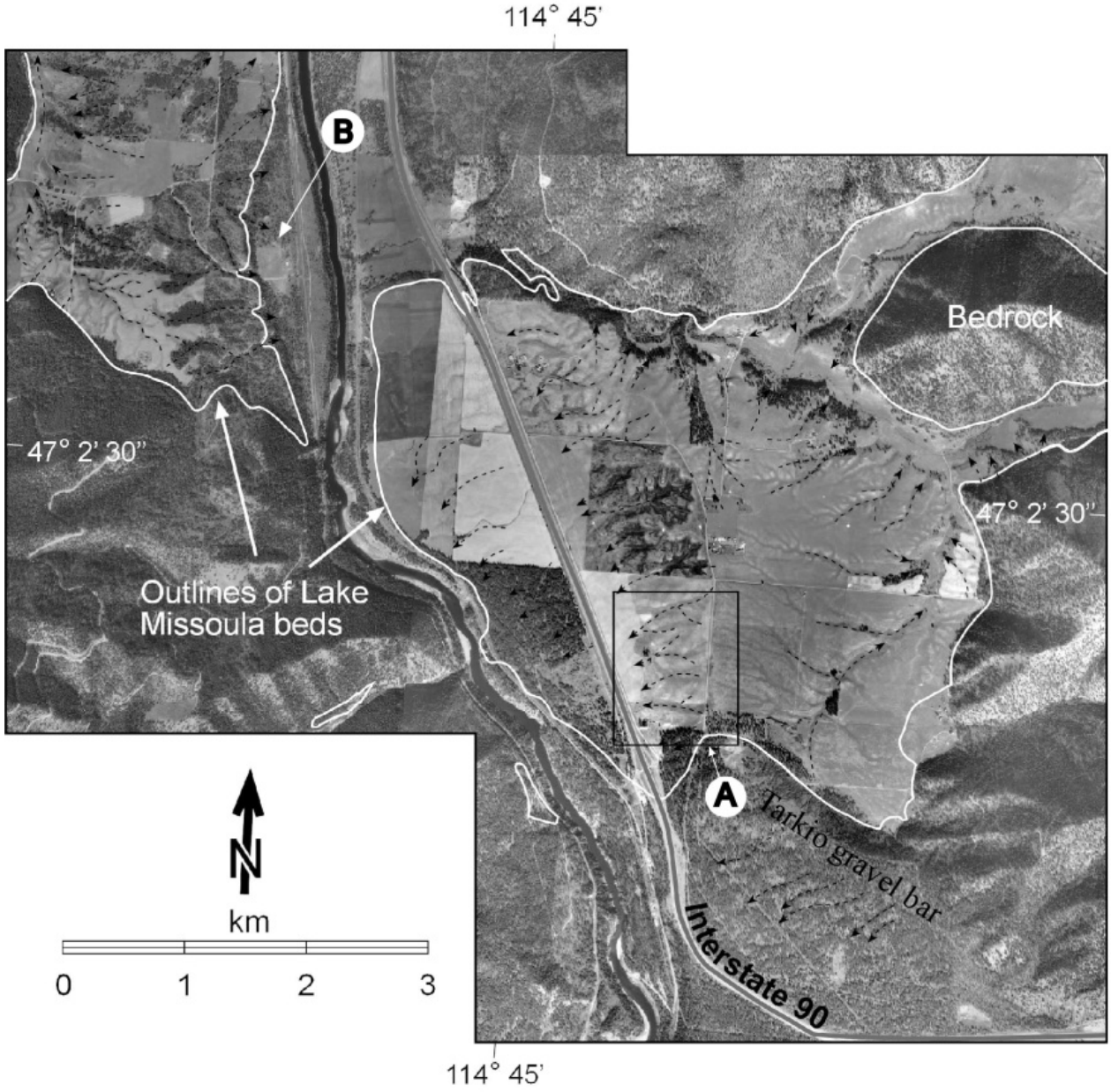

Figure 4. Digital orthophotos show the drainage networks that developed on the Lake Missoula beds in the Tarkio and Quartz flats areas and some of the drainage basins. Site "A" is rolling topography previously interpreted as a down-valley train of giant dunes. Site "B" is the location where drainage basins end in a depositional environment at a stream terrace remnant. However, the alluvial fans in this area are very small compared to the amount of sediment eroded from the drainage basin; dashed lines with arrows show some of the channels in lake-bed silts (modified from Smith, 2006).

Alluvial fans at the outlets of the stream valleys either do not exist, or contain a much smaller amount of sediment than that eroded from the stream network ("B" in fig. 4).

The basins appear to grade to terrace levels below the bench we are standing on (the upper surface of the Lake Missoula beds). The lack of alluvial sediments on these terraces suggests the sediments from the drainage basins eroded when the Clark Fork River was downcutting the terrace levels.

I think that the drainage basins were mostly cut during the final GLM flood.

What evidence is needed to further support or refute this?

If this is a typical record for GLM floods, and the Lake Missoula beds represent multiple lake stands, where are the gullies in the sedimentary record?

Return to I-90 and travel north about 6 miles to Exit 55. Turn right on Quartz Loop Road and cross the Clark Fork within about 1 mile. Note the large boulders in outcrop downstream of the bridge. Turn left (north) on Mullan Road East, travel an additional ~4.5 miles, and park on the right, across street from the Superior Airport.

STOP 4

Stop 4. Scabland topography (47º 09' 52" N, 114º 50' 48" W, 2,800 ft)

Scabland topography in the GLM drainage basin is an erosional landscape where Belt Supergroup bedrock has been stripped of most of the overlying unconsolidated sediments along a surface characterized by internally drained basins. As in the Channeled Scablands of Washington, scablands along the Clark Fork River are evidence of high-velocity flows associated with GLM drainage, forming "kolk" flows that caused bedrock plucking. A kolk is a helical fluid vortex that is created by rapidly rushing water. Vertical lifting forces in kolk flow can lift large boulders of bedrock, forming the internally drained bedrock basins known as scabland features. Scablands near the Clark Fork River below the glaciolacustrine deposits likely resulted from drainage of the lake stand that deposited the Lake Missoula beds (Smith, 2006).

At this stop, we can walk around in the area NE of Mullan Road, where scabland features were developed on a terrace remnant. Lake Missoula beds have not been mapped in the immediate area, but were mapped on small benches about 100 feet above this surface. Gravelly alluvium occurs in the area. The distribution of terraces and scabland features in the area is discussed in Smith et al. (this volume).

Things to note at this stop:

The scabland topography is evidence of catastrophic flows during a lake drainage event at a level below the Lake Missoula beds.

The scablands were likely formed by drainage of the last GLM, which drained in such a way that many deep-water lake deposits were preserved. High flow velocities were restricted to the inner canyon area, and some stream terraces were formed and downcut at the same time (Smith et al., this volume).

An alternate possibility would be that the scablands were formed during earlier (pre-Lake Missoula bed) flows, but they were exhumed during the last drainage. This exhumation would likely leave coarse clastics within the depressions. …is this reasonable?

Return to Mullan Road and drive into Superior; at about 3.3 miles continue onto Mullan Road another 2.2 miles west to Stop 5.

STOP 5

Stop 5. Miller Gravel Pit (47º 12' 42" N, 114º 56' 07" W, 2,730 ft)

Gravel mined from this pit underlies the Lake Missoula beds, which is being stripped off the top. Holocene alluvial fans emanate from the bedrock drainages northwest and southeast of the pit. The stratigraphy in the pit displays at least two gravel units, separated by a (discontinuous?) silty sand unit with climbing ripples (fig. 5).

Things to note at this outcrop (this is a working mine on private land, so access may not be possible):

The distribution and scale of sedimentary features in the gravel beds

The distribution and continuity(?) of the silty sand bed

Existence of erosional contacts in the system, suggesting multiple flow events

Return to Superior, cross the Clark Fork River and travel across I-90 onto the Westside frontage road (Diamond Road). Continue traveling southeast past Cedar Creek, and then southwest 5 miles up Trout Creek.

Stop 6. Deposits near the mouth of Trout Creek (47º 08' 24" N, 114º 50' 54" W, 2,800 ft)

STOP 6

In road cuts and the gravel quarry above this site there are gravelly deposits with large-scale cross stratification. This type of deposit is common near the confluence of the Clark Fork River and its side drainages. Stratification in these "eddy deposits" is not always evident; some exposures are of massive, very poorly sorted gravel. However, the sediment in this exposure was deposited in a protected embayment and transported up Trout Creek, away from the main flood route.

Figure 5. Photograph, looking NE, of the Miller Gravel Pit taken June 20, 2002 (at Stop 5). Large-scale cross stratification was evident in gravel below the silty sand bed. Lake Missoula beds were stripped from above the gravel. Optical dating of quartz in the silty sand bed suggests an age of about 21,000 yr for the catastrophic flooding at this site (Baker et al., 2009).

Modification of the area above the road cut has made interpretation of the entire area difficult. Holocene colluvial deposits that may contain Mazama tephra, which has an age of 7627 ± 150 cal yr B.P. (Zdanowicz et al., 1999), overlie gravel higher in the section.

Travel 5 miles to return to I-90 at Superior and travel 13 miles to St. Regis. Exit and travel northwest on MT-135 for 4.2 miles.

You will exit to the right onto a small dirt road, so be prepared. About 1 mile before the turn, MT-135 enters a narrow canyon and turns east. Slow down; the turnoff will be the first road on the right, just past the end of a guardrail. Take the dirt roads about 0.25 mile down to an unofficial crossing of the rail line.

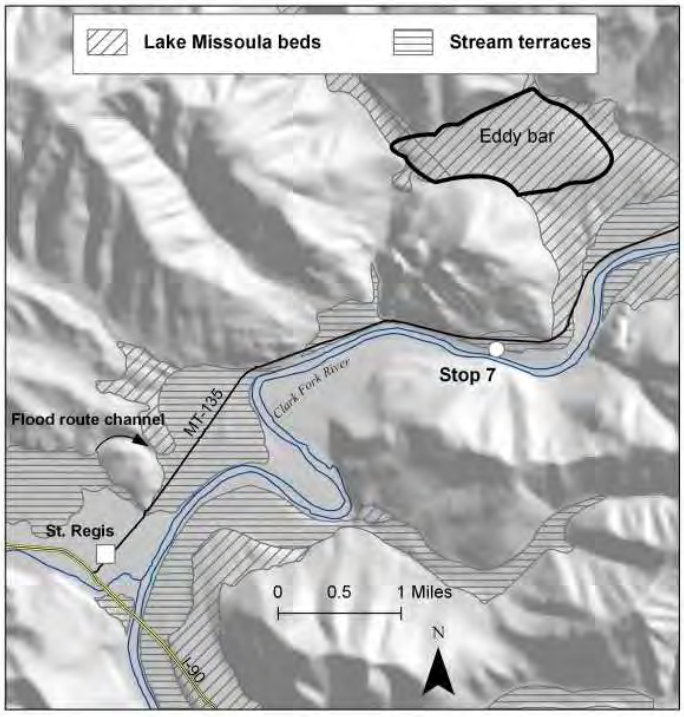

Figure 6. Geology and landforms in the area near and downstream of St. Regis, showing the location of Stop 7 and a large eddy bar downstream of a canyon reach.

STOP 7

Stop 7. Toole Siding (47º 19' 37" N, 115º 02' 02" W, 2,630 ft)

The rail line here is active, so be aware of the possibility of trains coming from either direction!

This stop is at the top of a canyon reach of the Clark Fork River, downstream from St. Regis. The geology and landforms of the area are shown in Figure 6. The large accumulation of boulders with diameters of 2-6 m is unusual and important. Glenn Koepke, a resident of St. Regis, showed this locality to me. Boulders are well exposed, and some are in original sedimentary position, along the north side of the rail cut. These large clasts are spread for an unknown distance above the rail grade, down to the active channel of the Clark Fork.

Rough calculations of the fluid shear stresses required to transport the clasts shows they could not have been moved by normal-sized floods. Their position on the bank and within the channel suggests they originated from erosion of the upstream portion of the bedrock knob, and accumulated where the channel widened slightly in this area. Their position very near or at stream grade (2,600–2,630 ft) here shows that the Clark Fork River has downcut very little, or not at all, at this location since the late Pleistocene.

Things to notice at this stop:

Boulder size and imbrications

The distribution of boulders from above the rail grade to rapids in the Clark Fork River

Return to MT-135 by the same route, turn right, and travel about 17.5 miles to the intersection of MT-135 and MT-200. Along the way notice:

1.5 miles—The 300–400-foot-high, tree-covered hill to the north is made up of gravel, formed as an eddy bar formed where the valley widened. Lake Missoula beds are exposed in the slopes around the hill.

12.2 miles—Cascade Creek USFS campground—possible rest stop. Scoured bedrock surfaces in the canyon have a few remnant gravels that are evidence of terrace remnants or flood gravel deposits.

STOP 8 Stop 8. Confluence of the Flathead and Clark Fork rivers (47º 21' 15" N, 114º 46' 43" W, 2,500 ft)

From this vantage, we can see Lake Missoula beds south and southeast of the intersection, and a prominent "gulch fill" eddy deposit above the town of Paradise, north-northwest of the stop. Preservation of Lake Missoula beds in the bottom of the valleys shows that drainage of the last lake could not have been as catastrophic as earlier floods, which produced the "gulch fills" (Pardee, 1942; Chambers, 1971; Smith, 2006). The larger floods caused dramatic scouring and high-elevation eddy deposits in this area, and large bedforms were deposited in the upstream areas of the Clark Fork River, including the area near Tarkio. The last draining of the GLM eroded scabland features only along inner canyon reaches. I believe that the last lake stand either was deep and its dam failed in such a way that water was slowly released or was shallow and released a smaller volume water.

Sediments deposited during catastrophic draining of GLM are better preserved in the southern basins than in the northern basins. No large eddy bars like those near Cyr, Tarkio, and St. Regis have been found yet in the northern basins. This difference in preservation may be due to the much larger volume of water stored in the northern basins of GLM, which caused generally higher durations of extreme flow velocities, and more erosion during draining events.

Return to Superior (about 35 miles), or proceed on an additional 53-mile loop to two more stops, at Rainbow Lake and Markle Pass.

To proceed to Rainbow Lake, turn left (northwest) on MT-200 and travel 8.3 miles; turn right (northeast) onto MT-28E. Go an additional 9.4 miles. As we travel up Boyer Creek on MT-28E, we will pass gravelly alluvium deposits, and cut terraces formed by floodwaters coming down from the "Rainbow Lake bypass" from the Little Bitterroot valley. The stop will be near the east end of the lake, pull over onto dirt roads on the left (west).

Stop 9. Rainbow Lake (47º 31' 35" N, 114º 44' 38" W, 3,610 ft) **STOP 9**

The depression filled by Rainbow Lake was cut by high-energy GLM floodwaters. This "Rainbow Lake bypass" was a shortcut for the massive amounts of water stored at high lake stands in the Little Bitterroot and Mission Valley subbasins. This lake sits in a large scabland basin. Maximum water depths in this area were only about 600 feet. When the dam failed downstream from Plains, water spilled through this valley at high speeds, forming kolks.

Proceed NE on MT-28 for 7 miles, turn right on County Road 382, and travel about 1.8 miles to a good overlook of the Camas Prairie Basin. Joseph Pardee's famous "giant ripples", which are now referred to as dunes, are visible from here.

STOP 10 Stop 10.—Markle Pass (47º 32' 46" N, 114º 37' 08" W, 3,310 ft)

When the light is right, the giant dunes emanating from Markle Pass and other gaps along the northern side of the Camas Prairie Basin are striking. The trains of rounded (in profile), straight-crested bedforms are made up of cobble-sized gravel. The dunes are overlain by glaciolacustrine silts correlative to the Lake Missoula beds. The silts are only inches to a few feet think in the inter-dune areas. These relationships are similar to what is seen elsewhere in the basin: the high-velocity flows occurred during earlier drainages of GLM; the silts represent transgression and deposition in a later lake-stand; and its drainage did not cause the higher velocity flows characteristic of the earlier events (Pardee, 1942; Chambers, 1971, 1984; Smith, 2006).

Continue south on County Road 382 for about 14 miles to MT-200 and turn right (west)

Things to look for on return:

Mile 18.5—A beautiful "gulch fill" eddy deposit described by Pardee (1942) is across the river. The top of the gravelly alluvium deposit is about 700 feet above river level here. Burgess Lake is out of view on the south side of the valley, about 400 feet above river level. Scabland features in bedrock by "kolk" erosion.

Mile 24—Turn left (south) on MT-135 and return to Superior.

Acknowledgements

The Montana Bureau of Mines and Geology Groundwater Assessment Program supported most of the initial fieldwork, for the purpose of understanding the distribution of aquifers in the area. Use of Google maps allowed mileage figure calculation from the comfort of my office chair. Marie Garsjo reviewed the manuscript and improved its clarity.

References

Alho, P., Baker, V., and Smith, L.N., 2010, Paleohydraulic reconstruction of the largest Glacial Lake Missoula draining(s): Quaternary Science Reviews, v. 29, p. 3067-3078.

Alt, D., 2001, Glacial Lake Missoula and its Humongous Floods: Mountain Press, Missoula, 208 p.

Alt, D., and Chambers, R.L., 1970, Repetition of the Spokane flood: American Quaternary Association Meeting 1, Yellowstone Park and Bozeman, Montana, Abstracts, Montana State University, Bozeman, p. 1.

Atwater, B.F., 1986, Pleistocene glacial-lake deposits of the Sanpoil River valley, northeastern Washington: U.S. Geological Survey Bulletin 1661, 39 p.

Atwater, B.F., Smith, G.A., and Waitt, R.B., 2000, The Channeled Scabland: back to Bretz?, Comment: Geology, v. 28, p. 574-575.

Baker, V.R., 1973, Paleohydrology and sedimentology of Lake Missoula flooding in Eastern Washington: Geological Society of America Special Paper 144, p. 1-79.

Baker, V.R., Bjornstad, B.N., Greenbaum, N., Porat, N., Smith, L.N., and Zreda, M.G., 2009, Possible revised chronology of late Pleistocene megaflooding, northwestern U.S.: Geological Society of America Abstracts with programs, v. 41, no. 7.

Booth, D.B., Troost, K.G., Clague, J.J., and Waitt, R.B., 2004, The Cordilleran ice sheet: *in* Gillespie, A.R., Porter, S.C., and Atwater B.F., eds., The Quaternary Period in the United States: Developments in Quaternary Science 1, Elsevier, Amsterdam, p. 17-43.

Breckenridge, R.M., 1989, Lower Glacial Lakes Missoula and Clark Fork ice dams: *in* Breckenridge, R.M., ed., Glacial Lake Missoula and the Channeled Scabland: Missoula, Montana to Portland, Oregon: American Geophysical Union, 28th International Geological Congress, Field Trip Guidebook T310, p. 13-21.

Bretz, J.H., 1969, The Lake Missoula floods and the Channeled Scabland: Journal of Geology, v. 77, p. 505-543.

Chambers, R.L., 1971, Sedimentation in glacial Lake Missoula: MS thesis, University of Montana, Missoula.

Chambers, R.L., 1984, Sedimentary evidence for multiple glacial Lakes Missoula: *in* McBane, J.D., and Garrison, P.B., eds., Northwest Montana and Adjacent Canada: Montana Geological Society, Billings, p. 189-199.

Curry, R.R., 1977, Glacial geology of Flathead Valley and catastrophic drainage of Glacial Lake Missoula: Geological Society of America, Rocky Mountain Section Field Guide 4, University of Montana, Missoula.

Fritz, W.J., and Smith, G.A., 1993, Revisiting the Ninemile section: Problems with relating glacial Lake Missoula stratigraphy to the Scabland-floods stratigraphy: Eos, Transactions American Geophysical Union 74:43 (supplement), p. 302.

Langton, C.M., 1935, Geology of the northeastern part of the Idaho Batholith and adjacent region in Montana: Journal of Geology, v. 43, p. 27-60.

Levish, D.R., 1997, Late Pleistocene sedimentation in glacial Lake Missoula and revised glacial history of the Flathead Lobe of the Cordilleran Ice Sheet, Mission valley, Montana: PhD dissertation, University of Colorado, Boulder.

Pardee, J.T., 1910, The glacial Lake Missoula, Montana: Journal of Geology, v. 18, p. 376-386.

Pardee, J.T., 1942, Unusual currents in glacial Lake Missoula, Montana: Geological Society of America Bulletin, v. 53, p. 1569-1599.

Shaw, J., Munro-Stasiuk, M., Sawyer, B., Beaney, C., Lesemann, J.-E., Musacchio, A., Rains, B., and Young, R.R., 1999, The Channeled Scabland: back to Bretz?: Geology, v. 27, p. 605-608.

Shaw, J., Munro-Stasiuk, M., Sawyer, B., Beaney, C., Lesemann, J.-E., Musacchio, A., Rains, B., and Young, R.R., 2000, The Channeled Scabland: back to Bretz?, Reply: Geology, v. 28, p. 576.

Smith, L.N., 2006, Stratigraphic evidence for multiple drainings of glacial Lake Missoula along the Clark Fork River, Montana, USA: Quaternary Research, v. 66, p. 311-322.

Waitt, R.B., 1980, About forty last-glacial Lake Missoula jökulhlaups through southern Washington: Journal of Geology, v. 88, p. 653-679.

Waitt, R.B., 1985, Case for periodic, colossal jökulhlaups from Pleistocene glacial Lake Missoula: Geological Society of America Bulletin, v. 96, p. 1271-1286.

Zdanowicz, C.M., Zielinski, G.A., and Germaini, M.S., 1999, Mount Mazama eruption: Calendrical age verified and atmospheric impact assessed: Geology, v. 27, p. 621-624.

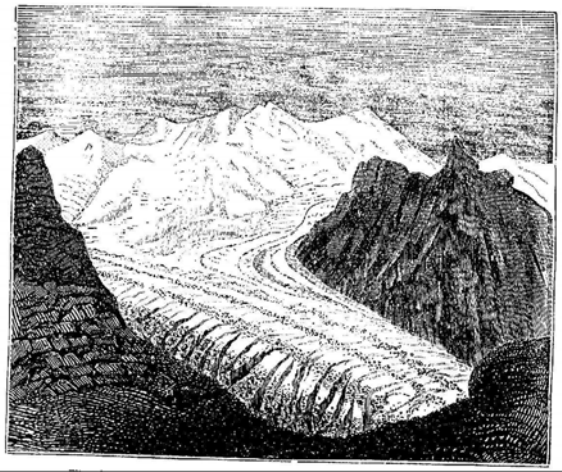

PRECIOUS METALS IN CEDAR AND TROUT CREEKS, MINERAL COUNTY, MONTANA

Robin McCulloch
Montana Bureau of Mines and Geology, 1300 W. Park St., Butte, MT 59701
rmcculloch@mtech.edu

Cedar and Trout Creeks flow northward into the Clark Fork River upstream of Superior, MT (fig. 1). Wallace Formation rocks near the upper ends of the drainage basins host precious metal deposits, and will be the locations of most stops on this trip (fig. 2). The area is cut by NE- and NW-trending faults (fig. 2). Placers in the area include those in alluvial/gulch deposits, debris deposits, and residual deposits (fig. 3). Most of the placers in the area can be tied, at least in a general way, to lode sources (fig. 3; McCulloch et al., 2003).

Road Log

Travel southeast from Superior on Diamond Road, the south-side frontage road for about 5 miles and follow the road upstream in the Trout Creek drainage (fig. 1).

STOP 1 – Lower end of Trout Creek. We will discuss the placer drift mining activities from the 1920s and 1930s at the mouth of Trout Creek

STOP 2 – At Gulls gulch placer deposit, near Slaughter House Gulch, we will look at gold-bearing quartz veins on the roadside and discuss the placers in Windfall and Deep creeks as well as the potential placers at the junction. Time will also be spent discussing the lode source on Landowner Mountain and its location.

STOP 3 – Gold Mountain Mine portal and discuss the placer operations and the lode structure that crossed the valley at that point. Soils adjacent to the forest service road run as high as 859 ppb Au.

STOP 4 – Prospect Gulch placer deposit where drift mines are exposed near the main forest service road. The alluvial fan between the canyon mouth and the road, shows extensive placer activity ranging from booming to drift mining.

STOP 5 – Lost Dutchman mine. This segment of the gold-bearing structure contains chalcopyrite that was mined and shipped to the smelter in Anaconda.

STOP 6 – We will walk into Freeze Out Basin and view the buried placer. Deep cuts reveal extensive placer deposits buried by valley fill.

STOP 7 – At the divide, we will walk a short distance into a barite mine located along one of the structures. In this valley, the western structure is a barite-lead-zinc zone while the eastern structure changes from gold to copper and is the source of the primary placers in Cedar Creek.

STOP 8 – We will stop at the Gildersleeve Placer camp, which is one of the few remaining camps still intact. Out of this camp, George Gildersleeve hydraulicked residual gold deposits at the head of Snowshoe creek as late as 1972. The lead-zinc vein is exposed in a drift at the west side of the camp.

STOP 9 – The Brockbank placer will be discussed. A narrow-gauge railroad was built to transport a bucket-ladder dredge that operated for a short period. After the war, gold was mined using trucks and a

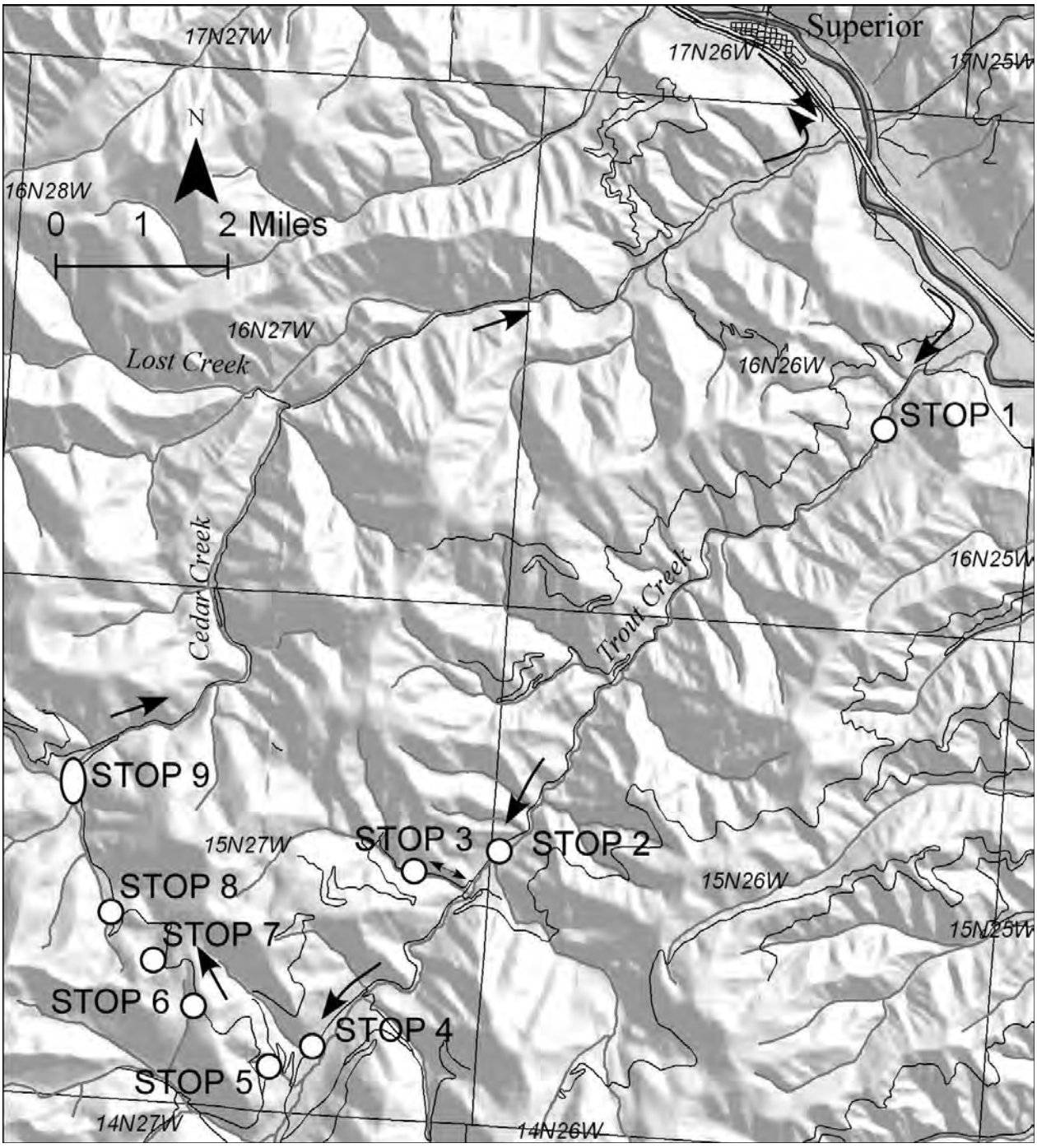

Figure 1. Location map of roads and stops.

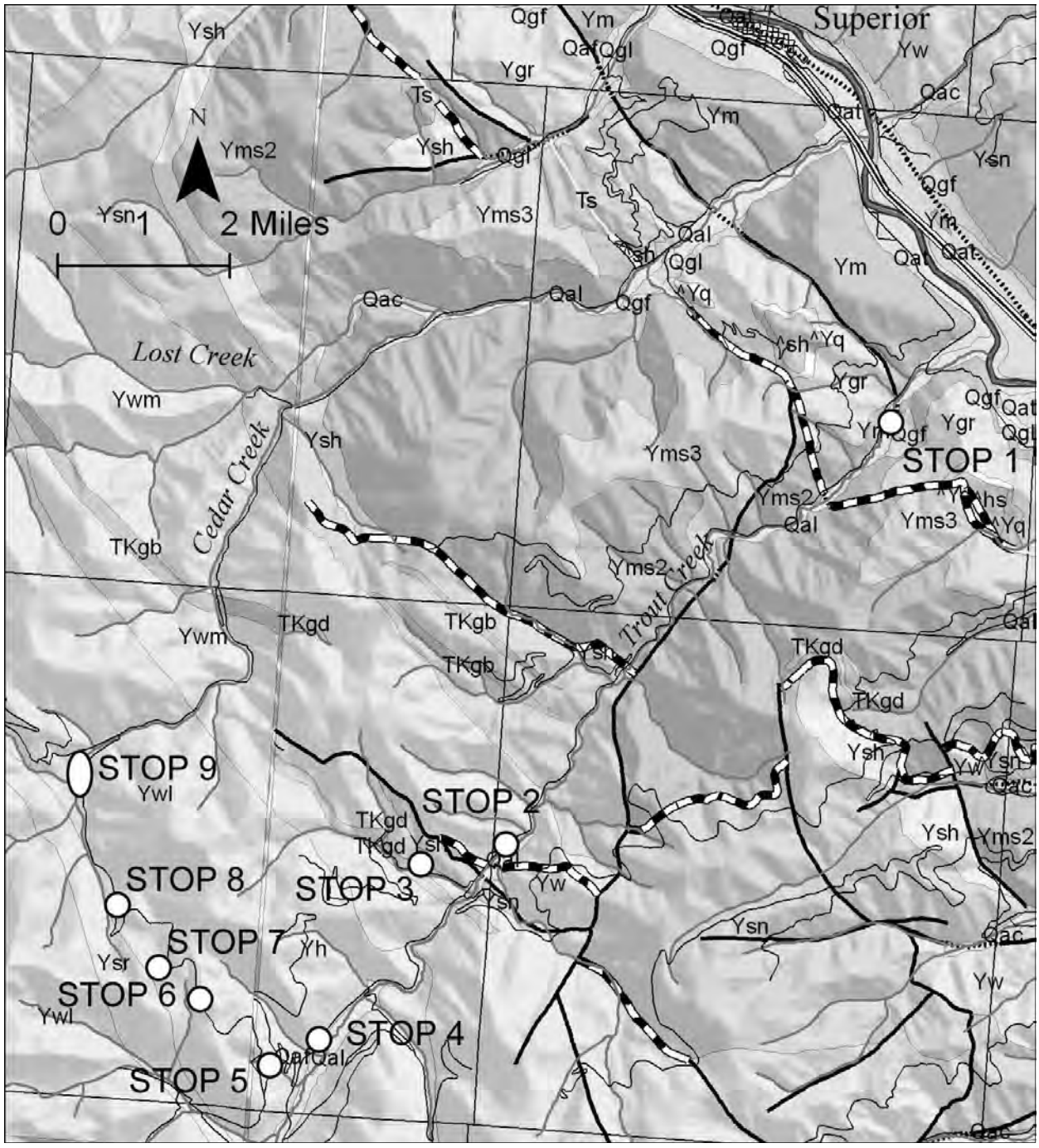

Figure 2. Geologic map of the Cedar and Trout Creek area; Ysr – St. Regis Fm.; Ywl, Ywm – Wallace Fm., lower and middle members: Ysn – Snowslip Fm.; Yms2,3 – Mount Shields Fm.; Ysh – Shepard Fm.; Ygr – Garnet Range Fm.; ^Yq – Precambrian or Cambrian quartzite; ^sh – Cambrian Silver Hill Fm.; Ts – Tertiary sedimentary rocks; Qgf – Quaternary glacial flood deposits; Qgl – glacial lacustrine deposits; Qao – older alluvium; Qat – terrace deposits; Qac – alluvial or colluvial deposits; bold lines – faults (dotted where covered); black and white line – thrust fault; modified from Lonn and McFaddan (1999) and Lonn et al. (2007).

shovel. In the 1990s, a dragline was used to produce gold from placer deposits.

Lode deposits yielded gold from vein deposits just above the road in the late 1880s until 1910 when most of the country burned in the 1910 fire.

STOP 10 – we will discuss the mining of the bench placers and the deposits within the Cedar Creek drainage.

References

Lonn, J.D., and McFaddan, M.D., 1999, Geologic map of the Montana part of the Wallace 30' x 60' quadrangle: Montana Bureau of Mines and Geology Open-File Report 388, 16 p., scale 1:100,000.

Lonn, J.D., Smith, L.N., and McCulloch, R.B., 2007, Geologic map of the Plains 30'x60' quadrangle, western Montana: Montana Bureau of Mines and Geology Open-File Report 554, scale 1:100,000.

McCulloch, R.B., Lewis, B., Keill, D., and Shumaker, M., 2003, Applied Gold Placer Exploration and Evaluation Techniques: Montana Bureau of Mines and Geology Special Publication 115, 267 p.

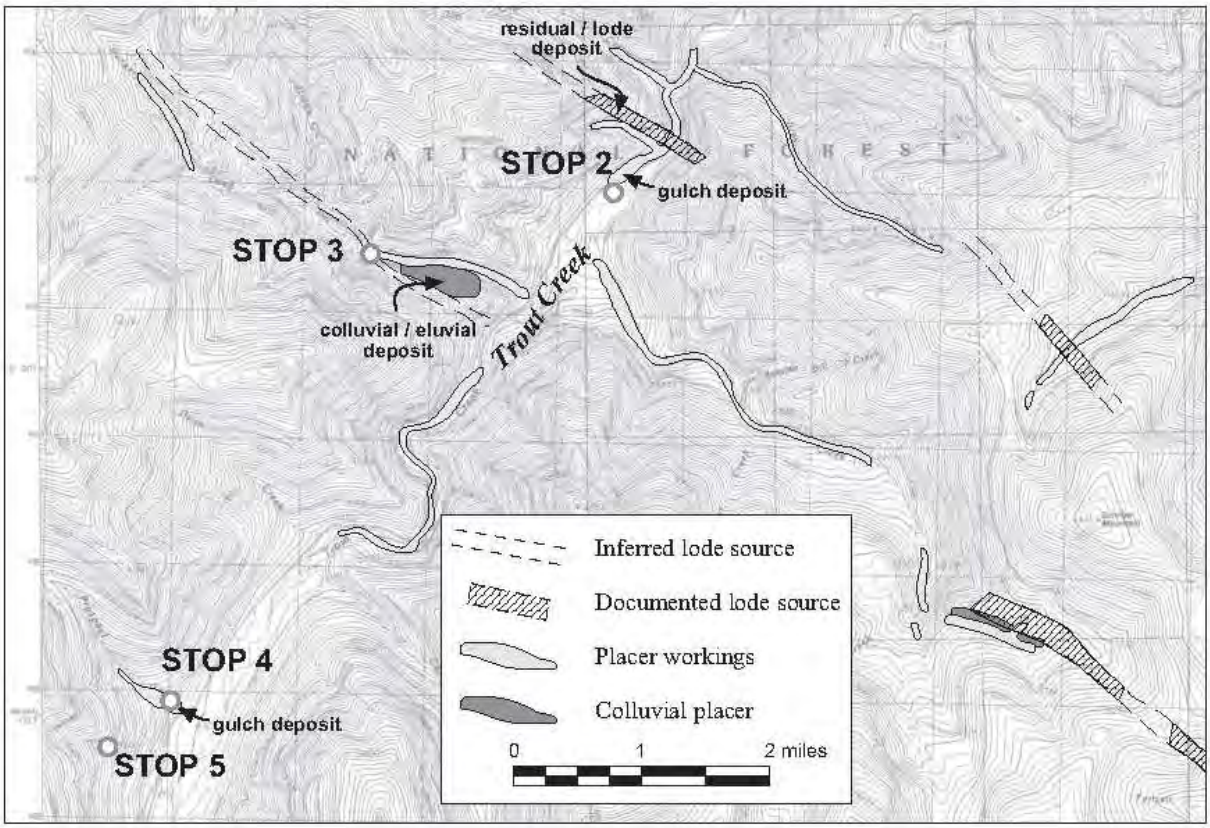

Figure 3. Map of placer and lode deposits in the Quartz Creek area (modified from McCulloch et al., 2003).

Placer operation along Trout Creek.

Sluice box in Gold Mountain mine placer along Trout Creek.

Boom operation in Gold Mountain mine placer along Trout Creek.

Sluice box in Gold Mountain mine placer along Trout Creek.

BELOW THE BELT: A ROAD LOG OF ARCHEAN AND PALEOPROTEROZOIC ROCKS IN THE EASTERN CLEARWATER COMPLEX, IDAHO

Reed S. Lewis[1], Rachel A. Brewer[2], Andrew C. Jansen[2], Victor E. Guevara[3], Jeffrey D. Vervoort[2], and Julia A. Baldwin[3]
[1]Idaho Geological Survey; [2]Washington State University; [3]University of Montana

INTRODUCTION

The spatial distribution and ages of the basement rocks in northern Idaho and western Montana are poorly understood due to coverage by overlying metasedimentary rocks of the Belt-Purcell Supergroup, multiple widespread metamorphic events, and Late Cretaceous to early Tertiary magmatism (fig. 1). Outcrops of Precambrian basement rocks are rare, but have been documented in several locations including the Priest River complex in northern Idaho (Doughty et al.,1998), the Boehls Butte area in north-central Idaho (Doughty and Chamberlain, 2007), and in the northern Bitterroot Range southwest of Missoula, Montana (Baldwin et al., 2011).

This field trip focuses on the Clearwater metamorphic core complex of north-central Idaho. It was first proposed as a metamorphic core complex by Seyfert (1984) and this suggestion has been substantiated by Doughty et al. (2007), based on kinematic analyses, thermobarometric data, and Eocene $^{40}Ar/^{39}Ar$ cooling ages. They describe an "internal zone" composed of 1787 Ma anorthosite and 1587 Ma amphibolite, and an "external zone" of amphibolite facies metamorphic rocks of the lower Belt Supergroup that extend as far east as the Collins Creek fault. The Clearwater complex is a manifestation of Eocene extension that occurred in a releasing bend between the St. Joe fault to the north and the Kelly Forks-Benton Creek fault to the south, both of which are part of the Lewis and Clark line. Foster et al. (2006) designated basement in this area as part of the Selway terrane, which they proposed to be a southwestern extension of the Great Falls tectonic zone and to contain primarily Paleoproterozoic crust overlain by the Belt-Purcell metasedimentary rocks. Our more recent U-Pb data, however, has revealed the presence of previously unrecognized 1.86 Ga Paleoproterozoic rocks as well as a significant component of 2.67 Ga Archean basement (Vervoort et al., 2007; Brewer et al., 2008). The presence of the two distinct age groups of basement indicate more widespread Archean basement than previously recognized and extends the Clearwater complex to the southeast into the Kelly Creek area, well east of the Collins Creek fault.

Documenting previously unidentified Paleoproterozoic and Archean rocks within the Clearwater complex has resulted in a new geologic piercing point along the western margin of the North American craton. During the assembly of Nuna (1.8–1.6 Ga) and Rodinia (1.1–0.9 Ga), North America's central location acted as nucleation point for supercontinent growth. Therefore, understanding the distribution and age relationship of these rocks is crucial in determining the extent of the original craton, the fundamental evolution of North America, and correlation with similar rocks that occur on previously adjoined cratons (e.g., Siberia, Australia, and Antarctica).

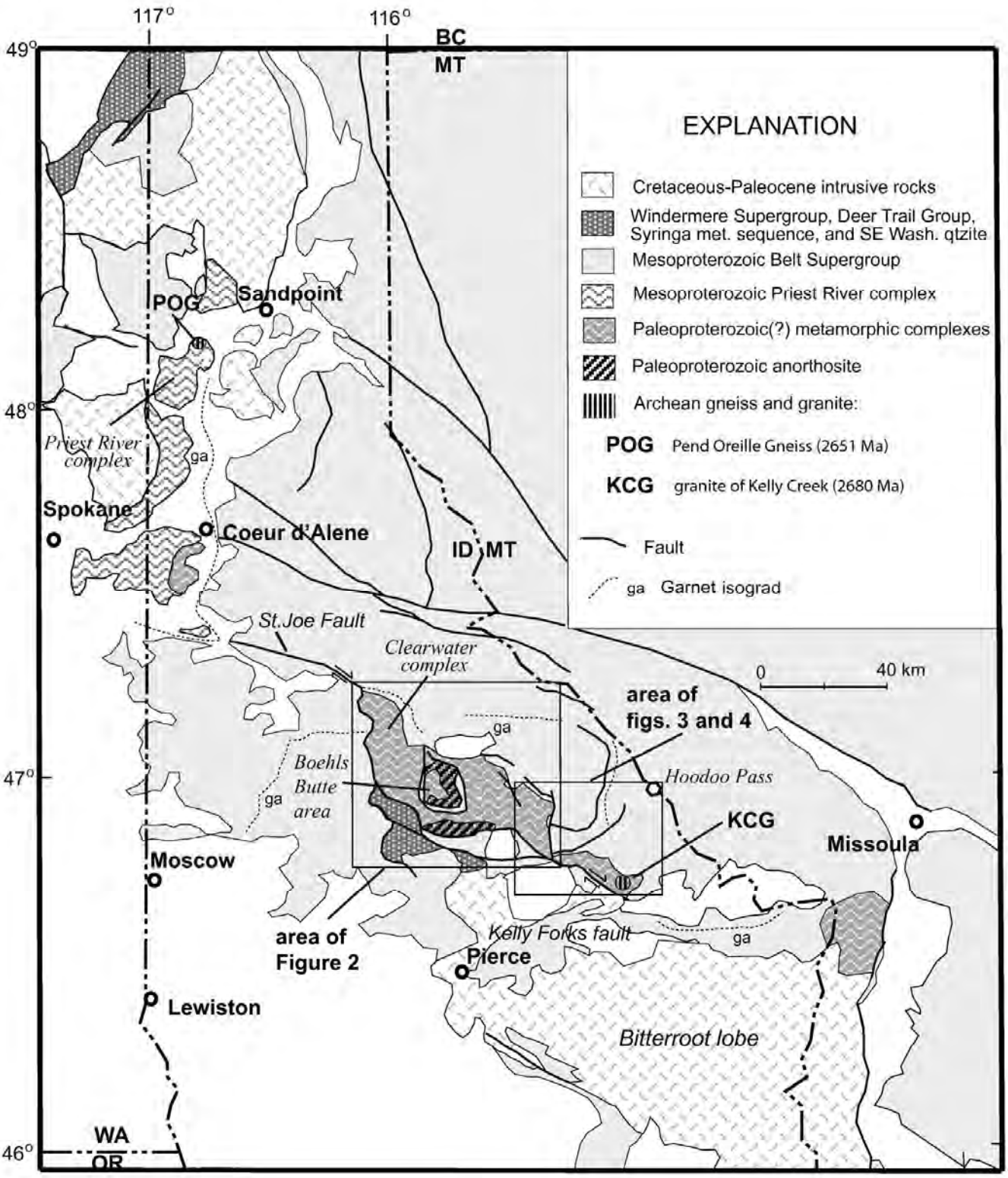

Figure 1. Regional geologic map showing exposures of basement rocks that pre-date the Belt-Purcell Supergroup. Modified from Lewis et al. (2010).

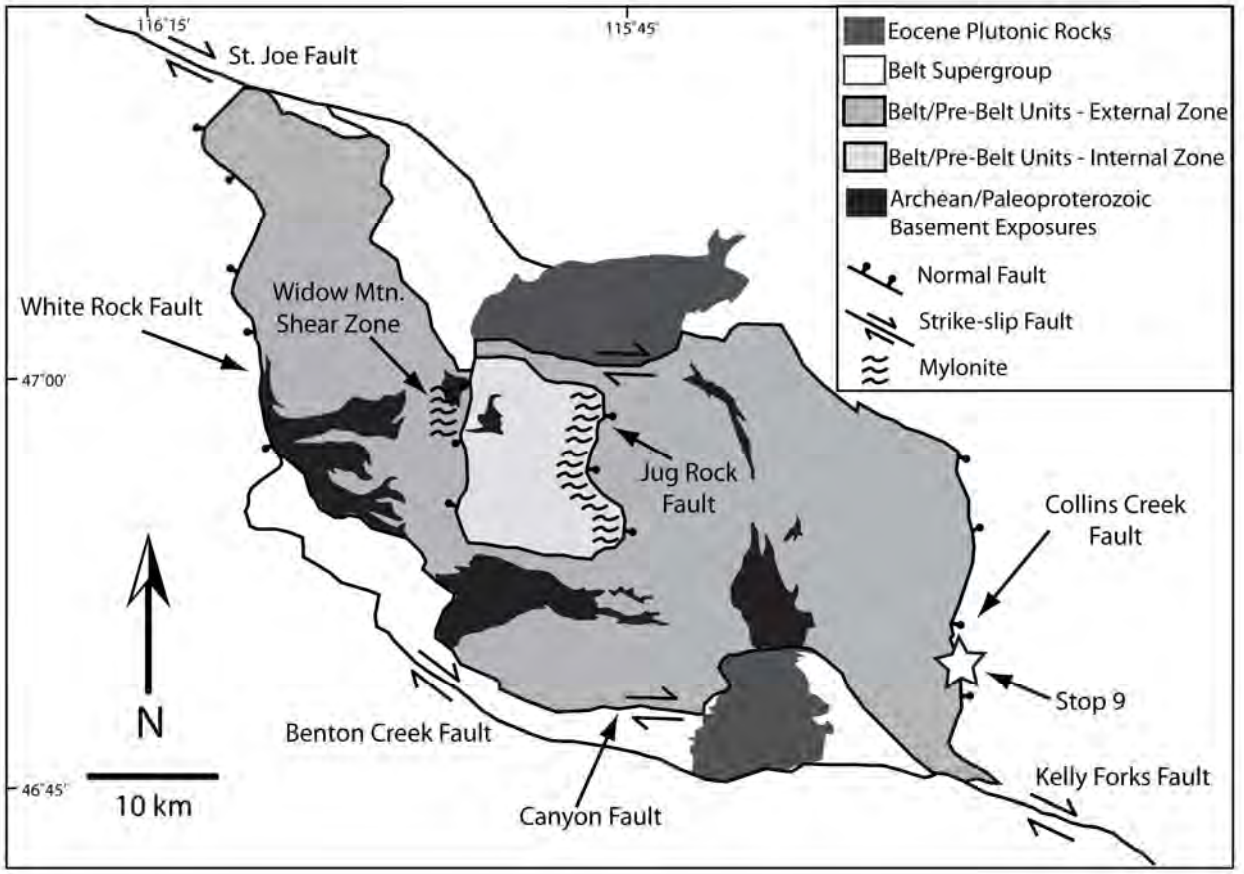

Figure 2. Generalized geologic map of the Clearwater complex showing lithologies, major structures, and the location of Stop 9. Modified from Nesheim (written communication, 2010).

This field trip includes stops within the Clearwater complex at exposures of both Paleoproterozoic and Archean orthogneiss as well as metasedimentary outcrops believed to provide links between the overlying Belt sediments and its underlying basement. The purpose of this field trip is to see rocks of the Clearwater complex in light of new geochronological data in order to understand the spatial, structural, and temporal relationships between the Precambrian intrusive and metasedimentary rocks of the region. Ages presented here were determined by laser ablation inductively coupled plasma mass spectrometry (LA-ICPMS) at Washington State University.

ROAD LOG

Stops are noted on the maps in figures 3 and 4 and latitude and longitude is given for each stop in NAD 27. The trip starts at Hoodoo Pass, south of Superior, Montana and proceeds south on U.S.F.S. road 250.

STOP 1: Hoodoo Pass (46° 58′ 31″ N, 115° 1′ 29″ W). Park at the pass and walk along the road south into Idaho. The rocks exposed here are lower greenschist facies metasedimentary rocks of the Belt Supergroup. They have been mapped as lower Wallace Formation (Lewis et al., 2007a), part of the Piegan Group as defined by Winston (2007), and are correlative with the Helena Formation. The primary rock

STOP 1

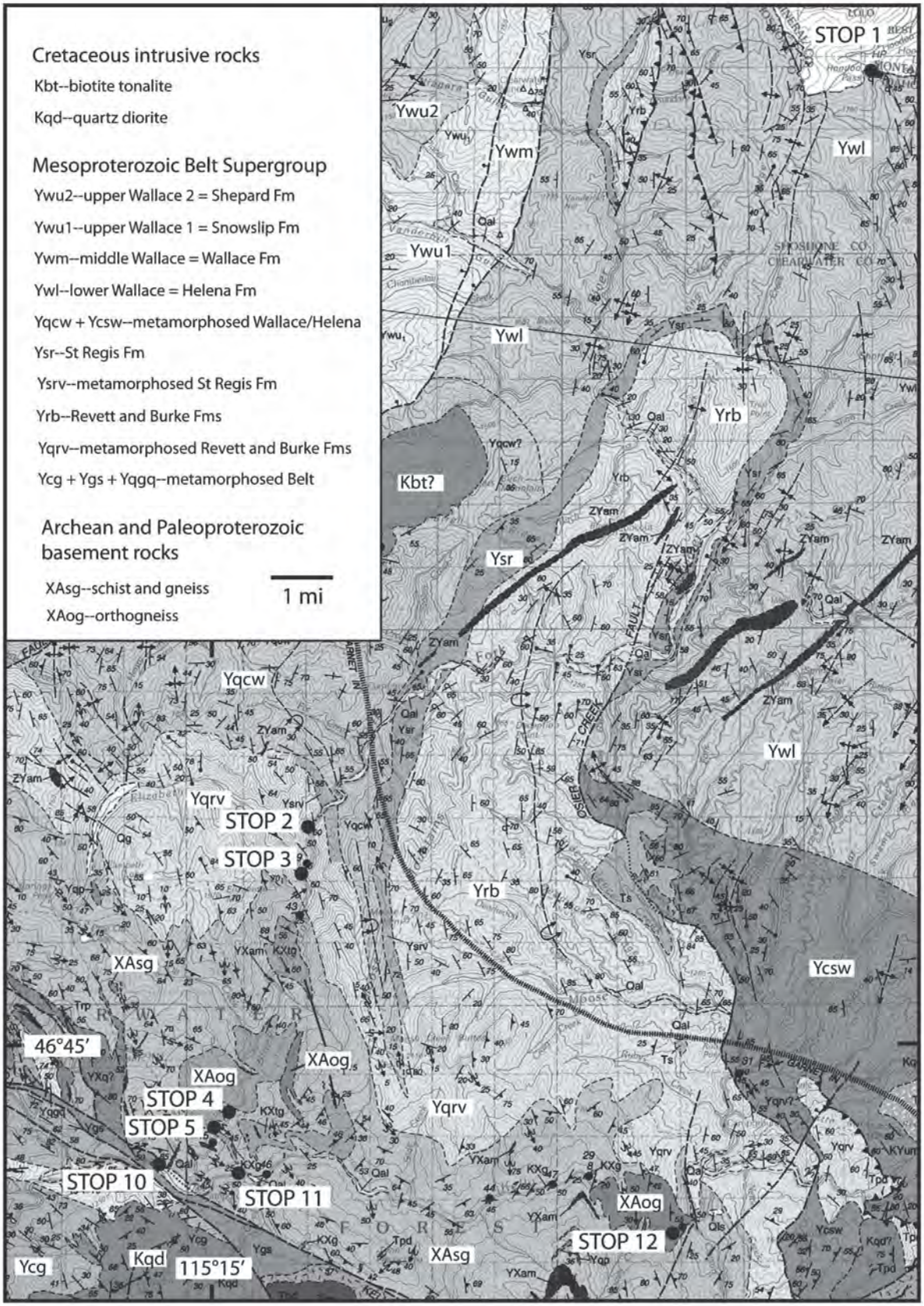

Figure 3. Geologic map of the area between Hoodoo Pass and Kelly Creek showing field trip stops. Modified from Lewis et al. (2007a).

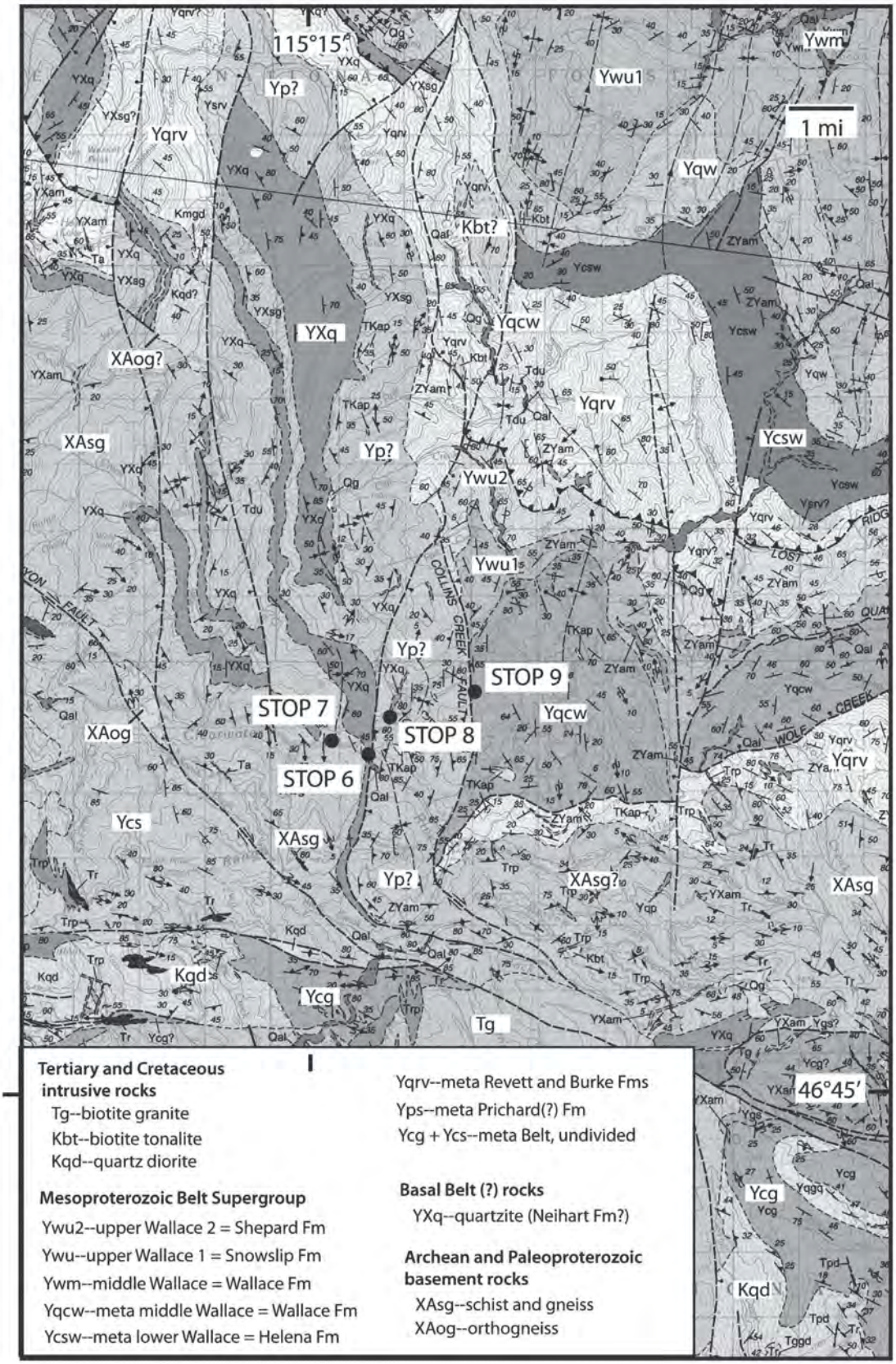

Figure 4. Geologic map of the Quartz Creek and Skull Creek areas showing field trip stops. Modified from Lewis et al. (2007a). Eastern edge of map corresponds to western edge of Figure 3.

types here are dolomitic siltite and quartzite. Detrital zircon grains from a sample collected here yielded an abundance of U-Pb ages between 1450 and 1900 Ma (Lewis et al., 2007b), typical of the western part of the Belt basin.

Drive south along Long Creek to its confluence with the North Fork of the Clearwater River at the Cedars campground. On the way you will pass the mouth of Rawhide Creek on the right and go down section into the Ravalli Group. Continue south from the campground along the North Fork of the Clearwater along road 250. The canyon will narrow once the turnoff to Deception Saddle is passed. Rocks here are quartzite of the Ravalli Group that core a large north-plunging anticline that is west verging. You will drive through the core of the anticline and then back up section into the upper Ravalli Group (metamorphosed St. Regis Formation) at the Hidden Creek campground. South of the Hidden Creek campground you will go up section into calc-silicate rocks of the Piegan Group, through a tight syncline, and then back down into the Ravalli Group. The rocks here are now amphibolite facies. Continue past the campground approximately 3.3 miles to the next stop.

STOP 2 STOP 2: North of mouth of Elizabeth Creek between Elizabeth Creek and Can Creek along the North Fork of the Clearwater (46° 48′ 2″ N, 115° 12′ 58″ W). Park in one of the narrow turnouts along the river. Rocks here are Ravalli Group (Belt Supergroup) strata consisting of feldspathic quartzite with micaceous layers. Approximately 100 concordant U-Pb zircon analyses from sample 08RAB020 were compiled to develop a probability density age plot of this detrital sample (fig. 5). The main peak is at ~1600 Ma; the presence of grains with ages within the "North American magmatic gap" (1610-1490 Ma) is similar to Ravalli Group quartzite sampled by Ross and Villeneuve (2003) approximately 100 km to the NW.

Continue approximately 1 mile to the next stop.

STOP 3 STOP 3: Mouth of Elizabeth Creek (46° 47′ 26″ N, 115° 13′ 10″ W). Park at the pullout at the mouth of the creek and walk to the roadcut to the north. Rocks here are more thinly layered than the last stop and may be metamorphosed Burke Formation of the Ravalli Group. Walking south of Elizabeth Creek, one encounters massive, iron-stained quartzite. From here and south for 1.5 miles, the rocks are gneiss, schist, and quartzite of uncertain age. The massive quartzite could be the base of the Belt Supergroup, but we have no radiometric age information from this locality. The southernmost contact of the Ravalli Group was originally mapped as depositional, with the gneissic and schistose rocks to the south being assigned to the Prichard Formation (Lewis et al., 1992). Based on new pre-Belt ages from orthogneiss to the south (Stop 4 below), it is uncertain as to whether any of these rocks are part of the Prichard. Also unknown is whether the contact with the Ravalli Group is depositional or a down-to-the-north normal fault.

Continue south along road 250 approximately 9 miles. You will pass a wide variety of gneissic and schistose rocks, most or all of which are basement to the Belt Supergroup.

STOP 4 STOP 4: Lower Black Canyon about 1.5 miles south of Pete Ott Creek (46° 44′ 5″ N, 115° 14′ 39″ W). Park along the river and observe the gneissic roadcuts. One outcrop at this locality contains augen

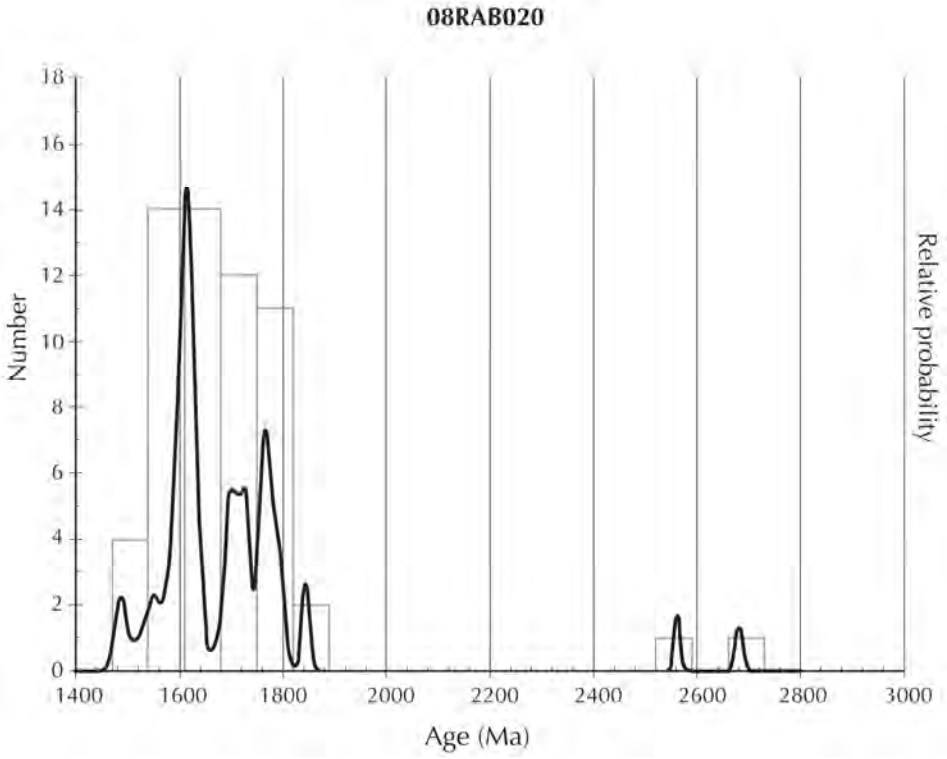

Figure 5. Density-age plot of zircon $^{206}Pb/^{207}Pb$ ages from 08RAB020 showing a prominent peak at ~1600 Ma. This is similar to age plots of the Ravalli Group of the Belt-Purcell Supergroup (Ross and Villeneuve, 2003). Only zircon ages less than 10 percent discordant are plotted.

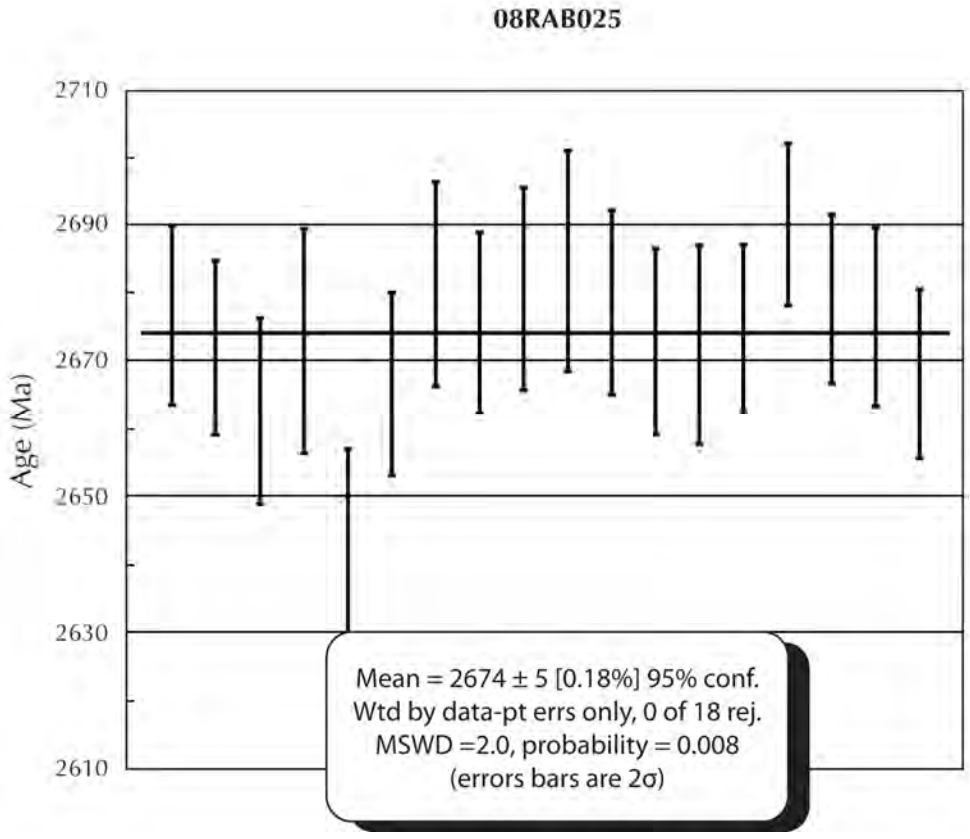

Figure 6. Weighted mean plot for orthogneiss sample 08RAB025 that yielded an Archean $^{206}Pb/^{207}Pb$ age of 2674 ± 5 Ma.

gneiss with large (1-3 cm) plagioclase porphyroblasts surrounded by lenses of gneissic material composed primarily of biotite, muscovite, and quartz. U-Pb zircon analysis of sample 08RAB025 from this outcrop yielded an age of 2674 ± 5 Ma (fig. 6). The zircons from this sample appear relatively undisturbed in CL images despite the metamorphic nature of the rock.

We believe this outcrop is Archean intrusive basement whose igneous characteristics have been lost due to deformation. The nature of the contact between this orthogneiss and the surrounding paragneiss and schist is uncertain. Yet to be determined is whether the orthogneiss intruded older sedimentary rocks, or was basement upon which the sedimentary rocks were deposited.

Continue south along road 250 about 0.3 miles to the next small drainage coming in from the west.

STOP 5 STOP 5: Lower Black Canyon about 1.3 miles north of Kelly Forks Work Center (46° 43′ 52″ N, 115° 14′ 56″ W). Park in pullouts along the river. This stop includes rocks interpreted as both paragneiss and orthogneiss. Two samples (07RAB003 and 07RAB004) were taken from the same outcrop. Initial mineralogical evaluation of 003 indicated that it was a medium-grained biotite-quartz-feldspar gneiss with >40 percent quartz and with a probable metasedimentary origin (fig. 7). 07RAB004 was a medium-grained biotite-feldspar-quartz gneiss, interpreted as orthogneiss, with a well-defined foliation (fig. 8). The presence of euhedral epidote within biotite, as well as epidote with sparse allanite cores, indicate possible high-pressure conditions during crystallization of the orthogneiss. U-Pb zircon analysis of 07RAB004 yielded an age of 2662 ± 8 Ma (fig. 9), similar to the orthogneiss at Stop 4. Analysis of 07RAB003 revealed populations of both 2670 and 1860 Ma grains (fig. 10).

The Archean age determined for 004 orthogneiss is a reasonable one, but its relationship to the adjacent sample 003 (possible paragneiss) is unclear, and the results from sample 003 are not fully understood. A possibility for the two ages of zircons found in 003 is that they are representative of a magmatic event during which Archean basement (orthogneiss?) was intruded at ~1860 Ma by thin granitic stringers which could be related to nearby Paleoproterozoic intrusions. Another possibility is that sample 003 really is metasedimentary and the two outcrops are in depositional contact. The presence of only two populations of zircons could simply be due to its only having sources of those ages.

Continue south along road 250 to the Kelly Forks Work Center. Turn west on road 250 and continue 29 miles downstream to the site of the old Bungalow Ranger Station. Road 250 turns south here and goes up Orogrande Creek. You will continue on Road 247 downstream along the North Fork. Note how the canyon has widened out slightly as you entered the Eocene Bungalow pluton. You will leave the Bungalow pluton after crossing Larson Creek and will shortly cross the Kelly Forks fault and then the Canyon fault, which splays off the Kelly Forks fault to the northwest. Exposures are poor in this area and the first good outcrops are garnet-rich schist (possible Prichard Formation of the lower Belt Supergroup) south of the mouth of Quartz Creek. Quartzite right at the mouth of Quartz Creek is thought to be Ravalli Group. Continue to the mouth of Skull Creek where road 252 takes off to the right.

STOP 6 STOP 6: East of mouth of Skull Creek (46° 49′ 32″ N, 115° 28′ 51″ W). Park in pullout at mouth of Skull Creek and walk east

Figure 7 (above). Photo of the gneiss at Stop 5 (sample 07RAB003), which contains two age populations of zircons (~1860 Ma and ~2670 Ma).

Figure 8 (right). Photo of the Archean tonalite gneiss at Stop 5 (sample 07RAB004) near the outcrop shown in Figure 7 (sample 07RAB003).

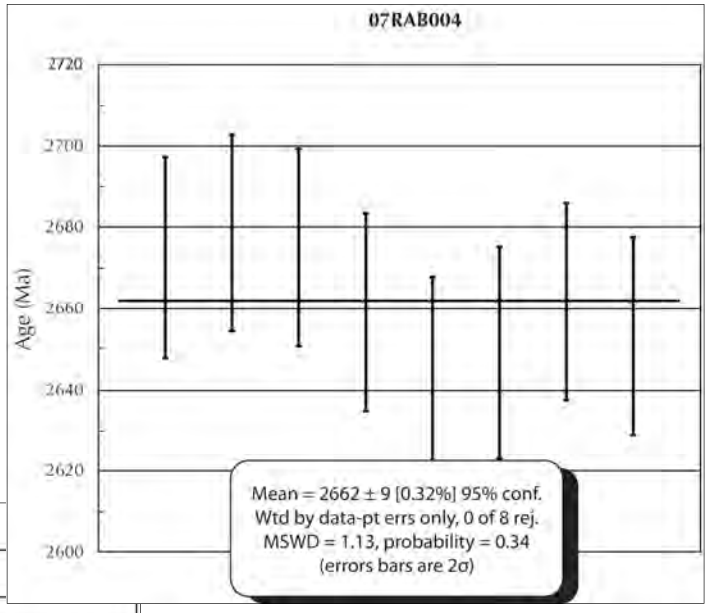

Figure 9. Weighted mean plot for orthogneiss sample 07RAB004 that yielded an Archean $^{206}Pb/^{207}Pb$ age of 2662 ± 9 Ma.

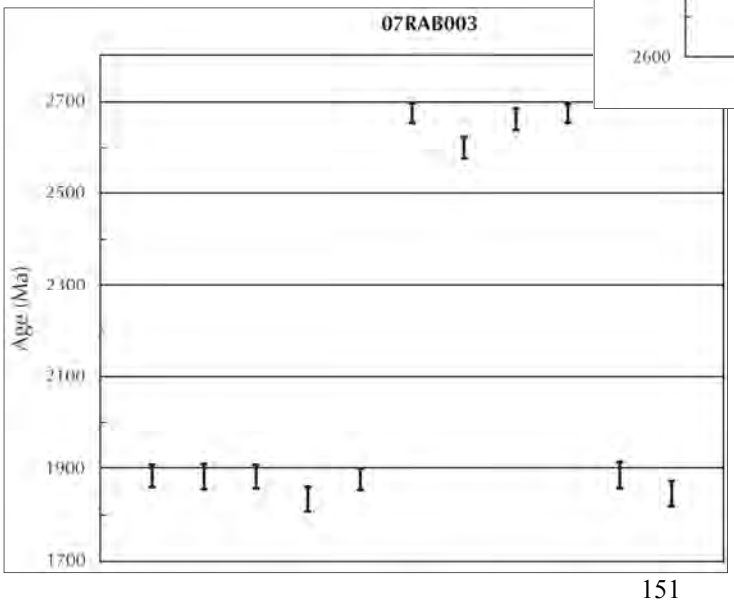

Figure 10. Weighted mean plot of $^{206}Pb/^{207}Pb$ ages for gneissic sample 07RAB003 that yielded both Paleo-proterozoic (~1860 Ma) and Archean (~2670 Ma) ages.

back up the North Fork to the first large outcrops. These are coarse-grained quartzite with sparse feldspar and small (<1 mm) grains of biotite (fig. 11; sample 07RAB006). The rock here was originally mapped as Burke Formation of the Belt Supergroup by Hietanen (1968) and later as Paleoproterozoic or Mesoproterozoic quartzite by Lewis et al. (2007a). Approximately 120 U-Pb zircon analyses were completed to develop a probability density age plot of this detrital sample (fig. 12). The plot reveals three main clusters of ages with the largest peak ~1860 Ma. In conjunction with a smaller peak at 2670 Ma, the results are quite similar to the detrital age peaks of the Neihart quartzite, which has been interpreted to represent a pre-Belt quartzite unit that lies between the basement and the Belt Supergroup metasediments (Winston et al., 1989; Ross and Villeneuve, 2003). The presence of this quartzite may indicate that there is a complete sequence of rocks in the area from Archean basement (next stop) up into the lower part of the Belt-Purcell Supergroup.

Continue west along the North Fork of the Clearwater about 1.1 miles. You will pass Owl Creek, which comes in from the south, go around a corner, and park.

STOP 7 STOP 7: West of the mouth of Owl Creek (46° 49′ 46″ N, 115° 30′ 26″ W). Park in a pullout along the river. The outcrop consists of a small exposure of Archean augen gneiss surrounded by massive to thickly layered, fine- to medium-grained, rusty weathering, mica schist. The gneiss consists of 0.5-1 cm thick relatively even spaced alternating bands of biotite and plagioclase with quartz. Augen are composed of 1.5-2 cm lenticular white plagioclase (fig. 13). These rocks were originally mapped as metamorphosed Prichard Formation by Hietanen (1968). Later mapping by Lewis et al. (1992) reclassified similar rocks as deformed Cretaceous-aged orthogneiss related to the Idaho batholith. Both of the studies failed to recognize the antiquity of rocks in the complex. Zircons dated by LA-MS-ICPMS yield a crystallization age of 2662 ± 7 Ma (fig. 14).

This is the westernmost extent of the road log. Basement rocks continue from here west to the Canyon fault. Turn around here, return to Skull Creek, turn left, and drive up the Creek about 0.7 miles.

STOP 8 STOP 8: Up Skull Creek (46° 49′ 58″ N, 115° 28′ 28″ W). Park along Skull Creek.

The pale white to buff colored outcrop here is composed of medium-to-coarse-grained muscovite-bearing quartzite with trace amounts of calc-silicate minerals (sample ACJ038; fig. 15). Possible relic bedding in the quartzite ranges from a few centimeters up to a decimeter, and is marked by the appearance of coarse-grained muscovite layers ~0.5 cm thick. Mapped as quartzite within schist of the St. Regis Formation by Hietanen (1968), the sample differs from other quartzites and inferred Belt rocks farther to the southeast (at mouth of Quartz Creek) in its higher degree of recrystallization and low mica and feldspar content. Approximately 130 zircon grains from this sample were analyzed by LA-ICPMS. The results show a depositional age for this unit to be 1446 Ma ± 13 or younger (fig. 16). This depositional age, and the abundance of ~1600 Ma (non-North American) zircons are similar to results reported by Ross, and Villeneuve (2003) for lower Belt (Prichard Formation) metasedimentary rocks. The results are significant in that they help delineate the first known Belt-aged sediment east of probable Neihart Quartzite at field trip Stop 6. Thus, we are probably near the base of the Belt Supergroup at this locality.

Figure 11. Photo of the coarse-grained quartzite at Stop 6 (sample 07RAB006). This quartzite is feldspar poor and thus similar to the Neihart Formation in western Montana.

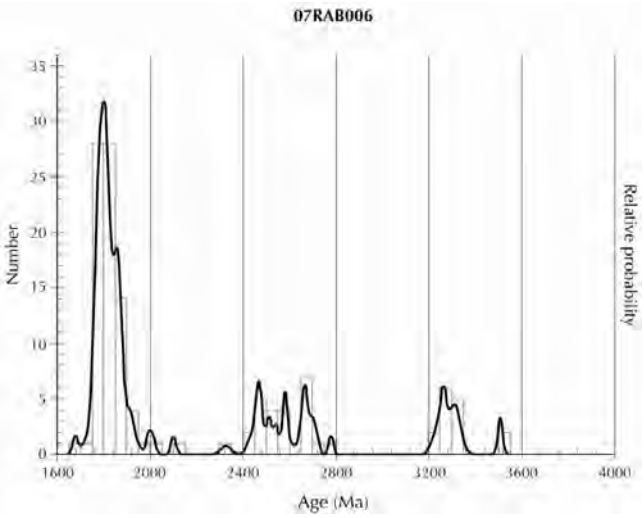

Figure 12. Density-age plot of zircon $^{206}Pb/^{207}Pb$ ages from 07RAB006 showing one large peak at 1800 Ma and two smaller Archean components. This pattern is similar to the results from the Niehart Quartzite (Ross and Villeneuve, 2003). If Niehart, this outcrop may represent the

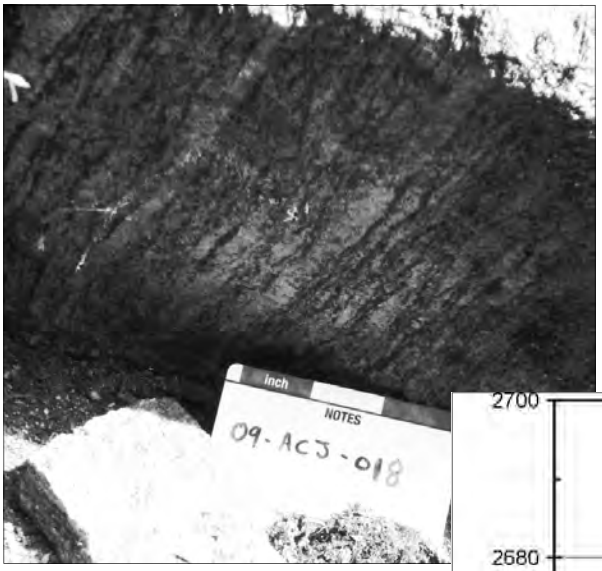

Figure 13. Photo of Archean augen gneiss outcrop at Stop 7 (08ACJ018); photo card for scale (3 inches wide).

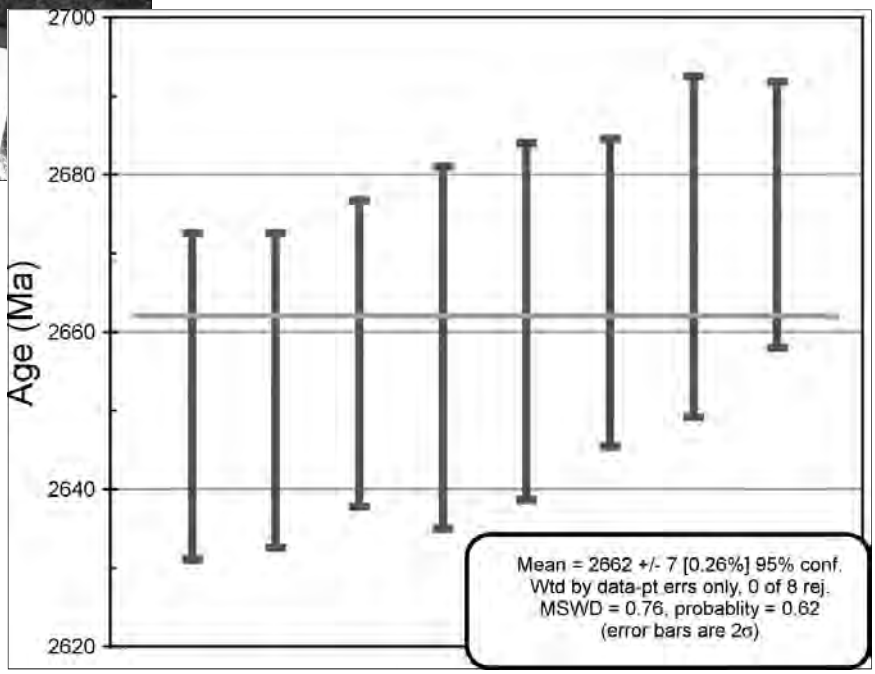

Figure 14. Weighted mean plot for augen gneiss sample 08ACJ018 that yielded an Archean $^{206}Pb/^{207}Pb$ age of 2662 ± 7 Ma.

Figure 15. Photo of the Prichard (?) quartzite at Stop 8 (sample10ACJ038).

Continue up Skull Creek along road about 2 miles and take road 710 (hard right) back to the south. For larger groups it is best to park here and walk up road 710 about 0.2 miles.

STOP 9

STOP 9: Road 710 above Skull Creek (46° 50′ 42″ N, 115° 26′ 51″ W). The purpose of this stop is to walk across the Collins Creek fault. The Collins Creek fault is a north-south striking, east-dipping normal fault that juxtaposes amphibolite-facies metapelites and quartzites of the lower Belt Supergroup against less metamorphosed rocks of the Wallace Formation. This structure is believed to be responsible for the Eocene exhumation of highly metamorphosed mid-crustal rocks of the Clearwater metamorphic core complex to the west (Doughty and Chamberlain, 2007). The first road cuts encountered here are calcareous quartzite in the Wallace Formation on the east side of the fault. Continuing west and up the road we cross the fault (which is not exposed) and are now in the footwall, here composed of garnet-mica schist (locality 46° 50′ 42″ N, 115° 26′ 56″). This schist is possibly metamorphosed Prichard Formation. The equilibrium mineral assemblage of garnet-muscovite-biotite-plagioclase-quartz in this rock indicates peak pressure and temperature conditions of about 5.5-6.0 kbar and 580-590°C (Baldwin, unpublished data).

Return to the North Fork of the Clearwater, turn left, and head upstream toward Kelly Forks Work Center. We will stop about 0.5 miles west of the Work Center at a quarry next to the road.

STOP 10

STOP 10: West of Kelly Forks Work Center (46° 43′ 21″ N, 115° 16′ 3″ W). Park opposite the quarry on the south side of the road. This quarry exposes chlorite breccia along the Kelly Forks fault, a major west-northwest striking fault that bounds the basement rocks on the south side. Plenty of loose rock is available, so avoid the unstable slopes of the quarry walls. Kell and Childs (1999) postulated both left-lateral and later right-lateral motion along this structure. Burmester et al. (2004) documented Eocene right-lateral motion along this fault system southwest of the Boehls Butte area.

Continue east to Kelly Forks campground, and then about one mile up Kelly Creek on road 255.

STOP 11

STOP 11: Above Kelly Creek campground (46° 43′ 15″ N, 115° 14′ 24″ W). Park along Kelly Creek. This stop is in foliated, medium-grained, biotite tonalite gneiss (fig. 17). Trace minerals include epidote and apatite within the mafic layers. The zircons are euhedral and CL images reveal bright, thin rims with darker cores. U-Pb zircon analyses of the cores yielded an age of 1865 Ma (sample 07RAB002; fig. 18). Two rim analyses were dated at 86 Ma indicating a Cretaceous event which may be related to the Cretaceous intrusions found south of the area.

Continue up Kelly Creek about 9 miles to

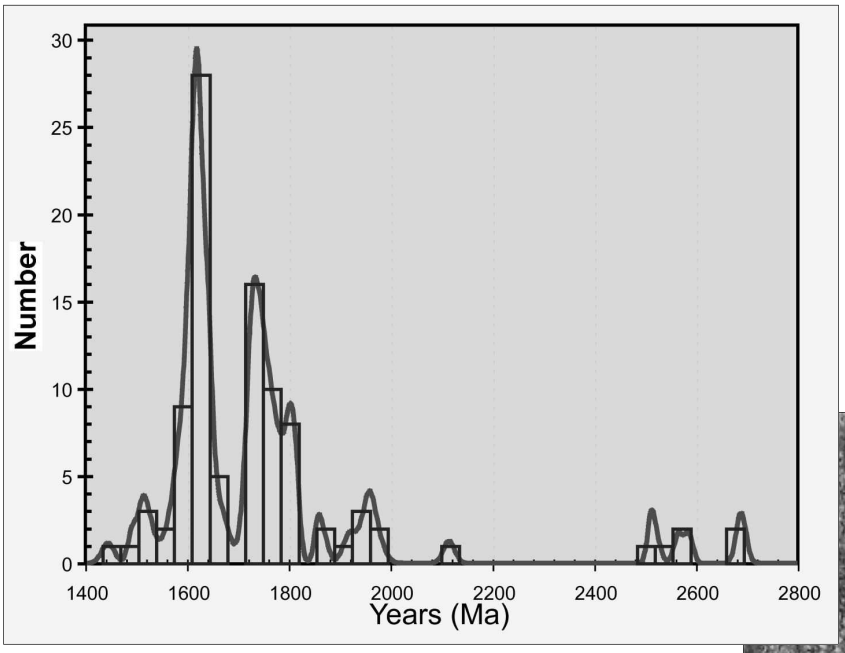

Figure 16. Density-age plot of zircon $^{206}Pb/^{207}Pb$ ages from 10ACJ038 yielded a depositional age younger than ~1446 Ma (Belt Supergroup age). Only zircon ages less than 10 percent discordant are plotted.

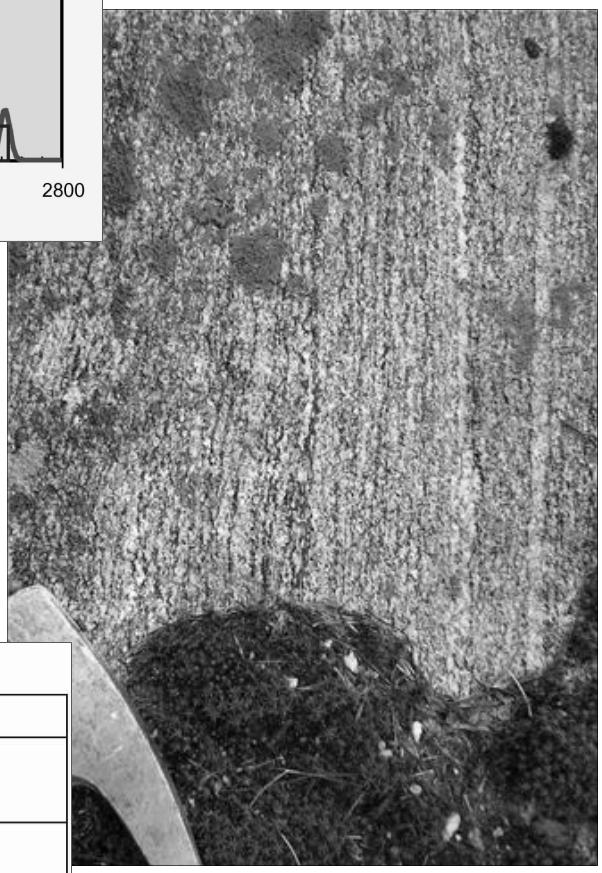

Figure 17. Photo of Paleoproterozoic tonalite gneiss at Stop 11 (sample 07RAB002).

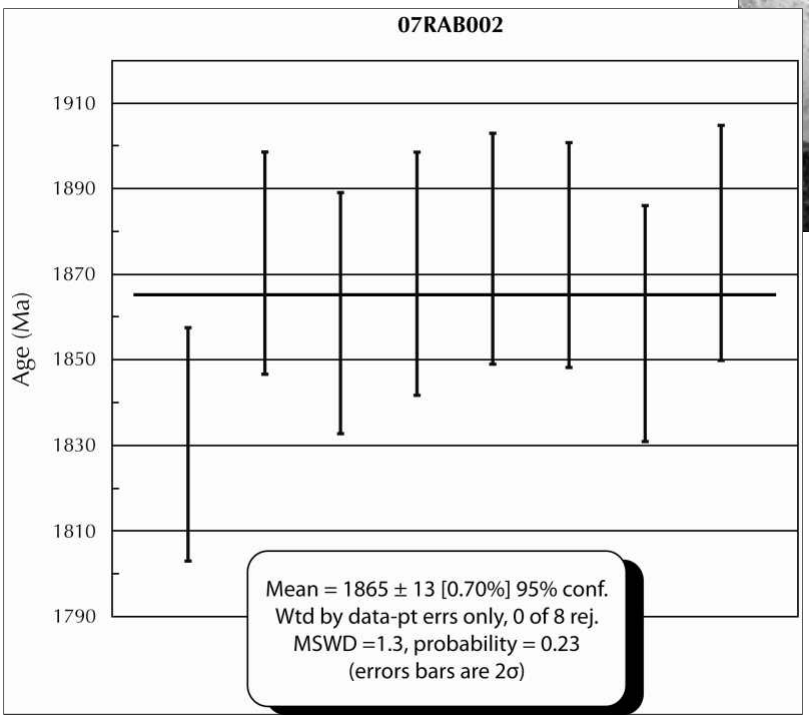

Figure 18. Weighted mean plot of $^{206}Pb/^{207}Pb$ ages for tonalite gneiss sample 07RAB002 that yielded a Paleoproterozoic age of 1865 ± 13 Ma.

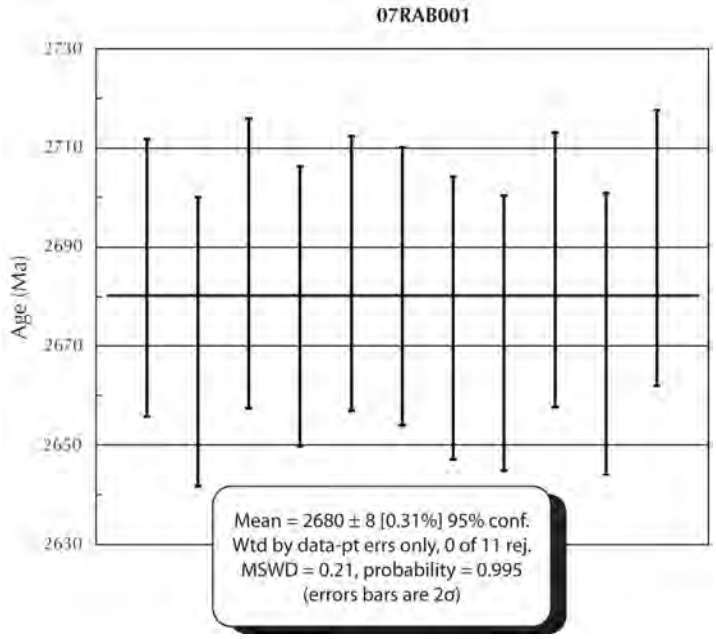

Figure 19. Weighted mean plot of $^{206}Pb/^{207}Pb$ ages for granite sample 07RAB001 that yielded an Archean age of 2680 ± 8 Ma.

where the road cuts sharply to the left. The rocks along this part of the route are schist and gneiss that are presumably basement to the Belt Supergroup.

STOP 12 Stop 12: Kelly Creek (46° 42′ 23″ N, 115° 5′ 33″ W). Park in pullout on point and walk about 0.1 miles back downstream. This stop is in a massive outcropping of iron-stained, medium-grained granite, here termed the granite of Kelly Creek. A faint lineation of biotite is the only obvious fabric in the rock. Thin sections reveal the primary minerals to be plagioclase, microcline, biotite, and quartz. U-Pb zircon analysis of sample 07RAB001 yielded an age of 2680 ± 8 Ma (fig. 19). The zircons from this sample are moderately euhedral despite having a slightly tattered appearance. CL images of the zircons reveal little to no zoning.

The presence of this rock in such large and extensive outcrops makes it unique to the area. The other Archean intrusions in the area are smaller and less easily mapped. While the relative lack of disturbance and its clear zircons belie its old age, they also reinforce the idea that the age is not a product of inheritance or resetting.

End of road log. Return to Superior by continuing east about 1.4 miles, taking a left (still on road 255) and going north over Deception Saddle. North of the saddle you will join U.S.F.S. road 250, the road we started on. Take a right to get to Hoodoo Pass and Superior.

ACKNOWLEDGMENTS

Russell Burmester kindly reviewed the manuscript, improved the content, and assisted with the figures.

REFERENCES

Baldwin, J.A., Graham, A., and DesOrmeau, J.W., 2011, U-Pb zircon geochronology of meta-anorthosites in the Bitterroot Range, western Montana: Implications for metamorphism and anatexis during core complex formation: Geological Society of America, Abstracts with Programs, v. 43, p. 76.

Brewer, R.A., Vervoort, J., Lewis, R.S., Gaschnig, R.M., and Hart, G., 2008, New constraints on the extent of Paleoproterozoic and Archean basement in the northwest U.S. Cordillera: EOS, Transactions, American Geophysical Union, Fall Meeting Supplement, 89, Abstract T23C-2066.

Burmester, R.F., McClelland, W.C., and Lewis, R.S., 2004, U-Pb dating of plutons along the transfer zone between the Bitterroot and Priest River metamorphic core complexes: Geological Society of America, Abstracts with Programs, v. 36, p. 72.

Doughty, P.T., and Chamberlain, K.R., 2007, Age of Paleoproterozoic basement and related rocks in the Clearwater complex, northern Idaho, U.S.A.: *in* Link, P.K., and Lewis, R.S., eds., Proterozoic

Geology of Western North America and Siberia: SEPM Special Publication 86, p. 9-35.

Doughty, P.T., Price, R.A., and Parrish, R.R., 1998, Geology and U-Pb geochronology of Archean basement and Proterozoic cover in the Priest River complex, northwestern United States, and their implications for Cordilleran structure and Precambrian continent reconstructions: Canadian Journal of Earth Science, v. 35, p. 39-54.

Foster, D.A., Mueller, P.A., Mogk, D.W., Wooden, J.L., and Vogl, J.J., 2006, Proterozoic evolution of the western margin of the Wyoming craton: Implications for the tectonic and magmatic evolution of the northern Rocky Mountains: Canadian Journal of Earth Sciences, v. 43, p.1601-1619.

Hietanen, A., 1968, Belt series in the region around Snow Peak and Mallard Peak, Idaho: U.S. Geological Survey Professional Paper 344-E, 34 p.

Kell, R.E., and Childs, J.F., 1999, Mesozoic-Cenozoic structural events affecting the Belt Basin between the Idaho batholith and the Lewis and Clark line: Implications on identifying syndepositional Belt-age structures: *in* Berg, R.B., ed., Belt Symposium III Abstracts, 1993: Montana Bureau of Mines and Geology Open-File Report 381, p. 32-34.

Lewis, R.S., Burmester, R.F., McFaddan, M.D., Eversmeyer, B.A., Wallace, C.A., and Bennett, E.H., 1992, Geologic map of the upper North Fork of the Clearwater River drainage, northern Idaho: Idaho Geological Survey Geologic Map 20, scale 1:100,000.

Lewis, R.S., Burmester, R.F., McFaddan, M.D., Kauffman, J.D., Doughty P.T., Oakley, W.L., and Frost, T.P, 2007a, Geologic map of the Headquarters 30- x 60-minute quadrangle, Idaho: Idaho Geological Survey Digital Web Map 92, scale 1:100,000.

Lewis, R.S., Vervoort, J.D., Burmester, R.F., McClelland, W.C., and Chang, Z., 2007b, Geochronological constraints on Mesoproterozoic and Neoproterozoic(?) high-grade metasedimentary rocks of north-central Idaho: *in* Link, P.K., and Lewis, R.S., eds., Proterozoic Geology of western North America and Siberia: SEPM Special Publication 86, p. 37-53.

Lewis, R.S., Vervoort, J.D., Burmester, R.F., and Oswald, P.J., 2010, Detrital zircon analysis of Mesoproterozoic and Neoproterozoic metasedimentary rocks of north-central Idaho: Implications for development of the Belt-Purcell basin: Canadian Journal of Earth Sciences, v. 47, p. 1383-1404.

Ross, G.M., and Villeneuve, M., 2003, Provenance of the Mesoproterozoic (1.45 Ga) Belt basin (western North America): Another piece in the pre-Rodinia paleogeographic puzzle: Geological Society of America Bulletin, v. 115, p. 1191-1217.

Seyfert, C.K., 1984, The Clearwater Core Complex, a new Cordilleran metamorphic core complex, and its relation to a major continental transform fault: Geological Society of America Abstracts with Programs, v. 16, no. 6, p. 651.

Vervoort, J.D., Zirakparvar, N.A., Lewis, R.S., and Burmester, R.F., 2007, Evidence for recurrent Paleoproterozoic and Mesoproterozoic magmatism and metamorphism in the Boehls Butte-Clarkia area, north-central Idaho, USA: Geological Society of America Abstracts with Programs, v. 39, no. 6, p. 245.

Winston, D., 2007, Revised stratigraphy and depositional history of the Helena and Wallace Formations, Mid Proterozoic Piegan Group, Belt Supergroup, Montana and Idaho: *in* Link, P.K., and Lewis, R.S., eds., Proterozoic Geology of western North America and Siberia: SEPM Special Publication 86, p. 65-100.

Winston, D., Horodyski, R.J., and Whipple, J.W., 1989, Middle Proterozoic Belt Supergroup, western Montana: American Geophysical Union, 28th International Geological Congress, Washington D.C., Field Trip Guidebook T334, p. 102.

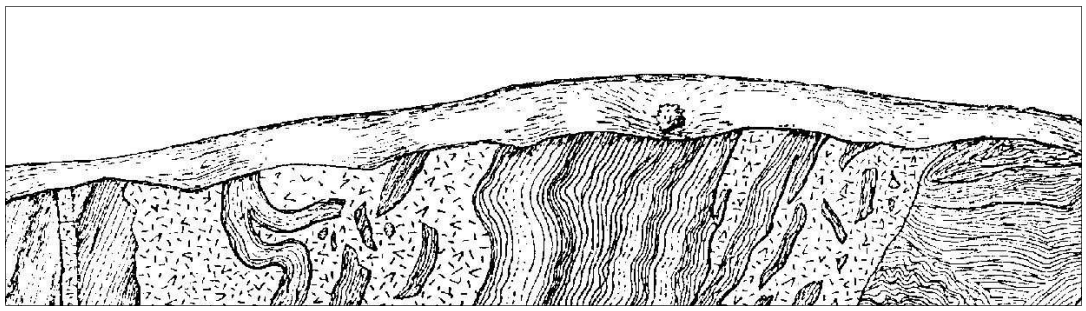

QUATERNARY GEOLOGY AND PLACERS IN QUARTZ CREEK, MINERAL COUNTY, MONTANA

Robin McCulloch
Montana Bureau of Mines and Geology, 1300 W. Park St., Butte, MT 59701
rmcculloch@mtech.edu

Larry N. Smith
Department of Geological Engineering
Montana Tech of the University of Montana, 1300 W. Park St., Butte, MT 59701
lsmith@mtech.edu

Quartz Creek is a small, steep stream that flows ENE into the Clark Fork River near the small community of Rivulet, MT (fig. 1). Alluvium and other unconsolidated Quaternary sediment along the drainage bottom have been mined for placer gold. The drainage basin is underlain mostly by Wallace Formation with some Snowslip Formation and Tertiary or Cretaceous granodiorite intrusions. The area is cut by NE- and NW-trending faults (fig. 1).

Placers in the area include those in alluvial/ gulch deposits, debris deposits, and residual deposits (fig. 2). Most of the placers in the area can be tied, at least in a general way, to lode sources (fig. 3; McCulloch et al., 2003).

The placer deposits formed through two distinct events. The early event formed as a debris flow/gulch placer in the main drainages of Quartz, Cedar and Trout creeks during the Tertiary period. During the Pleistocene, Glacial Lake Missoula filled the drainages to the 4,100 ft elevation causing the lower ends of the drainages to fill with reworked placer deposits and gravel. The draining of the lake caused much of the material to rework again leaving perched bars in the lower segments of the major streams.

Road Log

Travel southeast from Superior on Interstate 90 for about 19 miles, and exit to the south at Fish Creek (exit 66). Go under the freeway, across the Clark Fork River and travel through the historic place of Rivulet to where Quartz Creek crosses the dirt road.

STOP 1 – Lower end of Quartz Creek. Near the mouth of Quartz Creek is the remnant portions of the valley fill up the drainage while across the river, the paleo-stream channel can be seen above the old Milwaukee Railroad bed. The Clark Fork River has since eroded its channel well below this old stream channel. Pay gravels still remain 15-20 ft below the present stream while drift mining has exposed segments of the paleo-channel on the north side of the river.

STOP 1

We will walk up the gated road (with permission, onto private property) to view alluvial and gulch placers along the lower end of Quartz Creek. Gravelly alluvium depositd by high-energy alluvial flows are exposed in the high walls of excavated gravel (fig. 3). The gravelly deposits show crude bedding. A few fine-grained beds show rapid deposition, climbing ripples, and dewatering structures that may represent subaqueous debris-flow to turbidite deposition in Glacial Lake Missoula. Most

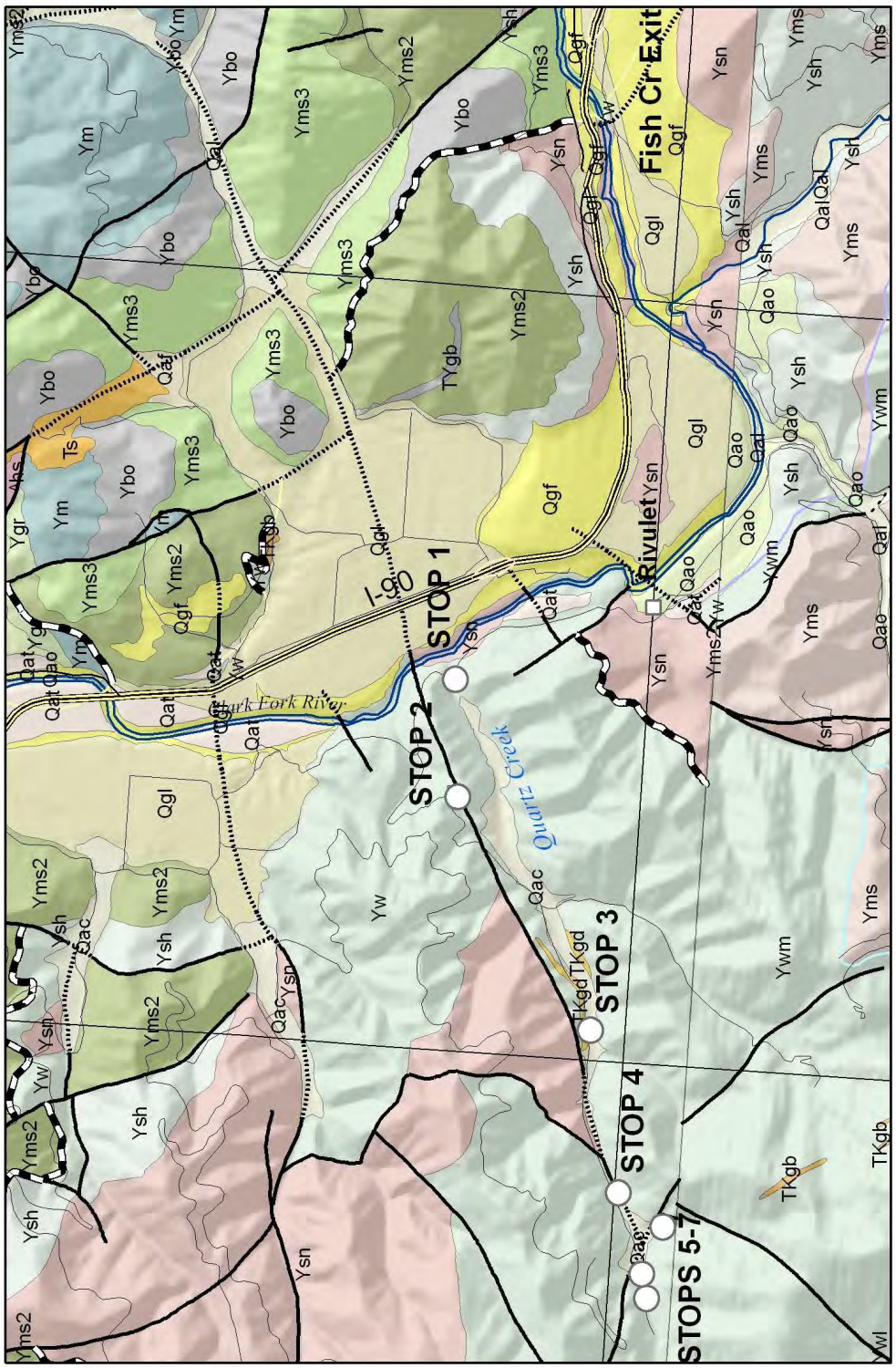

Figure 1. Location map of roads and stops and geologic map of the Quartz Creek area. Ywl, Ywm – Wallace Formation, lower and middle members: Ysn – Snowslip Formation; Yms – Mount Shields Formation; Qgf – Quaternary glacial flood deposits; Qgl – glacial lacustrine deposits; Qao – older alluvium; Qat – terrace deposits; bold lines – faults (dotted where covered); black and white line – thrust fault; modified from Lewis (1998) and Lonn et al. (2007); the east-west trending discordance are just "map boundary faults".

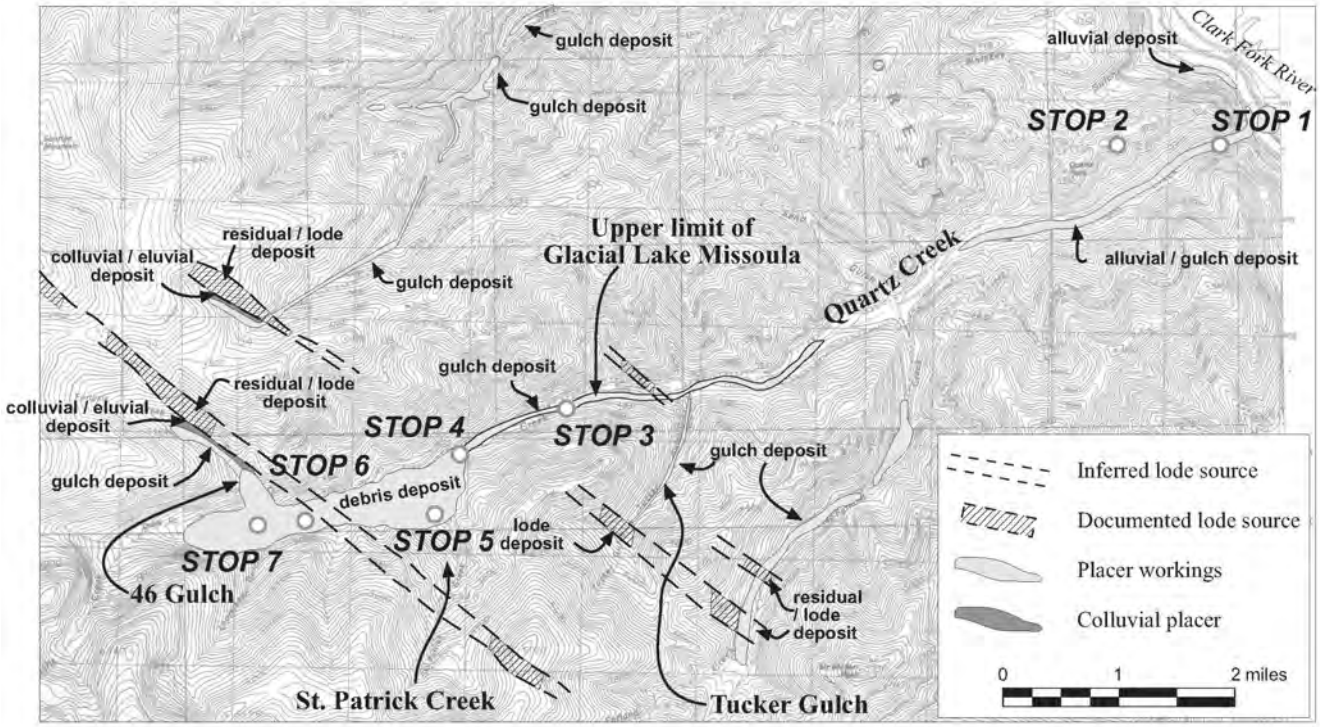

Figure 2. Map of placer and lode deposits in the Quartz Creek area (modified from McCulloch et al., 2003).

of the gravel (inadequately mapped as "Qac" in fig. 2) likely represents deltaic(?) deposits that prograded into the lake.

STOP 2

STOP 2 – Quartz Creek overlook – this represents the upper limit of Glacial Lake Missoula. The current operations of gold placering have exposed the bedrock and portions of the pay streak. At the stop, we will discuss the formation of the pay streak and subsequent burial from Glacial Lake Missoula followed by the erosion of a side drainage that has buried the deposit by an additional 15-20 ft. Boulders within the deposit indicate that the mineralizer of the lode may be granodiorite intrusive formed along a northwest trending fault that has yet to be exposed. Many of these boulders exhibit significant chloritic alteration. The pay streak through this area exhibits high energy, linear pathways following refraction from valley wall impacts similar to the ball in a billiard game.

STOP 3

STOP 3 – Near the historic Calumet placer deposit one of the lode zones is exposed above the road in the form of a mine dump. Slightly upstream, quartz crops out 200 ft across on the hillside.

STOP 4

STOP 4 – At the confluence of Quartz Creek and St. Patrick Creek it is possible to see where the debris flow plugged Quartz Creek and during the resulting flood, placer gold was deposited on the hillside until the blockage was eroded out.

STOP 5

STOP 5 - We will leave the vehicles and cross the creek on the St. Patrick Creek trail to the Dakota Placer mine. This was a surface mine in the 1930s that subsequently went underground in a drift 1,700 ft long. This was documented in a publication by the U.S. Bureau of Mines.

Figure 3. Photograph, taken with a telephoto lens, of gravelly alluvial deposits in the lower portion of Quartz Creek (looking northwest). Note crude bedding in the gravelly deposits and the extensive silty sand bed between the gravels. The silty sand displays climbing ripples and fluid escape structures that indicate rapid deposition, probably from a debris flow into the lake.

STOP 6 STOP 6 – We will view boulder piles that were stacked with a winch driven by a pelton wheel. The upper end of the road will show the remains of the boom dam and sluice box that was used and created the need for boulder stacking.

STOP 7 STOP 7 – Slightly above that the sluice box, we will cross a ford and bushwhack a short distance to the site of the hydraulic pit that was also operated in the 1930s. Although we will be near the source area for the gold, dense foliage and steep terrain preclude the opportunity for the group to see much of anything.

We will then return to the vehicles at Stop 4 and drive back to Superior.

References

Lewis, R.S., 1998, Geologic map of the Montana part of the Missoula West 30' x 60' quadrangle: Montana Bureau of Mines and Geology Open-File Report 373, 20 p., scale 1:100,000.

Lonn, J.D., Smith, L.N., and McCulloch, R.B., 2007, Geologic map of the Plains 30'x60' quadrangle, western Montana: Montana Bureau of Mines and Geology Open-File Report 554, scale 1:100,000.

McCulloch, R.B., Lewis, B., Keill, D., and Shumaker, M., 2003, Applied Gold Placer Exploration and Evaluation Techniques: Montana Bureau of Mines and Geology Special Publication 115, 267 p.